FIVE-FOLD SYMMETRIC PENTA-BIOCONJUGATED CORANNULENES: SYNTHESIS, PROPERTIES AND APPLICATIONS

Dissertation zur Erlangung
der naturwissenschaftlichen Doktorwürde
Dr. sc. nat.

vorgelegt der
Mathematisch-naturwissenschaftlichen Fakultät
der Universität Zürich

von
Martin, Mattarella
aus Italien

Promotionskomitee:
Prof. Dr. Jay S. Siegel (Vorsitz)
Prof. Dr. Kim K. Baldridge
Prof. Dr. Nathan W. Luedtke
Prof. Dr. Joseph M. O'Connor

Zürich, 2013

ABSTRACT OF THE DISSERTATION

FIVE-FOLD SYMMETRIC PENTA-BIOCONJUGATED CORANNULENES: SYNTHESIS, PROPERTIES AND APPLICATIONS

by

Martin Mattarella

University of Zurich, 2013

Prof. Dr. Jay S. Siegel, Chair

Corannulene is a C_{5v} symmetric polyaromatic hydrocarbon (PAH) and it can be considered the smallest fragment of buckminsterfullerene that displays a curvature of the carbon skeleton, which gives corannulene interesting physical properties differing from those of planar π-conjugated analogs (*i.e.* bowl-shaped structure, rapid bowl-to-bowl inversion at room temperature and a dipole moment). With the advent of corannulene in kilogram scale, and a robust procedure for converting corannulene into *sym*-pentachlorocorannulene, came the motivation to create an array of 5-fold symmetric pentasubstituted corannulene derivatives suitable for incorporation into polymers, materials, bioconjugates and supramolecular architectures. The development of a robust synthetic pathway for the preparation of C_5-symmetric pentasubstituted corannulenes functionalized with the main classes of biomolecules (carbohydrates, oligopeptide, lipids and nucleic acids) and their applications and properties are described in this dissertation.

The first goal is having access to a library of *sym*-pentasubstituted corannulene derivatives bearing a broad window of functional groups and displaying high solubility in organic solvents. Iron-catalyzed alkyl-aryl cross-coupling and further elementary chemical reactions allow the synthesis in hundreds of milligrams scale of a wide range of penta-substituted corannulenes displaying the principal organic functional groups.

Copper nanoparticles catalyzed and microwave assisted CuAAC "click" reaction provides optimal reaction conditions for the conjugation of *sym*-penta-(1-butyn-4-yl)-corannulene with azide-containing biomolecules; corannulene derivatives bearing nucleosides (thymidine and deoxy-adenosine), sugars (ribose and galactose), short oligopeptide and lipids can be prepared in good

yield and purity. In the case of the synthesis of sym-penta-(DNA) corannulene, the CuAAC reaction conditions need to be optimized using CuBr-TBTA as catalytic species. The assembling behavior of these molecules and the computational studies for the formation of supramolecular architectures are described in this dissertation.

Cholera toxin (CT) from *Vibrio cholerae* belongs to the AB_5 bacterial toxins family. Following the "Finger-Linker-Core" approach, several five-fold symmetric pentasubstituted corannulene derivatives conjugated to PEG-like chains functionalized with CT binders galactose and GM1os are synthesized and their inhibition potency toward CT evaluated. The synthesized GM1os-based inhibitors show high binding to CT with IC_{50} values in the range of nanomolar concentrations.

Several pentakis-lipido corannulene derivatives displaying different aliphatic chains are synthesized and their thermal and gelation behaviors investigated. While oleyl-functionalized corannulene derivative exists in a lamellar liquid-crystalline phase at room temperature and shows gelator properties, the saturated analog is partially crystallized at room temperature but forms gel in cyclohexane; heptyl-functionalized corannulene does not show neither gelator nor liquid-crystalline behavior. The results suggest that the length and geometry of the alkyl chains attached onto corannulene play an important role on the physical properties of pentakis-lipido corannulenes.

In summary, this PhD dissertation describes the development of a powerful "toolbox" for the synthesis of C_5-symmetryc pentasubstituted corannulene derivatives, which can find application in biology, pharmacology, material chemistry, polymers and supramolecular chemistry.

ZUSAMMENFASSUNG DER DISSERTATION

von

Martin Mattarella

Universität of Zürich, 2013

Prof. Dr. Jay S. Siegel, Vorsitz

Corannulene, ein C_{5v} symmetrischer polyaromatischer Hydrocarbon (PAH), ist das kleinstes Fragment der Buckminsterfullerene und weisst eine Wölbung des Kohlenstoffgerüstes auf. Dieses charakteristische Merkmal zeigt interessante physikalische Eigenschaften, welche im Vergleich zu den planaren π-Analogen komplett unterschiedlich sind (z.B. schalenförmige Struktur, rapide Inversion von Schale-zu-Schale bei Raumtemperatur, und der Dipolmoment). Mit dem Durchbruch Corannulene in Kilogramm-Massstab herzustellen und mit einer robusten Methode in *sym*-Pentachlorocorannulene umzuformen, kam die Motivation eine Reihe von fünfach symmetrischen, pentasubsitutierten Corannulenederivaten herzustellen, welche eine Andwendung in vielerlei Bereichen aufweisen, wie z.B. in Polymeren, Materialen, biokonjugierte und supramolekularen Strukturen. In dieser Dissertation wird die Entwicklung eines robusten Syntheseweges zur Herstellung von C_5-funktionalisieren, symmetrischen pentasubstituierten Corannulenen mit dem hauptsächlichem Anwendungsgebiet in Biomolekülen (Karbonhydrate, Oligopeptide, Lipide und Nukleinsäure) beschrieben.

Das erstes Ziel bestand aus einer weitreichenden Sammlung von *sym*-pentasubstituierten Corannulenderivaten, welche ein breites Spektrum von funktionellen Gruppen und eine hohe Löslichkeit in organischen Lösungsmitteln aufweisen. Eisenkatalysierte Alkyl-Aryl-Kreuzkupplung und weitere darauf folgende elementare chemische Reaktionen erlauben eine vielfältige Synthese im Milligrammmassstab unter Herstellung von einer solchen Sammlung an verschiedensten penta-substituierten Corannulenen mit grundlegenden organischen funktionellen Gruppen.

Die durch Kupfernanopartikeln katalysierte und Mikrowellen-unterstütze CuAAC “Klick”reaktion bietet optimale Bedingungen zur Konjugation von *sym*-penta-(1-butyn-4-yl)-Corannulen mit aziden Biomolekülen. Corannulenderivate, welche Nukleoside (Thymidin und

Deoxyadenosin), Zucker (Ribose und Galactose), kurze Oligopeptide und Lipide besitzen, können so in guten Ausbeuten und Reinheit gewonnen werden. Im Fall der Synthese von *sym*-penta-(DNA)-Corannulen musste die CuAAC-Reaktion optimiert werden, indem CuBr-TBTA als Katalysator verwendet wurde. Das sich aggregierende Verhalten dieser Moleküle und computeranimierte Studien zur Bildung dieser supramolekularen Architekturen sind in dieser Dissertation besschrieben.

Cholera Toxin (CT) der *Vibrio cholerae* gehört zur der AB_5 der Familie der bakteriellen Toxine. Verschiedene fünffach-symmertrische, pentasubstituierte Corannulenderivate verknüpft mit PEG-ähnlichen Ketten, welche mit CT-bindern Galactose und GM1os funkionalisiert sind, wurden gemäss dem "Finger-Linker-Core"-Prinzip synthetisiert und ihre inhibitorische Fähigkeit im Hinblick auf CT evaluiert. Die synthetisierten GM1os-Inhibitoren wiesen eine hohe Bindung zu CT mit einer IC_{50} –Werte in nanomolekularen Konzentrationen auf.

Verschiendenste pentakis-lipido-Corannulenderivate mit unterschiedlichen aliphatischen Ketten wurden synthetisiert und deren thermisches Verhalten und Gelierungsverhalten studiert. Während oleyl-funktionalisierte Corannulenderivate in einer lamellelenarigen flüssigkristallinen Phase bei Raumtemperatur existiert und gelatierende Eigenschaften aufweist, zeigt das gesättigte Analogon nur einen teilweisen kristallinen Zustand bei Raumtemperatur und formt Gele in Cylcohexan. Hingegen weist das heptylfunktionalisierte Corannulen weder gelatierenden Eigenschaften, noch flüssigkristallines Verhalten auf. Diese Resultate lassen darauf schliessen, dass die Länge und Geometrie der Alkylketten, welche an Corannulen gebunden sind, eine entscheidende Rolle hinsichtlich der physikalischen Eigenschaften der pentakis-lipido Corannulene spielen.

Zusammenfassend wird in dieser Doktorarbeit die Kreation eines vielversprechenden "Baukastens" zur Synthese von C_5-symmetrischen pentasubstituierten Corannulenderivaten mit einer ebenso vielversprechenden Anwendung in der Biologie, Pharmakolgie, Materialchemie, Polymer- und supramolekulare Chemie, beschrieben.

ACKNOWLEDGEMENTS

Prof. Dr. Jay S. Siegel

Prof. Dr. Kim K. Baldridge

Prof. Dr. Nathan W. Luedtke

Prof. Dr. Joseph M. O'Connor

Prof. Dr. Ehud M. Landau

Prof. Dr. Han Zuilhof

Prof. Dr. Raffaele Mezzenga

Prof. Dr. Janne Ruokolainen

Prof. Dr. Franco Cozzi

Dr. Ing. Tom Wennekes

Dr. Sofia Gallo

Dr. Ulrike Rieder

Laura Berstis

Jacopo Marino

Jaime Garcia-Hartjes

Johannes M. Haberl

UNIZH NMR Service

UNIZH MS Service

All Siegel, Finney, Landau, Stuparu and Baldridge group members past and present.

CONTENTS

LIST OF FIGURES

LIST OF SCHEMES

LIST OF TABLES

1. CORANNULENE: AN INTRODUCTION

1.1. STRUCTURE OF CORANNULENE

Corannulene (**1**) is a non-planar polycyclic aromatic hydrocarbon (PAHs) and its carbon skeleton can be found in the structure of another member of the non-planar PAHs family: buckminsterfullerene (**2**).

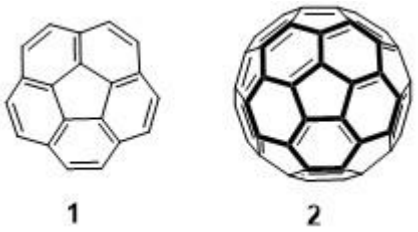

Figure 1.1. Corannulene **1** and buckminsterfullerene **2**.

The structure of **1** consists in five condensed benzene rings arranged around a central pentagon; this particular disposition imposes a bowl-shaped geometry to the molecule. This arrangement of the carbon atoms represents the optimal compromise between strain and electronic delocalization. A proposed polar resonance form of **1** consists in the presence of two concentric aromatic systems, the inner cyclopentadyenil anion and the peripheral cyclopentadecaheptaenyl cation. [1]

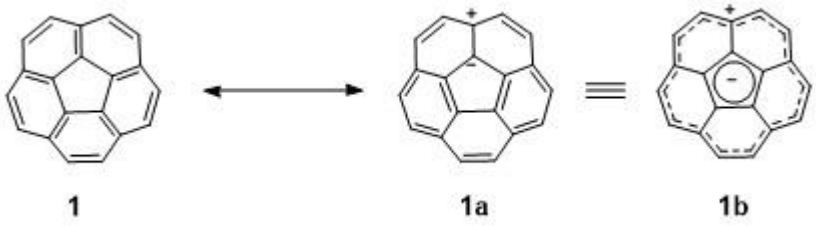

Figure 1.2. Resonance form of **1**.

Both of the aromatic systems in the resonance form satisfy the Hückel's rule and MO calculations suggest the resonance has a significant contribution on the π electron distribution. [2]

The first X-ray analysis reveals the bowl-shaped geometry of **1** and its C_{5v} symmetry, which is confirmed by the magnetic isochrony of the ten hydrogen atoms showed in ^{1}H-NMR experiment (δ= 7.81 ppm) and the presence of three signals in ^{13}C-NMR experiment (δ= 135.81, 130.84 and 127.18 ppm for hub, spoke and rim respectively). [3] These values suggest a dominant [5]-radialene structure of **1**; however, synchrotron measurements of the electron density at 12 K reveal a slightly negative region in the center of **1**, as expected from the resonance form **1b**. [4]

The symmetry of **1** imposes three chemically different carbon atoms and four different C-C bonds with different lengths: flank (1.45 Å), rim (1.38 Å), spoke (1.38 Å) and hub (1.42 Å). [5] In comparison, compound **2** show a shorter bowl-depth (1.50 Å) and only two different C-C bonds length (1.38 Å and 1.45 Å). [6] The value of the bowl-depth, defined as the distance between the imaginary planes defined one by the five central carbons and the other by the ten peripherial carbon atoms, has been determined to be 0.875 Å. [7,8]

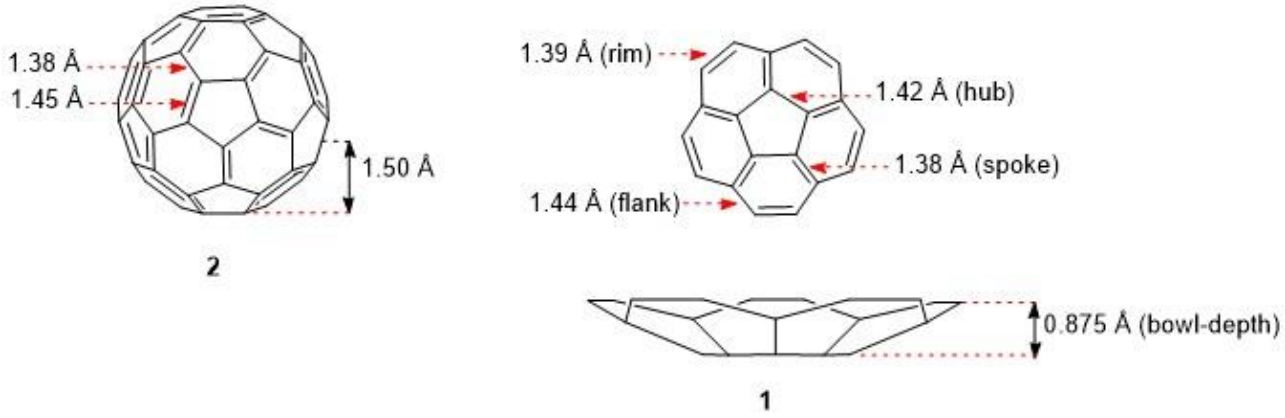

Figure 1.3. Structure of **1** and **2**.

While **2** shows a static spherical geometry, **1** has a dynamic structure: the bowl-to-bowl inversion process consist in the inversion of the bowl (ground state) through a high energetic flat form (transition state). [2] Given the symmetry of **1**, the inversion barrier cannot be measured by variable temperature NMR (VT-NMR) experiments; however, the value of the inversion barrier of **1** (11.5 kcal mol^{-1}) was estimated from VT-NMR measurements of several derivatives of **1** containing stereo probes, which have little effects on the bowl-to-bowl process. [9,10]

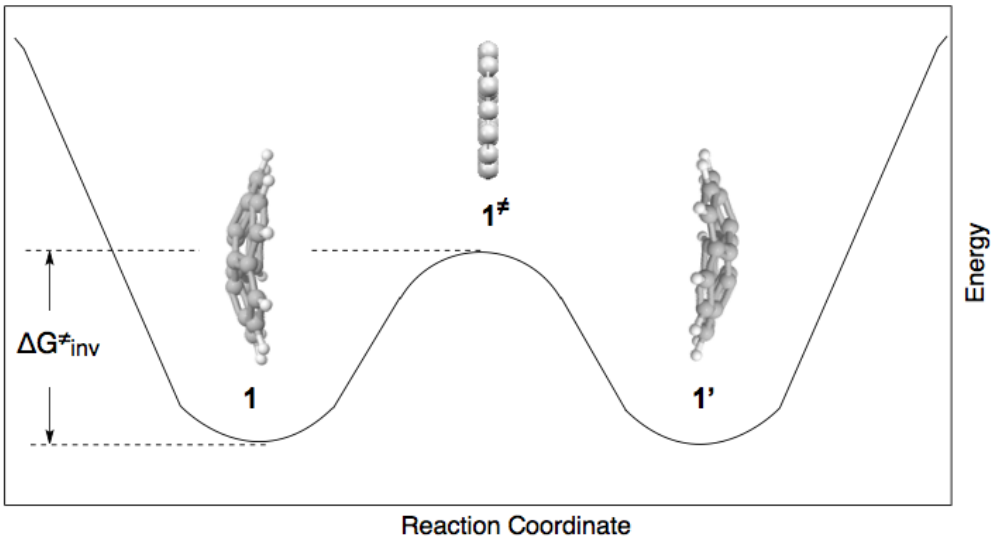

Figure 1.4. Energy diagram for the bowl-to-bowl inversion process of **1**.

1.2. SYNTHESIS OF CORANNULENE

1.2.1. PIONEERING SYNTHESIS OF CORANNULENE

The first synthesis of **1** was achieved in 1966 [11] by Lawton through a laborious synthetic pathway. The strategy for the formation of the carbon framework of **1** consists in a gradually introduction of 4-carbons fragments and sequent annulation of the carbon rings starting from acenaphthene (**3**), which represents an optimal starting substrate.

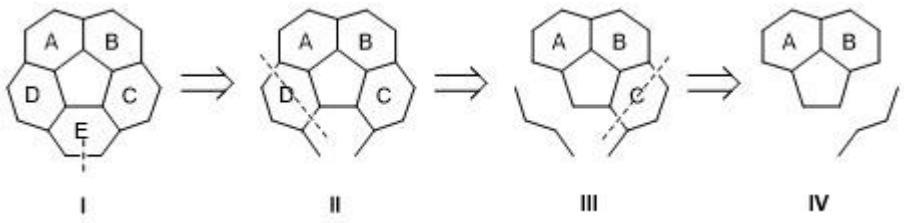

Scheme 1.1. Retrosynthetic disconnection for the carbon network of **1**.

The first part of the synthetic route is the formation of ring C: alkylation of **3** with maleic anhydride (4-carbon unit), intramolecular acylation and further chemical transformations lead to compound **4**. The formation of another ring (D) was achieved following the same strategy: a 4-carbon unit was attached to the methylene position of **4** and cyclized to **5**. The author claims the selective hydrogenation of **5** to acid **6**, whose apparent cup-like structure brings the carboxylic

groups in a position favorable for the ring closure. The last ring (E) was closed by intramolecular acyloin condensation and further reduction to alcohol **7**. The further dehydrogenation leads to the fully aromatic system **1**.

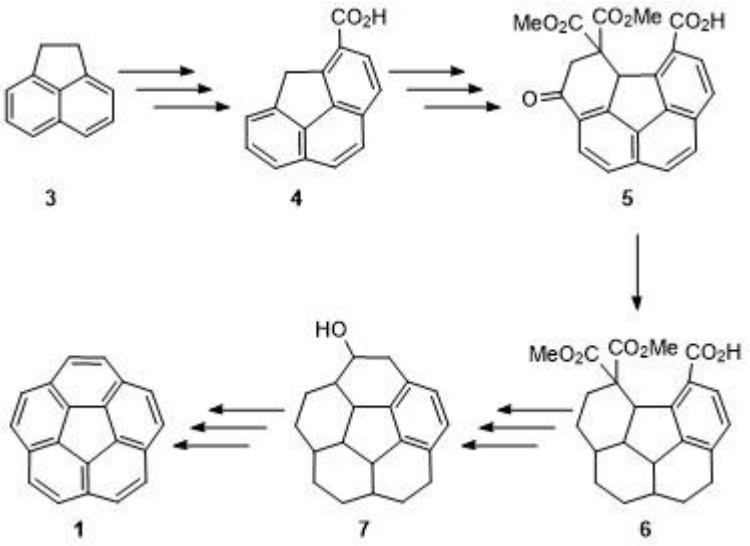

Scheme 1.2. First synthesis of **1**.

The formation of the saturated carbon network was crucial for the success of this synthetic pathway since the formation of strained structures by ring closure has been bypassed. Unfortunately, this long synthetic route is not optimal for the preparation of **1** in amounts large enough for detailed studies on its physical and chemistry properties (17 steps, and yield <1%).

1.2.2. Synthesis of Corannulene by Flash Vacuum Pyrolysis

After its first synthesis in 1966, the interest in non-planar PAHs decreased and only two new attempts for the synthesis of **1** were tried in the next 20 years and both of them failed. [12–14] The discovery of fullerene in 1985 [15] gave new energy and motivations to the synthesis of various curved PAHs, which can be considered as subunits of fullerene.

In 1991 Scott reported an improved synthesis of **1** using flash vacuum pyrolysis (FVP) starting from the diyne **8**. [3] This synthesis was inspired by the work of Brown who demonstrated the reversible rearrangement of terminal acetylenes to viniylidenes [16] and the cyclization of 2-ethynylbiphenyl to phenantrene [17] by apparent trapping of transient carbene via intramolecular C-H insertion, when FVP conditions are applied.

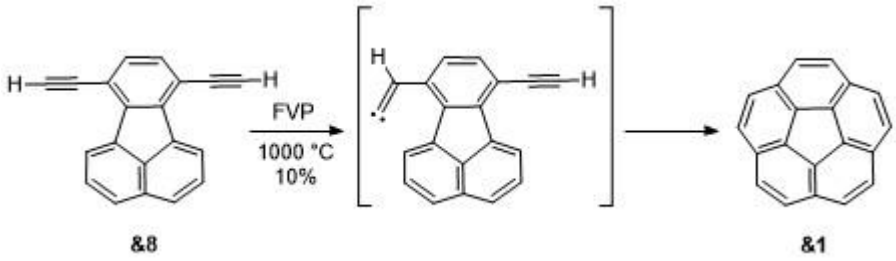

Scheme 1.3. First synthesis of **1** via FVP.

The success of FVP in the synthesis of strained non-planar PAHs depends on the high temperature applied, which allows the bending of the planar precursors to curved geometries in which the reaction centers are close in space. Furthermore, since the reaction takes place in gas phase, the polymerization of the precursor is minimized.

Due to the success of the FVP approach, several works report different syntheses of **1** starting from various precursors. After his first synthesis, Scott reports that tetrabromide **9** leads to better yield due to its small thermal polymerization during sublimation. It's also reported that bis(1-chlorovinyl)fluoranthene **12** allows access to **1** in gram scale with good yield; the authors speculate that **12** thermally eliminate HCl to form **8** in situ. [18] Rabideau showed that silyl vinyl ethers **13** can also be deployed, however with less efficacy. [19] In 1992 Siegel reported the syntheses of **1** from tetrakis(bromomethyl)-fluoranthene **10** and from bissulfone **11**. [5] In 1999 Knölker devised an alternative route from bis(trimethylsilyl)fluoranthene **14**, which produces **1** upon FVP condition. [20] Although slightly different, all the above precursors have fluoranthene as common basic structure. Zimmermann in 1994 [21] and Mehta in 1997 [22] reported the synthesis of **1** starting from precursors with a different carbon skeleton: diyne **15** and helicenes **16** were converted to **1** under FVP conditions.

Despite the success of FVP in the production of **1**, this procedure suffers from some disadvantages: the FVP equipment restricts the synthesis to several hundred milligrams from which only modest amount of **1** can be obtained. Since high temperatures are applied, the FVP procedure does not tolerate functional groups, which limits the methods for the synthesis of unsubstituted corannulenes.

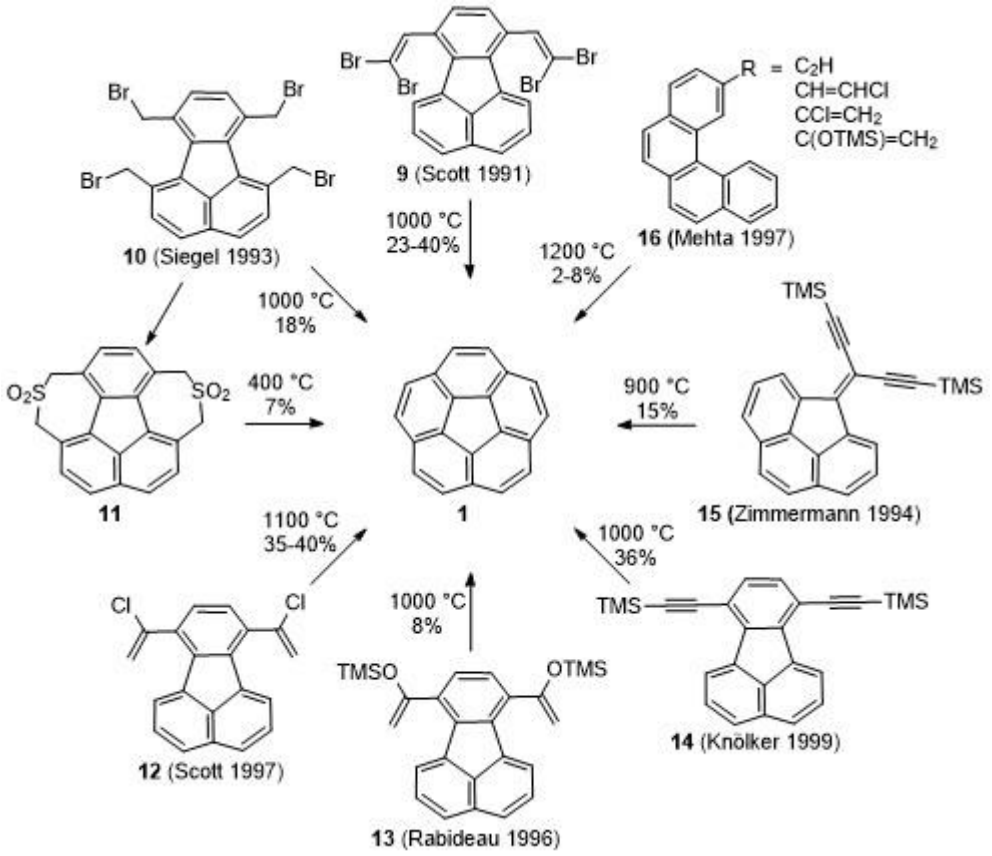

Scheme 1.4. Alternative syntheses of **1** via FVP.

1.2.3. Solution Phase Synthesis of Corannulene

Since the attempts to prepare **1** by formation of the flanking bonds under intramolecular Friedel-Crafts conditions were unsuccessful, [12–14] new restrosynthetic approach based on the disconnection of the rim bonds was proposed.

The first solution phase synthesis of a corannulene derivative **21** was reported by Siegel in 1996. [23] The key step of this synthetic approach is the reductive coupling reaction of the brominated fluoranthene derivatives (**20**) with low-valent titanium followed by hydrogenation (Scheme 1.5).

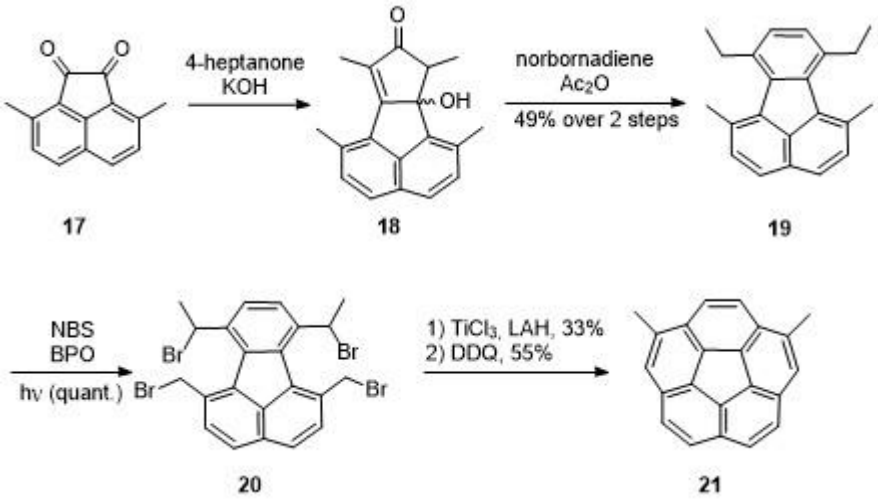

Scheme 1.5. First solution phase synthesis of a corannulene derivative.

A slightly modified pathway was applied for the synthesis of **1** reported by Siegel;[24] the 11 steps synthesis gave an overall yield of 20% starting from the commercial available 2,7-dimethyl acenaphtalene **22**. In the same year Rabideau reported new condition for the reductive coupling based on low-valent vanadium species. [25]

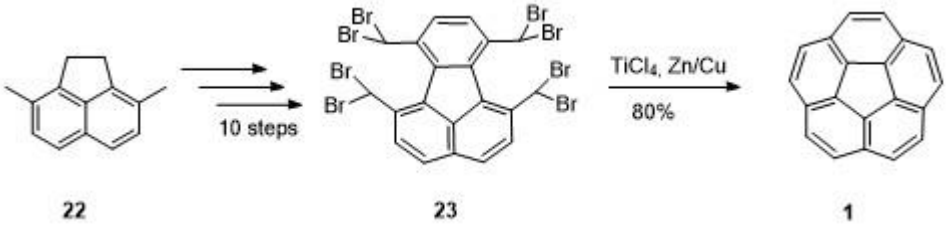

Scheme 1.6. Solution phase synthesis of **1**.

Recently Siegel reported the optimization and scale-up to kilogram production for the synthesis of **1** following an analogous synthetic route. [26]

A disadvantage of the use of low-valent titanium or vanadium in the reductive coupling step is the lack of functional group compatibility. Rabideau suggested a refinement for the reductive coupling based on the use of sodium hydroxide (Scheme 1.7). [27,28]

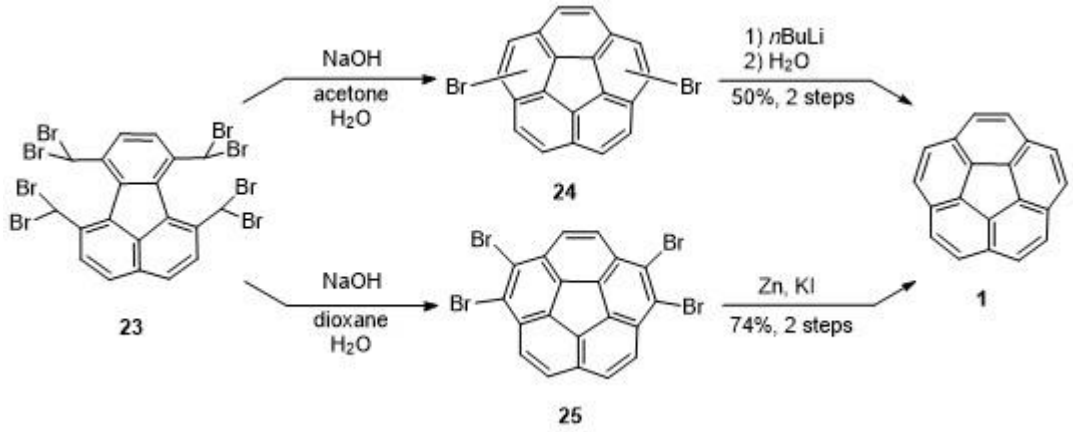

Scheme 1.7. Base-catalyzed synthesis of **1**.

This new approach shows a solvent dependency: when the ring closure is run in water and acetone, a complicated mixture of dibrominated corannulenes is obtained which is then converted to **1** by reaction with *n*-butyl lithium followed by quenching with water. On the other hand, the use of a mixture of dioxane and water as solvent leads to 1,2,7,8-tetrabromocorannulene, which undergoes to reductive debromination affording **1** in better yield.

1.3. Corannulene Derivatives and Their Symmetry

In the following section, a general view on the synthesis of various substituted corannulene derivatives with different symmetry will be discussed. Benzo-fused, [29] indenoannelated [30–32] and other ring-extended system, [10,23,33] as well as metal complexes of **1** will not be covered. As an overview, three different symmetries are possible for substituted corannulenes: C_s, C_5 and C_1.

1.3.1. C_s-Symmetric Corannulene Derivatives

The synthetic route to **1** through 1,6,7,10-tetrasubstituted fluoranthenes retains the bilateral symmetry of the initial disubstituted naphthalene. In general, the synthesis of fluoranthenes by this pathway is based on the retrosynthetic analysis shown in Scheme 1.8.

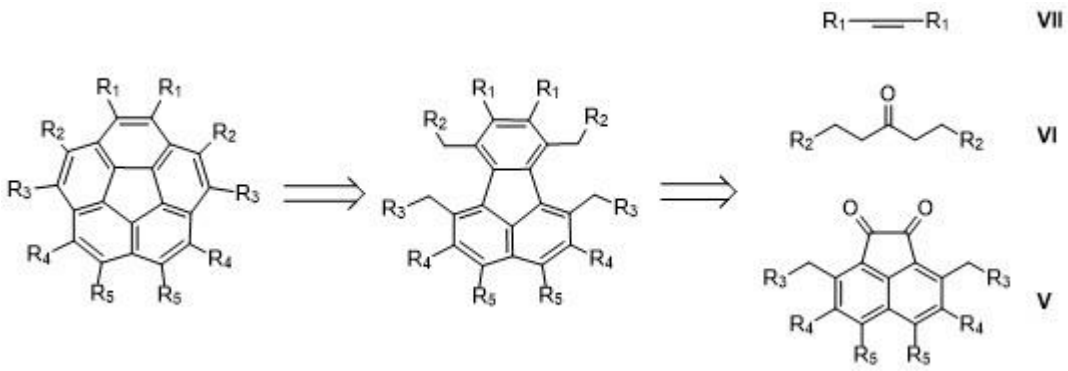

Scheme 1.8. 1,2- and 1,3,4,6-substituted corannulene derivatives.

Following this synthetic route, the desired substituents of the final C_s-symmetric corannulene derivative must be chosen at the level of acenaphthenequionone **V**, dialkylketone **VI** and disubstituted dienophile **VII**. Depending on the particular location of the desired substituents and their position on corannulene, changes in the synthetic strategy are required.

By following this strategy, a number C_s-symmetric of di- and tetrasubstituted corannulene have been synthesized (Figure 1.5).

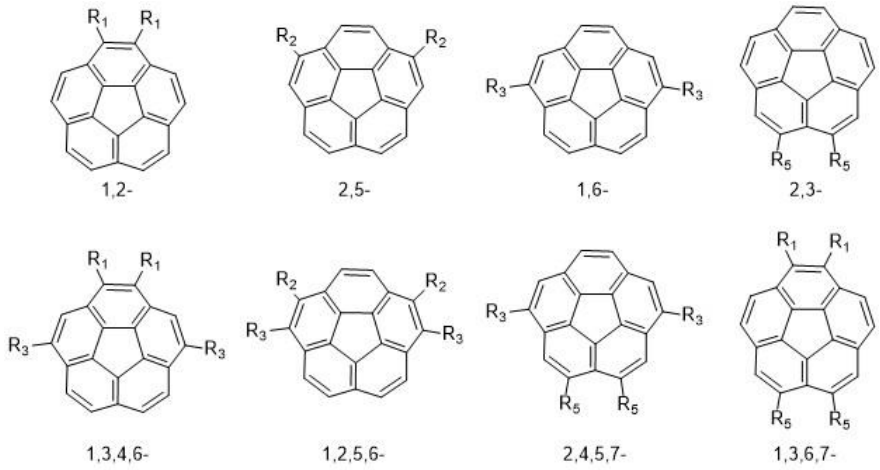

Figure 1.5. C_s-symmetric di- and tetrasubstituted corannulenes.

1,2-Disubstituted corannulenes can be readily accessed as reported by Rabideau. [34] The Ni-mediated ring closing method [28,35] was applied to brominated fluoranthene diester **26** and the dicarboxylated corannulene **27** was obtained in good yield. The authors suggest that the formation of intermediate tetrahydrocorannulene **28**, which has not been observed probably due to the facile double elimination of HBr.

Although accompanied by hydrolysis of the esters, the base mediated ring closing method delivers the hydrolyzed 1,6-dibromo derivative **29** in low yield (Scheme 1.9).

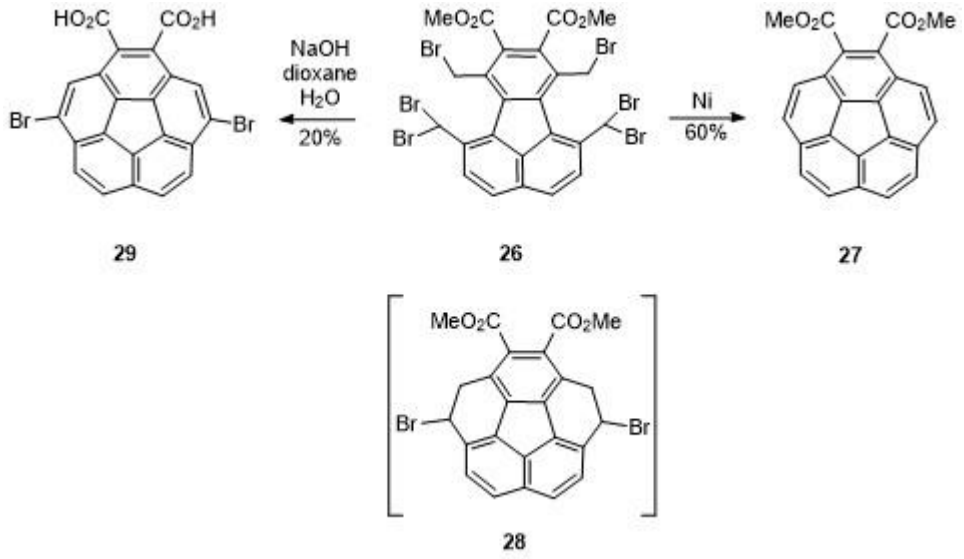

Scheme 1.9. General disconnection for the synthesis of C_s-symmetric corannulene derivatives.

Siegel was the first to publish the preparation of alkyl substituted corannulenes starting from adequately presubstituted fluoranthene derivatives. [23,24] The synthesis of 2,5-disubstituted corannulene **21** from tetrabromide **20** was achieved by low-valent metal reductive coupling (Scheme 1.5). When the base-mediated ring closing condition in dioxane/water is applied to hexabromide **30**, the dialkyl dibromo corannulene **31** is obtained directly in over 60% yield. [36,37] Compound **31** can then be hydrodehalodenated [38] to disubstituted compound **21** (Scheme 1.10). The same procedure can be followed for the synthesis 1,6-disubstituted corannulene [24] **32** and its 2,5-dibrominated analog **33**.

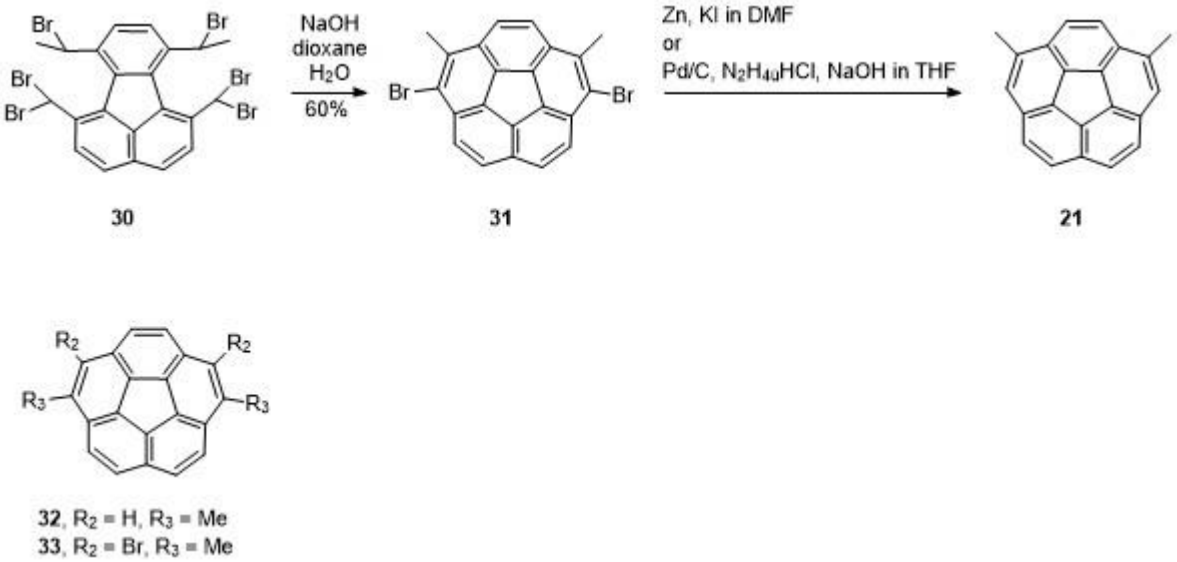

Scheme 1.10. 1,2 and 1,2,5,6-substituted corannulene derivatives.

For the introduction of R_5 substituents needed for the 2,5-disubstituted corannulenes (Figure 1.5), the synthesis of the acenaphthenequinone moiety must be modified. Starting from acenaphthene **3**, chlorination leads to peri-substituted 5,6-dichloroacenaphtene **34**. [39] Further bromination delivers 5,6-dichloro-3,8-dibromoacenaphthene **35**, which is then oxidized to acenaphthenequinone **36** (Scheme 1.11). The preparations of the corresponding fluoranthene **37** and corannulene derivative **38** are analog to the cases explained above.

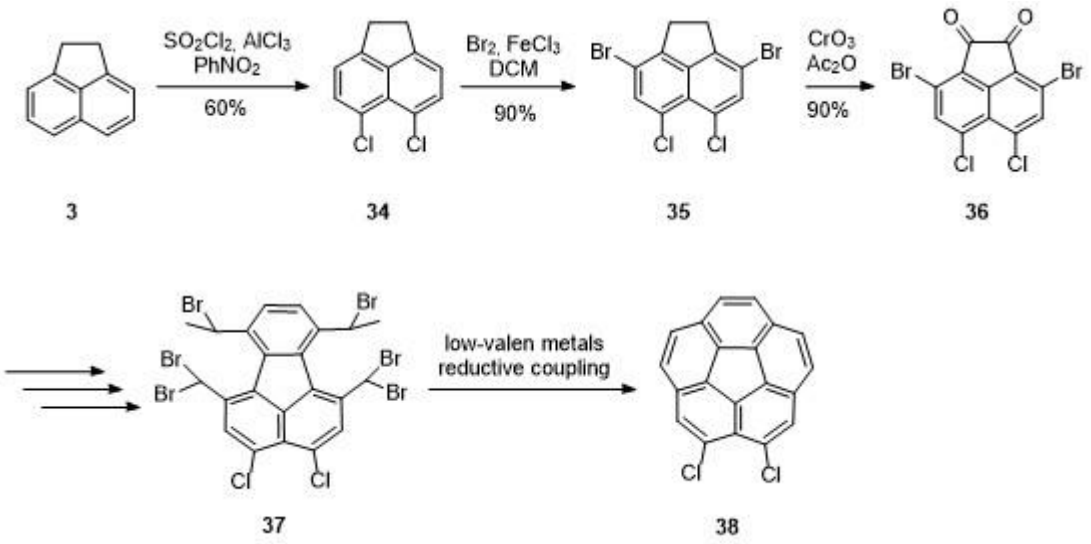

Scheme 1.11. Synthetic route to 2,3-dichlorocorannulene **38**.

C_s-symmetric tetrasubstituted corannulene derivatives have almost all been obtained by a combination of the methods described above; depending on the functional groups present, one of the several ring closing methods was chosen.

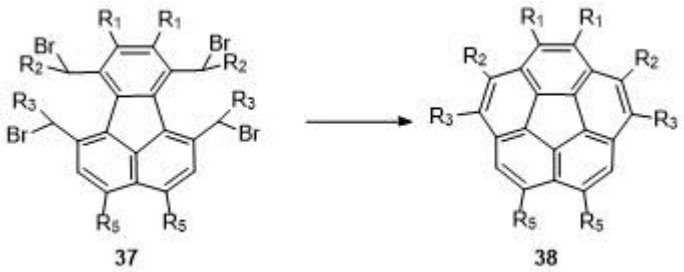

Scheme 1.12. General synthesis of C_s-symmetric tetrasubstituted corannulene derivatives.

1.3.2. C_5-Symmetric Corannulene Derivatives

While the synthesis of C_s-symmetric corannulenes is generally accomplished by starting from the corresponding fluoranthene precursor that already possess the desired carbon skeleton for the final corannulene derivatives, the synthesis of C_5-symmetric penta- and deca-substituted corannulene derivatives starts from corannulene (Scheme 1.13).

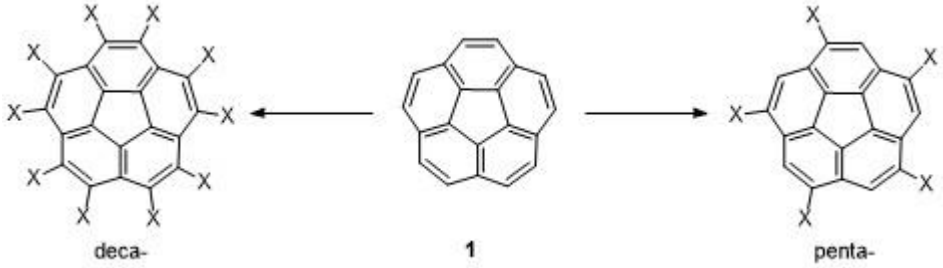

Scheme 1.13. C_5-symmetric penta- and decasubstituted corannulene derivatives.

Five-fold symmetric pentasubstituted corannulene derivatives are synthesized from **1** by controlled pentachlorination [40,41] to *sym*-pentachlorocoranulene [a] **39** or by direct electrophilic aromatic substitution with bulky groups under Friedel-Crafts conditions. [8] Reaction with sterically less demanding alkyl- or acyl groups, as well as bromination, gives multiple isomers with different degrees of substitution.

[a] *Sym*- here means 1,3,5,7,9-pentasubstitution.

Recently Scott [42] reported the synthesis of *sym*-pentakis[(pinacolato)boryl]corannulene (**40**) by direct Ir-catalyzed borylation of **1**.

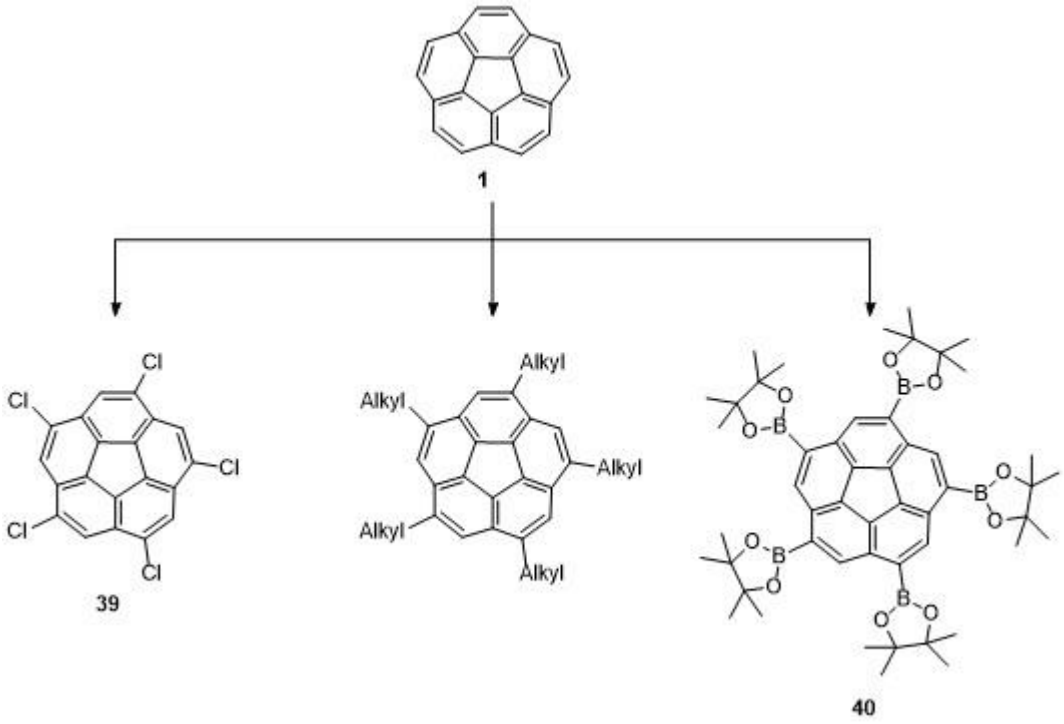

Scheme 1.14. C_5-symmetric penta-substituted corannulene derivatives.

Sym-pentachloro corannulene **39** is synthesized from **1** by reaction with iodine monochloride with surprising high selectivity. Furthermore, due to the polarization of the I-Cl bond towards the more electronegative chlorine atom, iodination instead of chlorination would be expected. The proposed mechanism for the chlorination suggests a first addition of iodine to the hub bond of **1**, followed by the attack of chloride to the rim. The corannulene system is then restored by rearomatization by HI elimination. Repetition of these steps eventually leads to **39** in about 50% yield along with small amounts of under- and over-chlorinated corannulenes as side products (mainly tetra- and hexa-chlorinated). [40] The formation of under-substituted side products is also observed for the synthesis of compound **40**. However, the higher solubility of these molecules allows an easy isolation of the desired *sym*-pentaborylated corannulene.

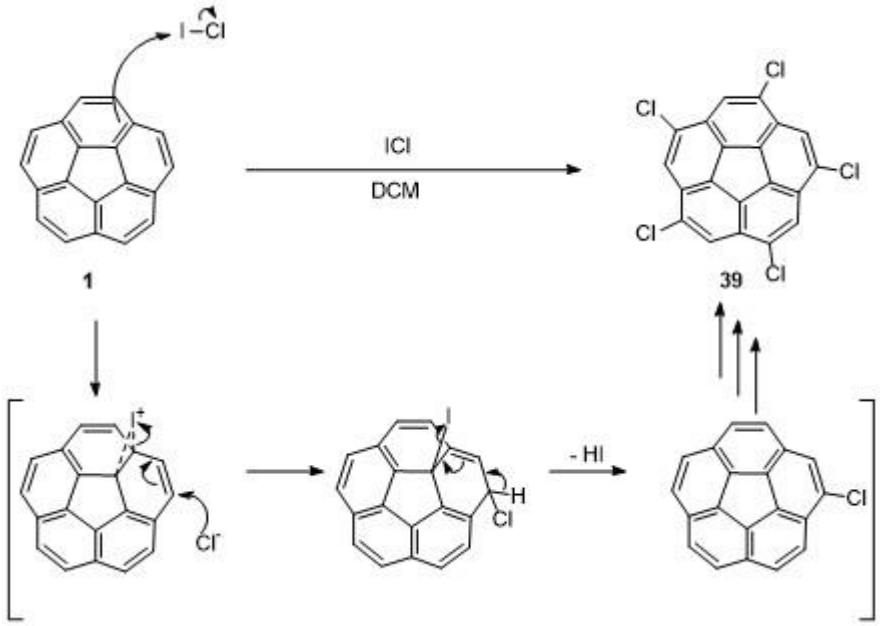

Scheme 1.15. Proposed chlorination mechanism of **1** with ICl.

The proposed chlorination mechanism is strongly supported by the addition of the dichlorocarbenium ion $CDCl_2^+$ to the one of the hub carbon atoms of **1**. [43]

Sym-pentachloro corannulene **39** is the common starting point for the five-fold derivatization of the corannulene core, but it is far from to be an ideal synthetic intermediate. **39** is sparingly soluble in common organic solvents, even at high temperatures, making it difficult to manipulate at reasonable concentrations. However, as the coupling advances, the solubility of the respective intermediates usually gradually increase, accelerating further the coupling reaction. Furthermore, aryl chlorides are generally less reactive in transition-metal catalyzed cross-coupling reaction than aryl bromides or iodides and, since the pentasubstitution, the catalytic cycle has to be completed five times per molecule, demanding high reaction yield per site. Moreover, due to the difficulties of isolation of **39**, the under- and over-chlorinated corannulenes present lead to a mixture of isomers of tetra- and hexasubstituted byproducts.

Although all the issues described, several synthetic procedures for the preparation of C_5-symmetric pentasubstituted corannulene derivatives starting from **39** have been developed. *Sym*-pentaalkylcorannulenes **41** have been synthesized by 1,3-bis(diphenylphosphino) nickel (II) chloride catalyzed alkylation of **39** with trialkylaluminiums (*i.e.* $Al(CH_3)_3$, $Al(C_2H_5)_3$, $Al(C_8H_{17})_3$) in between 30 and 50% yield (Scheme 1.16). [24,44] In the synthesis of *sym*-pentaarylated corannulenes **42**, Zn-based Negishi-type coupling conditions were employed using $Ni(dppp)Cl_2$. [45] The catalyst system with $Pd(OAc)_2$ or $Pd_2(dba)_3$ and Nolan's N-heterocyclic carbene (NHC) ligand

1,3-bis(2,6-diisopropylphenyl)imidazoliumchloride) (IPr·HCl), [46] or alternatively (IPr)Pd(allyl)-complex could be used as well. [47] The thermal more stable NHC ligands proved to be successful in the coupling of sterically hindered aryl zincates (*i.e.* manisyl), and yields could be improved from 7 to 18–35%. The yields for unhindered coupling partners range from about 30–50%. Buchwald's system for the coupling of amines to arylchloride, RuPhos palladium (II) phenethylamine chloride, [48] was recently used by Scott and coworkers to give *sym*-pentakis(2,6-dichlorophenyl)corannulene in more than 50% yield. [49] Suzuki-type chemistry was also successful using Nolan's NHC ligand. [31] Improved conditions with Pd-catalyst, bearing Fu's bulky phosphine ligand tri(*tert*-butyl)phosphine, [50,51] which tolerates boronic acids with a variety of functional groups were claimed by Keinan and coworkers to deliver the *sym*-pentaarylated corannulene derivatives in 59-83% yield (Scheme 1.16). [52]

The introduction of five *sp* carbons to form *sym*-pentaethynyl corannulene **43** has been solved in several different approaches. Scott and coworkers report a Kumada-type coupling with trimethylsilylethynyl magnesium bromide catalyzed by $Ni(acac)_2$. [40] Indipendently, the Siegel group also reported a protocol developed by Eberhard group, [53] in which the trimethylsilyl acetylene is used in large excess with the pincer catalyst and zinc dichloride to give *sym*-pentakis(trimethylsilylacetylene)corannulene in 53% yield. [45] An important improvement in the introduction of five acetylenes onto corannulene core has been recently reported by Wu and coworkers utilizing a Stille-kind coupling. [37] Stannanes of the corresponding acetylenes were employed with Nolan's NHC ligand, and yields between 70-95% could be reached for a variety of acetylenes. [37]

Finally the chlorine atoms allow nucleophilic aromatic substitution with strong nucleophiles. Aromatic and aliphatic thiolates have been introduced onto corannulene by the Scott [54] and Siegel [45] groups giving the corresponding corannulene thioethers **44** in 35-55% yield. Displacement of chlorines by thiolates occurrs at ambient temperature or at 120 °C in the polar solvent 1,3-dimethylimidazolin-2-one (DMEU), whereas the synthesis of aryl ethers (**45**) requires more elevated temperature of 180 °C. Alternatively, Keinan and coworkers described a copper-catalyzed Ullmann condensation whith a variety of phenols. [55] Yields for coupling of sterically unhindered and electron rich phenols range from 75-85%, whereas hindered and electron deficient substrates gave between 17-50% of the corannulene ethers **45**.

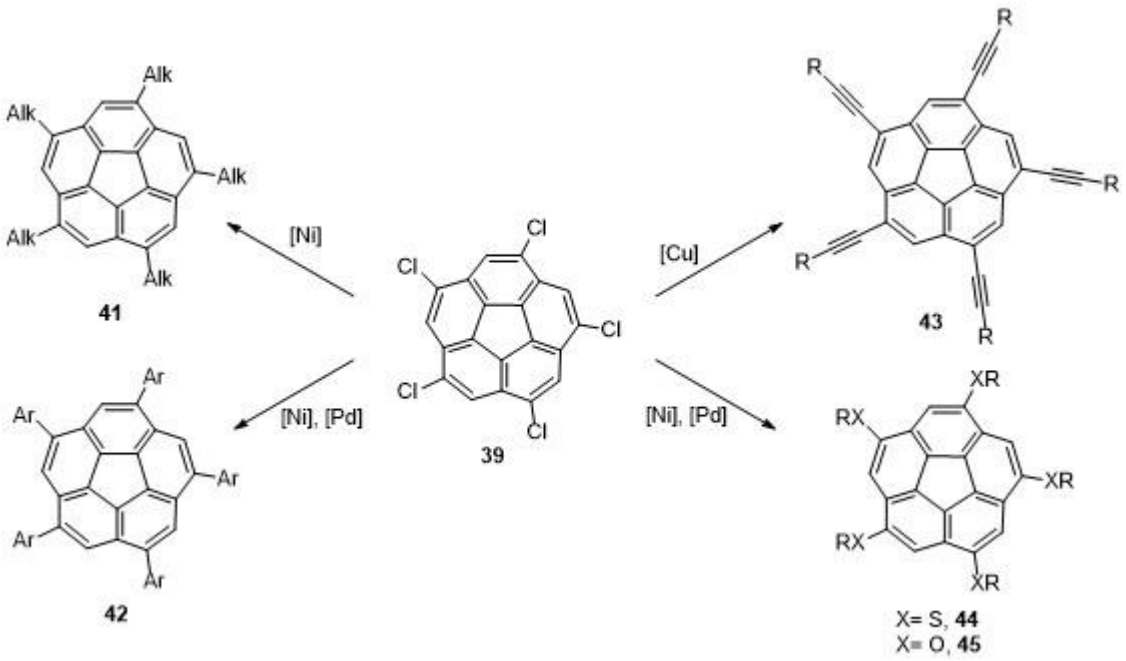

Scheme 1.16. Synthesis of *sym*-pentasubstituted corannulene derivatives.

The synthetic intermediate for the preparation of decasubstituted corannulene is decachlorocorannulene **46**. [40,54,56] Corannulene undergoes to perchlorination under Ballester conditions, [57] which delivers an overhalogenated tetrahydro intermediate **47**. Refluxing in high boiling ether extrudes four chlorines yielding **46** (Scheme 1.17).

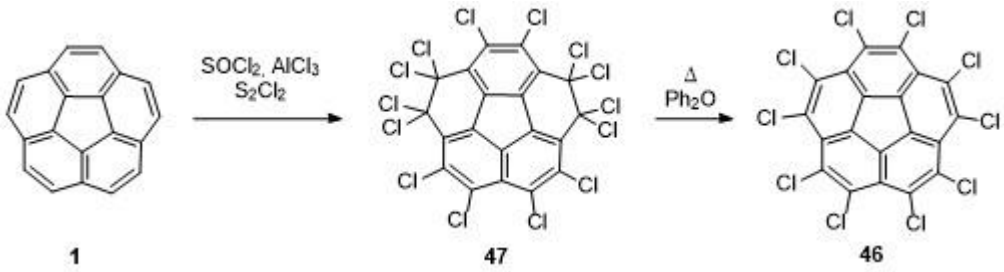

Scheme 1.17. Synthetic route to decachlorocorannulene.

Conversion of **46** to other decasubstituted corannulene derivatives is achieved by Pd-catalyzed reation with stannylalkyne and the NHC ligand IPr·HCl; under these reaction conditions delivered decaethynylated corannulenes are prepared in about 10% yield (80% yield for each reaction site). [58] Furthermore, the addition of a variety of thioethers has been reported. [40,45,54,56,59]

Recently Keinan [60] reported the synthesis of a C_5-symmetric deca-heterosubstituted corannulene derivative starting from *sym*-pentachlorocorannulene **39** by Ullmann condensation and further electrophilic aromatic substitution to produce 1,3,5,7,9-pentaX-2,4,5,8,10-pentaY-corannulene derivatives (Scheme 1.18).

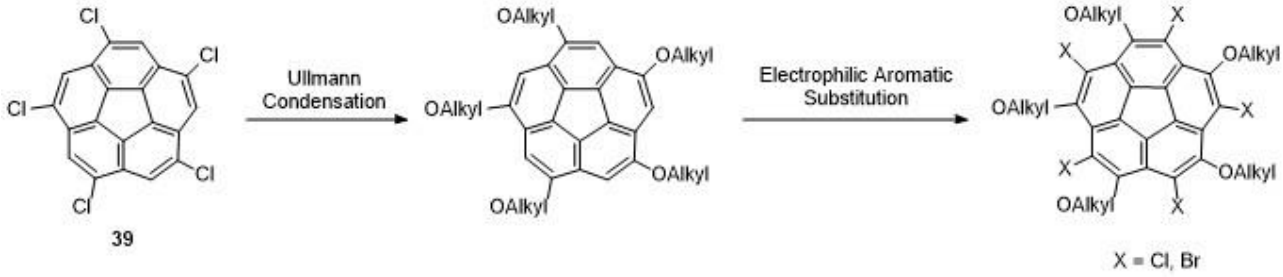

Scheme 1.18. Synthesis of C_5-symmetric deca-heterosubstituted corannulene derivatives.

1.3.3. C_1-SYMMETRIC MONOSUBSTITUTED CORANNULENE DERIVATIVES

As seen previously for the synthesis of decachlorocorannulene **46**, **1** undergoes to electrophilic aromatic substitution with several electrophiles. Although formylation, bromination, acylation and nitration have been previously reported, [45] experimental details are only available for the bromination [61] and nitration. Nitrocorannulene **48** has been synthesized by reaction of **1** with nitronium terafluoroborate on excellent yield. [62]

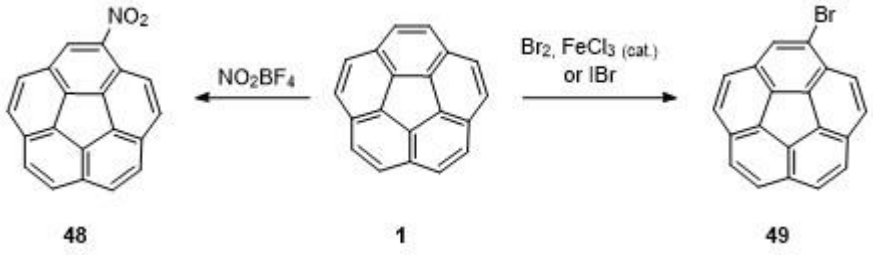

Scheme 1.19. Synthesis of C_1-symmetric monosubstituted corannulene derivatives.

2. Synthesis of Five-fold Symmetric Pentabioconjugated Corannulene Derivatives

Five-fold symmetry is quite abundant in flowers, fruits and molecules, although somewhat less frequent than other symmetry *e.g.* six-fold symmetry. [63] At the molecular scale, five-fold symmetry is common in metal complexes [64] and in biomolecules such as proteins [65] and DNA-based nanostructures. [66–68] However, C_5-symmetrical organic molecules can be considered quite rare. Only a few pentameric examples allow substitution of the periphery, and most of them consist of conformally flexible macrocycles, such as pentapeptides **50**, [69] crown ethers and aza-crown ethers **51**. [70,71] Structurally more rigid examples are calix[5]arene **52**, [72] calix[5]furans and -pyrroles, [73] cucurbit[5]urils [74] and pillar[5]arenes **53**. [75] A recently reported pentaamidic structure [76] folds into an almost planar disk arrangement with nearly C_5-symmetry due to an interior H-bonded network.

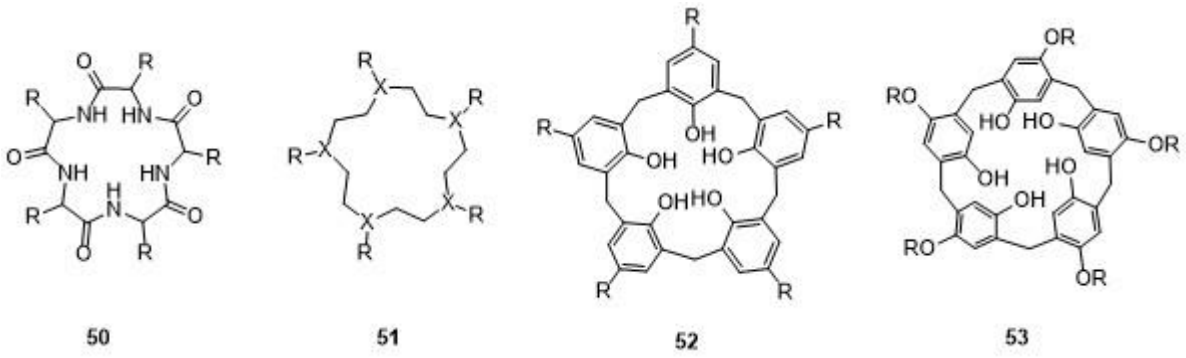

Scheme 2.1. Selected pentameric structures.

More generally, five-fold symmetrical molecules can serve as scaffolds for extended supramolecular structures that might found application in material science, biology and pharmacology.

2.1. Aim of the Current Work

C_5-symmetric pentasubstituted corannulene derivatives represent a new class of five-fold symmetric scaffold. With the advent of the kilogram scale synthesis of corannulene **1**, [26] and a robust procedure for converting it into 1,3,5,7,9-pentachloro corannulene **39**, [40,41] came the motivation to improve the general knowledge on the reactivity of **39** and to develop a robust

synthetic procedure that would make accessible a broad spectrum of C_5-symmetric pentasubstituted corannulene derivatives suitable for incorporation into polymers, [77] materials, [78] bioconjugated [79] and supramolecular architectures. [80]

The purpose of this thesis is the development of a synthetic route for the preparation of five-fold symmetric bioconjugated corannulene derivatives functionalizated with the main classes of biomolecules *i.e.* carbohydrates, lipids, peptides and nucleic acids. This new family of compounds based on corannulene would open the door to the study of high-order multivalent ligands, [47,81–83], corannulene-based material, template for protein folding mimics [84] or aromatic/nucleic acid conjugate assemblies, respectively (Scheme 2.2). [68,85,86]

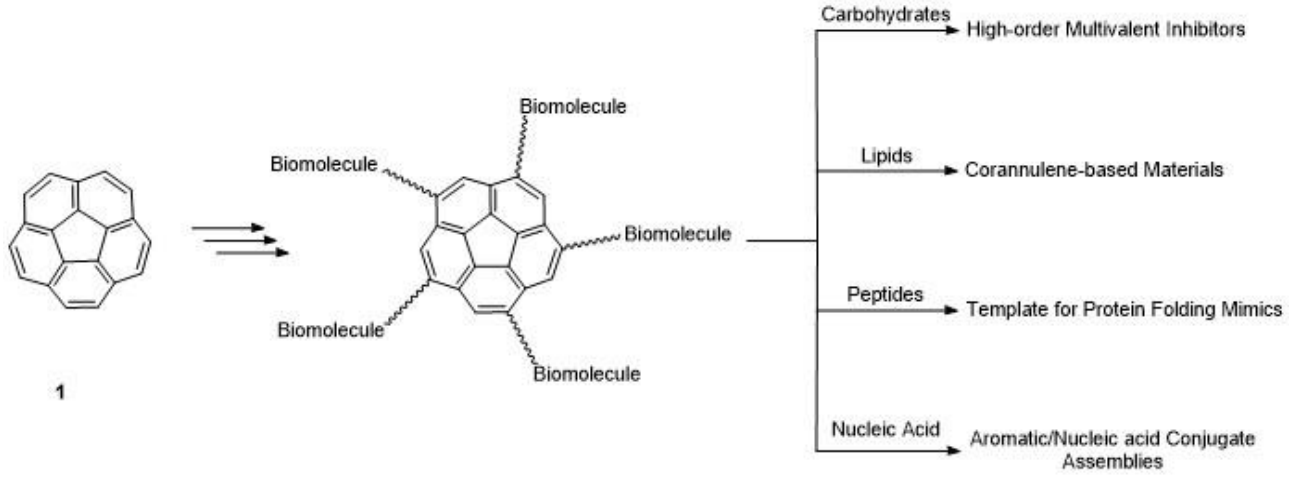

Scheme 2.2. Possible applications of C_5-symmetric corannulene derivatives.

The research focus will be addressed to:

1. develop an efficient synthetic route to access to five-fold symmetric corannulene derivatives bearing a broad spectrum of functional groups;
2. develop an efficient procedure for the introduction of biomolecules onto corannulene core.
3. investigate the material, supramolecular and biological properties of C_5-symmetric bioconjugated corannulene derivatives.

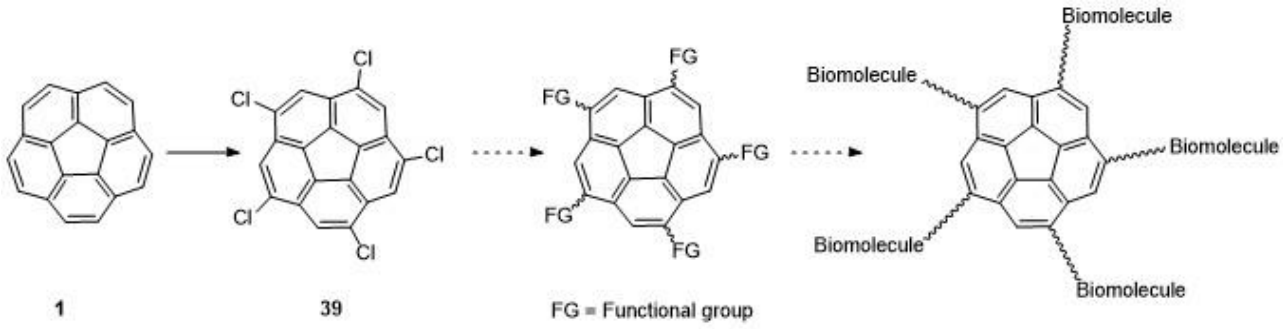

Scheme 2.3. Proposed schematics synthetic pathway for the preparation of *sym*-pentabioconjugated corannulene derivatives.

3. SYNTHESIS OF ω-FUNCTIONALIZED C_5-SYMMETRIC PENTASUBSTITUTED CORANNUELENE DERIVATIVES

3.1. INTRODUCTION

The first hurdle for the synthesis of C_5-symmetric pentabioconjugated corannulene derivative is to access to a wide class of synthetic corannulene derivatives with a broad spectrum of functional groups with orthogonal reactivity. The synthetic route for the preparation of this family of compounds needs to tolerate the presence or the introduction of functional groups or their synthetic equivalents. Having access to several terminal functionalized corannulenes, would makes these compounds especially suitable for developing tectons for supramolecular chemistry, building blocks for dendrimer chemistry, cores for multivalent bioconjugate chemistry or active elements for liquid crystal and optoelectronic materials.

In 2009, Keinan reported the synthesis of a variety of *sym*-pentaaryl corannulene derivatives bearing different functional groups that might be a good starting point for the synthesis of bioconjugated pentapods (Scheme 3.1). [52] These compounds have been prepared starting from **39** and the appropriate arylboronic acids using Fu's bulky phosphine ligand, tri(*tert*-butyl)phopshine [50,51,87] and, if necessary, further deprotection.

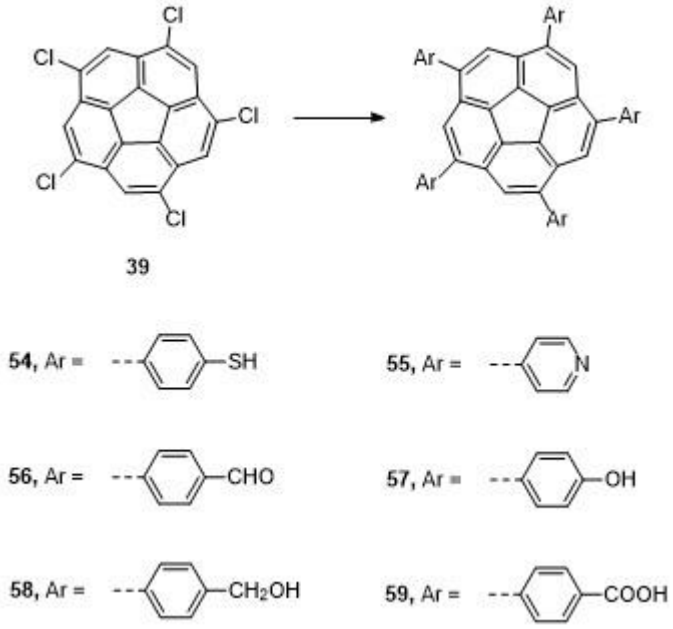

Scheme 3.1. *Sym*-pentaaryl corannulene derivatives bearing different functional groups.

Unfortunately, these compounds display low solubility in common organic solvents, [52] most probably due to the rigidity of the molecule. Solubility issue limitates the reactions conditions that can be tested for the synthesis of five-fold symmetric pentapods based on corannulene. In order to overcome the low solubility issue, it was planned to prepare an array of five-fold substituted corannulene derivatives in which the aromatic linker between corannulene and the functional group will be replaced with more flexible alkyl chains.

At first, the introduction of functionalized alkyl chains was tested by Ni(II)-catalyzed cross-coupling following the condition reported for the synthesis of **41**. [45] Unfortunately, the cross-coupling reaction between **39** and 2-(1,3-dioxolan-2-yl)ethyl magnesium bromide under Kumada's condition (Scheme 3.2) led to a complicated mixture of di-, tri-, tetra- and pentasubstituted coupled products, which were detected by HRMS analysis. Since the introduction of functionalized alkyl chains onto corannulene is the first step for the preparation of more complicated pentapods, better cross-coupling reaction conditions for **39** have to be developed in order to increase the reaction yields and purity of the product.

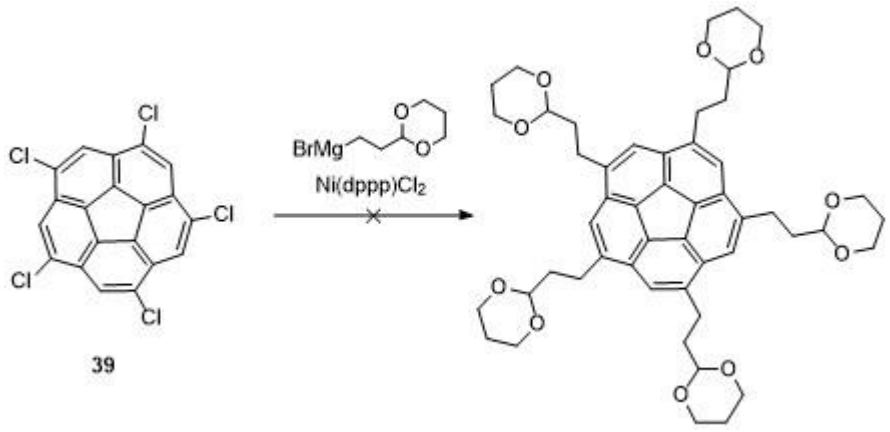

Scheme 3.2. Ni(II)-catalyzed cross-coupling between **39** and 2-(1,3-dioxolan-2-yl)ethyl magnesium bromide.

3.2. IRON-CATALYZED ALKYL-ARYL CROSS-COUPLING REACTION

In 1971, Kochi et al. [88] proposed the use of iron salt as catalyst for coupling reaction of Grignard reagents with alkenyl halides. Although the promising results, the iron-catalyzed methodology remained limited for cross-coupling reaction of Grignard or organomanganese species with alkenyl

halides, [89–91] alkenyl sulfones, [92] acid chlorides or thiolesters [93] and allylic phosphate. [94] An important improvement in this field was given by Cahiez et al., [89,90] which demostrated and recognized the advantages associated with the use of *N*-methyl-2-pyrrolidone (NMP) as cosolvent. [89,90]

Advancements in the field of "inorganic Grignard reagent" by Bogdanovic et al. [95] re-evaluated the iron-catalyzed cross-coupling reaction. It was established that iron(II) chloride reacts with four equivalents of ethyl or higher Grignard to give a new species of formal composition $[Fe(MgX)_2]$, an "inorganic Grignard reagent" (Scheme 3.3). [96]

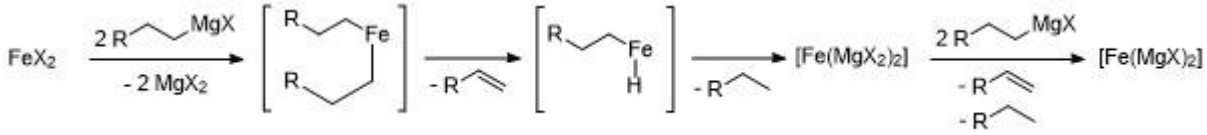

Scheme 3.3. Synthesis of iron "inorganic Grignard reagent".

The rigorously established stoichiometry of this reaction implies that the reduction process does not stop to zerovalent iron species, but leads to species bearing a formally negative charge at iron Fe(-II). Such highly nucleophilic entities lacking of any stabilizing ligands are able to oxidatively add to aryl halides. [96,97] The resulting organometallic iron compounds, formally Fe(0), are again alkylated by the excess of the Grignard reagent present in the medium; subsequent reductive coupling of the organic ligands should then form the desired product and regenerate the propagating Fe(-II) species (Scheme 3.4).

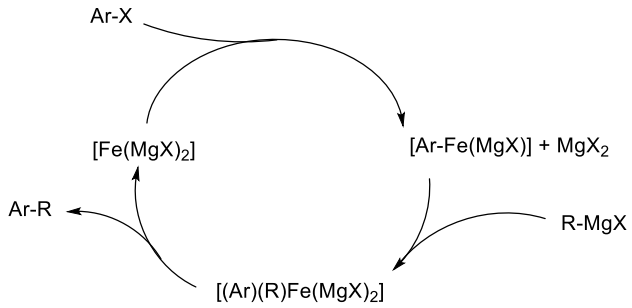

Scheme 3.4. Proposed "low valent iron" catalytic cycle for Fe-catalyzed cross-coupling.

In the past decade, Fürstner research groups reported iron-based procedures for cross-coupling reaction of Grignard compounds with aryl chloride and aryl-pseudohalide (aryl bromides and iodides undergo to reductive dehalogenation). [98–100]

The "low valent iron" catalytic cycle requires the formation *in situ* of the catalytic specie [$Fe(MgX)_2$] which can only be obtain if the alkyl Grignard compound can undergo to β-elimination. However, reactions with methyl- phenyl- and vinyl donors lead to organoferrate complexes which react with activated electrophiles only (Scheme 3.5); in this cases, an "organoferrate manifold" is followed. [101]

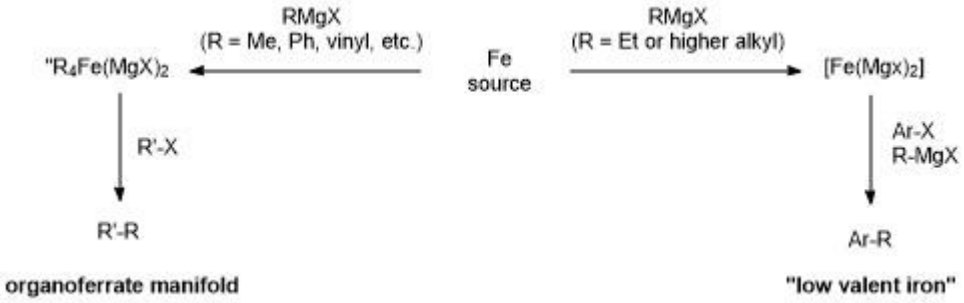

Scheme 3.5. Iron-catalyzed cross-coupling reaction conditions.

3.3. IRON-CATALYZED CROSS-COUPLING REACTION ON *SYM*-PENTACHLORO CORANNULENE

Iron-catalyzed cross-coupling shows several advantages for reactions with aryl chloride than Ni- or Pd-catalyzed coupling: lower temperature, short reaction time, high tolerance to functional groups, higher yield, absence of side reactions (*i.e.* reductive dehalogenation), cheap catalyst and high reactivity on aryl chloride. [98,99] Therefore, Fe-catalyzed procedure is an optimal candidate for further functionalization of **39**.

3.3.1. *SYM*-PENTAALKYL CORANNULENE DERIVATIVES

The synthesis of *sym*-pentaalkyl corannulene derivatives was already achieved by Ni(II)-catalyzed alkylation. *Sym*-pentamethyl- (**60**), [24,44] pentaethyl- (**61**) [45] and pentaoctyl corannulene (**62**) [45] derivatives were synthesized in 33%, 51% and 31% yield, respectively, by reaction of **39** with the correct trialkyl aluminium species in refluxing DME for 24, 16 and 46 hours, respectively (Scheme 3.6).

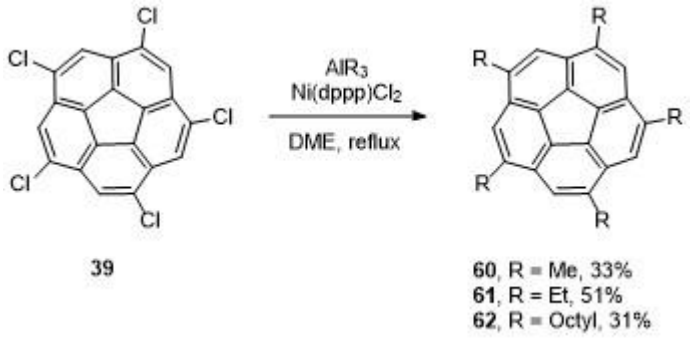

Scheme 3.6. Ni-catalyzed synthesis of *sym*-pentaalkyl corannulene derivatives.

In order to test the iron-catalyzed cross-coupling procedure, the synthesis of compounds **60** and **61** was performed under Fürstner conditions (Scheme 3.7). [102]

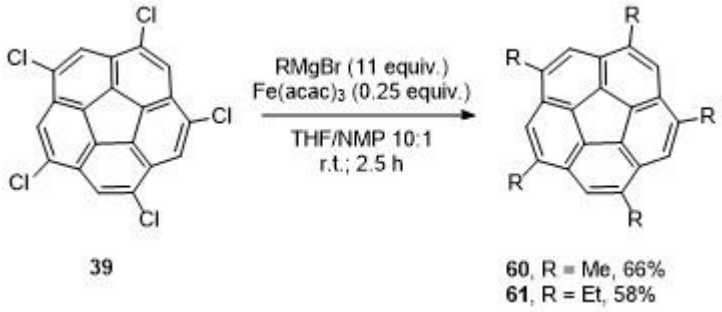

Scheme 3.7. Synthesis of **60** and **61** by Fe-catalyzed reaction.

Both the desired compounds were obtained in good yield and high purity. This new coupling conditions display several advantages compared to the Ni-catalyzed procedure: under Fe-catalyzed conditions the reaction requires shorter reaction times (from days to few hours), it leads to higher yield of the desired product (from 30-50% to 60-70%) and it needs a very cheap precatalyst (*i.e.* iron (III) acetylacetonate). Since both **60** and **61** were obtain, the Fe-catalyzed cross-coupling on **39** works following both the "low valent iron" pathway, in the case of **61**, and the "organoferrate manifold" pathway in the case of **60**, which implying an higher reactivity of **39** compared to normal aryl chlorides.

The promising results gave the motivation to further explore the application and versatility of Fe-catalyzed cross-coupling for the preparation of more complicated five-fold symmetric pentaalkyl corannulene derivatives displaying bulky (1-methyl-adamantyl, **63**) or homochiral (*S*-2-methyl-butyl, **64**) moieties (Scheme 3.8). [102]

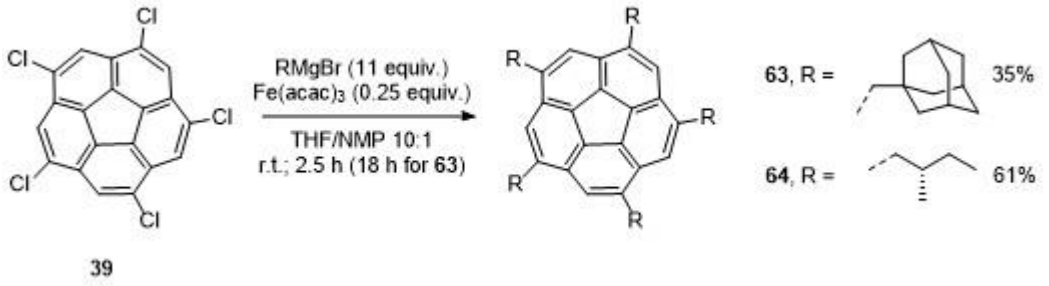

Scheme 3.8. Synthesis of **63** and **64** by Fe-catalyzed reaction.

While the preparation of **64** gave similar results of the previous Fe-catalyzed reaction on **39**, compound **63** was obtained in lower yield and the reaction requires longer reaction time to reach full conversion of **39**. The presence of the tetra-substituted product in the reaction mixture gave an hint for the explanation of the low yield obtain for **63**: the bulky nature of adamantane might increases the energy of the transition state of the cross-coupling reaction decreasing the rate of the reaction; this makes the reductive dehalogenation pathway a competitive reaction. This explains the long reaction time, the low yield and the presence of the tetrasubstituted corannulene as side product of the coupling.

3.3.2. *SYM*-PENTAALKENYL AND PENTAALKYNE CORANNULENE DERIVATIVES

The results obtained using the Fe-catalyzed procedure for the functionalization of **39** with alkyl chain gave motivation for the application of this promising reaction for the synthesis of corannulene derivatives bearing terminal alkene and terminal protected alkynes group. The preparation of *sym*-penta-(1-buten-4-yl)-corannulene **65** and *sym*-penta-(1-(trimethylsilyl)-1-butyn-4-yl)-corannulene **66** was achieved by Fe-catalyzed cross-coupling on **39** (Scheme 3.9). [102]

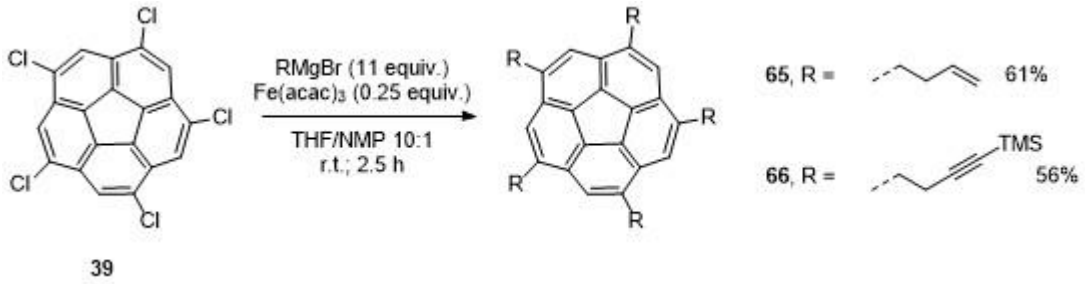

Scheme 3.9. Synthesis of **65** and **66** by Fe-catalyzed reaction.

The terminal acetylene corannulene derivative **67** was obtained in high yield and purity by deprotection of compound **66** under basic conditions (Scheme 3.10). [102]

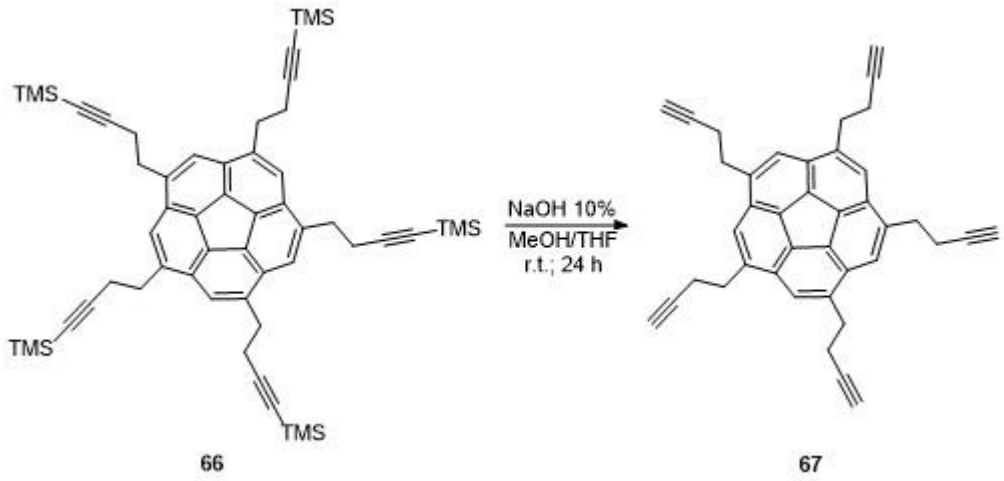

Scheme 3.10. Synthesis of **67** by deprotection of **66**.

Both the desired compounds **65** and **66** were obtained in yield and reaction time comparable to *sym*-pentaalkyl corannulene derivatives; this suggests that the mild conditions of Fe-catalyzed coupling procedure tolerates the presence of double and triple bonds.

Based on the promising results obtained, the synthesis of the first *sym*-pentabioconjugated corannulene derivatives, functionalized with the terpenoid *S*-(+)-citronellyl chain (**68**), was achieved by Fe-catalyzed procedure (Scheme 3.11).

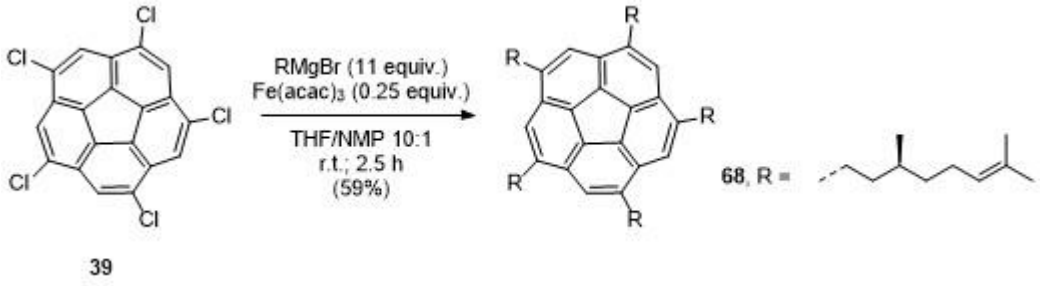

Scheme 3.11. Synthesis of sym-pentaterpenoid corannulene derivative **68** by Fe-catalyzed reaction.

All the compounds described so far show high solubility in common organic solvents.

3.3.3. *SYM*-PENTA-(ω-CARBONYL)- AND PENTA-(ω-CARBOXYL) CORANNULENE DERIVATIVES

The preparation of C_5-symmetric pentasubstituted corannulene derivatives functionalized with alkyl chains bearing carbonyl and carboxyl groups was achieved in two-steps pathway because these functional groups are not stable under Fe-catalyzed condition. The first step of the synthetic route is the introduction of a protected precursor of both carbonyl and carboxyl group on corannulene core. Alkyl acetal has been chosen as protective group since this chemical specie is stable under cross-coupling conditions and it can lead both to carbonyl and carboxyl group by hydrolysis [103] and oxidative deprotection, [104] respectively. The synthesis of five-fold terminal alkyl acetal corannulene **69** was achieved by Fe-catalyzed cross coupling (Scheme 3.12). [102] The key intermediate **69** was obtained in high yield and purity.

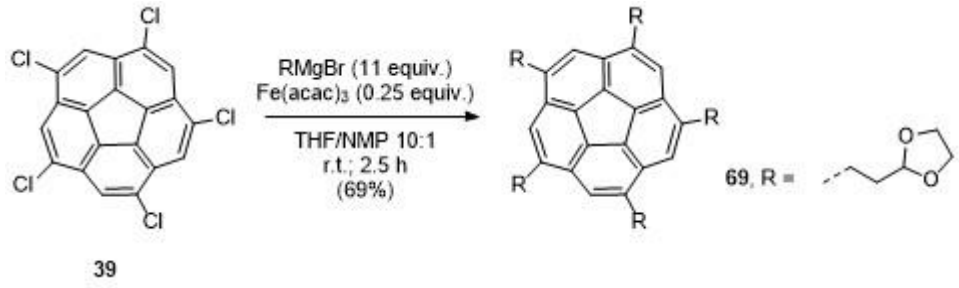

Scheme 3.12. Synthesis of **69** by Fe-catalyzed reaction.

The deprotection of acetal **69** under acidic condition [103] leads to the pentacarbonyl derivative **70** in high yield and purity (Scheme 3.13.) [102]

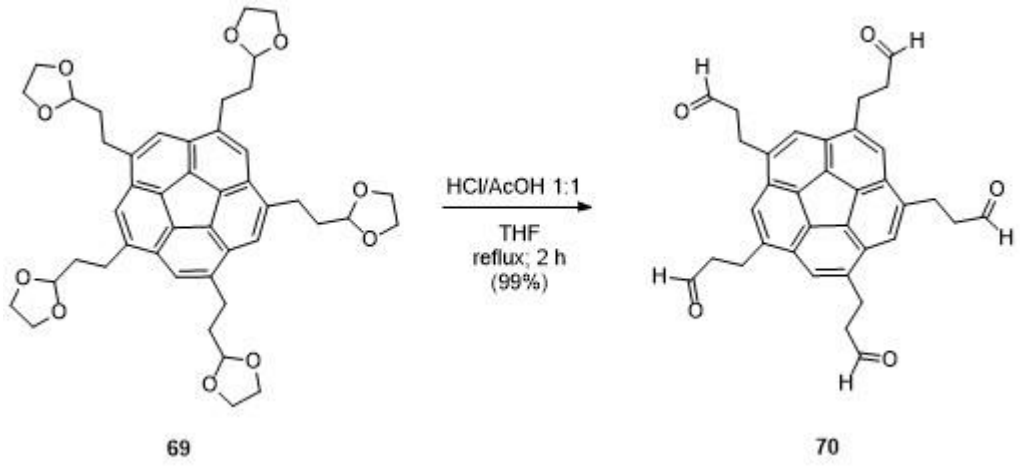

69 70

Scheme 3.13. Acidic deprotection of compound **69**.

The treatment of compound **69** with the mild oxidizer Oxone® (potassium peroxymonosulfate, $KHSO_5$) in THF/water resulted in both deprotection and oxidation of the acetal to directly furnish carboxylic acid **71** (Scheme 3.14). [102]

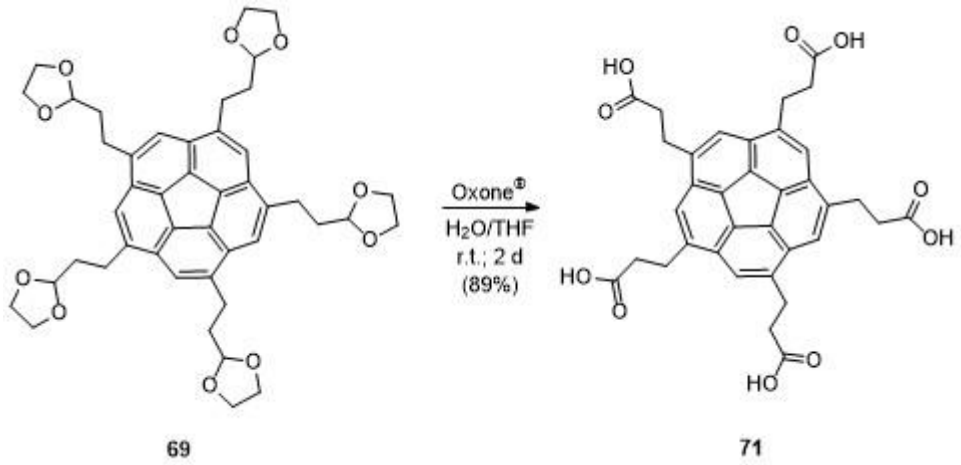

69 71

Scheme 3.14. Oxidative deprotection of compound **69**.

Compound **71** was obtained in high yield and purity. According to this procedure, the acetal group serves as a protective specie for the carboxylic group; since the base-tolerant protection of this group is not easy, the acetal protocol offers a useful method. [104]

The reduction of carbonyl compound **70** to the correspondent alcohol **72** was performed under different reaction conditions (temperature, reducing agent, addition rate of reducing agent, etc.). However, yields higher than 50% were never achieved due tothe formation of byproducts **73** by

dehydroxylation of semi-acetals formed during the course of the reaction. The best result in order of yield of **72** was obtained when a solution of $NaBH_4$ in methanol was added over 24 hours to a ice-cold solution of the carbonyl in methanol (Scheme 3.15).

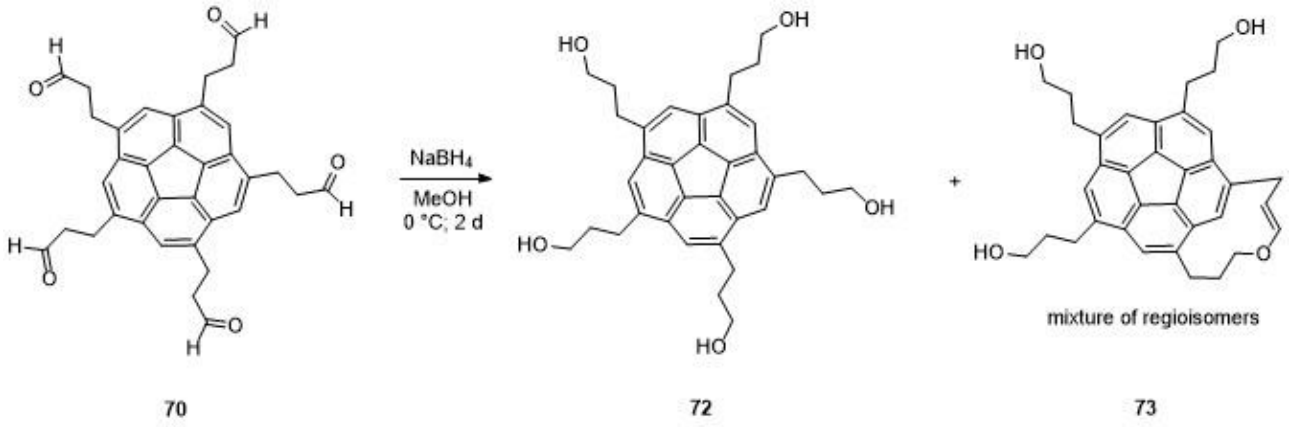

70 72 73

Scheme 3.15. Reduction of compound **70**.

All compounds **70**, **71** and **72** display high solubility in common organic solvents; therefore, as expected, the introduction of alkylic linker between the corannulene core and the functional group increases the solubility of the functionalized corannulene derivatives. In comparison, the analog corannulene derivatives in which these functional groups are connected to corannulene through a benzene ring (Scheme 3.1) are poorly soluble in hot DMSO.

3.3.4. *SYM*-PENTA-(ω-HYDROXY)-, PENTA-(ω-BROMO)- AND PENTA-(ω-THIOL) CORANNULENE DERIVATIVES

The poor yield obtained for the reduction of carbonyl **70** gave the motivation to follow a different synthetic route for the preparation of alcohol **72**. The new strategy is based on the direct introduction of a protected hydroxylic group onto corannulene core; the synthesis of compound **74** was achieved by Fe-catalyzed cross-coupling on **39** in high yield and purity (Scheme 3.16). [102]

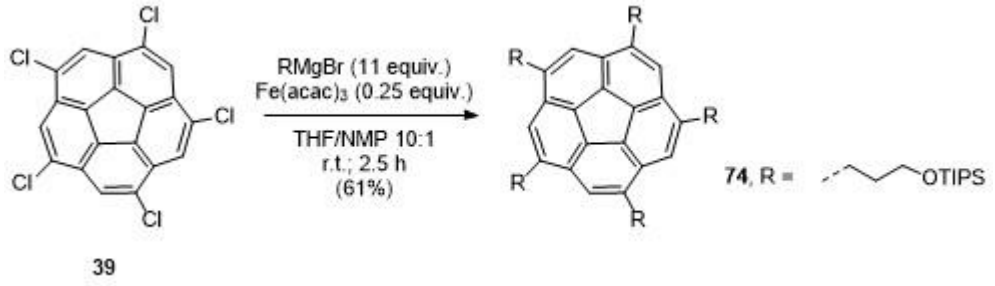

Scheme 3.16. Synthesis of **74** by Fe-catalyzed reaction.

The deprotection of compound **74** (Scheme 3.17) was performed using trifluoroacetic acid in mixture of acetone, water and THF; these conditions are necessary to provide an high nucleophilic medium [105] since common deprotection procedures did not afford product **72** but a mixture of tetra- and penta-desilylated product. [102,103]

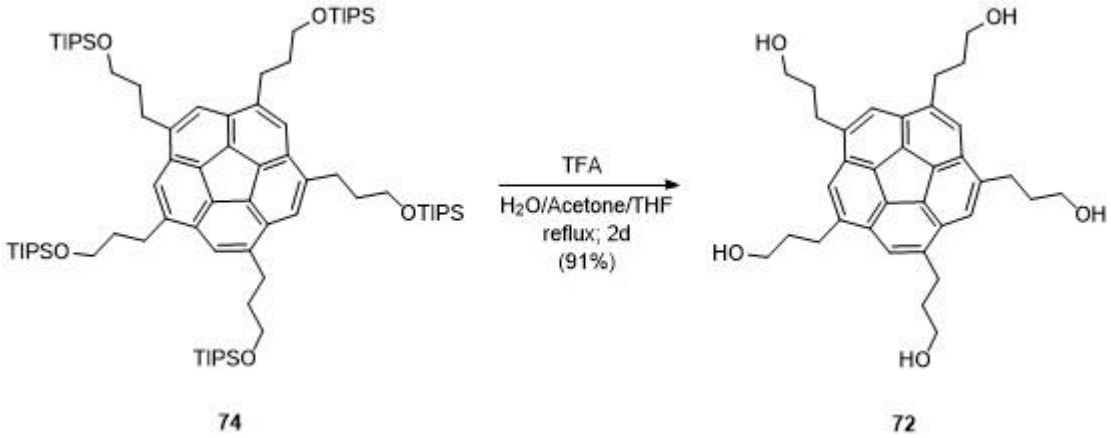

Scheme 3.17. Synthesis of **72** by deprotection of **74**.

By treatment of compound **72** with NBS and triphenylphosphine, five-fold symmetric bromide **75** was obtained in high yield and purity. C_5-symmetric pentaalkylthiol corannulene was prepared in two-steps synthesis by further reaction of compound **75** with thiourea and sequent basic hydrolysis (Scheme 3.18). [102]

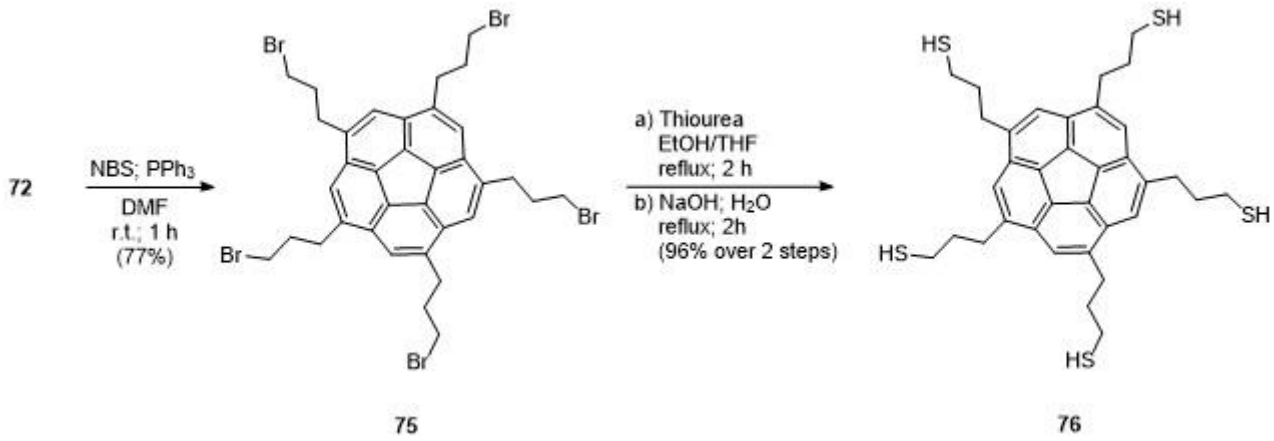

Scheme 3.18. Synthesis of derivative **75** and **76**.

The synthesis of the C_5-symmetric penta-alkylamino corannulene derivative **77** was tried under several conditions. The first strategy involves the reduction of the C_5-symmetric penta-alkylazido corannulene derivative **78** prepared from nucleophilic substitution on bromide **75**. Unfortunately, this synthetic pathway did not lead to the desired pentasubstituted product, but to a complicate mixture of compounds. Mass spectrometry analysis of the crude reveals a distribution of pentasubstituted corannulene derivatives functionalized both with azido and alkene groups; the nature of the byproduct suggests that under these condition, compound **75** undergoes both to nucleophilic substitution with sodium azide and elimination of HBr yielding the respective azido-alkene corannulene derivative. The same strategy has been followed starting the synthesis from an activated form of alcohol **72** (*i.e.* tosylate, mesylate and triflate); however it was not possible to find reaction conditions in which all the five hydroxyl group of compound **72** react.

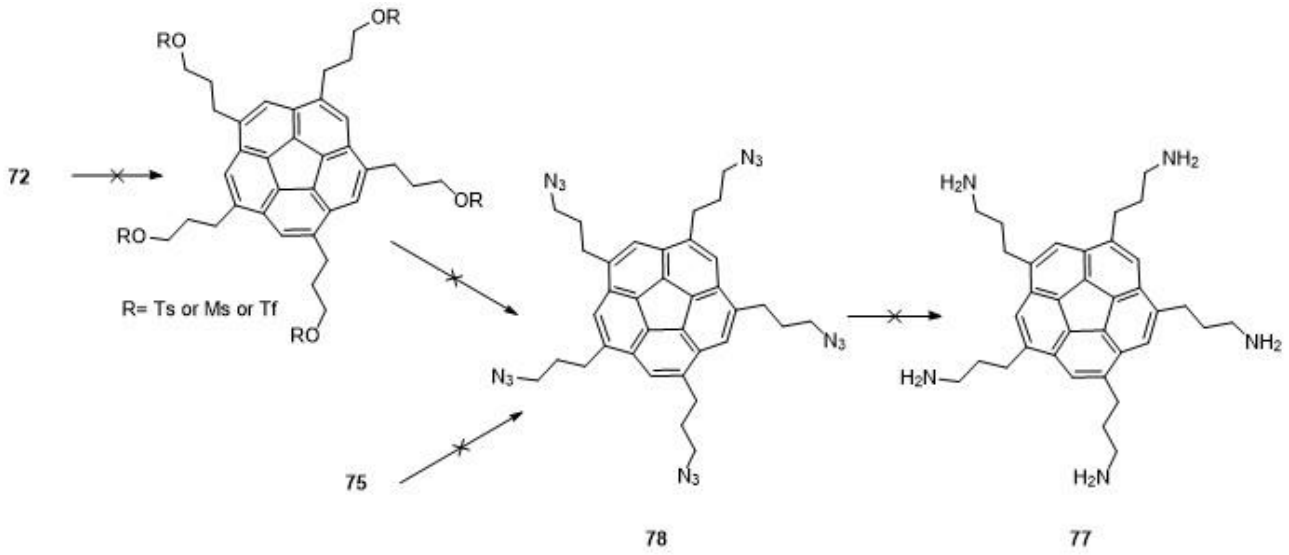

Scheme 3.19. Proposed synthetic strategy for the preparation of compound **77** from bromide **72** or alcohol **75**.

The second synthetic strategies involves the introduction of a protected amino group on corannulene core by Fe-catalyzed procedure. Two protected amino compounds have been selected: 1-(3-bromopropyl)-,2,2,5,5-tetramethyl-1-aza-2,5-disilacyclopentane **79** and 1-(3-bromopropyl)-2,5-dimethylpyrrole **80**.

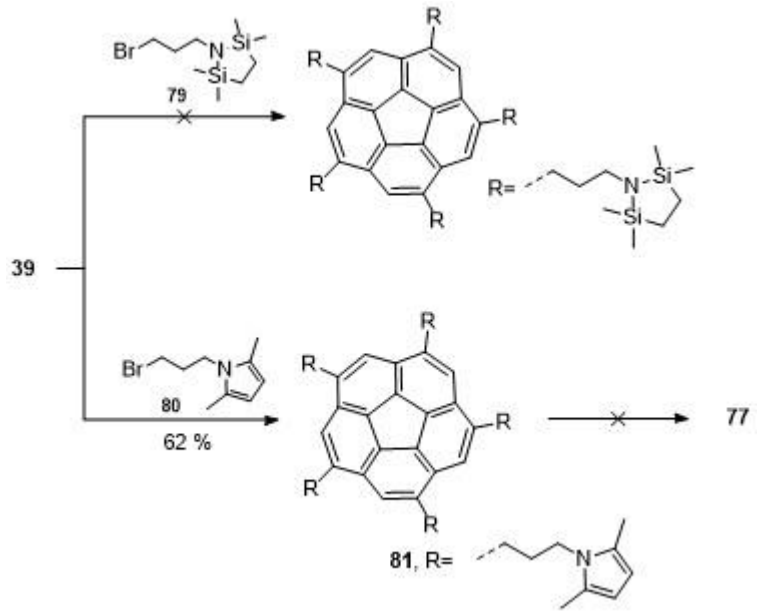

Scheme 3.20. Proposed synthetic strategy for the preparation of compound **77** from **39**.

While the reaction between compound **39** and **79** did not lead to the desired product due to low stability of this protective group, compound **81** was obtained in high yield and purity. [102] However, the deprotection of this corannulene derivative with hydroxylamine did not lead to the desired pentaamino compound **77** but to a complex mixture of product not easily characterizable by NMR and MS analysis.

3.4. PROPERTIES OF ω-FUNCTIONALIZED C_5-SYMMETRIC PENTASUBSTITUTED CORANNUELENE DERIVATIVES

The most of the compounds synthesized by Fe-catalyzed cross-coupling are well soluble in common organic solvents (THF, DCM, MeOH, etc.); the only exception is compound **76**, which shows good solubility only in strong polar organic solvents like DMF and DMSO.

The five-fold symmetric corannulene derivatives **63**–**72**, **74**–**76** and **81** show a small red shift of the π-π* absorption band in the UV-vis spectra compared to corannulene (**1**) (Table 3.1). [102]

Compound	Absorption λ_{max}	Emission λ_{max}	Compound	Absorption λ_{max}	Emission λ_{max}
1[24]	251, 286	421	**60**[24]	260, 295	431
61[45]	263, 297	431	**63**	263, 301	438
64	261, 299	438	**65**	261, 298	436
66	262, 299	438	**67**	262, 299	435
68	264, 300	437	**69**	263, 298	433
70	261, 298	438	**71**	263, 298	433
72	261, 298	435	**74**	263, 298	439
75	261, 299	438	**76**	263, 301	438
81	262, 299	519			

Table 3.1. Absorption and emission measurements of corannulene derivatives in THF (in DMSO for **76**), wavelengths in nm.

The red shift follows what expected by Woodward-Fieser rules for UV absorption in substituted aromatic system. [106] Otherwise, the absorption profiles of these corannulene derivatives are relatively constant within the error of band shape and position. The data collected show that the

derivatives bearing functionalized alkyl chains have similar absorption behavior to those with unfunctionalized alkyl chains. Also the emission spectra show no serious differences in the properties of functionalized and unfunctionalized alkyl-chain derivatives; one exception is compound **81**, which shows an higher Stokes'shift, probably due to the presence of the electron rich pyrrole ring.

Sym-pentaalkyl functionalized corannulene derivatives undergo to a rapid a bowl-flip mechanism that interconverts equal proportions of enantiomeric conformations. When the arms bear chiral substituents, as in the case of compound **64**, the interconversion is between diasteromers and the symmetry required equality of proportions is then broken. One might expect to detect this in a deviation from van't Hoff's additivity rule for optical rotation; [107] *i.e.* the specific rotation for **64** should deviate from 5 times the specific rotation for a reference "arm". As such the specific rotation of compound **64** was measured: this compound has a $[\alpha]_D$ value of +68.9° which is 6.5 times the specific rotation value of *S*-2-methyl-butylpheny ($[\alpha]_D$= +10.5°). [102] [108] This result indicates that the contribution to the optical activity from the bias is small. This result could come about because the rotary power of an enantiomer of a *sym*-pentaalkyl corannulene derivative is small or because the energetic bias for one diasteromeric conformation of **64**.

3.5. Conclusion and Outlook

In conclusion, a robust and efficient procedure for the synthesis of C_5-symmetric pentasubstituted corannulene derivatives functionalized with alkyl chains bearing functional groups has been developed using Fe-catalyzed cross-coupling reaction. This procedure allows the functionalization of *sym*-pentachloro corannulene **39** under mild condition and using a cheap pre-catalyst yielding the desired product up to hundreds of milligrams scale. As expected, the introduction of aliphatic chains between the corannulene core and the functional groups led to an increased solubility in organic solvent of the molecule respect to the one presenting a aromatic linker.

Further studies should be performed in order to have access to the missing corannulene derivative functionalized with an amino group (compound **77**). Moreover, the synthesis and reactivity of the side product **73** obtained from the reduction of the penta carbonyl derivative **70** should be further investigated in order to study its potential as possible starting point for the desymmetrization of C_5-symmetric pentasubstituted corannulene to C_1-symmetric 1,3,5,7,9-functionalized analog.

The possibility to synthesize hundreds of milligrams of a broad class of soluble corannulene derivatives with a broad spectrum of functionality facilitates the access to *sym*-pentapodal corannulenes conjugated to active molecular modules. This core-module approach should further stimulate to create molecular design and engineering of material based on these components.

4. SYNTHESIS OF C_5-SYMMETRIC BIOCONJUGATED CORANNULENE DERIVATIVES

4.1. INTRODUCTION

Pentakis-bioconjugated corannulenes combine the properties of biomolecules (*e.g.* molecular recognition, biological activity, etc.) and the symmetric and structural features of corannulene derivatives leading to a new family of pentapods suitable as template for protein folding mimics, high-order multivalent ligands and aromatic/nucleic acid conjugate assemblies as explaned in Chapter 2.

The availability of highly soluble corannulene derivatives bearing a broad window of functional groups [102] permit the screening of different synthetic routes for the preparation of five-fold symmetric corannulene derivatives functionalized with the main classes of biomolecules (*i.e.* carbohydrates, peptide, nucleosides, lipids and terpenes). The synthesis of a C_5-symmetric terpenoid corannulene derivative (**68**) achieved by Fe-catalyzed cross-coupling has been already reported in the previous chapter.

In this chapter, the various synthetic pathways and the preparation of basic bioconjugated pentapods using corannulene scaffold will be described.

4.2. PROPOSED SYNTHETIC ROUTES

The synthesis of the first bioconjugated corannulene derivative functionalized with a terpenoid chain (**68**) has been achieved by Fe-catalyzed cross-coupling (Chapter 2). However, the reaction conditions used for this synthesis do not allow the introduction of other classes of biomolecule onto corannulene core unless estensive use of protective groups. Therefore, different and more convenient synthetic routes have been proposed and tested (Scheme 4.1).

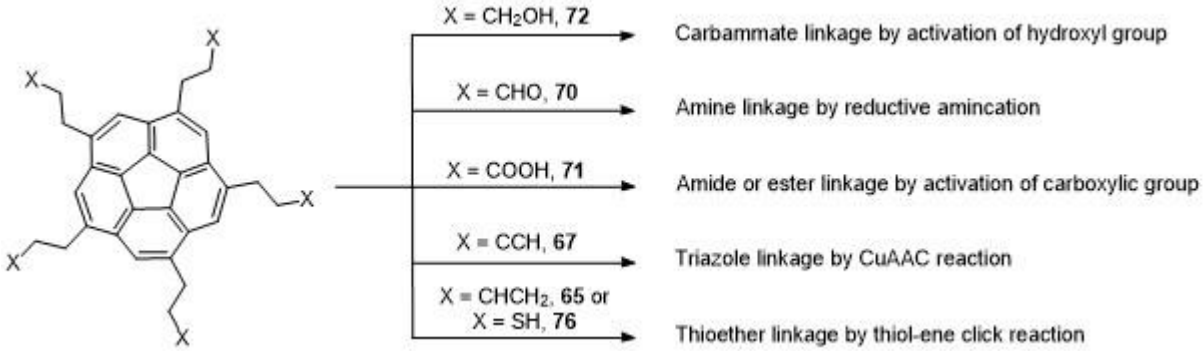

Scheme 4.1. Synthetic route proposed and tested for the synthesis of bioconjugated pentapods of corannulene.

The conjugation of corannulene derivatives **72** and **71** with biomolecules was tried under different conditions. Upon reaction with 4-nitrophenyl chloroformiate, the activated form of alcohol **72** did not yield to the desired pentaconjugated product after reaction with amino functionalized biomolecules (5'-amino thymidine and glycine methylester). The presence of tri- and tetrafunctionalized products and the formation of intramolecular carbonate linkage was detected by mass spectrometry analysis of the crude mixture.

Condensation reaction of compound **71** with the same amino functionalized biomolecules using several condensing agents (HATU, DCC, BOPCl) yield to a mixture of under-substituted corannulene derivatives. Similar results were obtain when the carboxylic acid **71** was activated by reaction with thionyl chloride or 1,1'-carbonyldiimidazole: under these conditions, the presence of intramolecular anhydride derivatives was detected by MS analysis.

Promising preliminary results were obtained for reductive amination reaction of pentacarbonyl corannulene derivative **70** with the methyl ester of glycine; the desired pentabioconjugated corannulene derivative **82** was obtained in high yield and purity and short reaction time (Scheme 4.2).

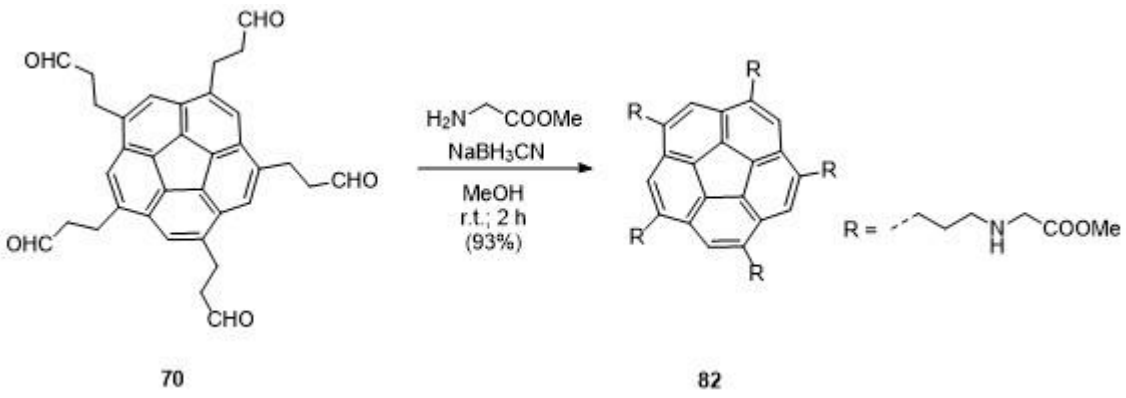

Scheme 4.2. Synthesis of **82** by reductive amination reaction on corannulene derivative **70**.

However, the introduction of the tripeptide H_2N-Ala-Ala-Ala-OMe onto corannulene core by reductive amination did not lead to complete conjugation: a mixture of tri- and tetraconjugated products were detected in the crude mixture by MS analysis. The reaction of **70** with 5'-amino thymidine under reductive amination conditions was not tried. Therefore, reductive amination was abandoned as protocol for the introduction of biomolecule onto corannulene.

The formation of under-substituted corannulene derivatives or different byproducts under the reaction conditions described in this chapter might be caused by a intramolecular steric effect of tri- or tetrasubstituted corannulene derivatives. The bulky substituents hide the missing reacting site or, in the case of the trisubstituted product, give access to different reaction pathway leading to intramolecular bounded species.

4.3. Synthesis of Bioconjugated Corannulene by Copper Catalyzed Azide-Alkyne Cyclization

Copper catalyzed azide-alkyne cycloaddition reaction (CuAAC) [109] is one of most representative member of the "click reaction" family. [110] High yield, high purity and functional groups orthogonality make this class of reactions widely used in different fields of science: bioconjugation, [111] material science [112] and drug discovery. [113] Furthermore, due to the large number of azides known or commercial available, this procedure should be representative for the preparation of a wide window of corannulene architectures.

Several CuAAC reaction conditions on corannulene derivative **67** were screened: copper source, temperature, solvent and heating system were varied. The best outputs in terms of purity and yield of the desired product wer obtained when CuAAC reaction was performed using copper

nanoparticles (CuNPS) [114] in DMF at 60 °C or 80 °C, depending from the azide, under microwave irradiation. [102] Under other CuAAC conditions the regioselectivity of triazole formation decreases and under-substituted corannulene derivatives were obtained.

A library of pentakis-bioconjugated corannulene derivatives displaying the main classes of biomolecule was synthesized following the new CuNPs-catalyzed CuAAC procedure.

4.3.1. Synthesis of Deoxynucleoside-conjugated Corannulene Derivatives

A member for each of the two families of deoxynucleoside have been conjugated to corannulene: deoxyadenosine (**83**) for purine and thymidine (**84**) for pyrimidine.

5'-azido-2'-deoxy-adenosine **85** was prepared in good yield and high purity by nucleophilic substitution reaction of 5'-tosylated-2'-deoxy adenosine **86** [115] with lithium azide in DMF; the low yield obtained for the synthesis of compound **86** is due to the formation of 2'-tosylated and 5'-2'-tosylated products. 5'-azido thymidine **87** was synthesized following the reported [116] one-step procedure by reaction of thymidine **64** with carbon tetrabromide, triphenylphopshine and sodium azide (Scheme 4.3).

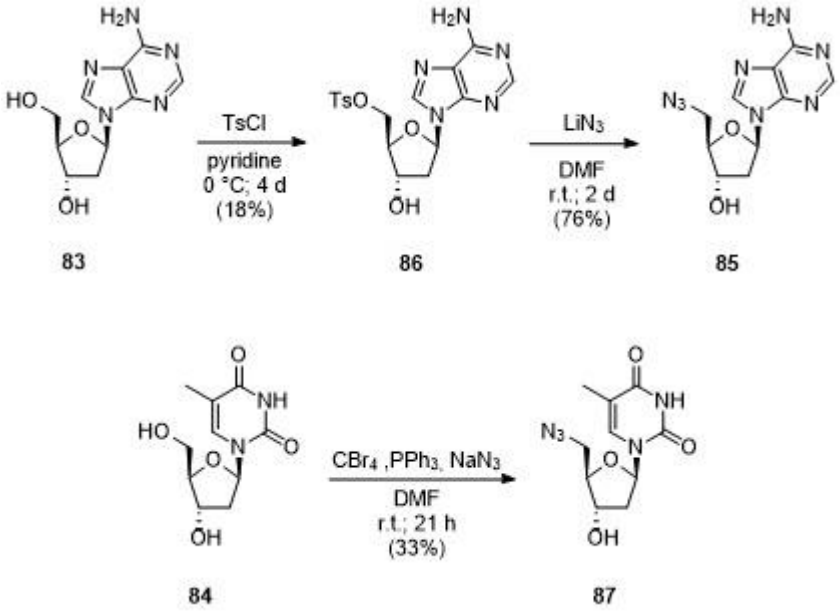

Scheme 4.3. Synthesis of 5'-azido deoxynucleosides **85** and **87**.

Five-fold symmetric pentanucleoside corannulene derivatives **88** and **89** were then synthesized in good yield and high purity by CuAAC reaction of alkyne **67** with azides **85** and **87**, respectively (Scheme 4.4).

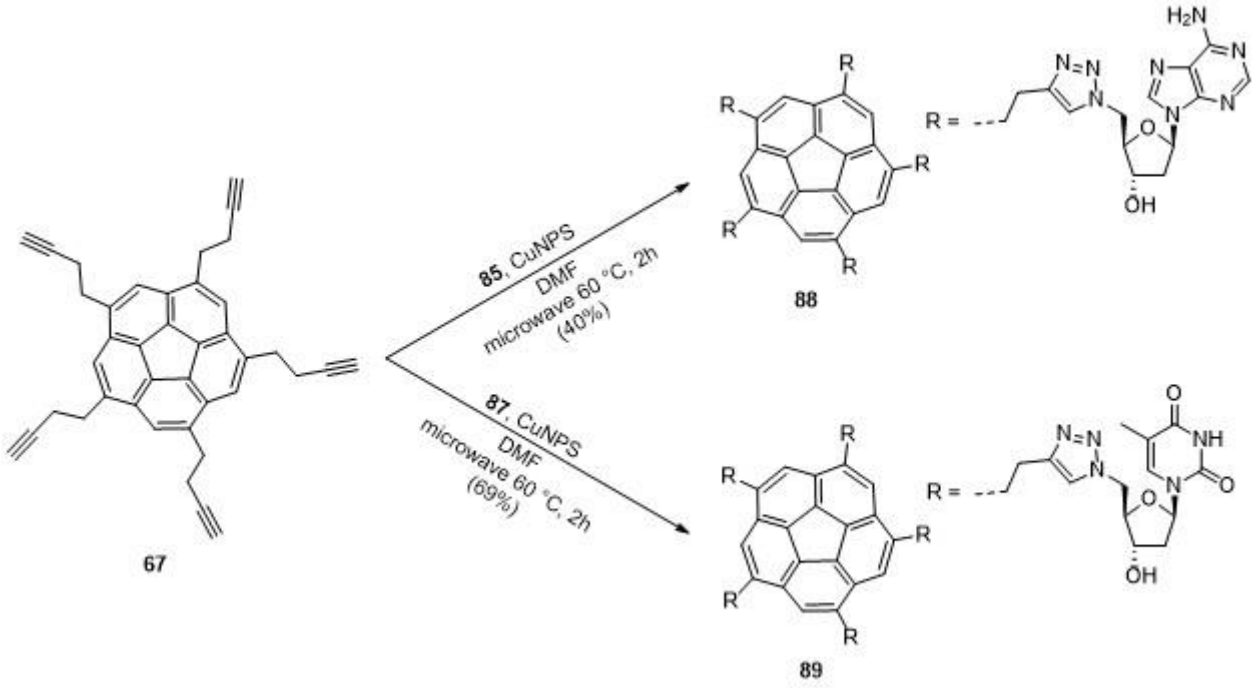

Scheme 4.4. Synthesis of deoxynucleosides pentapods **88** and **89**.

The poor solubility of corannulene derivatives **88** and **89** in non-polar organic solvents does not permit investigation on the formation of supramolecular assemblies by formation of H-bonding network. These bioconjugated compounds display high solubility in strong polar solvents such as DMF, DMSO and TFE. However, ^{1}H-NMR and UV-vis investigation of solutions of **88** and **89** in these solvents did not substantiate the formation of any aggregates; most probably, the absence of supramolecular constructs is due to the saturation of the H-bonding sites by the solvent. The formation of supramolecular heteroaggregates between **88** and **89** in solid state have been studied by HRMS analysis: the high sensitivity of this technique allows the study of highly diluted solution of compounds **88** and **89** in methanol. The MS spectrum of a solution nearly equimolar of **88** and **89** shows a peak corresponding to the heterodimer **88**-**89** (Figure 4.1).

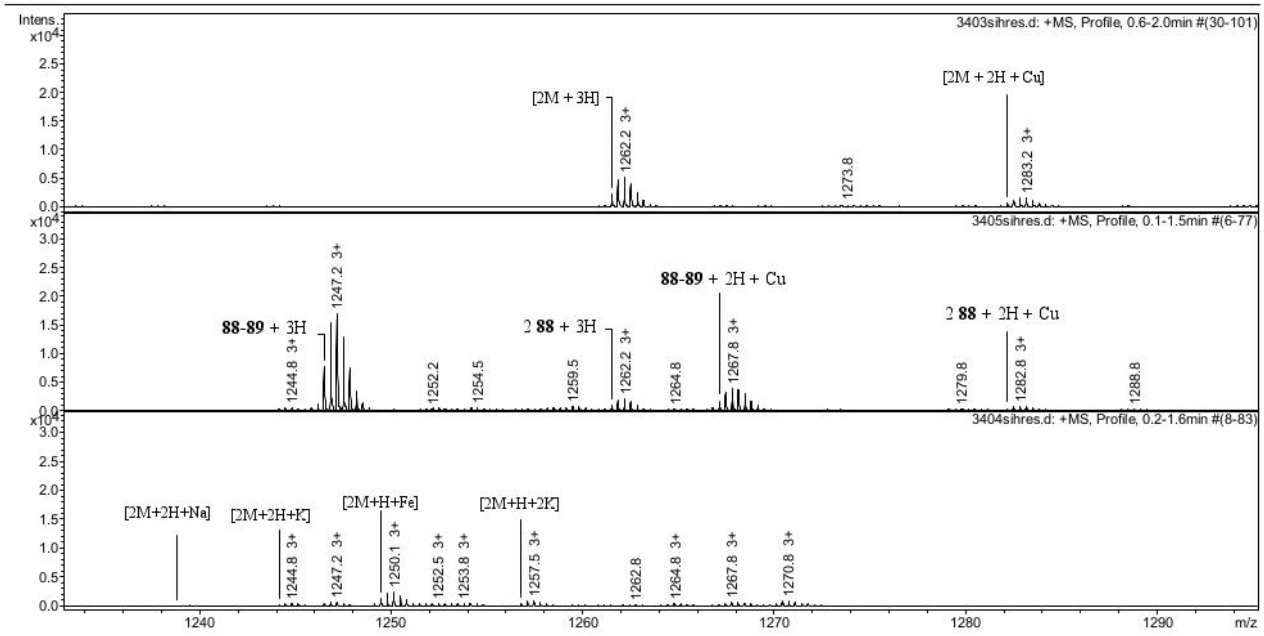

Figure 4.1. HR-ESI-MS in MeOH + 0.05% formic acid of **88** (top), mixture of **88** and **89** (middle) and **89** (bottom).

The higher intensity peak of the **88-89** heterodimer than the intensity of the homodimers is an evidence of the formation of dimeric aggregates between the two pentakis-nucleosides corannulenes. However, information about the geometry and symmetry of the dimer, and the intermolecular forces involved cannot be obtained from the MS data.

4.3.2. Synthesis of Oligopeptide-conjugated Corannulene Derivative

For this class of bioconjugated pentapods, the tripeptide H-Ala-Ala-Ala-OMe **90** was introduced onto corannulene core; this oligopeptide was selected due to its capability to form β-strands in solution. [117] Five-fold substituted corannulene derivative functionalized with this oligopeptide might form supramolecular architectures in solution by formation of H-bonding network.

Corannulene derivative **91** was prepared in good yield and high purity by CuAAC reaction of **67** with azide **92**, which was synthesized by reaction of amine **90** with triflic azide prepared *in situ* (Scheme 4.5). In the case of azide on secondary carbon, like **92**, the CuAAC reaction requires higher temperature and longer reaction time to have full conversion of **67**; this is most probably due to steric hindrance effects.

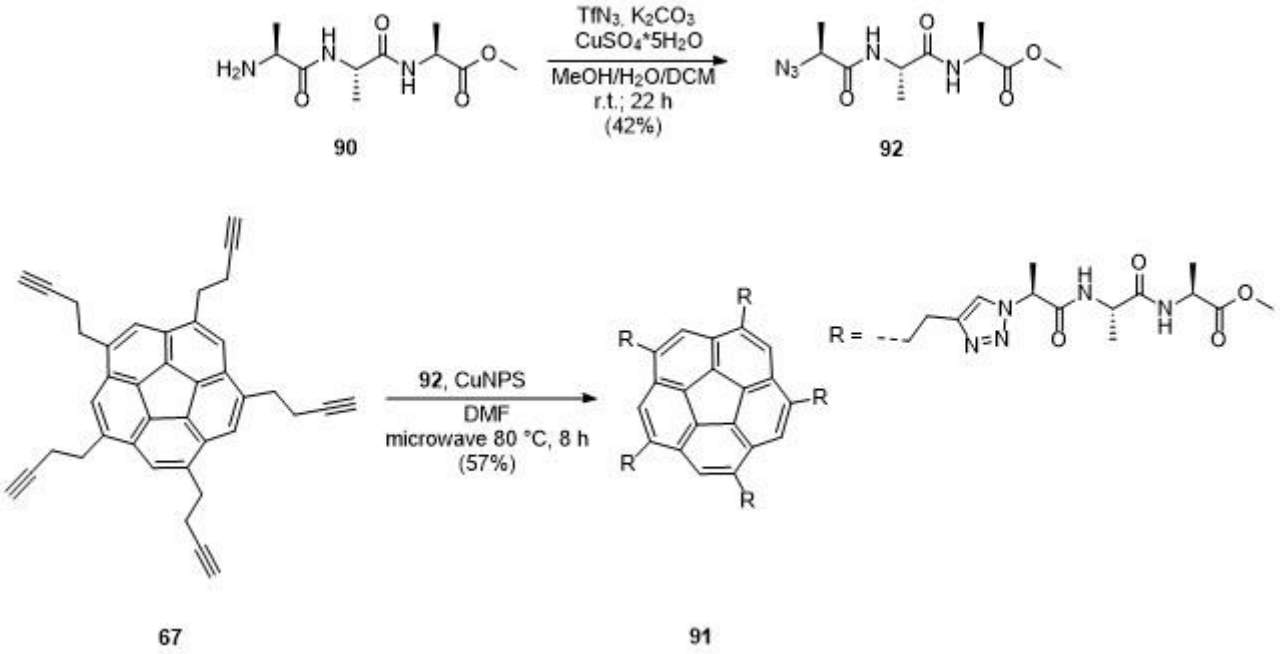

Scheme 4.5. Synthesis of oligopeptide pentapod **91**.

Compound **91** has been obtained in modest yield and high purity. This corannulene derivatives is well soluble only in polar H-bonding solvents like DMSO, DMF and trifluoroethanol which saturate the H-bonding sites of pentapod **91**. Thus the formation of homodimers of **91** in solution has not been detected by UV-vis, emission and NMR studies. Like for compounds **88** and 89, a diluted solution of oligopeptide 91 in methanol was analyzed by HRMS; however, peaks relative to aggregates of this molecule were not detected suggesting the absence of any supramolecular structure.

4.3.4. Synthesis of Lipid-conjugated Corannulene Derivative

Oleic acid **93** has been chosen as representative member of lipids for the synthesis of pentakislipido corannulene derivatives. This fatty acid has been chosen due to the important application of its glycerol ester in protein crystallization and soft material field. [118]

Five-fold symmetric pentalipido corannulene **94** was prepared in high yield and purity by CuAAC reaction of alkyne **67** with oleic acid derivative **95** [119] (Scheme 4.6). [120]

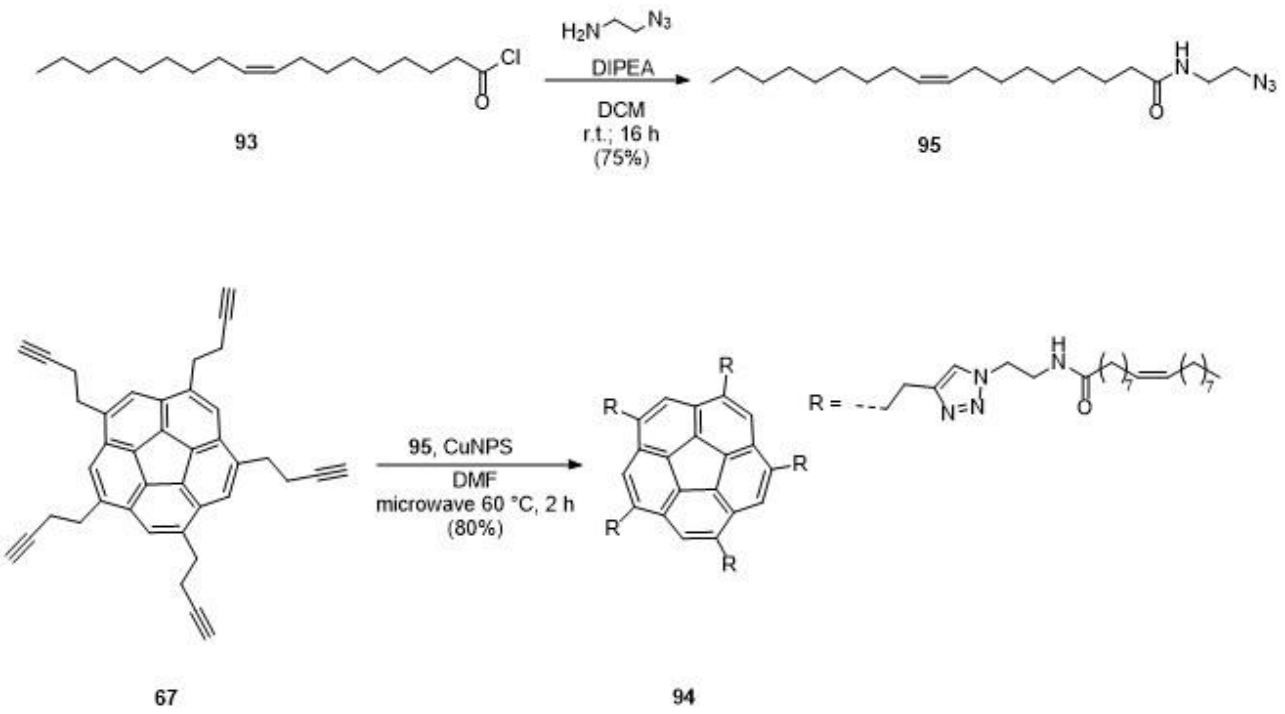

Scheme 4.6. Synthesis of pentakislipido corannulene **94**.

The physical properties of compound **94** will be discussed in details in Chapter 6.

4.3.5. Synthesis of Carbohydrated-conjugated Corannulene Derivative

Two different corannulene derivatives conjugated to carbohydrates were prepared; galactose and ribose have been selected as sugar units.

Pentakis-glicosidic corannulene derivatives represent a leit-motif for potential multivalent binder to biological complex. [82,102,121]

The synthesis of the azidoalkyl galactoside **96** was a prerequisite to the coupling for the synthesis of galactoside **100**. The preparation of **96** starts from 2,3,4,6-tetra-*O*-acetyl-α-D-galactopyranosyl bromide **97**, which undergoes to a Koening-Knorr displacement with 2-bromoethanol affording compound **98**. [122] Azide **99** can be prepared in excellent yield by treatment of **98** with sodium azide in DMF, followed by removal of acetyl groups with sodium methoxide to afford the sugar azide **96** in high yield and purity. CuAAC reaction of alkyne **67** with azide **96** yields pentakis-galactoside corannulene **100** (Scheme 4.7). [102,123]

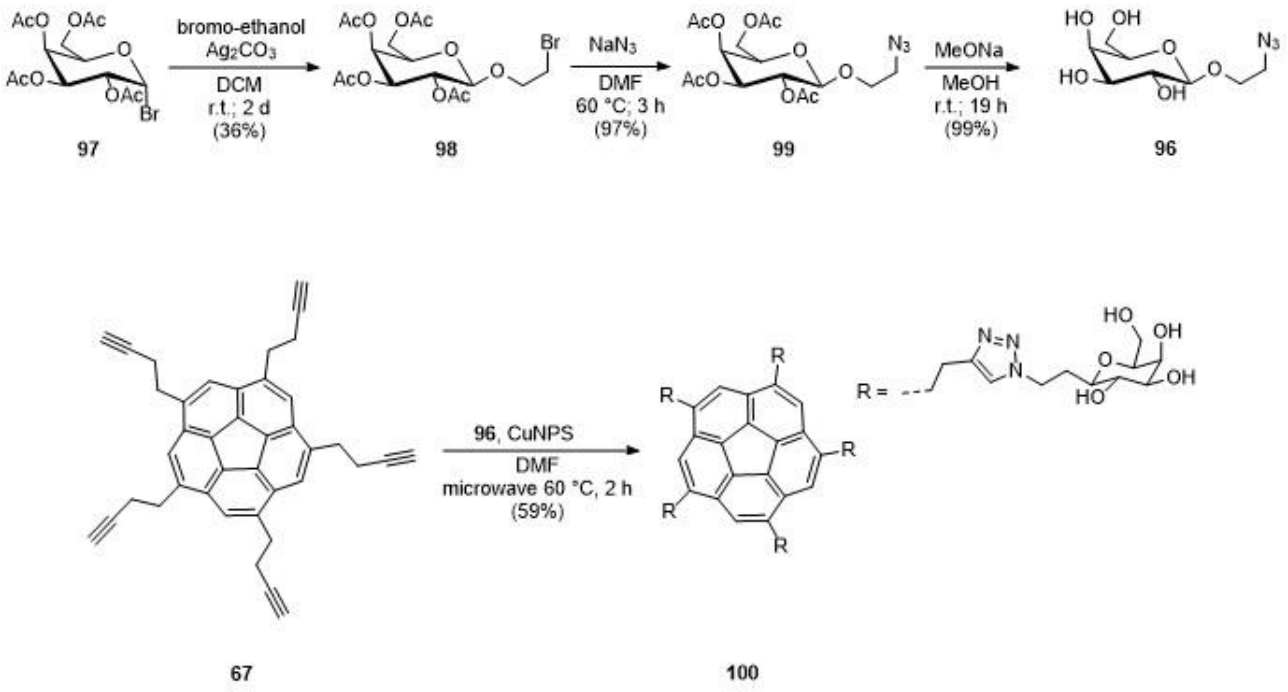

Scheme 4.7. Synthesis of carbohydrate pentapod **100**.

The synthesis of pentakis-riboside **101** was achieved by CuAAC reaction of alkyne **67** with 2,3,5-tri-*O*-acetyl-β-D-ribofuranosyl-1-azide **102** synthesized following a reported procedure. [124] Deprotection of **101** with sodium methoxyde yields corannulene derivative **103** (Scheme 4.8). The protection of the hydroxyl groups of ribose was necessary for the isolation in high purity of compound **101** from the crude reaction mixture due to low solubility of riboside **103**.

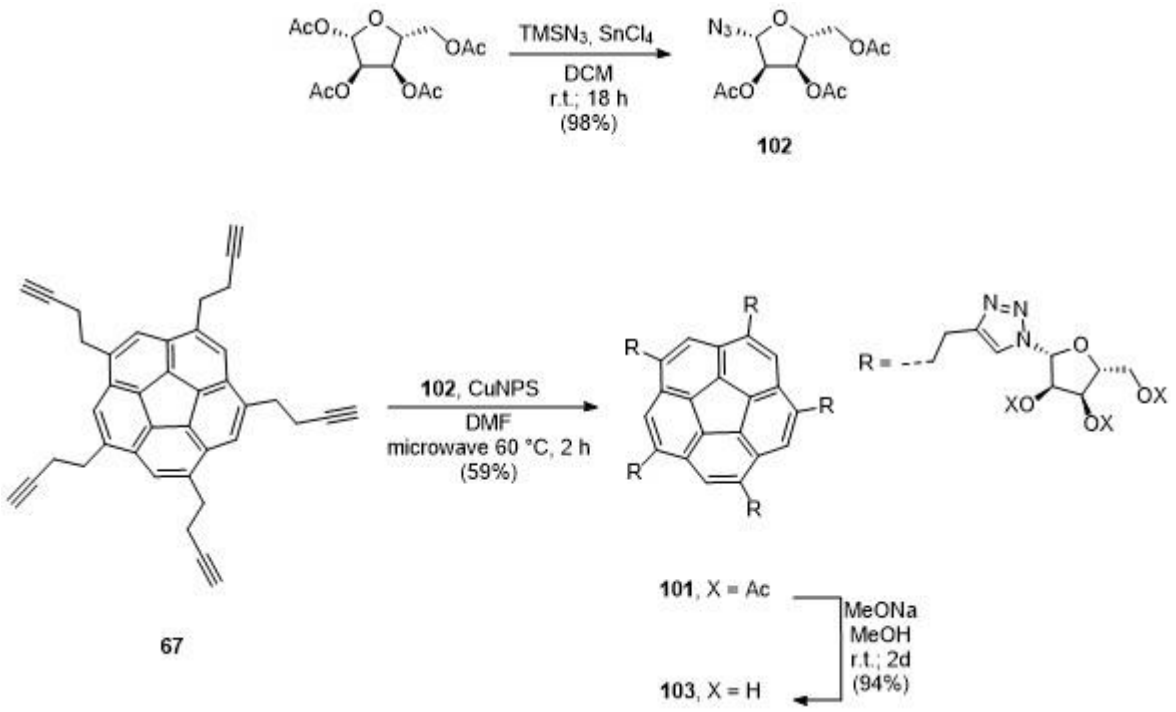

Scheme 4.8. Synthesis of corannulene pentapods **101** and **103**.

Due to the hydrophobic corannulene core of the amphiphilic sugar pentapods **100** and **103,** combined with the strongly hydrophilic galactoside and riboside functionalization, these molecules may form stacked supramolecular aggregates in aqueous solution. Unfortunately, riboside corannulene **103** did not show any solubility in water, but was only soluble in strongly polar solvent such as DMF and DMSO. Therefore, the formation of aggregates in water was investigated only for galactoside **100** by ^{1}H-NMR, absorption and emission spectroscopy. The assembling behavior of galactoside **100** will be described in details in Chapter 5.

4.4. Conclusion and Outlook

In conclusion, a powerful and robust procedure for the synthesis of five-fold symmetric pentabioconjugated corannulene derivatives has been developed. CuAAC "click" reaction catalyzed by Cu nanoparticles allowed the functionalization of terminal acetylene **67** with the main classes of biomolecules: sugars, oligopeptide and nucleoside. The studies characterizing the aggregation behavior of these new compounds support the formation of supramolecular architectures. Water-soluble galactoside derivatives of corannulene were observed to form H-dimers in solution (details are reported in Chapter 5), while dimeric structures can be formed via H-bonding between pentakis-nucleosides corannulene derivatives.

The facile synthesis of this new family of compounds, the results and observations on the assembling behavior of these molecules should motivate the design and synthesis of improved bioconjugated systems using corannulene scaffold. An example of such kind of system is described in Chapter 7.

5. Synthesis of Cholera Toxin Inhibitors Based on C_5-Symmetric Corannulene Derivatives

5.1. Cholera Toxin: An Introduction

The World Health Organization (WHO) estimates that annually 3–5 million people worldwide are infected with cholera, resulting in over a hundred thousand fatalities. [125] The responsible pathogen, the *Vibrio cholerae* bacterium, produces the cholera toxin (CT) protein that is the cause for the severe clinical symptoms.

CT belongs to the protein family of AB_5 bacterial toxins. [126] These proteins consist of two distinct domains (A and B) with different roles. [127] The A-subunit is an enzyme that - once inside the host cell - is toxic and responsible for the subsequent disease symptoms. A-subunit consists of two functional domains: wedge-shaped A1 moiety and elongated A2 moiety. The cholera toxin B-subunit (CTB) is a lectin ans plays a crucial role in the recognition and interaction of the toxin with its natural ligand, ganglioside GM1, on the periphery of intestinal cells (Figure 5.1). [128]

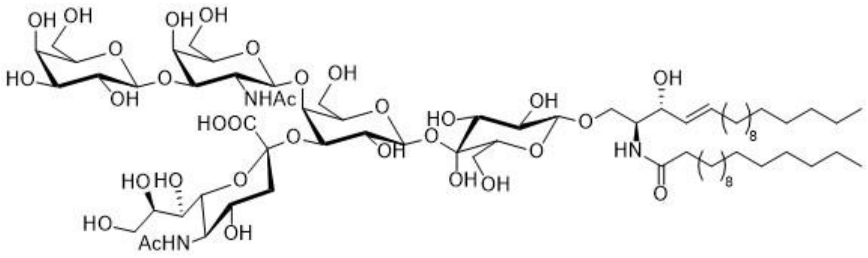

Figure 5.1. Structure of CTB's natural ligand, ganglioside GM1.

The crystal structure of CT [129] shows that the protein complex consists of five identical monomeric CTB subunits, arranged in a pentagonal symmetry, and each of those subunits can bind the ganglioside GM1 in a one-to-one stoichiometry. Detailed calorimetric studies revealed that CT exhibits allosteric cooperativity, [130] which contributes to increasingly higher binding affinities to CT when more ligands are bound. [131]

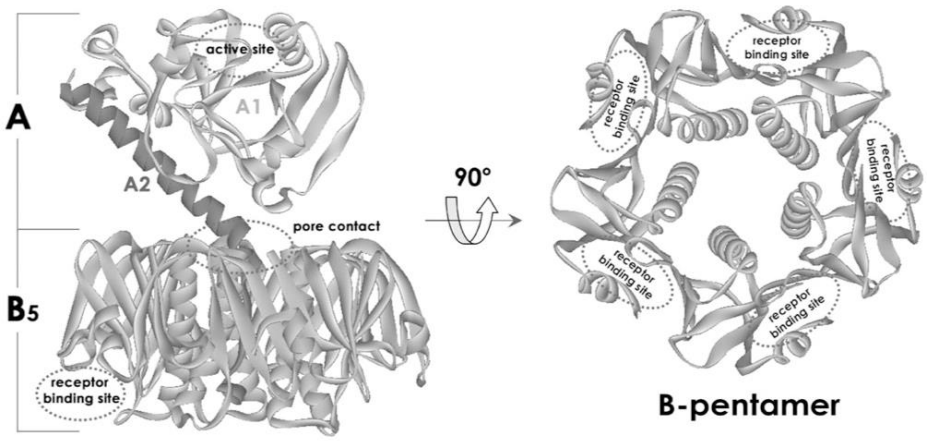

Figure 5.2. Crystal structure of CT with the sites for molecular recognition.

The mechanism of the Cholera Toxin's reaction cascade has already been elucidated at the molecular level. [132,133] First of all, B-subunit binds to ganglioside GM1 on intestinal epithelial cell membranes, followed by cleavage of the A-subunit and disulfide bond reduction to yield the two separated fragments A1 and A2. Then after A1 is translocated across the cell membrane by endocytosis, it modifies the alpha subunit of the stimulatory G protein through a NAD-dependent ADP-ribosylation reation. This locks the G protein in its GTP-bound form, which continually stimulates adenylate cyclase to produce the second messenger cAMP whose intracellular concentration increases to more than 100-fold over normal and over-activates cytosolic protein kinase A (PKA). These active PKA then phosphorylate the cystic fibrosis transmembrane conductance regulator (CFTR) chloride channel proteins, which leads to ATP-mediated efflux of chloride ions and secretion of water, sodium and potassium cations and bicarbonate anions into the intestinal lumen. In addition, the entry of sodium and, consequently, of water into enterocytes are diminished. The combined effects result in rapid fluid loss from the intestine, up to two liter per hour, leading to severe dehydration and other factors associated with cholera. [133]

From the structural point of view, there are three potential target areas for drug design: blocking the enzyme-active site A1, the interruption of A2-B pentamer interaction or prevent the receptor-recognition process. [134] The inhibition of receptor binding has received the most attention because of the relative ease of making antagonist that led to the structural studies of the receptor-binding sites on the CTB. Two major routes can be discerned in the literature to achieve this goal. The first strategy, monovalent receptor-binding approach, focuses on the design and synthesis of ligands that closely mimic the natural ligand on the cell surface [135] in order to obtain a strong interaction with the CTB receptor. To improve the affinity for the toxin pentamer, modified galactose derivatives

were explored: this led to the discovery of *m*-nitrophenyl-*a*-D-galactopyranoside (MNPG), which has a 100-fold increase in affinity relative to D-galactose. [136] Based on this result, the inhibitor design using MNPG was reported. [137] So far, many different kinds of galactose or MNPG derivatives have been investigated and utilized as monovalent inhibitor for CT. [138]

The second approach, multivalent receptor-binding, [81–83] exploiting chelate cooperativity, takes the advantages of the pentavalent character of the ligand-binding sites of CT. This approach is based on the synthesis of a functionalized branched system, in which each arm carries a single-site inhibitor, like galactose [47,139–141] or lactose, [70,71,142,143] leading to a compound that has an overall stronger interaction with the toxin than the sum of the independent inhibitors. The synthesis of dendritic multivalent inhibitors functionalized with GM1os has been reported: these inhibitors displayed unprecedented high inhibitor potencies for CTB, in the picomolar range. [144]

The most dramatic improvement in receptor-binding antagonist design using multivalent systems was achieved with a symmetrical pentavalent molecule by Fan and co-workers. [138] The basic concept to improve the affinity was a modular approach of "Finger-Linker-Core" (Figure 5.3). The pentavalent "Core" is connected by flexible "Linkers" to "Finger" that include the monovalent receptor-binding ligand.

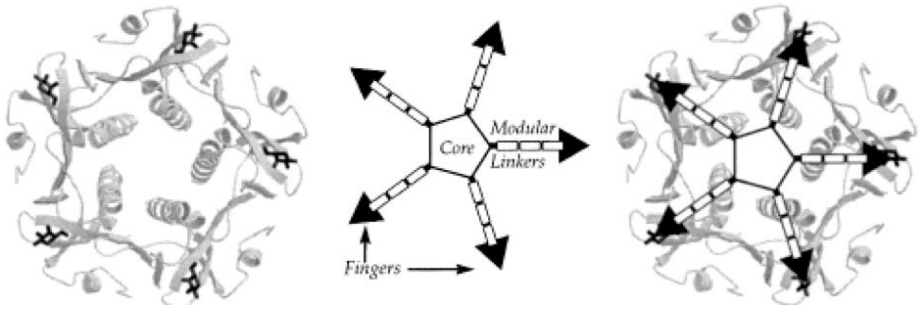

Figure 5.3. B-pentamer (left), pentavalent inhibitor (middle) and their complex (right).

Pentavalent CT inhibitors were synthesized using various "cores": acylated pentacyclen, [70] large cyclic peptide [71] and calix[5]arene. [145]

5.2. SYMMETRICAL PENTAVALENT INHIBITORS BASED ON CORANNULENE SCAFFOLD

5.2.1. SYNTHETIC ROUTE

The five-fold symmetry of *sym*-pentachlorocorannulene **39** can be utilized for the synthesis of coranulene-based AB_5 toxin antagonists using the "Finger-Linker-Core" approach (Scheme 5.1).

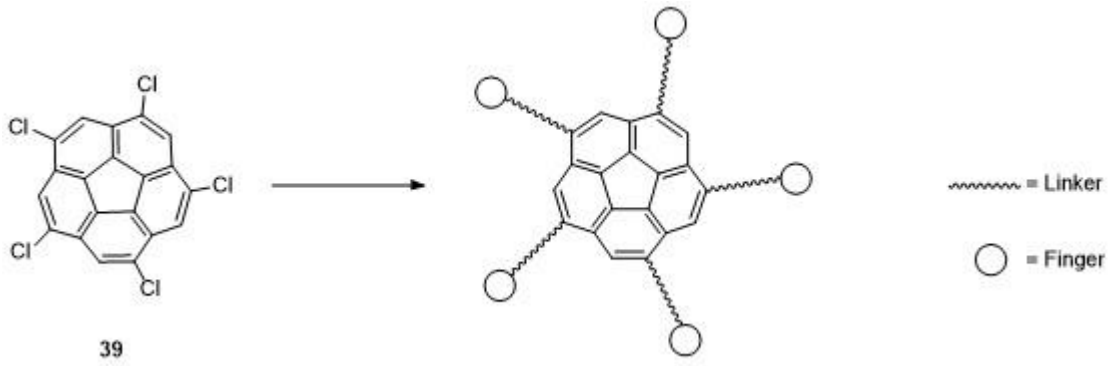

Scheme 5.1. General corannulene-based AB_5 toxins inhibitor.

A first attempt of the synthesis of AB_5 toxins inhibitors based on corannulene has been reported by Siegel group. [47] In this first approach, rigid linkers designed basing on the crystal data of AB_5 toxin have been used. Two ethylene glycol units were inserted in the linker structure in order to increase the water solubility of the inhibitor: a feature necessary for perform affinity assay with the toxin. In this approach, the rigid linkers should allow an optimal interaction of all the five galactose moieties of the inhibitor with the binding sites of the toxin, while corannulene adjusts the recognition circle by modulating the bowl depth.

Galactose has been chosen as week binder of the toxin and conjugated to the "Core-Linker" moiety by CuAAC reaction (Scheme 5.2). The sugar pentapod **105** was prepared starting from **39** by in a 4-steps pathway; in the first two reactions the linkers were introduced onto corannulene core as TIPS protected acetylene by Suzuki coupling and then deprotected by treatment with TBAF. In the last two steps, the conjugation of acetyl-protected galactose and its deprotection were achieved by CuAAC reaction followed by basic hydrolysis with sodium methoxide. [47]

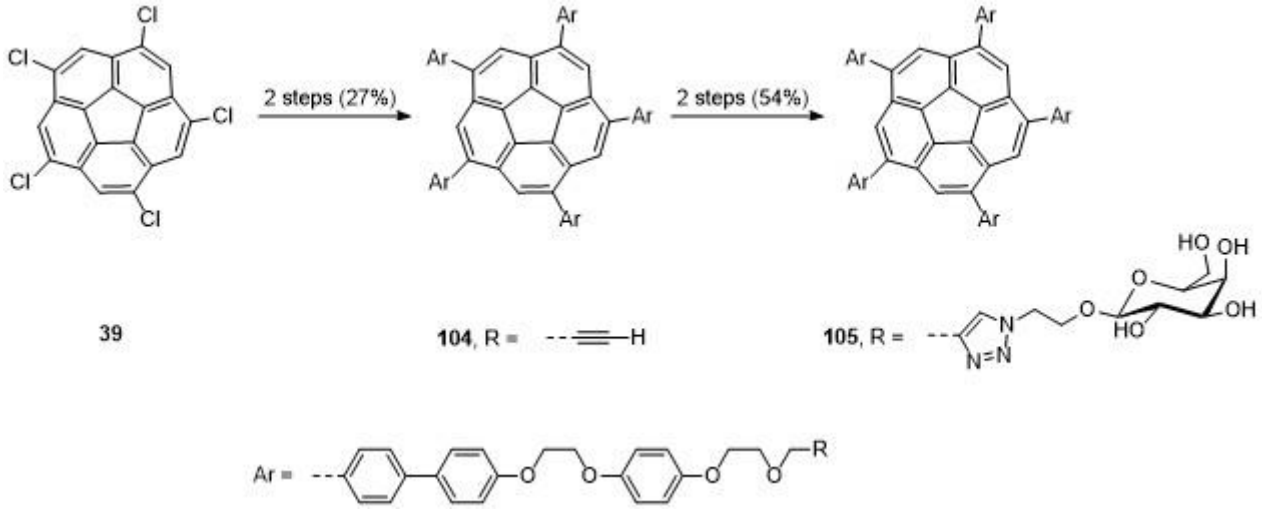

Scheme 5.2. Synthesis of first AB_5 toxin inhibitor based on corannulene.

Unfortunately. pentakisgalactoside **105** shows unexpected low solubility in water and DMSO/water mixtures; therefore affinity test with the toxin cannot be performed. Although the presence of five hydrophilic galactoside units, the high rigidity of the aromatic "Core-Linker" system of **105** might cause the low solubility of this molecule in water.

The recent developments achieved on the functionalization of *sym*-pentachlorocorannulene **39** [102] make accessible new classes of five-fold symmetric pentasubstituted corannulene derivatives. In order to achieve the preparation of CT inhibitors based on corannulene the rigid linkers will be substituted with more flexible *n*-mers of α-azidoethyl-ω-propargyl diglyme (*n* = 1, 2, 4) (Scheme 5.3) in order to increase the water solubility of the product. The design and synthesis of pentavalent GM1os-presenting inhibitors based on a five-fold symmetrical *sym*-pentasubstituted corannulene scaffold will combine the two strategies (multivalent system and strong monovalent binder) and obtain an optimal binding to CT.

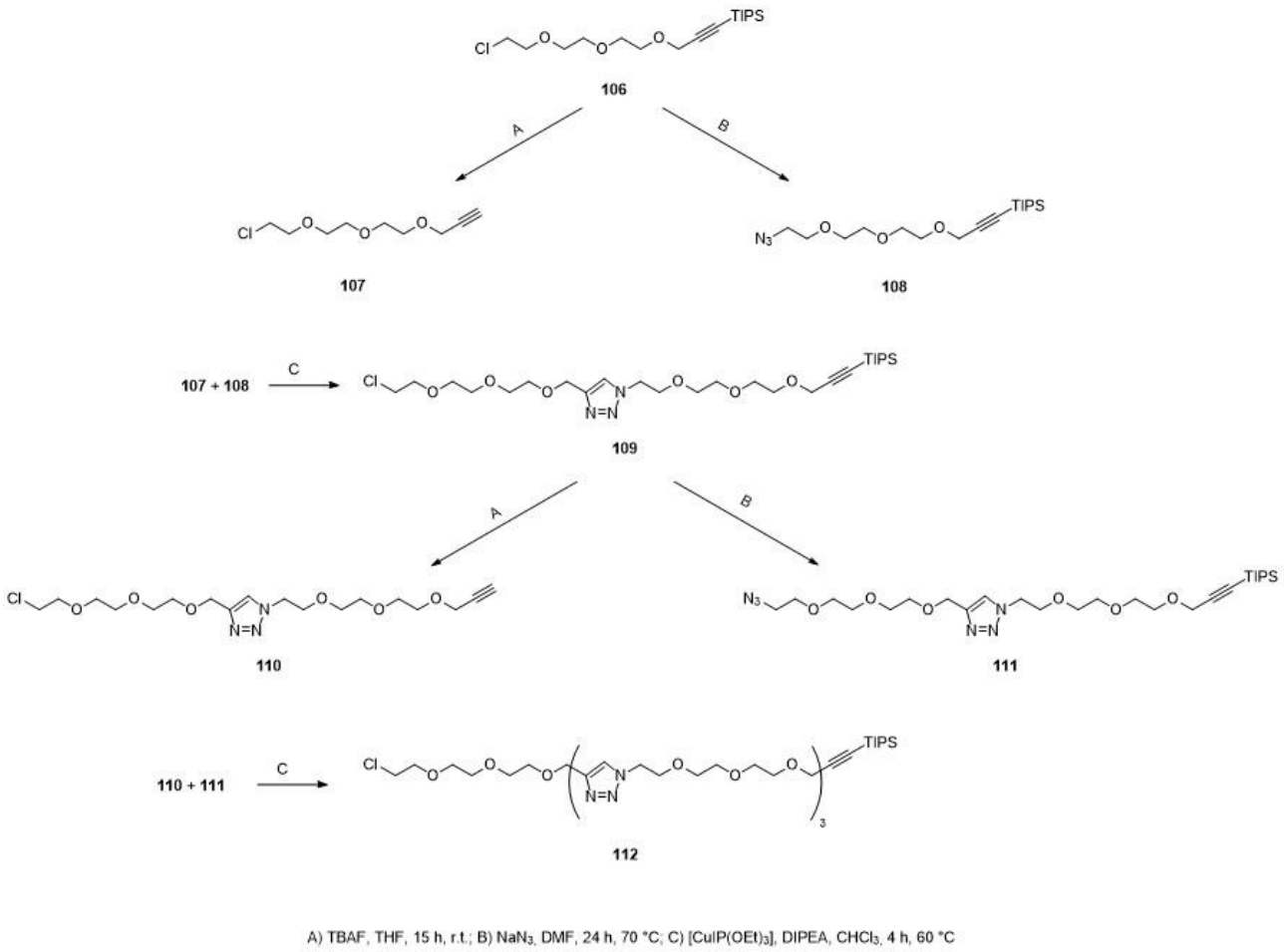

Scheme 5.3. Synthesis of *n*-mers α-azidoethyl-ω-propargyl diglyme (**108** *n* = 1; **111** *n* = 2 and **112** *n* = 4). A) TBAF, THF, 15 h, r.t. B) NaN_3, DMF, 24 h, 70 °C. C) $[CuIP(OEt)_3]$, DIPEA, CHCl3, 4 h, 60 °C.

The synthesis of the three linkers was achieved following a reported iterative strategy starting from compound **106**, which was chosen as elementary building block. [146] This strategy allows the preparation of monodispersed PEG-based linker with exponential growing of the lengths in high yield and purity. Compounds **108**, **111** and **112** were selected as linkers based on the crystal structure of CT: these linkers will cover a wide range of length permitting to reach an optimal binding of the inhibitor to CT. Moreover, they will improve the flexibility and the water solubility of the inhibitors.

The synthetic pathway towards the corannulene-based inhibitors starts with the introduction of the linker systems onto corannulene core by conjugation of the terminal acetylene **67** with poly diglimes **108**, **110** and **111** by copper nanoparticle-catalyzed CuAAC reaction (Scheme 5.4). [121] This synthetic route gave satisfactory results for the synthesis of the "Core-Linker" systems in good yield and purity. The terminal TIPS-protected acetylenes **113**, **114** and **115** were deprotected by

reaction with TBAF yielding the alkyne-terminated PEG-corannulene **116**, **117** and **118** (Scheme 5.4). [121]

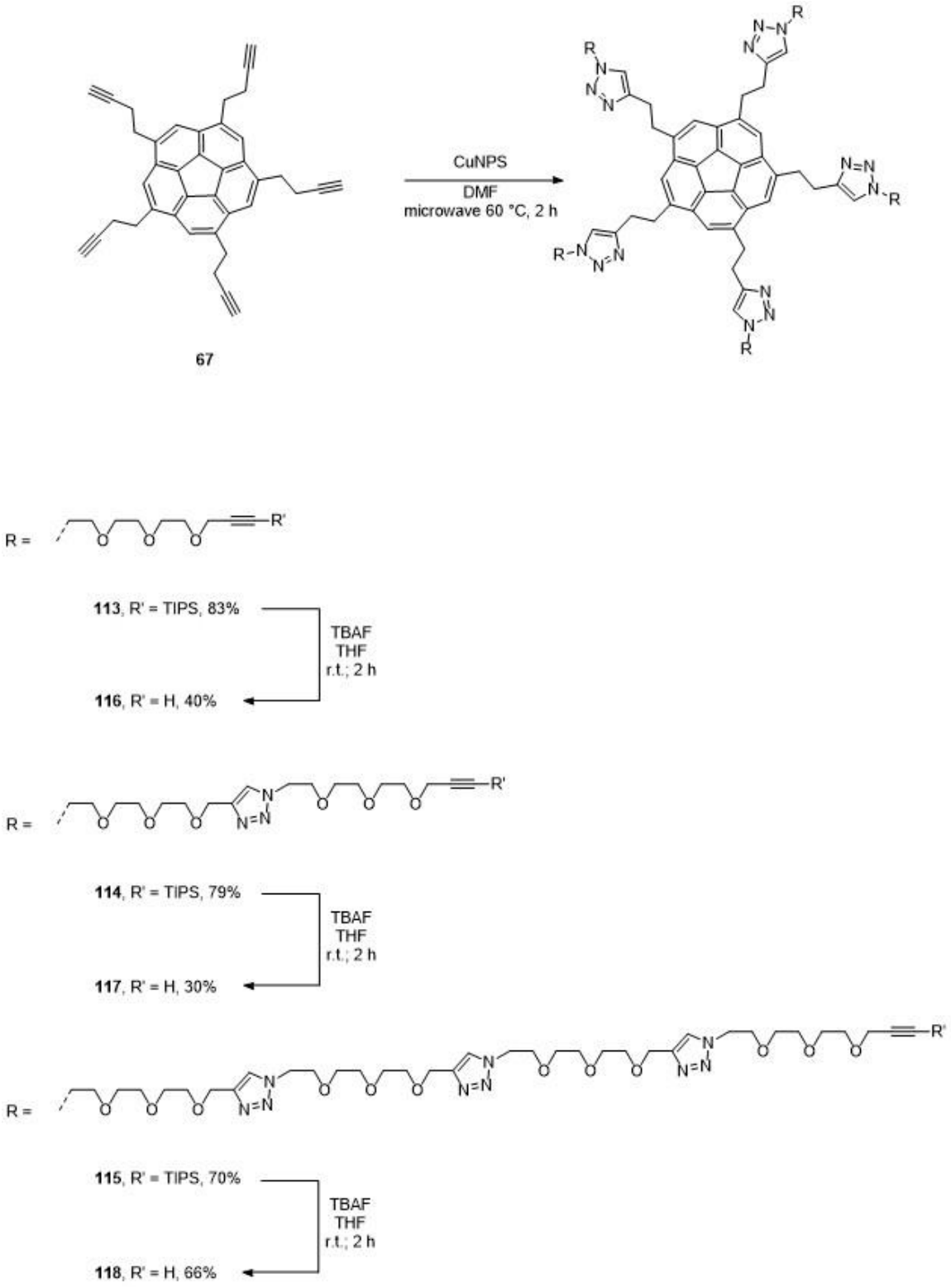

Scheme 5.4. Synthesis of "Core-Linker" systems **116**, **117** and **118**.

Two different "Finger" systems has been selected: galactose, an easily obtainable but quite poor binder of CT, and the oligosaccharide moiety of ganglioside GM1 (GM1os), the natural binder of Cholera Toxin.

The galactose-functionalized "Finger" **121** was synthesized by Koenigs-Knorr type glycosilation of azido-PEG hydroxide **119** [147,148] with peracetylated α-bromo-galactoside **97** followed by deprotection by treatment of glycoside **120** with sodium methoxide (Scheme 5.5). [121]

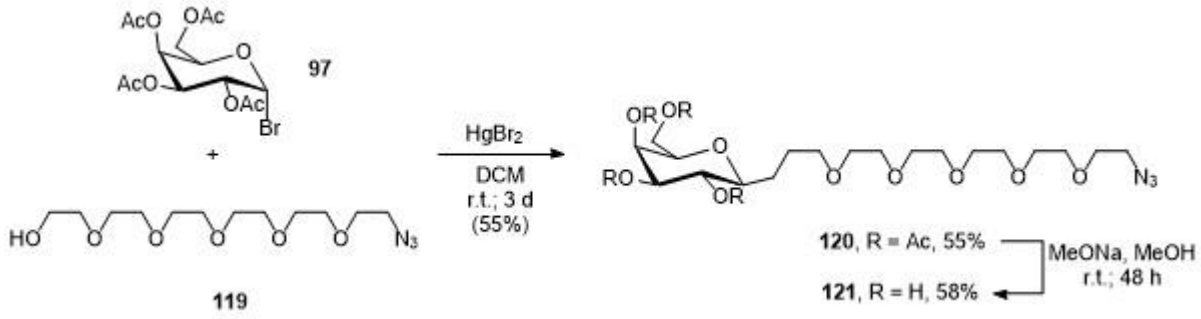

Scheme 5.5. Synthesis of galactose-functionalized linker **121**.

An array of pentavalent galactoside-functionalized *sym*-pentasubstituted corannulenes inhibitors was prepared employing the microwave-assisted CuAAC reaction of terminal acetylenes **67** and **116** – **118** with azido galactose derivative **121** affording four galactose-based CT inhibitors **122** – **125** (Scheme 5.6). [121]

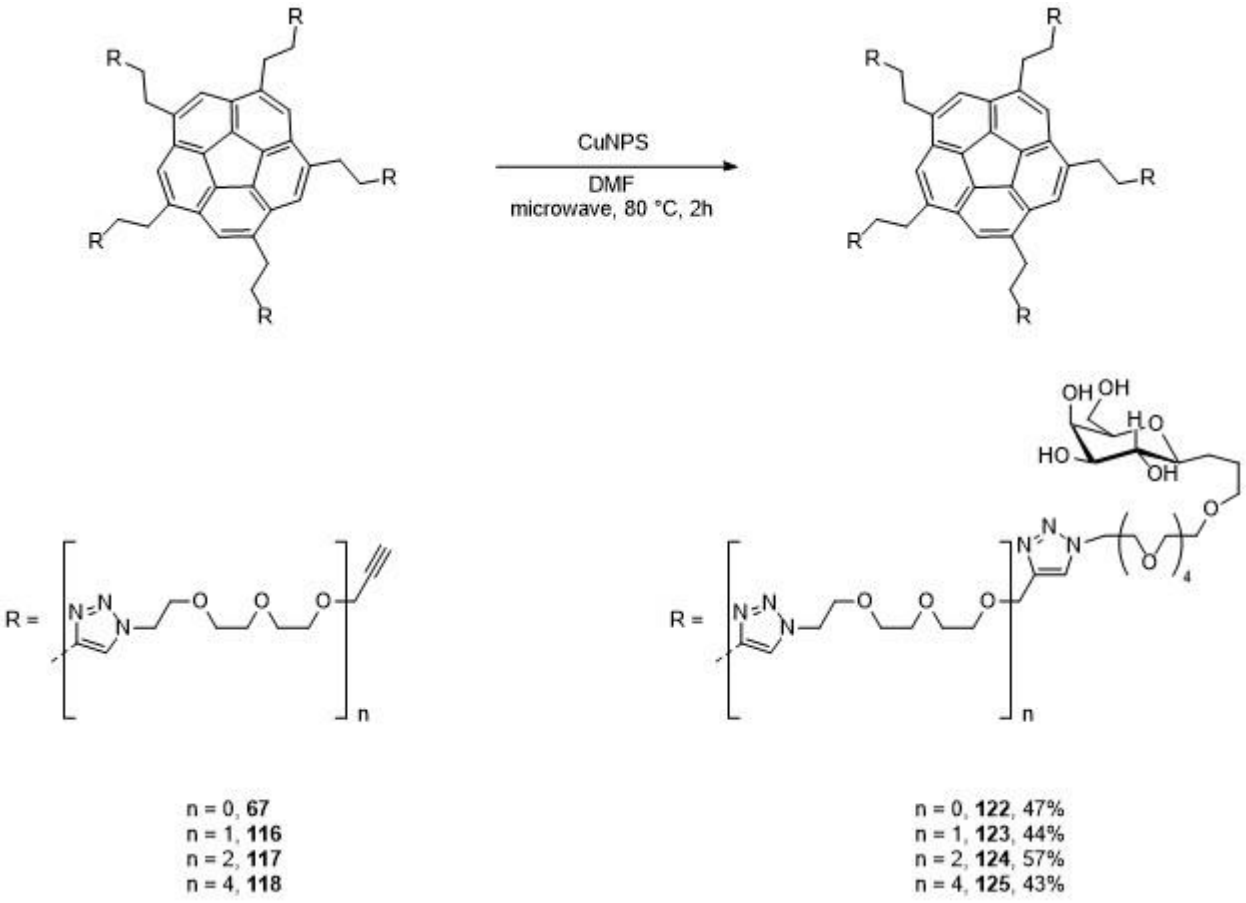

Scheme 5.6. Synthesis of galactose-functionalized corannulene-based CT inhibitors **122** – **125**.

Pentakis-galactose corannulene derivatives **122** – **125** were obtained in good yield and high purity. [121]

The second family of pentavalent inhibitors displays five GM1os moieties. The synthesis of GM1 mimic **130** has been previously achieved by a chemo-enzymatic pathway starting from lactoside **126**, which is synthesized from lactose (Scheme 5.7). [149]

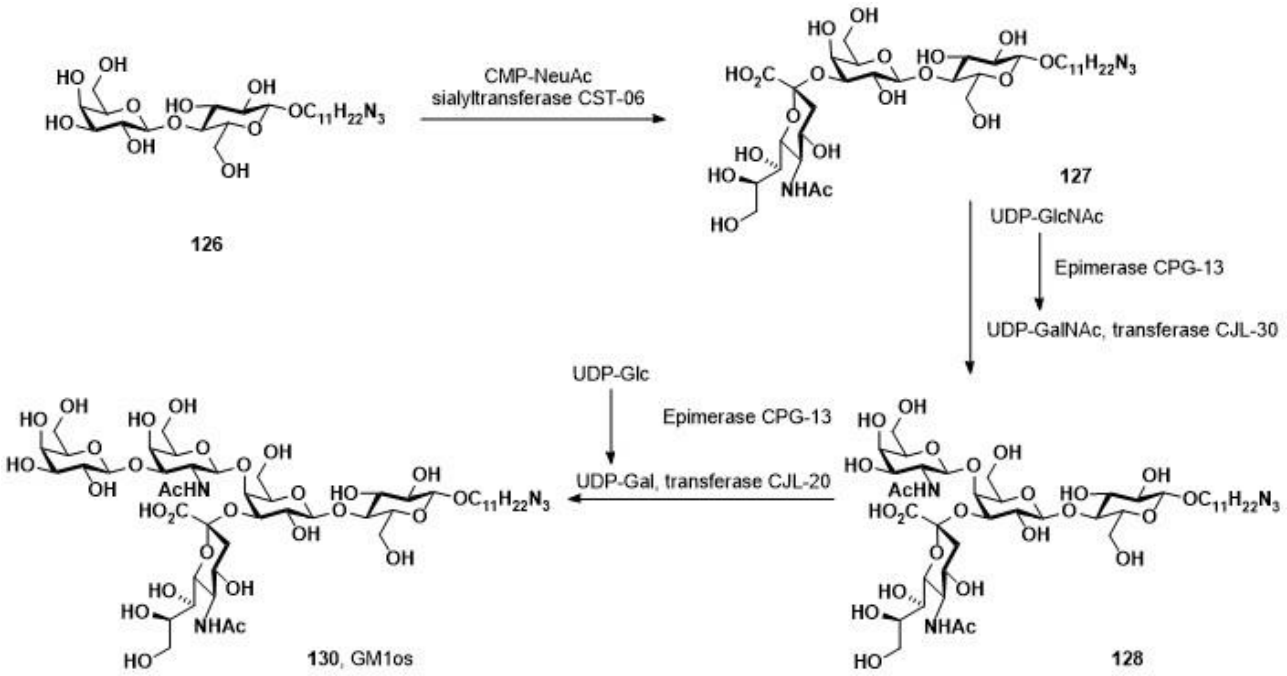

Scheme 5.7. Chemoenzymatic synthesis of GM1os **130**.

The pentakis-GM1os corannulene derivatives **131** – **132** were synthesized by CuNPs-catalyzed microwave-assisted CuAAC reaction of azido pentasaccharide **130** with terminal acetylenes **116** – **118**. Due to the low solubility of **130** in DMF, the "click" reaction were performed in water in order to have complete dissolution of GM1os in the reaction media. (Scheme 5.8). [121]

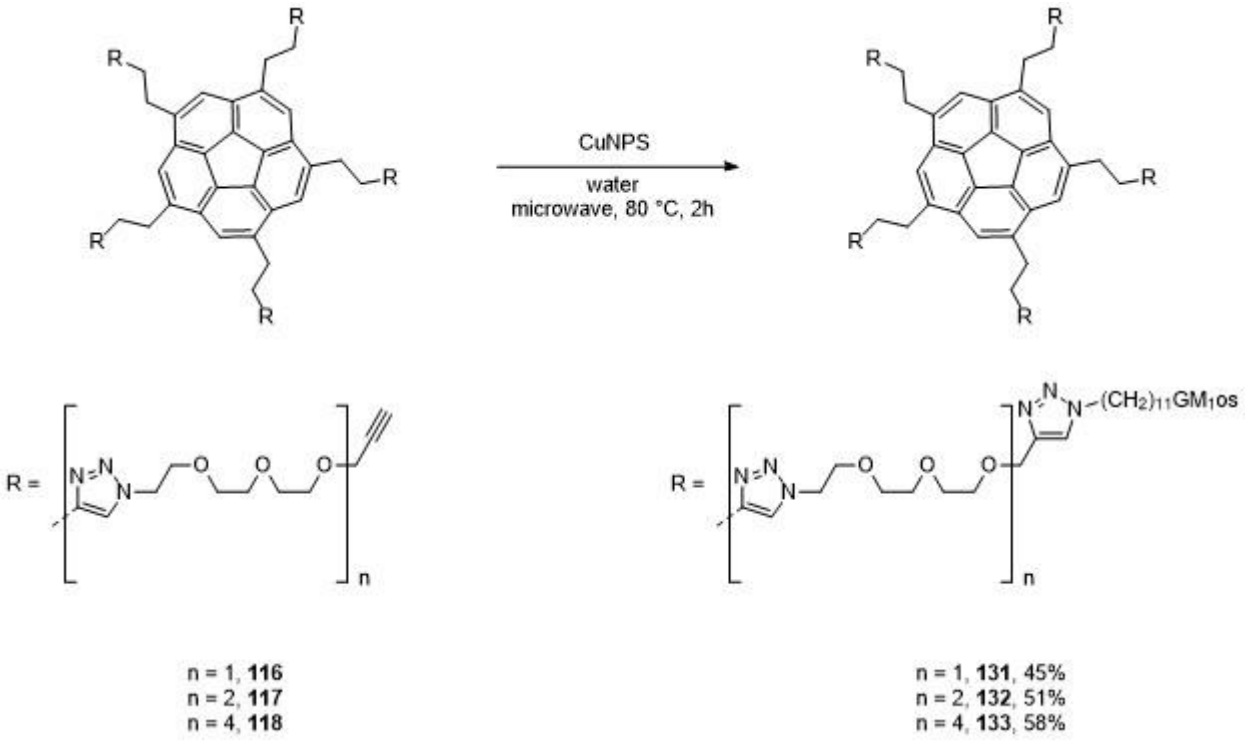

Scheme 5.8. Synthesis of GM1os-functionalized corannulene-based CT inhibitors **131** – **133**.

5.2.2. INHIBITION ASSAY

The inhibition efficiencies of corannulene-based CT binders **122** – **125** and **131** – **133** towards the B-subunit of CT (CT-B) were evaluated by enzyme-linked immunosorbent assay (ELISA) on 96-wells plate, in which each well was coated with native GM1. [150] Following a logarithmic serial dilution, solutions of each of the pentakis-saccharide corannulenes were mixed with CTB-HRP (*HorseRadish Peroxidase*) and incubated at room temperature for 2 hours and then transfered in the GM1-coated wells. The unbound CTB-HRP-corannulene complex were removed by washing. The amount of CTB-HRP on each well was determined by colorimetric analysis after addiction of ODP (*o*-phenylenediamine) and hydrogen peroxide (Scheme 5.9). [121]

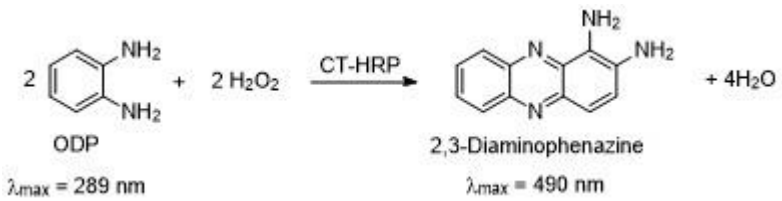

Scheme 5.9. Oxidation of ODP catalyzed by CTB-HRP.

Solubility issues at concentrations higher than 1 mM limited the experiments intended to find the IC_{50} (half maximal inhibitory concentration) value for galactose-based compounds **122** – **125**. [121] When compared to previously reported IC_{50}-values for multivalent CTB ligands functionalized with galactose, [47,139–141] these concentrations should not have been limiting. One hypothesis to account for this observation is that supramolecular aggregation of these amphiphilic molecules competes against binding to CTB. If the formation of the supramolecular assemblies is thermodinamically and kinetically favored over the interaction with CTB, the competition of these two processes might be a plausible explanation for the unexpected results obtained from the ELISA assays.[121] The investigation on the aggregation of pentakisgalactose derivative **100** will be discussed in details in Session 5.3.

ELISA-type assay on GM1os-functionalized inhibitors **131** – **133** showed high, nanomolar inhibitory potencies (Figure 5.4, Table 5.1).

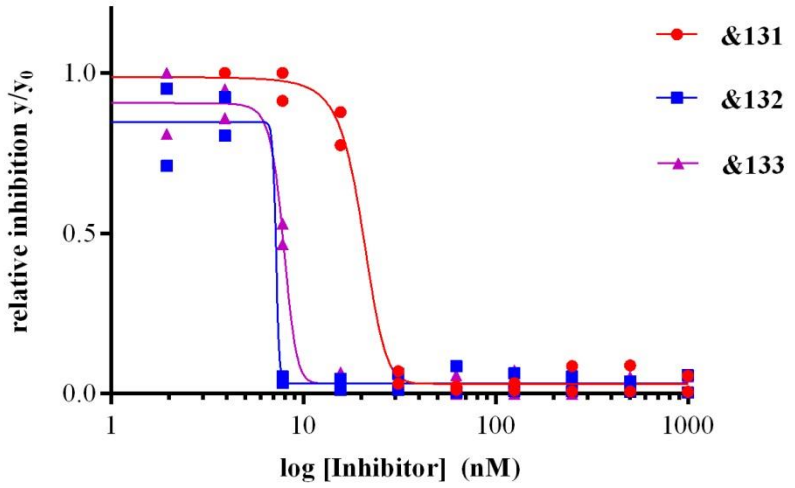

Figure 5.4. Fitted inhibition curves of GM1os-functionalized inhibitors **131**, **132** and **133**.

Compound	IC_{50} (nm)	RIP	Hill coefficient
131	25 ± 4	770	14 ± 5
132	5 ± 2	3700	9 ± 7
133	7.3 ± 0.9	2600	3.2 ± 0.6

Table 5.1. Inhibitory potency of pentakisGM1 corannulene-based ligands towards CTB.

The pentavalent GM1os-functionalized inhibitors **131** – **133** bind CTB at lower IC_{50} values than the monomeric GM1os. [143] The lowest IC_{50}-value measured is for **132** with an inhibition potency that is nearly 4000 times stronger than that of the monomeric GM1os. [143] The lower binding affinity for CTB by compounds **131** and **133** is most probably due to the effects related to the linker length: if the linker is not long enough (compound **131**), not all of the five ligands can simultaneously bind the five binding sites of CTB. In the opposite case (*i. e.* compound **133**), binding would lead to a substantial ordering in the chain, making it entropically less favorable, while enthalpically the necessary folding of the longer linkers to enable binding of CTB by the GM1os fingers might create sufficient steric hindrance to cause an increased IC_{50}-value. A further complicating factor is the possibility that also GM1os derivatives undergo to supramolecular aggregation that competes with binding to CTB and results in apparent higher inhibitory concentrations.

In the assay, more information about the cooperativity of binding can be obtained from the Hill coefficients. [151] Hill plots have been used as a method to assess cooperativity in binding of a multivalent ligand to a multivalent receptor [152] (Hill coefficient >1 and <1 being diagnostic for positive and negative cooperativity, respectively).Interestingly, monovalent binders **130** shows negative cooperativity with a Hill coefficient of around 0.5: [143] after the first molecule of **130** binds to CTB, subsequent molecule of the ligand binds less strongly. For the pentavalent-GM1os inhibitors **130**, **131** and **132** the Hill coefficients calculated are higher than 1, meaning that the binding event of these ligands is a cooperative phenomenon.

However, other studies criticized this approach showing that attribution of a Hill coefficient higher than 1 to positive cooperativity is not always justified. [153] The cooperativity of CT binding has been previously claimed in calorimetric experiments. [154] However, it is not fully clear whether the effects observed for these compounds are in line with such claim. The observation depicted in Figure 5.4, low IC_{50}-values and Hill coefficients >1, can indicate cooperative binding of the pentavalent inhibitors to CTB. On the other hand, they could also be result of increased local concentration of the ligands due to multivalency of the inhibitors, making binding of each following arm easier compared to the very first. Isothermal titration calorimetry (ITC) experiments are required to clarify this issue.

Ceveats notwithstanding, **132** is as of yet one of the strongest multivalent CT inhibitors, [147,155] and display the power of combining the pentavalency with the natural ganglioside to reach optimal blocking of multivalent lectins. Design efforts to create systems that optimize spacer geometry and

avoid self complexation will likely lead to new derivatives with inhibitory concentrations more favorably comparable to other previously reported GM1os-based inhibitor.

5.3. SUPRAMOLECULAR ASSEMBLING STUDIES ON PENTAKIS-GALACTOSIDE **100**

The formation of aggregates in water of **100** was investigated by ^{1}H-NMR, absorption and emission spectroscopy. Compound **100** is an amphiphilic molecules since it display an hydrophobic part (corannulene core) and a strong hydrophilic rim (galactoses); this property might lead to the formation of supramolecular aggregates in aqueous solution.

The thermodynamic behavior of the aggregation phenomenon was studied by ^{1}H-NMR experiments. The chemical shift (δ_{obs}) of the five homotopic hydrogens atoms on corannulene core was measured at different concentrations and temperatures. A downfield shift is observed upon increasing of the temperature of **100** (Figure 5.5).

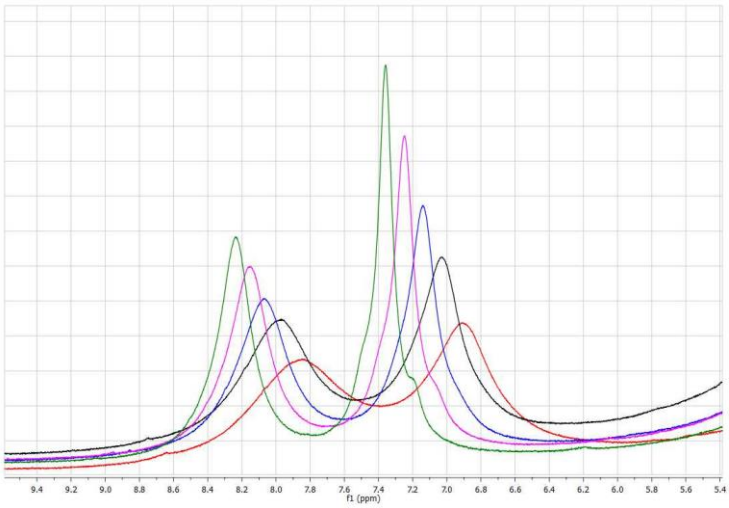

Figure 5.5. Aromatic region of ^{1}H-NMR spectra of a solution 0.28 mM of **100** at 300 K (red), 310 K (black), 320 K (blu), 330 K (violet) and 340 K (green).

The ^{1}H-NMR spectra of several solutions of **100** with a broad range of concentration were measured at different temperatures. The association constant K_a of the aggregation of **100** in water was calculated at each temperature by non-linear least-square regression based on the equal *K* or isodesmic (K_E) model of indefinite self-association described by Martin (Figure 5.6). [156] This model assigns all equilibrium constants for self-association of all the *n*-mers as equal.

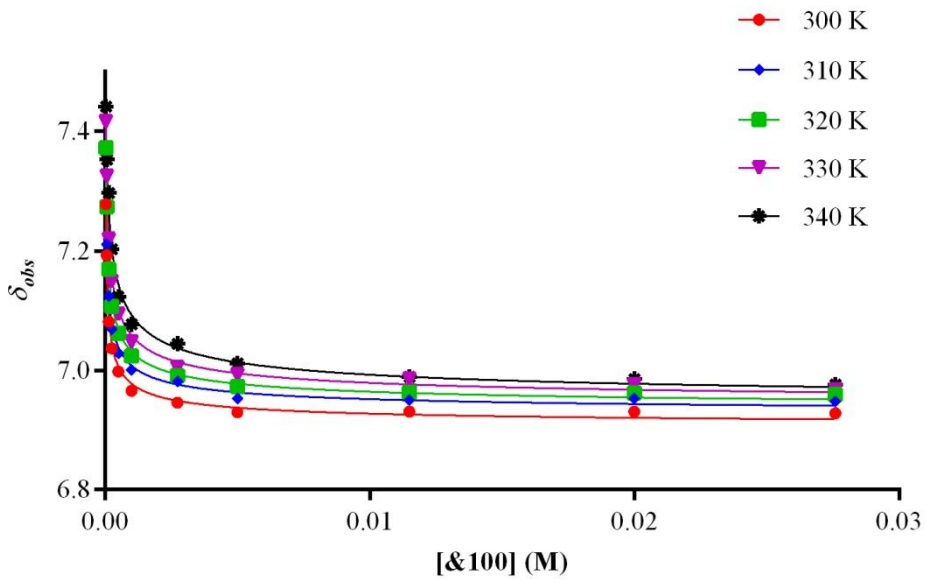

Figure 5.6. Fitted curves of δ_{obs} values of corannulene hydrogens measured for several solutions of **100** at different temperatures.

The K_a-values (Table 5.2) where obtained by fitting the experimental data with Equation 5.1, where δ_{obs} is the observed chemical shift, δ_{mon} is the chemical shift of monomer, K_a is the association constant, c is the molar concentration of the sample, and Δ is the different of the chemical shift of the monomer and the aggregate.

$$\delta_{obs} = \delta_{mon} - \Delta\left\{1 + \frac{\left[1 - \sqrt{(4K_a c + 1)}\right]}{2K_a c}\right\}$$

Equation 5.1

T (K)	K_a (x10^4)
300	20 ± 10
310	5 ± 2
320	6 ± 2

330	3 ± 1
340	1.4 ± 0.3

Table 5.2. Association constant K_a for the aggregation of **100** at different temperature.

The aggregation number *N*, *i. e.* the number of the monomers included in the aggregates, was determined using Equation 5.2, where δ_{obs} is the observed chemical shift, δ_{mon} is the chemical shift of monomer, K_a is the association constant, *c* is the molar concentration of **100** and *N* is the aggregation number.

$$\ln[c(\delta_{mon} - \delta_{obs})] = N \ln\left[c\left(\delta_{obs} - \delta_{agg}\right)\right] + \ln K_a + \ln N - (\mathrm{N} - 1)\ln\left(\delta_{mon} - \delta_{agg}\right)$$

Equation 5.2

The aggregation number was estimated to 2, assuming that **100** is in equilibrium between the monomer and the aggregate. [157]

The thermodynamic parameter ΔH (-13 ± 1 kcal mol^{-1}) and ΔS (-18 ± 4 cal mol^{-1}) of the dimerization process were determined by van't Hoff plot from the K_a calculated at various temperatures (Figure 5.7).

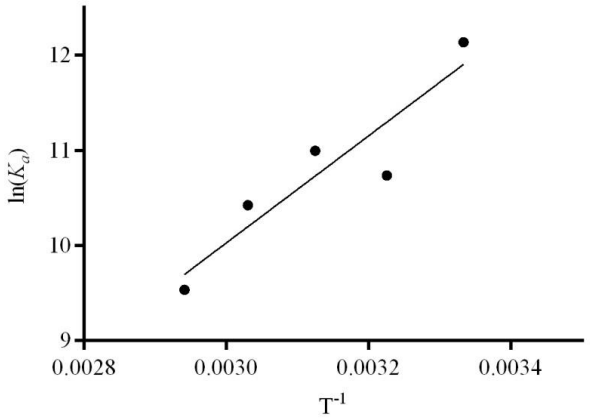

Figure 5.7. Van't Hoff plot for compound **100**.

Surprising, the driving force for the aggregation of **100** in solution is not the increasing of the entropy of the system (hydrophobic effect), like for the most amphiphilic molecules, but the exothermicity of the process. This suggest that other kind of intermolecular interaction are involved

like dipole-dipole interaction, π-π stacking, hydrogen bonds, nonspecific van der Waals interactions, electrostatic interactions and repulsive steric forces.

Further information about the geometry and the organization of the corannulene cores in the dimeric system can be obtained by absorption and emission spectroscopy analysis.

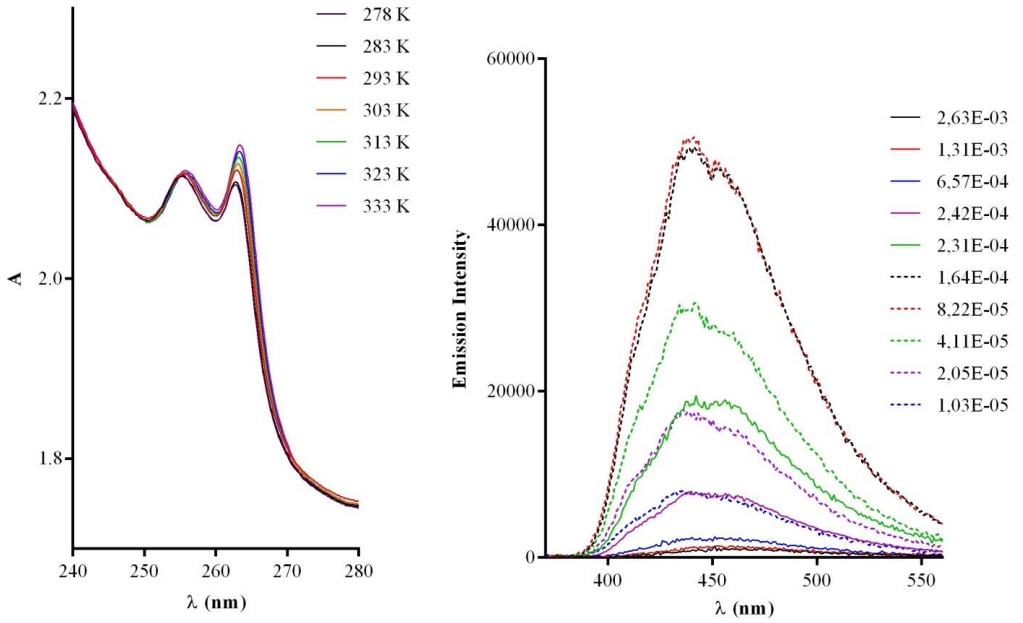

Figure 5.8. Absorption (left) and emission spectra (right) of compound **100** in water.

The hypsochromic shift in the absorption spectra (Figure 5.8 left), upon increasing of the temperature, and the quenching of the fluorescence (Figure 5.8 right) due to the increasing of the concentration of **100** suggest the formation of H-dimers in solution. [158,159] CD analysis of this aggregation did not show any significant signal in the range of the studied concentration, because of the low signal-to-noise ratio obtained at these conditions.

5.4. Conclusion and Outlook

In conclusion, this chapter reports powerful method for the synthesis of a new class of Cholera Toxin inhibitors with a design based on a C_5-symmetric pentasubstituted corannulene as core unit equipped with galactose and GM1os as CT binders. The Cu nanoparticles catalyzed and microwave-assisted CuAAC reaction described in Chapter 4 were employed for the conjugation of the monovalent CTB ligands (galactose and GM1os) onto corannulene core via azide-presenting PEG-linkers of various length. It was proven that the presence of such kind of linkers improves the

water solubility of the corannulene-based inhibitors when compared to the one that presents an aromatic linker (compound **105**). The potent CTB inhibition in the nanomolar range observed for the penta-GM1os corannulenes, **131** – **133** proves that multivalent systems functionalized with strong CTB binders represent a solid strategic approach for the synthesis of CT inhibitors with high potency in comparison with previously reported mono- and multivalent inhibitors.

The developed method allows the use of *sym*-substituted corannulenes as a possible core unit for the development of new multivalent binders of Cholera Toxin or other possible biological targets that rely on multivalent binding of their target ligand. Further investigation should be performed on the effect of the length of the linker to the inhibition potency: the PEG-like linker can be replaced by a polyproline moiety. This new system is highly hydrophilic, rigid and its length can be easily controlled changing the number of proline units. Crystal structure analysis of CT with GM1os-based corannulene derivative should be performed in order to obtain better information regarding the stoichiometry of the binding phenomena of CTB with the pentavalent inhibitors.

6. C_5-SYMMETRIC PENTA-SUBSTITUTED CORANNULENE WITH GELATION PROPERTIES AND LIQUID CRYSTALLINE PHASE

6.1. INTRODUCTION

Liquid crystals (LCs) [160,161] are a state of matter intermediate between that of a crystalline solid and an isotropic liquid. The liquid crystalline state has been discovered more than 100 years ago when in 1888 Reinitzer [162] and Lehmann [163] investigated some esters of cholesterol. LCs posses many of the mechanical properties of an isotropic liquid, like high fluidity, inability to support shear, formation and coalescence of droplets. At the same time LCs are similar to crystalline solid in that they exhibit anisotropy in their optical, electrical and magnetic properties. [160] The most important property of a liquid crystal is its anisotropy.

LCs are found among a wide window of organic molecules and the role of molecular geometry on liquid crystals has been discussed by Gray. Certain structural features are often found in the molecule forming liquid crystal phases and they may be summarized as follow: [160]

(a) liquid crystallinity is more likely to occur if the molecule has flat segments;

(b) a fairly rigid backbone containing double bonds defines the long axis of the molecule;

(c) the existence of a strong dipole and easily polarizable groups in the molecule seems important;

(d) the groups attached to the extremities of the molecule give disorder to the system.

With its unique geometry, corannulene **1** is a good candidate as backbone for liquid crystalline molecule: it's a fairy rigid aromatic system and it has a dipole moment of roughly 5 D, [164] which is due to the different electron densities on the concave and convex π-face of **1**. Moreover, a material comprising derivatives of **1** ordered in a columnar manner might orient in an electric field and show ferroelectric properties. [165] Extended columnar order of corannulene core has been found in the solid state for few corannulene derivatives. [30,37,166]

In 2009 Aida [78] reported the synthesis of two decasubstituted corannulene derivatives **134** and **135** starting from decachlorocorannulene **46** (Figure 6.1). These compounds are able to form liquid

crystalline assemblies; in particular, compound **135** forms columnar hexagonal LC phase which responds to an applied electric field, giving rise to a homeotropic alignment of the hexagonal columns with respect to the electrode surface. [78]

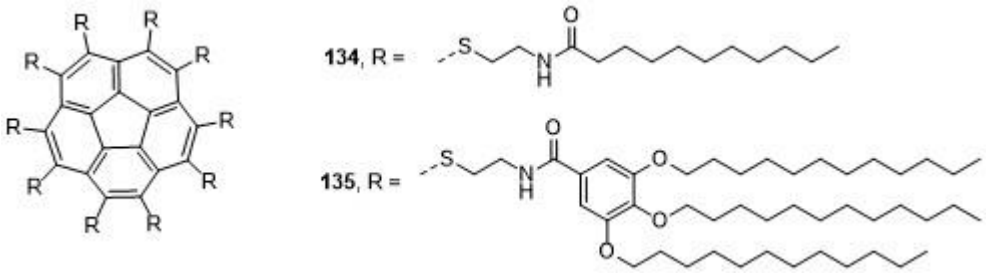

Figure 6.1. LC decasubstituted corannulene derivatives **134** and **135**.

6.2. *SYM*-PENTAKIS-LIPIDO CORANNULENE DERIVATIVES: SYNTHESIS AND PROPERTIES

The development on the synthesis of *sym*-pentasubstituted corannulene derivatives described in the previous chapters gave access to new classes of C_5-symmetric corannulenes. The easy preparation of the starting material **39** and the accessibility to a broad window of functionalized derivatives by high yielding procedures make *sym*-pentasubstituted corannulene derivatives possible new candidates for the preparation of LC materials instead of decasubstituted systems.

The structure features of pentakis-lipido corannulene derivatives makes this family of molecules a good candidate for the preparation of material showing a liquid crystalline mesophase. Three fatty acids with different alkyl chain have been chosen: oleic acid **136**, stearic acid **137** and heptanoic acid **138** (Figure 6.2). These three fatty acids were selected in order to study the effects of the nature of the alkyl chain (length and geometry) on the physical behavior of the corannulene derivatives of these compounds.

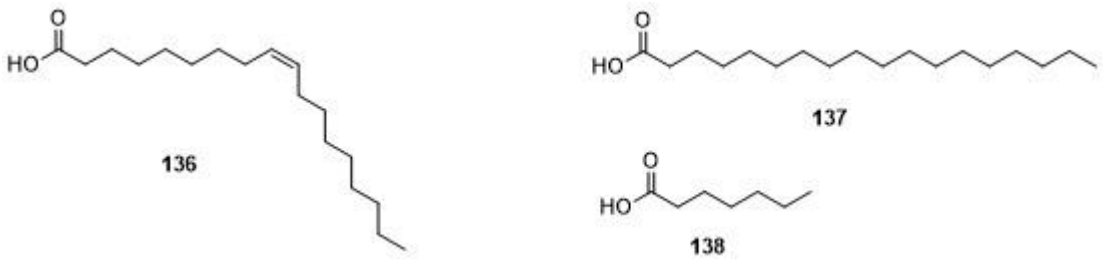

Figure 6.2. Selected lipids for the preparation of pentakis-lipido corannulene derivatives.

In order to be introduced on corannulene core by CuAAC procedure, acids **136**– **138** have to be functionalized in such a way that they bear an azido functional group. Moreover, Aida reported that the presence of amide bonds close to the aromatic core helps the formation of LC material. [78] Therefore, the introduction of the azidic and amidic moieties was achieved by condensation reaction of the acyl chlorides of **139** – **141** with 2-azidoethanolamine to give amide azides **95**, [119] **142** and **143** (Scheme 6.1).

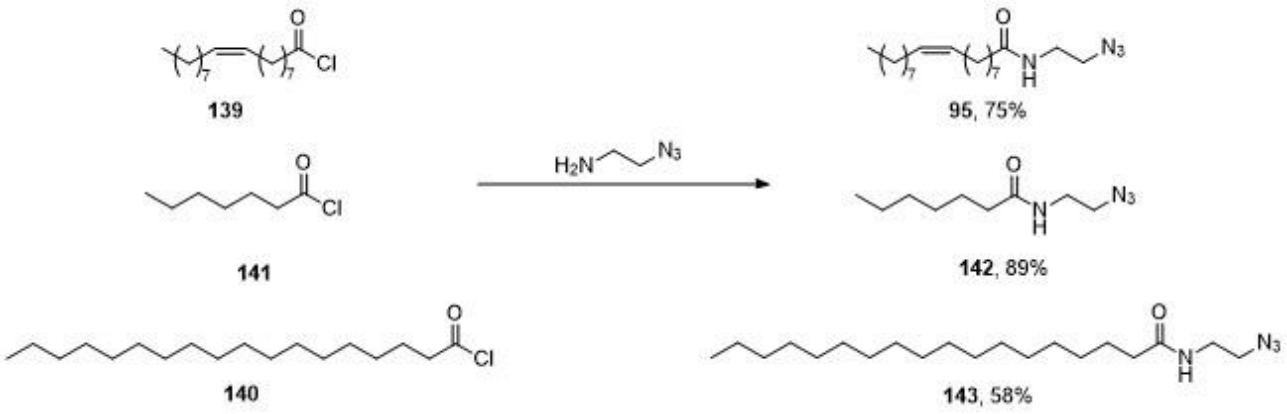

Scheme 6.1. Synthesis of lipid azides **95**, **142** and **143**.

Pentakis-lipido corannulene derivatives **94**, **144** and **145** were synthesized by CuAAC reaction of *sym*-pentabutynyl corannulene **67** with azide **95**, **142** and **143**, respectively (Scheme 6.2). [120]

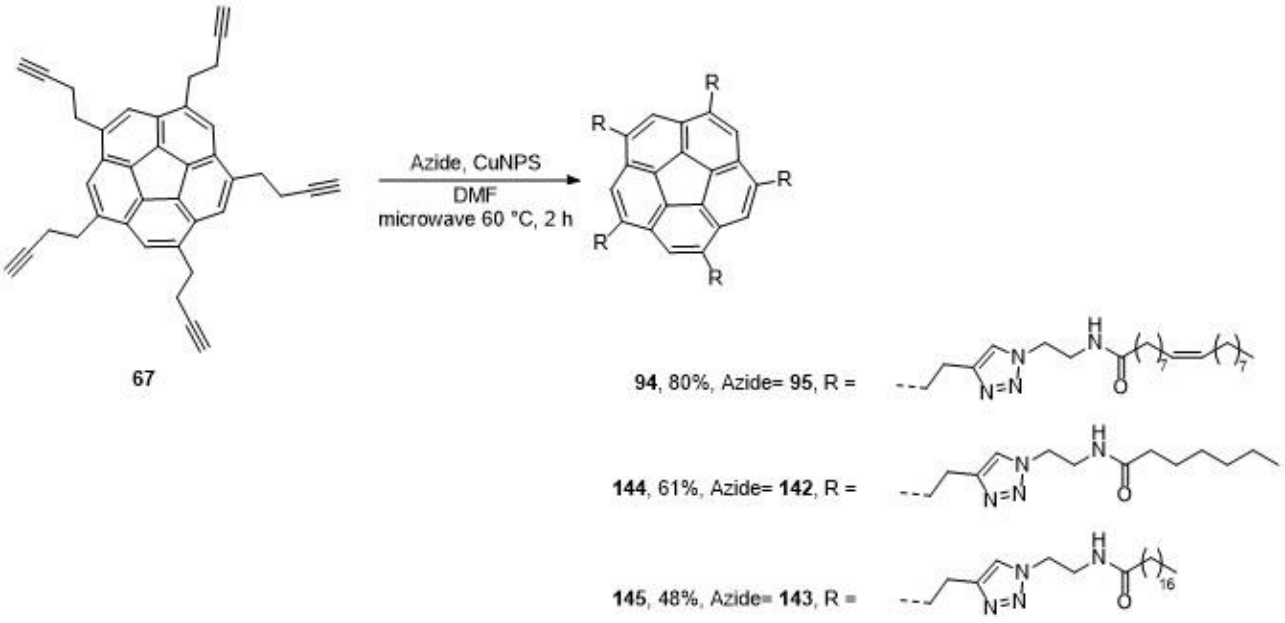

Scheme 6.2. Synthesis of C_5-symmetric lipido corannulenes **94**, **144** and **145**.

6.3. Physical Properties Study on Pentakis-Lipido Corannulene Derivatives **94**, **144** and **145**

6.3.1. Differential Scanning Calorimetry and Polarized Optical Microscopy

Differential scanning calorimetry or DSC is a thermoanalytical technique in which the difference in the amount of heat required to increase the temperature of a sample and reference is measured as a function of temperature. From DSC measurements, information regarding the number, type, transition temperature and enthalpy change of phase transition can be easily determined.

Polarized optical microscopy (POM) is an optical microscopy technique that involves the irradiation of the sample with polarized light. POM technique is capable of providing information about the birefringence nature of the sample distinguishing between isotropic and anisotropic materials, thus POM finds application in the study of liquid crystalline compounds.

In order to prove the formation of liquid crystalline phase, the thermal and optical behavior of corannulene derivatives **94**, **144** and **145** were initially investigated by DSC and POM. While neither thermal signatures characteristic of phase transition in the DSC scan nor birefringence in

POM were not observed for pentakislipido **144**, compounds **94** and **145** present different phase transitions in the DSC scan and birefringence in POM (Figure 6.3 and Figure 6.4). [120]

For corannulene derivative **94**, thermal signatures characteristic for phase transition were observed at 132 °C and at 99 °C in the DSC cooling scan, and the birefringence texture in POM images is consistent with the presence of liquid crystalline phases below 132 °C (Figure 6.3). This study shows that **94** exists in three different phases: an anisotropic phase below 99 °C, a second anisotropic phase between 99 °C and 132 °C and an isotropic liquid phase above 132 °C (Figure 6.3). [120]

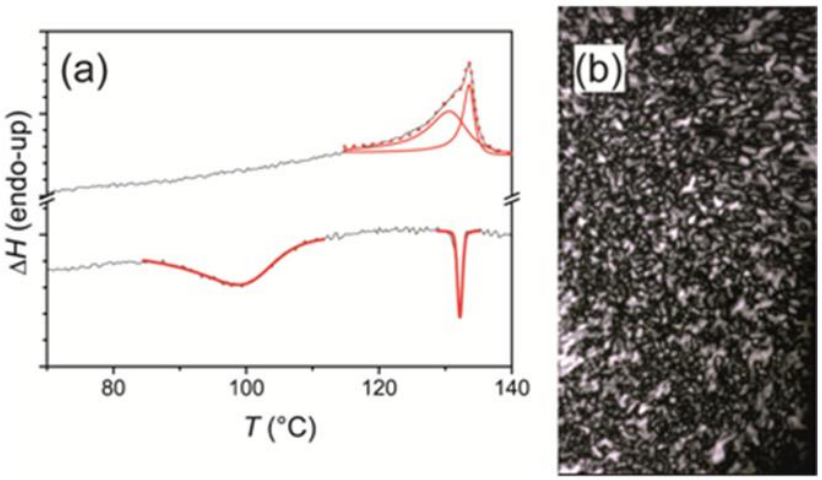

Figure 6.3. (a) DSC of compound **94** at 2 K min^{-1} and (b) POM image of **94** at 20 °C. The birefringent phase proves the presence of a liquid-crystalline phase at room temperature.

For compound **145**, DSC cooling scan reveals phase transitions at 30 °C and at 80 °C; the birefringence of the liquid phase indicates the presence of liquid-crystalline phases at temperature higher than the melting at 30 °C. Therefore, **145** exists in three phases: an isotropic solid phase at temperature lower than 30 °C, an anisotropic phase between 30 °C and 80 °C and a second anisotropic phase above 80 °C (Figure 6.4). [120]

The results obtained by DSC and POM measurements suggest that the thermal behavior of the pentakis-lipido corannulenes is strongly influenced by the nature (length and geometry) of the aliphatic chain attached to corannulene core.

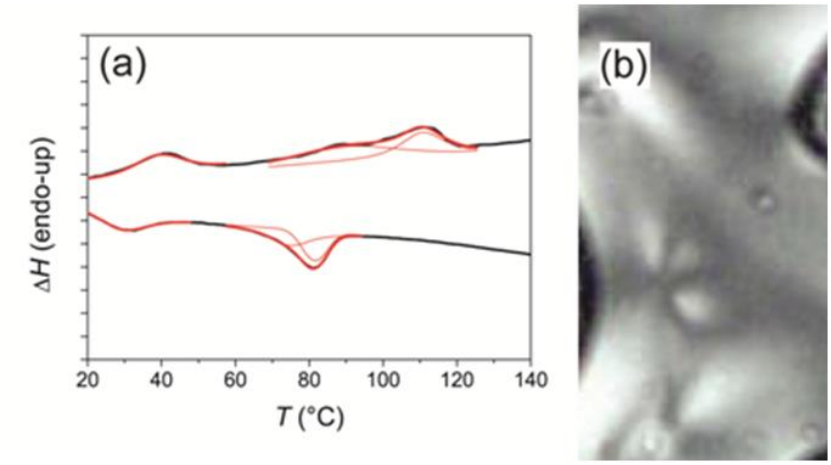

Figure 6.4. (a) DSC of compound **4** at 2 K min^{-1} and (b) POM image of **145** at 40 °C after melting, indicating a liquid-crystalline phase.

6.3.2. Small- and Wide-Angle X-ray Scattering

Small- and wide-angle X-ray scattering (SAXS and WAXS) are techniques where the scattering of X-rays by a sample, which shows inhomogeneities in the nm-range, is recorded at small and wide angles. The scattering gives information about the shape and size of molecules, characteristic distances of partially ordered materials, pore size, etc.

SAXS and WAXS are one of the most powerful techniques for investigating the structure of liquid crystalline phases. Since such phases possess long-range structural order, interaction with electromagnetic radiation of a suitable wavelength results in the generation of diffraction patterns. These are characterized by constructive interference when Bragg's law is fulfilled. From the relation between the diffraction peaks, the nature of the liquid crystalline phase can be identified. When the composition of the sample is known together with the nature of liquid crystalline phase, X-ray diffraction data can be used to extract information about the characteristic dimension in the liquid crystalline structure. Also with system without long-range order, SAXS and WAXS may provide useful information, e.g., on the size of micelles, liposomes and other disperse system, as well as on gel structure.

SAXS and WAXS were performed in order to obtain more information about the supramolecular organization on corannulene derivatives **94**, **144** and **145** at room temperature. [120] In the wide-angle region of X-ray scattering pattern of compound **94**, an isotropic halo indicates the liquid-like behavior of the component and the absence of a specific π-interaction peak indicated the absence of π-staked supramolecular organization of the molecules in this phase (Figure 6.5a). In the small-

angle region, the appearance of a strong reflection followed by a weak second order reflection at q_2:q_1 of 2:1 suggests a lamellar organization of the molecules in this liquid crystalline phase (Figure 6.5b). The azimuthally integrated X-ray scattered intensity shows the Bragg's reflections of lamella with a layer-to-layer distance of 4.4 nm after sample annealing (Figure 6.5c). [120]

SAXS and WAXS investigation of corannulene derivative **144**, bearing a shorter alkyl tails than derivative **94** and **145**, reveal only a diffuse peak, indicative of a correlation hole at 2.5 nm and corresponding to chemical heterogeneities on the scale of the molecule (Figure 6.5c). [167] These results further confirm that the length of the alkyl chains of fatty acid functionalized corannulene derivatives plays a central and important role on the phase behavior and the molecular organization for this class of five-fold symmetric corannulene derivatives. [120]

The SAXS and WAXS studies of compound **145**, which is the direct saturated analog of **94**, reveal the presence of a partially crystallized phase at room temperature (Figure 6.5c) suggesting that, not only the length, but also the geometry of the alkyl chain dictates the physical properties of C_5-symmetric pentalipid corannulene derivatives. [120]

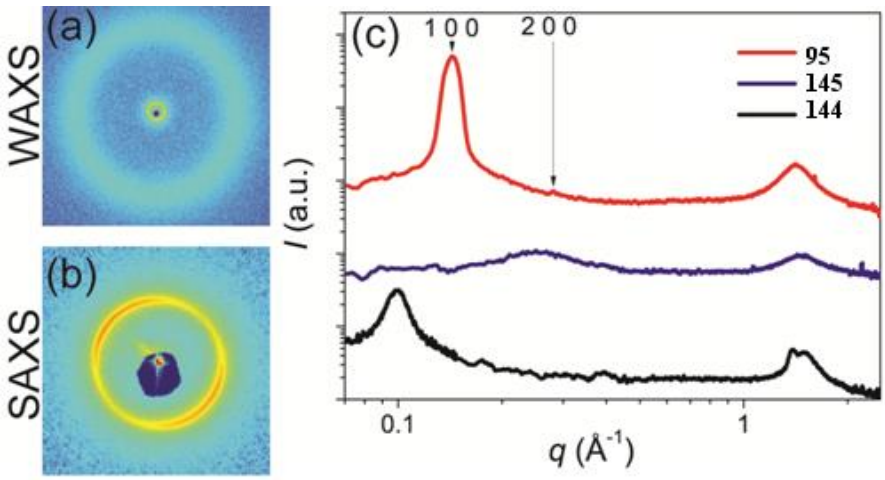

Figure 6.5. (a) 2D Wide and (b) Small Angle X-ray Scattering (WAXS, SAXS) patterns of **94** and (c) the 1D scattering intensity distribution of **94** (red), **144** (black) and **145** (blu) after annealing.

6.3.3. Transmission Electron Microscopy

Transmission electron microscopy (TEM) is a microscopy technique whereby a beam of electrons is transmitted through an ultra-thin specimen, interacting with the specimen as it passes through. An image is then formed from the interaction of the electrons transmitted through the specimen; the image is then magnified and focused onto an imaging device. TEMs are capable of

imaging at a significantly higher resolution than light microscopes, owing to the small de Broglie wavelength of electrons; this enables to examine fine details of the specimen.

After DSC, POM and SWAXS measurements, TEM images of compound **94** were performed in order to visualize and confirm the lamellar structure suggested from X-ray scattering pattern. TEM imagine (Figure 6.6a) show a very long-range ordered lamellar phase, with *d*-spacing of 4.1 – 4.3 nm measured after Fourier transformation, in good agreement with the X-ray analysis. [120]

All the results obtained from investigation on **94**, suggest a molecular model in which the microphase separation of the corannulene core and the symmetric substituents drives the molecule into a lamellar structure with partially interdigitated alkyl chains (Figure 6.6b) and reduced symmetry compared to the molecule itself.

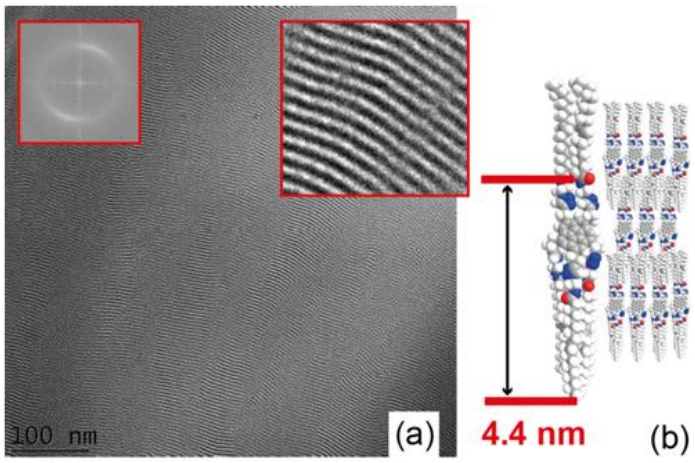

Figure 6.6. (a) Transmission Electron Microscopy (TEM) image of compound **94** with a lamellar structure. The insets show the Fourier transformation (FFT) and a zoom-up of a lamellar domain (edge size of 50 x 45 nm). (b) Possible molecular model of the molecular organization in the lamellar structure.

6.4. GELATION PROPERTIES OF COMPOUNDS **94**, **144** AND **145**

In 1999 Feringa and coworkers [168] reported the synthesis of 1,2-diaminobenzene derivatives functionalized with aliphatic or aromatic chains and their behavior as gelators for organic solvents was described. It has proven that the formation of intermolecular H-bonding network is the key phenomena for the gelating properties of this class of compounds. The similarity of the compounds described by Feringa *et. al.* with the the corannulene derivatives **94**, **144** and **145** (*i.e.* aromatic core, amide groups and long aliphatic chains) gave the motivation to investigate the gelation properties. In order to study the propensity of these compounds for molecular aggregation, the gelator behavior

of **94**, **144** and **145** was screened in organic solvents (Table 6.1), ethanol/water (Table 6.2) and isopropanol/water mixture (Table 6.3). [158,169]

Solvent	**94**	**144**	**145**
Heptane	I	I	I
Hexane	I	I	I
Cyclohexane	G (8)	I	G (10)
Methylcyclohexane	G (15)	I	S (> 40)
Benzene	VS	I	S (> 40)
Toluene	S (> 40)	I	S (> 40)
CCl_4	S (> 40)	I	S (> 40)
$CHCl_3$	S (> 40)	S (> 40)	S (> 40)
CH_2Cl_2	S (> 40)	S (> 40)	S (> 40)
THF	S (> 40)	S (> 40)	S (> 40)
Acetone	S (> 40)	S (> 40)	I
Ethyl Acetate	S (> 40)	I	I
Acetonitrile	I	I	I
Ethanol	S (> 40)	S (> 40)	S (> 40)
Isopropanol	S (> 40)	S (> 40)	S (> 40)
Water	I	I	I

Table 6.1. Gelation test for compounds **94**, **144** and **145** in common organic solvents. The following abbreviations are used: gelation: G (minimum gelation concentration in mg compound per mL solvent); insoluble: I; soluble (solubility in mg mL^{-1}): S; viscous solution: VS.

Water : EtOH ratio	**94**	**144**	**145**
90:10	S (< 40)	S	S (< 40)
75:25	I	S	I
60:40	I	S (< 40)	I
50:50	I	I	I
25:75	I	I	I

Table 6.2. Gelation test for compounds **94**, **144** and **145** in water/ethanol solutions. The following abbreviations are used:); insoluble: I; soluble (solubility in mg mL^{-1}): S.

Water : IPA ratio	94	144	145
90:10	S (> 40)	S	S (< 40)
75:25	S (< 40)	S	S (< 40)
60:40	I	S	I
50:50	I	S (< 40)	I
25:75	I	I	I

Table 6.3. Gelation test for compounds **94**, **144** and **145** in water/isopropanol solutions. The following abbreviations are used:); insoluble: I; soluble (solubility in mg mL^{-1}): S.

While corannulene derivative **144** does not show any gelation behavior, both compounds **94** and **145** form organogel in cyclohexane (1 w/w%) and, only for **94**, also in methylcyclohexane (2 w/w%) (Figure 6.7). [120] Interestingly, compounds **94** and **145** don't display gelator properties neither in benzene or toluene, which are isosteric to cyclohexane and methylcyclohexane, respectively. A possible explanation of this, is the formation of π-stacked or π-interactions in the gelation process which can be prevented by the presence of aromatic solvents, like benzene and toluene.

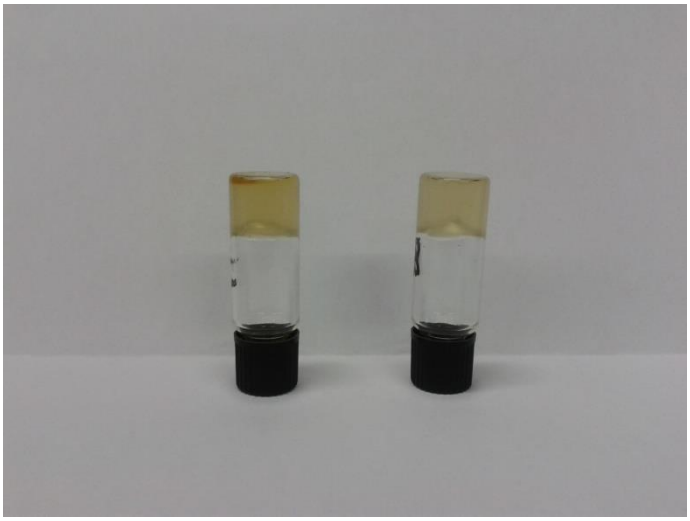

Figure 6.7. Gel in of **94** (left) and **145** (right) in cyclohexane at 10 mg mL^{-1}.

The results obtained show that, like for the thermal behavior of the neat substances, the gelation properties are strongly influenced by the length of the alkyl chains and, in minor way, by the geometry of these.

In order to study the influence of hydrogen bonding on the formation of the gel, FTIR spectra were measured as a function of concentration of **94** and **145** in cyclohexane. It was observed that, upon increasing of the concentration of these compounds and gelation, neither of the two amide bands (C=O, N-H) were shifted (Table 6.4). [120] Thus, no evidence for the formation of hydrogen bonds in the gelation process was found, suggesting that other phenomena are involved in this process and responsible for the gelation.

	94		**145**	
Concentration (mg mL^{-1})	ν NH (cm^{-1})	ν CO (cm^{-1})	ν NH (cm^{-1})	ν CO (cm^{-1})
1.0	3298	1649	3316	1646
5.0	3297	1650	3314	1647
15.0 (gel)	3300	1652	3317	1646
20.0 (gel)	3298	1647	3314	1645

Table 6.4. FTIR ν values of NH and CO bonds for solutions and gel of **94** and **145** in cyclohexane.

In order to obtain further information about the orientation of corannulene cores with respect to each other, UV-vis and emission spectroscopy measurements were performed (Figure 6.8). [120] Upon increasing of the gelator material, a quenching of the fluorescence was observed. However, the absorption spectra do not show any hypsochromic or bathochromic shift, which augurs poorly for the existence of π-stacked structures in the gel as well as *H*- and *J*-aggregate.

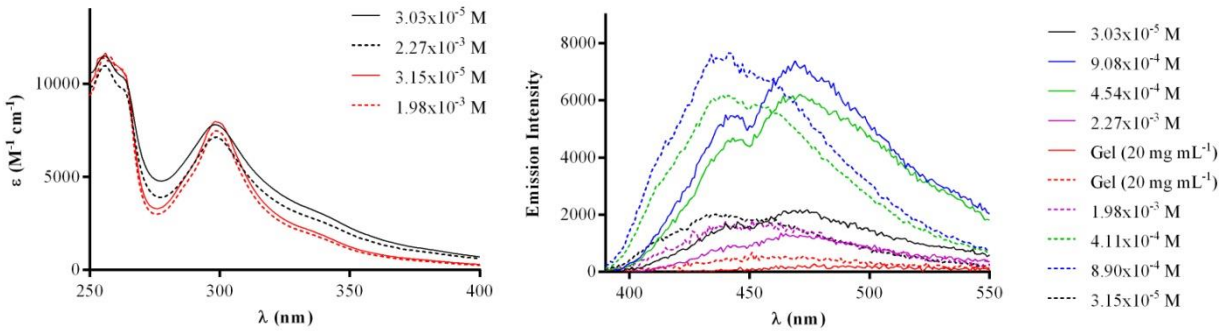

Figure 6.8. Left: UV-vis spectra of **94** (solid lines) and **145** (dashed lines) in cyclohexane. Right: Emission spectra of **94** (solid lines) and **145** (dashed lines) in cyclohexane.

Small and wide angle X-ray scattering measurements prove the absence of any ordered supramolecular organization in the gels; POM studies demonstrate the isotropic nature of the gels.

6.5. CONCLUSION AND OUTLOOK

The thermal behavior and gelation properties of pentakis-lipido-conjugated derivative of corannulene have been investigated. The results obtained and here described show that the nature of the hydrocarbon chains influence the phase behavior and the gelation properties of C_5-symmetric pentakislipido-corannulene derivatives. Specifically, the derivative functionalized with oleyl chains (**95**) forms gels in cyclohexane and methylcyclohexane, and, as a neat substance, exhibits a room temperature liquid.crystalline phase with lamellar order and a 4.4 nm layer-to-layer spacing. In contrast, the presence of short saturated chains lead to the absence of appreciable LC or gelation properties, while the saturated analog of **95** appears in a partially crystallized phase at room temperature and forms gels only in cyclohexane. Further study should be performed in order to gain more information regarding the effect of the length, geometry and nature of the aliphatic chain on the thermal behavior of this class of corannulene derivatives. VT-FTIR measurements can lead to a better understanding of the role of the amidic groups in the phase behavior of lipido-conjugated corannulene derivatives. Further investigation should be planned in order to study the behavior of this family of corannulenes under effect of electric or magnetic field.

The promising results obtained and the versatility of the synthetic strategy encourage the synthesis of a wide library of molecularly engineered *sym*-pentasubstituted corannulene derivatives suitable for numerous material application. Due to the structural features of these lipido derivatives of corannulene, the behavior of these compound at the air/water interface and the physical and electrochemical properties of their Langmuir-Blodgett films are being studied.

7. Five-Fold Symmetric Penta-DNA Corannulene: Synthesis and Investigation of Its Assembling Behavior

7.1. Introduction

The controlled construction of three-dimensional (3D) architectures with a designed supramolecular structure is an important and long-standing goal in the field of supramolecular chemistry. 3D architectures have diverse potential as scaffolds for molecular organization, [170] gas storage materials, [171] drug delivery vehicles, [172] templates for the development of new materials [173] and tools for encapsulating and controlling the reactivity of guest molecules. [174] In particular, noncovalent nanostructure are an interesting goal due to their thermal reversibility which is an important feature for guest releasing; promising results have been documented for amphiphilic systems functionalized with oligopeptide, [175] nucleosides [176] and carbohydrates. [177]

Over the past decades, a large number of methods for the formation of noncovalent nanostructure have been developed; [178] in particular, promising results were obtained using a DNA-functionalize approach. The pioneering work reported by Seeman [179] shows the potential of annealing complementary DNA strands as a high specificity approach to preparing nano-object with desired structure and symmetry. The linear ad rigid nature of double stranded DNA (dsDNA), the possibility to perform enzymatic amplification or modification of DNA strands and the accessibility to synthetic and chemically modified oligonucleotides all offers great advantages to a DNA-functionalized approach.

7.2. *Sym*-Pentasubstituted Corannulenes as Building Unit for the Construction of Icosahedral Supramolecular Arichitectures

The five-fold symmetry and the bowl-shaped aromatic core of *sym*-pentasubstituted corannulene derivatives suggest the potential application of these compounds as building units for the formation of icosahedral supramolecular assemblies by interaction of twelve self-recognizable C_5-symmetric building blocks (Figure 7.1). Each corannulene core will be positioned at each vertex of the

icosahedrons; the five-fold symmetry of *sym*-pentasubstituted corannulenes provide the correct geometry while the bowl-shaped aromatic core will provide the curvature needed for closure of the system in an icosahedral fashion.

Although icosahedra are found in nature and in inorganic clusters, [180] the synthesis of such structures from organic building blocks has never been achieved which makes the formation of such kind of assembling a challenging and interesting goal. Icosahedral nano-object can find application as host in host-guest system and be used as nano-carrier for gases, drugs, small proteins or short genes.

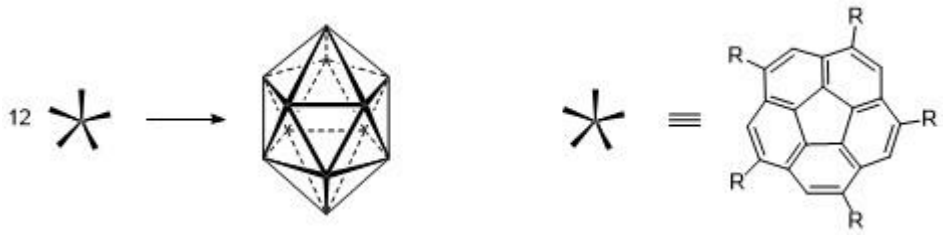

Figure 7.1. Formation of icosahedral polyhedra by assembling of twelve C_5-symmetric units based on corannulene core.

In 2007 Keinan and coworkes [181] conducted molecular dynamics simulation on corannulene-based molecule to demonstrate the formation of icosahedral structures. They also suggested several corannulene derivatives that can assembly into supramolecular structures using different binding mechanisms: hydrogen bonding, metal binding and formation of disulfide bonds (Figure 7.2).

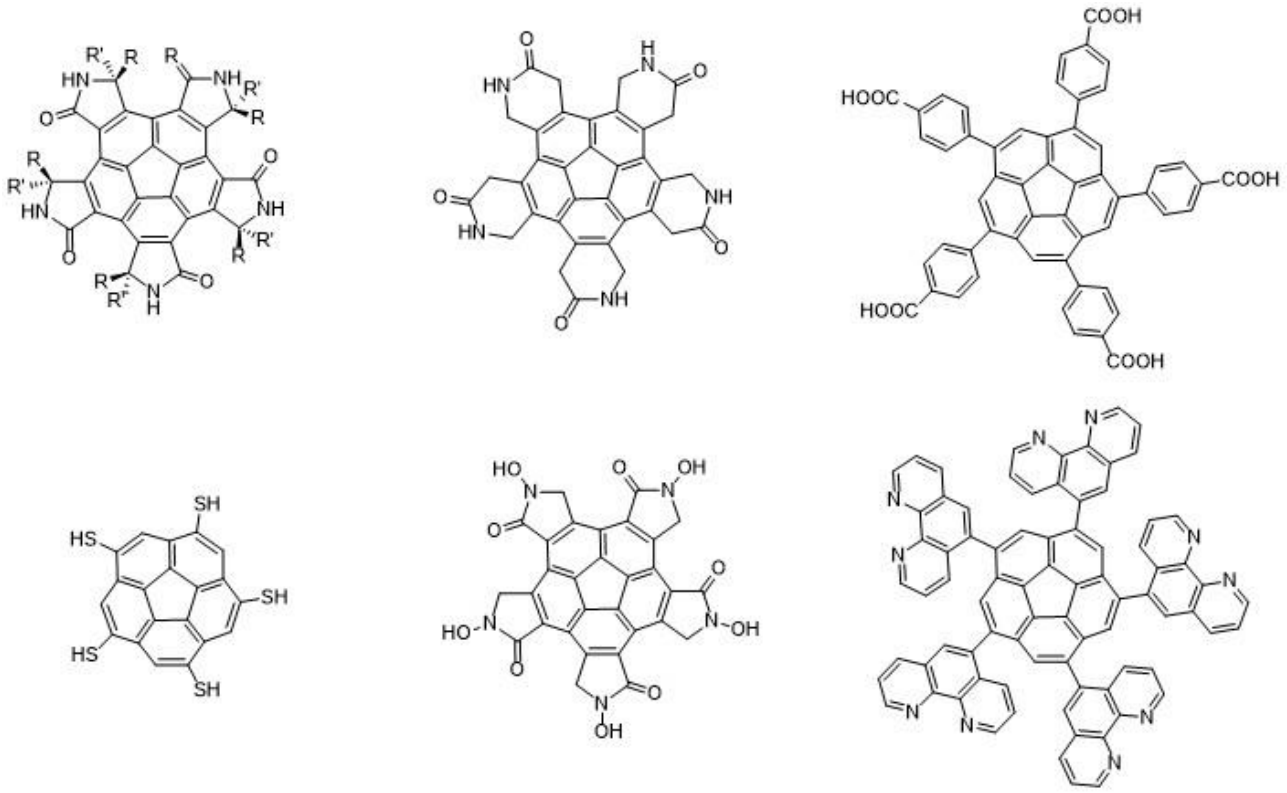

Figure 7.2. Proposed structures of corannulene-based building blocks

The development on the synthesis of five-fold bioconjugated corannulene derivatives and the many reported work on the formation of supramolecular architecture using DNA gave the motivation to design and prepare a DNA-functionalized corannulene which can act as building unit for the assembling of supramolecular construct with icosahedral symmetry.

7.3. DESIGN AND SYNTHESIS OF *SYM*-PENTA(OLIGONUCLEOTIDE) CORANNULENE DERIVATIVE

Four general strategies for the construction of 3D DNA-based architectures have been developed. The first strategy, named "DNA origami", involves the folding of long single stranded DNA (ssDNA) into the designed geometry by annealing with short "stable strands". [68] This procedure enables high geometrical control, [182] but requires the use of hundreds of different stable strands, as well as a long assembly time. The second strategy involves the use of identical branched DNA building blocks that assembly into DNA cages which present only dsDNA and a defined symmetry; [67,183] following this strategy Mao and coworkers were able to form regular polyhedral (tetrahedron, dodecahedron and buckyball). [67] The third strategy, developed by Sleiman group, is based on the assembly of ssDNA polygons - displaying organic corner units - which are then

assembled into 3D DNA architectures by ligation; [85,184] by this strategy, several nanostructures with prism shape have been prepared. [185] This strategy has been improved and simplified by developing a procedure in which the DNA polygon is formed without the separate ligation step. [185] The fourth approach, developed by von Kiedrowski, involves forming a fully dsDNA 3D-architecture by annealing poly-DNA-functionalized organic molecules. [186,187] Following this procedure, von Kiedrowsky and coworkers were able to form a nanostructure with dodecahedral symmetry from trisoligonucleotides with C_{3h} symmetric linkers. [187]

The bowl-shaped geometry and the C_5-symmetry make *sym*-pentasubstituted corannulene derivatives good candidates for the synthesis of icosahedral supramolecular aggregates following the last strategy. By this approach, twelve DNA-corannulene-based building units might form an isosahedral supramolecular architecture in which the corannulene cores will be positioned at each of the twelve vertexes of the icosahedron, while the dsDNA will form the thirty edges.

The structure of the pentakis-DNA corannulene was designed such that the ssDNA is a self-complementary 16-base palindromic sequence TATTACCGCGGTAATA. This sequence was designed with high concentration of T and A at the 5'- and 3'-end, to avoid the formation of loops, while the central C/G region increases the stability of the double stranded structure. Therefore, the ssDNA strands have the potential to fully anneal with the ssDNA strands of other molecules in solution into many polymeric structures, possibly including the expected supramolecular icosahedral capsid.

In order to be conjugated on corannulene core by CuAAC reaction, the 16-mer selected was modified at the 5'-end with an alkyl chain bearing an azido group (Scheme 7.1). The length of the alkyl linker was chosen in order to allow the formation of five double stranded DNA units around corannulene core where it's in an icosahedral fashion.

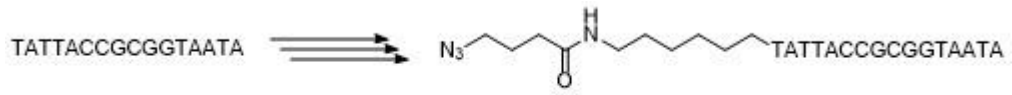

146

Scheme 7.1. 5'-alkylazido modified oligonucleotide **146**.

The synthesis of the C_5-symmetric penta(oligonicleotide) corannulene derivative **147** was achieved by a CuAAC "click" reaction of the alkyne **67** with the 5'-alkylazido-modified oligonucleotide **146**. Since the oligonucleotide **146** is not stable under the conditions used for the

CuNPS-catalyzed CuAAC reaction (oxidation of **146** and reduction of CuNPs was observed), a new synthetic procedure was developed for the synthesis of corannulene derivative **147**.

Several CuAAC reaction conditions were screened changing copper source (CuNPs, $CuSO_4$ and CuBr), solvent (water, DMSO, acetonitrile, THF and mixtures of these), temperature (room temperature or at reflux of the solvent) and heating system (oil bath and microwave). The best results in terms of yield and time were obtained by using Cu(I) bromide as the copper source together with *tris*-(benzyltriazolymethyl)amine (TBTA) [188] as a ligand and stabilizer of Cu(I) species in a mixture of THF and water (Scheme 7.2) avoiding any radical side reaction of Cu(I) species with oligonucleotide **146**.

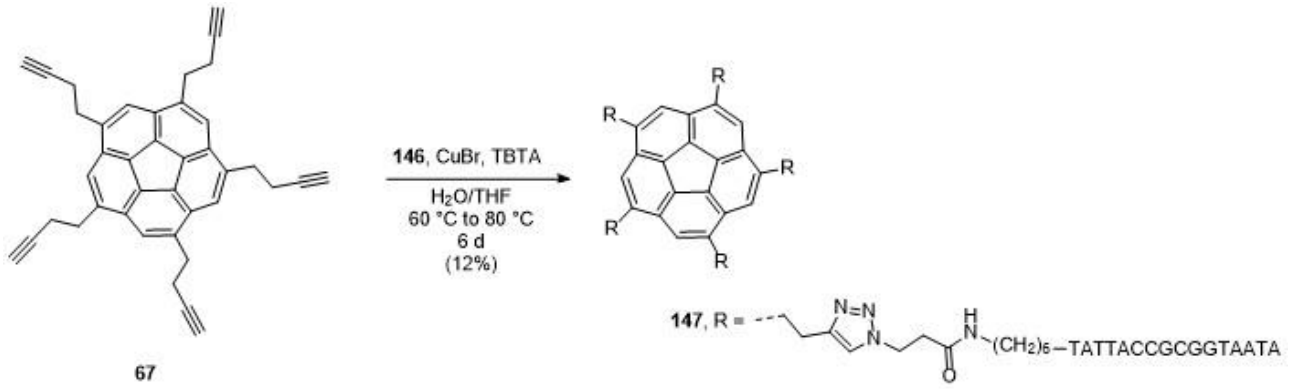

Scheme 7.2. Synthesis of oligonucleotide functionalized corannulene derivative **147**.

The desired compound **147** was obtained in high purity after D-PAGE purification, and the structure was verified by MALDI-TOF MS (Figure 7.3).

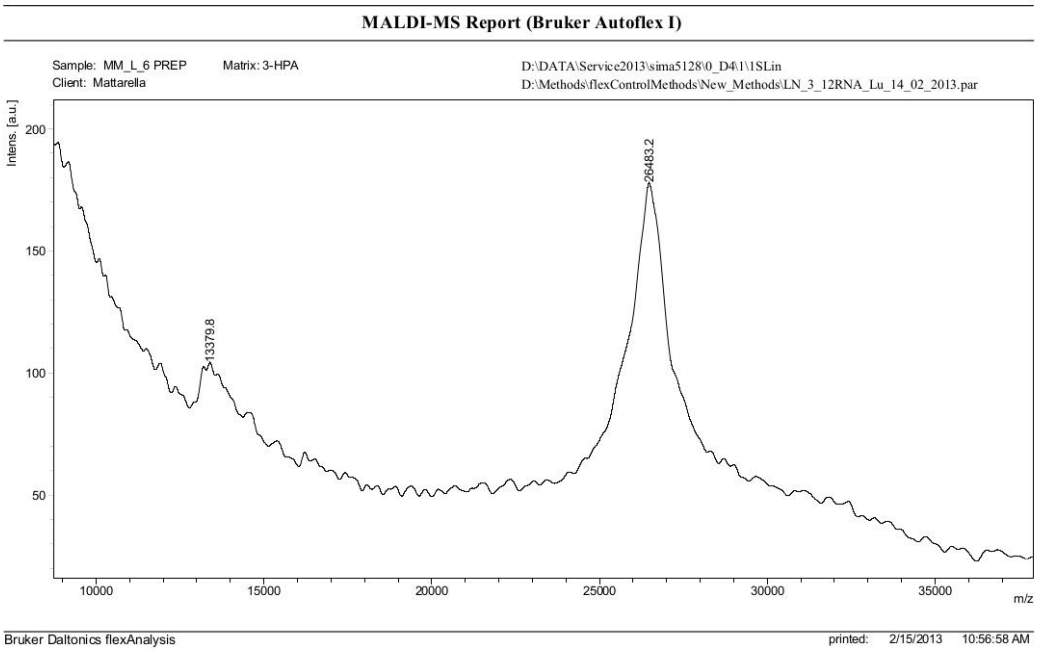

Figure 7.3. MALDI-TOF MS spectra of compound **147**.

7.4. ASSEMBLING STUDIES AND STRUCTURAL CALCULATIONS

The ability of DNA corannulene derivative **147** to form ordered supramolecular assemblies was investigated by native PAGE and ssDNA-selective enzymatic digestion.

Successful icosahedral supramolecular structure formation would require generating complete annealing of 12 units of compound **147**, generating 30 dsDNA edges. Two annealing strategies were pursued utilizing either kinetic control or thermodynamic control. In the kinetic strategy, a solution of **147** is first melted of any dsDNA at 95 °C, then cooled to 4 °C by immersion in an ice-bath. In the thermodynamic strategy, the melting step is followed by an annealing step at a temperature roughly 10 °C lower than the melting point of the double strand for at least an hour, and a final cooling step at 4 °C. Different outcomes were obtained from applying these two strategies to the same sample solution of **147** (1 μM in TE buffer with Na^+ 100 mM). The formation of small aggregates, mainly dimers and tetramers, was favored under thermodynamic control, whereas the kinetically-controlled strategy achieved aggregates up to 12-mers.

Based on this promising results, the annealing conditions were optimized, specifically the concentrations of **147**, Na^+ and Mg^{2+} and time of the annealing step, in order to mainly obtain the dimeric or 12-meric aggregate. The conditions maximizing formation of the 12-mer were found with the kinetically-controlled protocol with a solution 2 μM of **147** in TE buffer with Na^+ 100 mM and Mg^{2+} 5 mM (Figure 7.4). Applying the thermodynamically-controlled protocol, the optimal conditions for dimer formation were achieved with a solution 1 μM of **147** in TE buffer with Mg^{2+} 10 mM, and an annealing step of 50 hours (Figure 7.4).

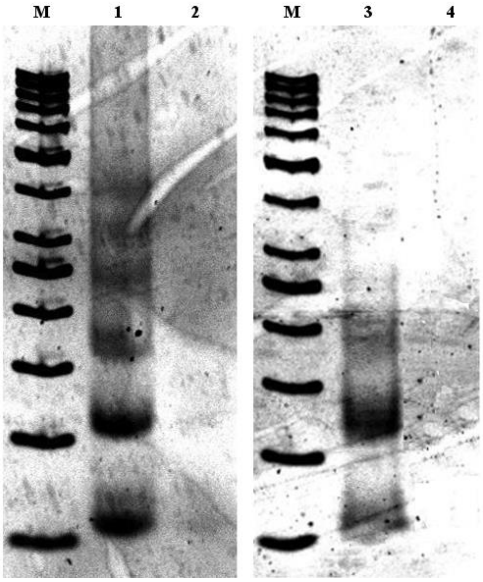

Figure 7.4. Native PAGE (4%) at 4 °C of assembling under kinetic (left) and thermodynamic control (right). Lanes M: 50-bp DNA ladder; lanes 1 and 3: assembled samples; lane 2 and 4: results from enzymatic digestion with MBN.

Enzymatic digestion reactions were performed in order to obtain more information regarding the structure of the aggregated formed during the annealing process. Mung bean nuclease (MBN) [189] is an enzyme that selectively digests ssDNA, while not disturbing dsDNA. Therefore, in order to investigate the formation of the fully double stranded dimer and 12-mer (icosahedral symmetric assembly), MBN digestion was performed on the two annealed solutions of the dimer and 12-mer of **147** from the above protocols. The native PAGE of the samples shows that all supramolecular aggregates were digested by MBN, implying that neither the dsDNA strands associated with the dimer nor icosahedral supramolecular structures were formed. The stability of dsDNA toward treatment with MBN was tested on double-stranded oligonucleotide TATTACCGCGGTAATA under the same digestion conditions used for the aggregates of **147**; the result proves that dsDNA is not hydrolyzed at these conditions (Figire 7.5).

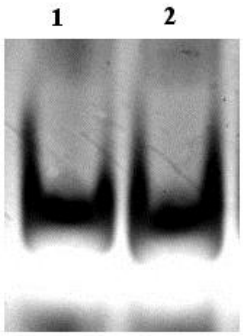

Figure 7.5. PAGE (15%) Lane 1: sample; lane 2: sample after MBN digestion.

Melting temperature (T_m) measurements were performed on compound **147** to study the stability of the annealed dimeric system; due to multivalent effect, [190] an higher T_m is expected compared to the one of the self-dimer of oligonucleotide TATTACCGCGGTAATA. Unfortunately, the temperature dependence of the absorption coefficient of corannulene at 260 nm did not permit accurate determination of T_m of the dsDNA formed under either kinetically- or thermodynamically-controlled conditions.

Due to the complexity of the interactions of compound **147**, it has been selected to theoretically study of this molecule's potential for interaction and aggregation into supramolecular arrangements. The RM1 methodology [191] was implemented in GAMESS [192] and validated on the MOPAC test sets. [193] RM1 calculations were performed on the neutral species of the ssDNA and complementarily paired dsDNA strands, optimizing each in gas phase.The final RM1-optimized structure is presented in Figure 7.6.

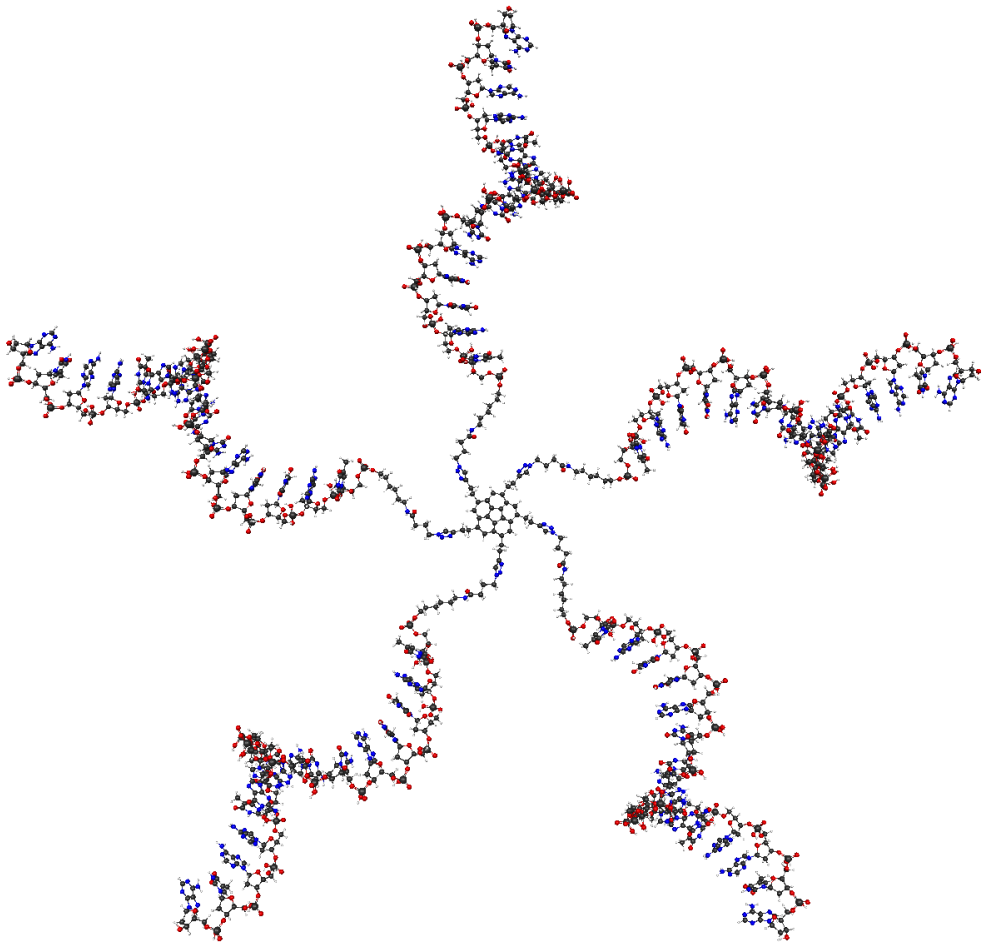

Figure 7.6. RM1-optimized ssDNA-conjugated corannulene structural model.

This optimized structure is characterized by an arm-length of 75.1 Å, measuring from the center of corannulene to the oxygen of the final hydroxyl group of the ssDNA. The RM1-optimzied bowl depth of unsubstituted corannulene is 0.88 Å, comparing well to the experimentally observed crystalline bowl-depth of corannulene, 0.87 Å. [10] In contrast, the bowl depth in **147** is slightly flattened to 0.84 Å. While corannulene itself has an intrinsic curvature, the final structure of this compound was comparatively flattened, indicating that this linker does not rigidly adopt and extend the curvature of corannulene. The angle between neighboring arms measured from the center of corannulene is 71.91˚, and 143.6˚ between non-neighboring arms. In an idealized icosahedron, these angles stemming from one vertex of a regular icosahedron are 60˚ and 108˚, respectively, as in Figure 7.7, and therefore a substantially smaller than observed in the optimized structure of **147**. This large discrepancy provides a further explanation for the lack of icosahedral 12-mer formation. Moreover, icosahedral aggregates are highly symmetric structures, and therefore strongly entropically disfavorable.

Given the conformational flexibility of the linker to the DNA strands, future theoretical studies could employ sampling techniques to search the potential energy surface of this molecule for other minima where this angle may be more conducive of icosahedral supramolecular aggregation. Nevertheless, this first *ab initio* minimum energy structure suggests the usage of a more rigid linker to the DNA to effectively restrict the angles of the bioconjugated arms nearer to 108˚, for increased probability of icosahedron formation.

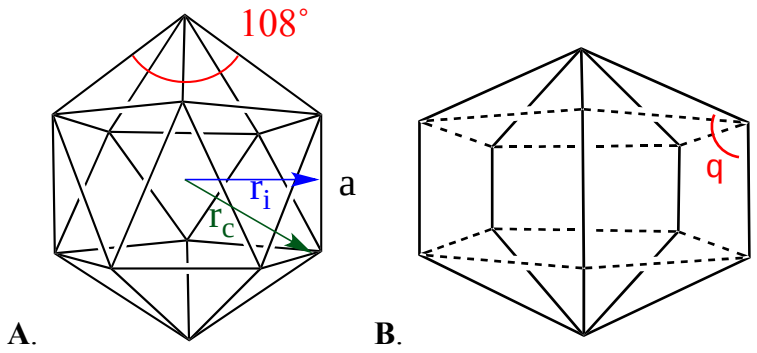

Figure 7.7. Supramolecular structures of **147** resulting from (A) 12-mer aggregation into an icosahedron, or (B) dimer formation of a pentagonal prism.

In contrast to the icosahedral structure, the dimer structure could easily accommodate a more flattened corannulene-linker structure as calculated for **147**, but would then necessitate the bending of the linker-to-DNA junction to an angle, θ in Figure 7.7, of 98˚ to properly orient the ssDNA strands for annealing. This angle in the calculated structure of **147** is a much more linear 165˚, therefore, suggesting again a design modification for promoting dimer formation, by rigidifying the linkers to DNA to achieve this orientation. The structural calculations also suggest that the fully double stranded dimer cannot be formed due to steric stress and strain since this molecular geometry is unsupportive of the annealing of all five dsDNA [194] strands when two molecules of **147** anneal in a dimeric fashion

With future optimization of the structure, the formation of this dimer supramolecular aggregate would be more successful, given the greater probability of two molecules joining in concert, opposed to twelve molecules in the correct orientation in the icosahedral aggregation.

7.5. Conclusion and Outlook

Although the formation of the icosahedron aggregate was not observed in this work, this predicted approximately 2 nm diameter nanocapsule offers interesting potential for applications

given both the size and nature of its construction. This cavity size offers the capacity to enclose large cargo, such as small proteins or genes. The release of cargo could also be directed by the same parameters that affect the annealing of the DNA sequence, namely, temperature, ion and denaturant concentrations, and enzymatic activity. With ever-increasing applications for nano-scale delivery mechanisms in the fields of targeted medicine and materials science, DNA-based nanocapsules are an option of growing interest. Specifically, a bioconjugated-organic construct offers appealing advantages, including increased stability and rigidity of the organic framework, and potential for a longer lifetime *in vivo* due to lower degradation rates of organic compounds compared to purely biomolecular constructs. This work encourages the continuation of efforts towards the synthesis of bioconjugated-corannulene supramolecular structures, and through *ab initio* structural calculations offers suggestions to improve the design and success of organized dimer or 12-mer formation.

The recent synthesis of C_1-symmetric 1,3,5,7,9-pentasubstituted corannulene derivatives achieved in Siegel group [195] can be a possible alternative for the formation of supramolecular aggregates with icosahedral symmetry. Using fifteen different couples of complementary oligonucleotide sequences and conjugating them on twelve C_1-symmetric 1,3,5,7,9-pentasubstituted corannulene in the correct order and in a way that they can only aggregate in an icosahedral fashion might lead to the formation of the desired 12-mer. This procedure was already used with success by von Kiedrowsk and coworkes [187] for the formation of a dodecahedral supramolecular aggregate starting from a designed series of trisoligonucleotides with C_{3h} linker.

8. CONCLUSION AND OUTLOOK

In conclusion, a robust and efficient synthetic procedure for the preparation of C_5-symmetric pentabioconjugated corannulene derivatives has been developed. Iron-catalyzed alkyl-aryl cross-coupling followed by copper nanoparticles catalyzed microwave-assisted CuAAC reaction give access to a new class of *sym*-pentasubstituted corannulene derivative bearing (oligo)saccharides, oligopeptide, lipids and (oligo)nucleotides.

The properties and applications of some of these derivatives have been described in this dissertation. Pentakis-saccharide corannulene derivatives functionalized with GM1os strongly interact with Cholera Toxin at nanomolar concentrations acting as inhibitors of this protein; pentakis-lipido corannulenes display organogelator behavior and liquid-crystalline phases. Interesting and promising results on the formation of supramolecular aggregates have been obtained for pentakis-galactose and pentakis-DNA corannulene derivatives.

The described "tool box" for the synthesis of C_5-symmetric pentasubstituted corannulenes opens the way for the application of corannulene scaffold in biology, pharmacology, material science, polymers, optoelectronic devices, soft materials, etc. The application of the synthetic procedure might be also used for the functionalization of other corannulene-based systems with substitution grade and symmetry different form the C_5-pentasubstitution.

9. EXPERIMENTAL SESSION

9.1. GENERAL

Reagents and Solvents: all reagents were used as purchased from commercial suppliers unless otherwise stated. For reactions, solvents of pro analysis grade were used. For reactions performed under dry atmosphere, solvents of puriss. grade were used. For work up and purification, distilled solvents of technical grade were used.

Chromatography: thin layer chromatography (TLC): Merck TLC aluminum sheets, silica gel 60 F254, 2 mm. Column chromatography (CC): Sigma-Aldrich Silica gel Merck Type 9385, 230-400 mesh, 60 Å.

Microwave Reaction:

Infrared Spectroscopy (IR): Jasco 4100 FT-IR spectrometer; absorption values in cm^{-1}.

UV-vis Spectrometry: UV-Vis measurements were carried out on an Agilent 8453 UV/Vis spectrophotometer using a 1 mm path quartz cuvette.

Emission Spectroscopy: emission spectra were recorded on an Edinburgh Instruments FLS920 spectrometer with excitation at 300 nm using 1 cm path quartz cuvette.

Optical Rotatory Power: $[\alpha]_D$ values were recorded on JASCO P-2000 Polarimeter at 25 °C.

Circular Dichroism (CD): circular dichroism spectra were recorded at room temperature on a Jasco J-810 spectropolarimeter using 1 mm path quartz cuvette.

Nuclear Magnetic Resonance (NMR): ^{1}H- and ^{13}C-NMR: Bruker AV-300, AV-400 or AV-500 instruments. ^{13}C-signal multiplicity was deduced from DEPT 90 and DEPT135 spectra. Peak assignment was performed by two-dimensional NMR experiment (NOESY, COSY).

Mass Spectrometry (MS): Finnigan Trace GC ultra instrument equipped with a Zebron ZB-5MS capillary GC column for CI and EI; Finnigan Surveyor MSQ quadrupole spectrometer for ESI; m/z (rel. %); Bruker Autoflex I spectrometer for MALDI-TOF (matrix assisted laser desorption/ionisation time of flight).

Quantification of DNA: Nanodrop 2000C was used for quantification of **147** in solution.

Differential Scanning Calorimetry (DSC): differential scanning calorimetry was performed on a DSC 2920 from TA Instruments equipped with a RCS cooling. The compounds were encapsulated in 40 µL crucibles and measured under nitrogen atmosphere in a temperature range from T=-10 to 150 °C with a heating and cooling rate of 2 $K \cdot min^{-1}$.

Polarized Optical Microscopy (POM): POM images were taken on a Leica DM LB optical microscope equipped with a Linkam CSS450 hot stage.

Small and Wide Angle X-ray Scattering (SAXS and WAXS): SWAXS experiments were performed on a Rigaku MicroMax-002+ microfocused beam (4 kW, 45 kV, 0.88 mA) with the wavelength $\lambda_{Cu\text{-}K\alpha}$= 0.15419 nm. The 2D scattering patterns were collected by a Fujifilm BAS-MS 2025 imaging plate system (15.2 x 15.2 cm^2, 50 µm resolution) with an effective scattering vector range of q= 1 nm^{-1} - 25 nm^{-1}.

Transmission electron microscopy (TEM): TEM experiments were carried out using aJeol JEM-3200FSC field emission cryo electron microscope operating at 300 kV voltage. The images were taken in bright field mode using zero loss energy filtering (omega type) with the slit width of 20 eV. Micrographs were recorded using a GatanUltrascan 4000 CCD camera. The specimen temperature was maintained at -187 °C during imaging. Thin sections (~70 nm) were cut at -80 °C

by Leica Ultracut UTC ultramicrotome using a 25o Diatome diamond knife. The sections were collected on 300 mesh lacey carbon grids. The samples were imaged without any staining.

Polyacrylamide Gel Electrophoresis (PAGE): preparative denaturating PAGE (D-PAGE) was peformed on 45x30 cm plates with 5 mm spacers at a constant power of 40 W. The DNA was visualized by UV irradiation (254 nm) of the gel placed on a fluorescent TLC plate. Analytical denaturating and native PAGE were performed on 10x10.8 cm plates with 1 mm spacers at constant current of 10 mA. Gels were stained with ethidium bormide and visualized with AlphaImager from AlphaInnotech.

9.2. ABBREVIATIONS

acac	acetylacetonate
AcOEt	ethyl acetate
APCI	atmospheric pressure chemical ionization
br	broad
BSA	bovine serum albumine
d	duplet
D-PAGE	denaturing polyacrilamide gel electrophoresis
dd	duplet of duplet
DEPT	Disortionless Enhancement by Polarization
DCM	dichloromethane
DMF	dimethylformamide
DMSO	dimethyl sulfoxide
ESI	electrospray ionization,,
HRMS	high resolution mass spectrometry
HRP	horseradish peroxidase
IR	Infrared spectroscopy

m	multiplet
MALDI	Matrix-assisted laser desorption/ionization
MeOH	methanol
NBS	*N*-bromosuccinimide
NMP	*N*-methyl-2-pyrrolidone
NMR	nuclear magnetic resonance
OPD	*o*-phenylenediamine
PAGE	polyacrilamide gel electrophoresis
PBS	Phosphate buffered saline
q	quartet
quint	quintet
s	singlet
t	triplet
TE	tris(hydroxymethyl)aminomethane, EDTA
TEA	triethylamine
THF	tetrahydrofuran
TIPS	triisopropylsilyl
TMS	trimethylsilyl
UV	ultraviolet

9.3. SYNTHETIC PROCEDURES

9.3.1. *SYM*-PENTAMETHYL-CORANNULENE (**61**)

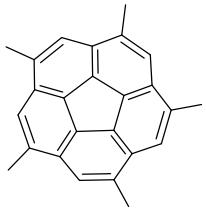

Chemical Formula: $C_{25}H_{20}$
Molecular Weight: 320,44

Methyl magnesium bromide (3.0 mL, 9.0 mmol, 3 M in THF) was added to a suspension of *sym*-pentachlorocorannulene (347 mg, 0.82 mmol) and $Fe(acac)_3$ (72 mg, 0.20 mmol) in THF (7 mL) and NMP (0.7 mL) at 0 °C. The reaction was stirred at room temperature for 2.5 hours. The solution was then cooled to 0 °C and quenched by slowly addition of diethyl ether followed by a 1 M solution of HCl in water. The organic layer was separated and the aqueous phase was extracted with diethyl ether. The collected organic phases were dried over Na_2SO_4 and evaporated to yield the crude product. The product was purified by column chromatography on silica gel eluted with hexane. The solvent was evaporated to yield a pale yellow solid (174 mg, 66%). The spectroscopic data were identical with those reported. [24,44]

9.3.2. *SYM*-PENTAETHYL-CORANNULENE (**62**)

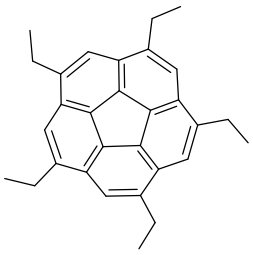

Chemical Formula: $C_{30}H_{30}$
Molecular Weight: 390,57

Ethyl magnesium bromide (4.6 mL, 9.2 mmol, 2 M in THF) was added to a suspension of *sym*-pentachlorocorannulene (350 mg, 0.83 mmol) and $Fe(acac)_3$ (73 mg, 0.21 mmol) in THF (7 mL) and NMP (0.7 mL) at 0 °C. The reaction was stirred at room temperature for 2.5 hours. The solution was then cooled to 0 °C and quenched by slowly addition of diethyl ether followed by a 1 M solution of HCl in water. The organic layer was separated and the aqueous phase was extracted with diethyl ether. The collected organic phases were dried over Na_2SO_4 and evaporated to yield the

crude product. The product was purified by column chromatography on silica gel eluted with hexane. The solvent was evaporated to yield a pale yellow solid (188 mg, 58%). The spectroscopic data were identical with those reported. [45]

9.3.3. *SYM*-PENTA-(1-METHYL-ADAMANTYL)-CORANNULENE (**63**)

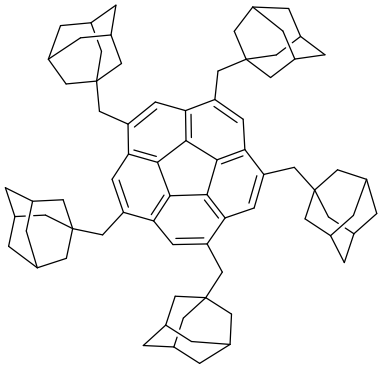

Chemical Formula: $C_{75}H_{90}$
Molecular Weight: 991,54

1-bromo-methyl-adamantane (2.2 g, 9.6 mmol) was added to a suspension of magnesium (1.0 g, 42.8 mmol) and a crystal of iodine in diethyl ether (70 mL) at 0 °C; the mixture was stirred at room temperature for 5 hours. The Grignard solution was added to a suspension of sym-pentachlorocorannulene (368 mg, 0.87 mmol) and $Fe(acac)_3$ (77 mg, 0.22 mmol) in THF (5 mL) and NMP (0.5 mL) at 0 °C. The reaction was stirred at room temperature for 18 hours. The solution was then cooled to 0 °C and quenched by slowly addition of diethyl ether followed by a 1 M solution of HCl in water. The organic layer was separated and the aqueous phase was extracted with diethyl ether. The collected organic phases were dried over Na_2SO_4 and evaporated to yield the crude product. The product was purified by column chromatography on silica gel eluted with hexane. The solvent was evaporated to yield a pale yellow solid (302 mg, 35%).

^{1}H-NMR (500 MHz, $CDCl_3$): δ 7.53 (s, 5H), 2.87 (s, 10H), 2.01 (s, 15H), 1.80 (s, 30H), 1.70 (dd, *J*= 12.5 Hz, *J*= 9.0 Hz, 30H).

^{13}C-NMR (125 MHz, $CDCl_3$): δ 136.78, 134.05, 130.48, 126.57, 47.89, 43.28, 37.31, 34.84, 29.20.

UV (THF) λ_{max}, nm: 263, 301.

HRMS (APCI) m/z: found 991.7109 (M + H); calc ($C_{75}H_{91}$) 991.7115.

9.3.4. *SYM*-PENTA-((*S*)-2-METHYL-BUTYL)-CORANNULENE (**64**)

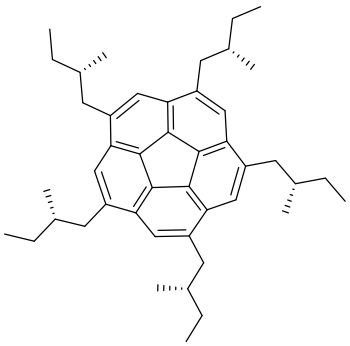

Chemical Formula: $C_{45}H_{60}$
Molecular Weight: 600,98

(S)-2-methyl-butylbromide (1.0 g, 6.6 mmol) was added to a suspension of magnesium (194 mg, 8.0 mmol) and a crystal of iodine in THF (5 mL) at 0 °C; the mixture was stirred at room temperature for 2.5 hours. The Grignard solution was added to a suspension of *sym*-pentachlorocorannulene (254 mg, 0.60 mmol) and $Fe(acac)_3$ (53 mg, 0.15 mmol) in THF (5 mL) and NMP (0.5 mL) at 0 °C. The reaction was stirred at room temperature for 2.5 hours. The solution was then cooled to 0 °C and quenched by slowly addition of diethyl ether followed by a 1 M solution of HCl in water. The organic layer was separated and the aqueous phase was extracted with diethyl ether. The collected organic phases were dried over Na_2SO_4 and evaporated to yield the crude product. The product was purified by column chromatography on silica gel eluted with hexane. The solvent was evaporated to yield a yellow solid (222 mg, 61%).

^{1}H-NMR (500 MHz, $CDCl_3$): δ 7.76 (s, 5H), 3.40 (dd, *J*= 13.5 Hz, *J*= 6.0 Hz, 5H), 3.02 (dd, *J*= 13.5 Hz, *J*= 8.0 Hz, 5H), 2.24 (m, 5H), 1.85-1.80 (m, 5H), 1.62-1.56 (m, 5H), 1.26-1.23 (m, 30H).

^{13}C-NMR (125 MHz, $CDCl_3$): δ 140.47, 135.02, 130.14, 123.87, 41.09, 37.75, 30.02, 19.73, 12.02.

UV (THF) λ_{max}, nm: 261, 299.

$[\alpha]^{25}_D$ = +68.9 (*c*=1.88 in $CHCl_3$)

HRMS (APCI) m/z: found 601.4765 (M + H); calc ($C_{45}H_{61}$) 601.4768.

9.3.5. *SYM*-PENTA-(1-BUTEN-4-YL)-CORANNULENE (**65**)

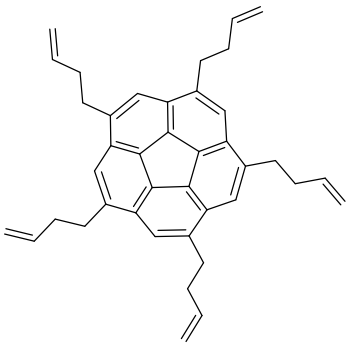

Chemical Formula: $C_{40}H_{40}$
Molecular Weight: 520,76

4-bromo-1-butene (1.1 g, 8.1 mmol) was added to a suspension of magnesium (219 mg, 9.0 mmol) and a crystal of iodine in THF (30 mL) at 0 °C; the mixture was stirred at room temperature for 2 hours. The Grignard solution was added to a suspension of *sym*-pentachlorocorannulene (311 mg, 0.74 mmol) and $Fe(acac)_3$ (65 mg, 0.18 mmol) in THF (5 mL) and NMP (0.5 mL) at 0 °C. The reaction was stirred at room temperature for 2.5 hours. The solution was then cooled to 0 °C and quenched by slowly addition of diethyl ether followed by a 1 M solution of HCl in water. The organic layer was separated and the aqueous phase was extracted with ethyl acetate. The collected organic phases were dried over Na_2SO_4 and evaporated to yield the crude product. The product was purified by column chromatography on silica gel eluted with a mixture hexane:ethyl acetate 98:2. The solvent was evaporated to yield a yellow solid (235 mg, 61%).

^{1}H-NMR (500 MHz, $CDCl_3$): δ 7.69 (s, 5H), 6.11 (m, 5H), 5.27 (dd, *J*= 17.0 Hz, *J*= 1.5 Hz, 5H), 5.17 (dd, *J*= 10.0 Hz, *J*= 1.5 Hz, 5H), 3.31 (t, *J*= 7,5 Hz, 10H), 2.76 (m, 10H).

^{13}C-NMR (125 MHz, $CDCl_3$): 140.80, 138.38, 135.13, 129.91, 122.75, 115.38, 36.54, 33.12.

UV (THF) λ_{max}, nm: 261, 298.

HRMS (ESI) m/z: found 521.3205 (M + H); calc ($C_{40}H_{41}$) 520.3203.

9.3.6. *SYM*-PENTA-(1-(TRIMETHYLSILYL)-1-BUTYN-4-YL)-CORANNULENE (**66**)

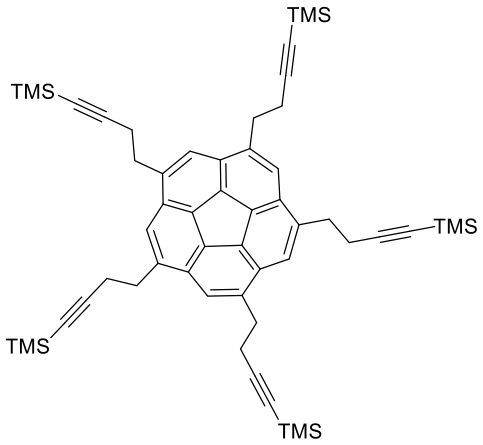

Chemical Formula: $C_{55}H_{70}Si_5$
Molecular Weight: 871,59

1-bromo-4-trimethylsilyl-3-butyne (2.4 g, 11.7 mmol) was added to a suspension of magnesium (575 mg, 19.7 mmol) and a crystal of iodine in THF (40 mL) at 0 °C; the mixture was stirred at room temperature for 3.5 hours. The Grignard solution was added to a suspension of *sym*-pentachlorocorannulene (465 mg, 1.1 mmol) and $Fe(acac)_3$ (97 mg, 0.27 mmol) in THF (10 mL) and NMP (1.0 mL) at 0 °C. The reaction was stirred at room temperature for 2.5 hours. The solution was then cooled to 0 °C and quenched by slowly addition of diethyl ether followed by a 1 M solution of HCl in water. The organic layer was separated and the aqueous phase was extracted with ethyl acetate. The collected organic phases were dried over Na_2SO_4 and evaporated to yield the crude product. The product was purified by column chromatography on silica gel eluted with a mixture hexane:diethyl ether 98:2. The solvent was evaporated to yield a yellow solid (537 mg, 61%).

^{1}H-NMR (500 MHz, $CDCl_3$): δ 7.64 (s, 5H), 3.33 (t, *J*= 7.5 Hz, 10H), 2.75 (t, *J*= 7.5 Hz, 10H), 1,53 (s, 45H).

^{13}C-NMR (125 MHz, $CDCl_3$): δ 139.65, 135.22, 129.64, 123.26, 106.53, 86.02, 32.86, 23.10, 0.35.

UV (THF) λ_{max}, nm: 262, 299.

HRMS (APCI) m/z: found 871.4396 (M + H); calc ($C_{55}H_{71}Si_5$) 871.4397.

9.3.7. *SYM*-PENTA-(1-BUTYN-4-YL)-CORANNULENE (**67**)

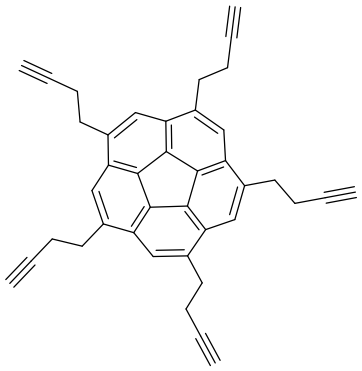

Chemical Formula: $C_{40}H_{30}$
Molecular Weight: 510,68

A solution of NaOH 10% in water was added to a solution of **66** (156 mg, 0.18 mmol) in MeOH (1.5 mL); THF was added until a clear solution was obtained. The reaction was stirred at room temperature for 24 hours. The solution was then cooled to 0 °C, acidified with a 1 M solution of HCl in water and extracted with diethyl ether. The collected organic phases were dried over Na_2SO_4 and evaporated to yield the crude product. The product was purified by column chromatography on silica gel eluted with a mixture hexane:DCM 6:4. The solvent was evaporated to yield a pale yellow solid (77 mg, 84%).

^{1}H-NMR (500 MHz, $CDCl_3$): δ 7.68 (s, 5H), 3.37 (t, *J*= 7.5 Hz, 10H), 2.73 (dt, *J*= 7.5 Hz, *J*= 2.5 Hz, 10H), 2.05 (t, *J*= 2.5 Hz, 5H).

^{13}C-NMR (125 MHz, $CDCl_3$): δ 139.35, 135.26, 129.66, 123.32, 83.88, 69.80, 32.54, 21.48.

UV (THF) λ_{max}, nm: 262, 299.

HRMS (ESI) m/z: found 511.2420 (M + 23); calc ($C_{40}H_{31}$) 511.2420.

9.3.8. *SYM*-PENTA-((*S*)-(3,7-DIMETHYLOCT-6-ENE)-1-YL)-CORANNULENE (**68**)

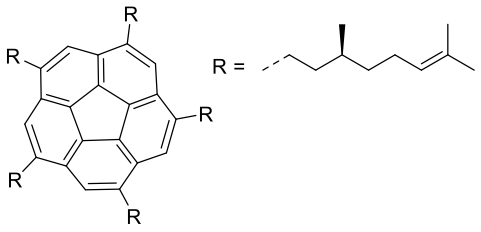

Chemical Formula: $C_{70}H_{100}$
Molecular Weight: 941,57

A flame-dried flask was charged with magnesium (176 mg, 7.24 mmol), THF (2 mL) and a crystal of I_2; the solution was stirred until the solution turns from brownish to uncolor. *S*-(+)-citronellyl bromide (332 mg, 1.51 mmol) was slowly added and the mixture was stirred at r.t. for 2 h. A flame-dried flask was charged with *sym*-pentachlorocorannulene (49.5 mg, 0.12 mmol) and $Fe(acac)_3$ (26.0 mg, 73.6 μmol), THF (1 mL) and NMP (100 μL) and put at 0 °C. The Grignard solution was added; the reaction mixture turned from red to black and the ice-water bath was removed. After 2.5 h ca. the reaction mixture was diluted with Et_2O and quenched with a solution of HCl 1M; the organic layer was separated and the aqueous phase was extracted with DCM. The collected organic phases were anhydrified over Na_2SO_4, filtered and the solvent was removed by low-pressure evaporation. The crude was purified by flash chromatography (silica; hexane:DCM 9:1). The product is a yellow oil (66.7 mg, 59%).

^{1}H-NMR (500 MHz, $CDCl_3$): 7.60 (5H, s), 5.18 (t, *J*= 10.0 Hz, 5H), 3.24 – 3.06 (m, 10H), 2.13 – 1.94 (m, 10H), 1.81 – 1.64 (m, 40H), 1.59 – 1.50 (m, 5H), 1.38 – 1.29 (m, 5H), 1.12 (d, *J*= 10.0 Hz, 15H).

^{13}C-NMR (125 MHz, $CDCl_3$): 141.92, 135.03, 131.30, 129.94, 125.06, 122.29, 39.97, 37.22, 32.83, 31.24, 25.89, 25.78, 25.76, 19.87, 19.85, 17.84. IR (film): ν cm^{-1} 2960, 2921, 2856, 1734, 1674, 1619, 1456, 1376, 1355, 1311, 1260, 1212, 1110, 1083, 984, 871, 827, 761, 739, 723, 466, 474.

UV (DMSO) λ_{max}, nm: 264, 299.

$[\alpha]^{25}_D$ = +3.4 (*c*= 0.007 in DMSO).

HRMS (APCI) m/z: found 941.7894 (M + H); calc ($C_{70}H_{100}$) 941.7898.

9.3.9. *SYM*-PENTA-(1-[1,3]-DIOXOLANE-2-ETHYL)-CORANNULENE (**69**)

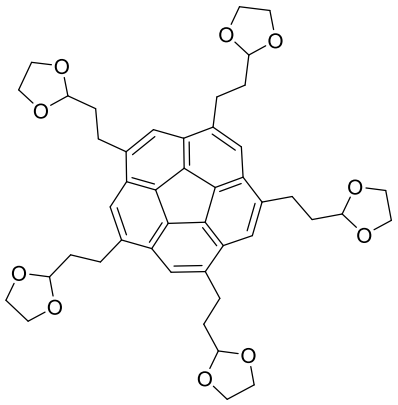

Chemical Formula: $C_{45}H_{50}O_{10}$
Molecular Weight: 750,88

2-(1,3-dioxa-2-cyclopentyl)-ethyl bromide (2.6 g, 14.4 mmol) was added to a suspension of magnesium (367 mg, 15.1 mmol) and a crystal of iodine in THF (60 ml) at 0 °C; the mixture was stirred at room temperature for 2.5 hours. The Grignard solution was added to a suspension of *sym*-pentachlorocorannulene (553 mg, 1.3 mmol) and $Fe(acac)_3$ (115 mg, 0.33 mmol) in THF (10 mL) and NMP (1.0 mL) at 0 °C. The reaction was stirred at room temperature for 2.5 hours. The solution was then cooled to 0 °C and quenched by slowly addition of diethyl ether followed by a 1 M solution of HCl in water. The organic layer was separated and the aqueous phase was extracted with ethyl acetate. The collected organic phases were dried over Na_2SO_4 and evaporated to yield the crude product. The product was purified by column chromatography on silica gel eluted with ethyl acetate. The solvent was evaporated to yield a yellow solid (674 mg, 69%).

^{1}H-NMR (500 MHz, $CDCl_3$): δ 7.65 (s, 5H), 5.04 (t, *J*= 4.8 Hz, 10H), 4.09 (m, 10H), 3,92 (m, 10H), 3.23 (t, *J*= 8.4 Hz, 10H), 2.24 (m, 10H).

^{13}C-NMR (125 MHz, $CDCl_3$): δ 140.68, 135.15, 130.00, 122.83, 104.17, 65.28, 36.45, 27.80.

UV (THF) λ_{max}, nm: 263, 298.

HRMS (ESI) m/z: found 773.3294 (M + Na); calc ($C_{45}H_{50}NaO_{10}$) 773.3296.

9.3.10. *SYM*-PENTA-(1-AL-3-PROPYL)-CORANNULENE (**70**)

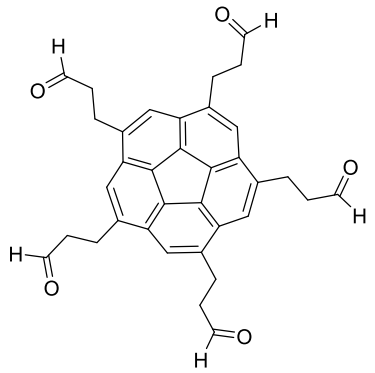

Chemical Formula: $C_{35}H_{30}O_5$
Molecular Weight: 530,62

Acetic acid (1.0 mL) and HCl 1 M (1.0 mL) were added to a solution of **69** (55 mg, 73.3 μmol) in THF (1.0 ml) and was heated to reflux and stirred for 2 hours. The mixture was cooled to 0 °C, neutralized with $NaHCO_3$ and extracted with ethyl acetate. The collected organic phases were dried over Na_2SO_4 and evaporated to yield an orange solid (41 mg, 99%).

^{1}H-NMR (500 MHz, $CDCl_3$): δ 9.92 (s, 5H), 7.60 (s, 5H), 3.45 (dt, *J*= 7.5 Hz, *J*= 7.0 Hz, 10H), 3.05 (t, *J*= 7.5 Hz, 10H).

^{13}C-NMR (125 MHz, $CDCl_3$): δ 201.18, 139.89, 135.32, 129.70, 123.02, 46.03, 25.68.

UV (THF) λ_{max}, nm: 261, 298.

HRMS (ESI) m/z: found 553.1983 (M + Na); calc ($C_{35}H_{30}NaO_5$) 553.1986.

9.3.11. *SYM*-PENTA-(1-CARBOXY-2-ETHYL)-CORANNULENE (**71**)

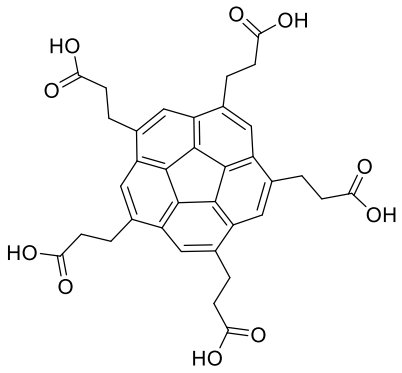

Chemical Formula: $C_{35}H_{30}O_{10}$
Molecular Weight: 610,62

A suspension of Oxone® (1.8 g, 2.88 mmol) in water (2 mL) was added to a solution of **69** (54 mg, 71.9 μmol) in THF (400 μL) at 0 °C. The reaction was stirred at room temperature for 2 days. The mixture was then diluted with water and ethyl acetate; the organic layer was separated and the aqueous phase was extracted with ethyl acetate. The collected organic phases were dried over Na_2SO_4 and evaporated. The crude was then dissolved in MeOH and a NaOH 1 M was slowly added until basic pH was reached; the aqueous phase was washed with ethyl acetate. The aqueous layer was then acidified with HCl 1 M to pH 1 and extractions with ethyl acetate were performed. The collected organic phases were dried over Na_2SO_4 and evaporated to yield a yellow solid (39 mg, 89%).

^{1}H-NMR (500 MHz, *d*^{4}-MeOD): δ 7.68 (s, 5H), 3.24 (t, *J*= 7.0 Hz, 10H), 2.87 (t, *J*= 7.0 Hz, 10H).

^{13}C-NMR (125 MHz, *d*^{4}-MeOD): δ 176.90, 141.21, 136.14, 130.81, 123.93, 37.54, 29.64.

UV (THF) λ_{max}, nm: 263, 298.

HRMS (ESI) m/z: found 609.1773 (M - H); calc ($C_{35}H_{29}O_{10}$) 609.1766.

9.3.12. *SYM*-PENTA-(1-OL-3-PROPYL)-CORANNULENE (**72**)

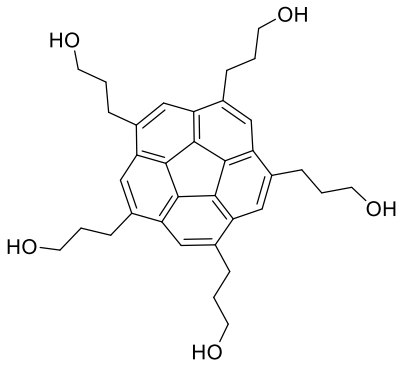

Chemical Formula: $C_{35}H_{40}O_5$
Molecular Weight: 540,70

*From compound **70**.*

A solution of $NaBH_4$ (284 mg, 7.5 mmol) in dry methanol (10 mL) was added over 24 hours by syringe pump to a solution of **70** (400 mg, 0.75 mmol) in dry methanol (10 mL) at 0 °C. The reaction mixture was stirred at room temperature for 1 day. The reaction mixture was then diluted with water and ethyl acetate; the organic layer was separated and the aqueous phase was extracted with ethyl acetate. The collected organic phases were dried over Na_2SO_4 and evaporated. The product was purified by column chromatography on silica gel eluted with a mixture dichloromethane:methanol 9:1. The solvent was evaporated to yield a pale yellow solid (203 mg, 50%).

*From compound **74**.*

Trifluoroacetic acid (2.0 mL, 26.1 mmol) was added to a well stirred solution of **74** (250 mg, 0.19 mmol) in acetone (2.5 mL), THF (1.75 mL) and water (1.0 mL). The reaction was heated to reflux for 2 days. The mixture was cooled to room temperature and the organic solvents were evaporated. The solid was then filtrated and was washed with water and diethyl ether. The product was purified by column chromatography on silica gel eluted with a mixture dichloromethane:methanol 9:1. The solvent was evaporated to yield a pale yellow solid (93 mg, 91%).

^{1}H-NMR (500 MHz, d^4-MeOD): δ 7.59 (s, 5H), 4.47 (br, 5H), 3.64 (t, *J*= 6.0 Hz, 10H), 3.11 (t, *J*= 7.5 Hz, 10H), 2.01 (m, 10H).

^{13}C-NMR (125 MHz, d^4-MeOD): δ 142.50, 136.04, 131.09, 123.86, 62.58, 36.45, 30.73.

UV (THF) λ_{max}, nm: 261, 298.

HRMS (ESI) m/z: found 563.2766 (M + Na); calc ($C_{35}H_{40}NaO_5$) 563.2768.

9.3.13. *SYM*-PENTA-(1-(TRIISOPROPYLSILYLOXY)-3-PROPYL)-CORANNULENE (**74**)

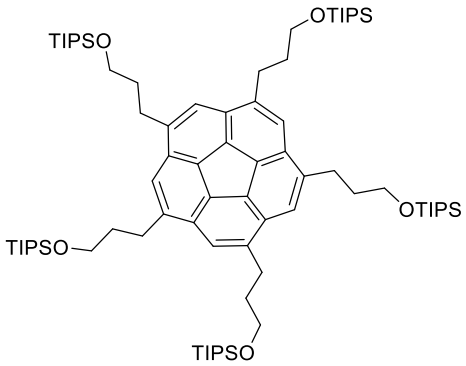

Chemical Formula: $C_{80}H_{140}O_5Si_5$
Molecular Weight: 1322,42

3-(triisopropylsilyloxy)-propylbromide (3.5 g, 11.9 mmol) was added to a suspension of magnesium (356 mg, 14.6 mmol) and a crystal of iodine in THF (25 mL) at 0 °C; the mixture was stirred at room temperature for 1 hours. The Grignard solution was added to a suspension of *sym*-pentachlorocorannulene (457 mg, 1.1 mmol) and $Fe(acac)_3$ (97 mg, 0.27 mmol) in THF (5 mL) and NMP (0.5 mL) at 0 °C. The reaction was stirred at room temperature for 2.5 hours. The solution was then cooled to 0 °C and quenched by slowly addition of diethyl ether followed by a 1 M solution of HCl in water. The organic layer was separated and the aqueous phase was extracted with diethyl ether. The collected organic phases were dried over Na_2SO_4 and evaporated to yield the crude product. The product was purified by column chromatography on silica gel eluted with ethyl acetate. The solvent was evaporated to yield a yellow oil (887 mg, 61%).

^{1}H-NMR (500 MHz, $CDCl_3$): δ 7.62 (s, 5H), 3.87 (t, *J*= 6.0 Hz, 10H), 3.19 (t, *J*= 7.5 Hz, 10H), 2.11 (m, 10H), 1.10 (m, 105H).

^{13}C-NMR (125 MHz, $CDCl_3$): δ 141.38, 135.14, 130.06, 122.82, 63.17, 36.00, 30.06, 18.35, 12.33.

UV (THF) λ_{max}, nm: 263, 298.

HRMS (ESI) m/z: found 1321.9610 (M + H); calc ($C_{80}H_{141}O_5Si_5$) 1321.9620.

9.3.14. *SYM*-PENTA-(1-BROMO-3-PROPYL)-CORANNULENE (**75**)

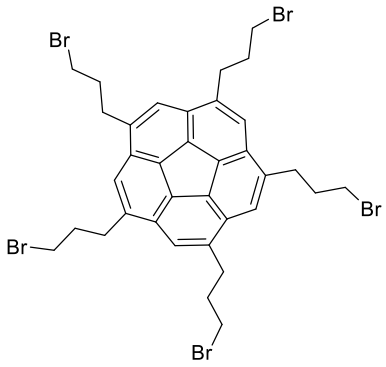

Chemical Formula: $C_{35}H_{35}Br_5$
Molecular Weight: 855,18

NBS (106 mg, 0.60 mmol) was added to a solution of **73** (37 mg, 68.4 μmol) and triphenylphosphine (149 mg, 0.57 mmol) in DMF (2.0 mL) at 0 °C. The reaction was stirred at room temperature for 1 hour. The DMF was evaporated at reduced pressure and the crude was diluted in dichloromethane. The organic phase was washed with water and brine, dried over Na_2SO_4 and evaporated to yield the crude product. The product was purified by column chromatography on silica gel eluted with a mixture hexane:ethyl acetate 9:1; hexane:ethyl acetate 1:1 and then ethyl acetate:methanol 9:1. The solvent was evaporated to yield a pale yellow solid (45 mg, 77%).

^{1}H-NMR (400 MHz, $CDCl_3$): δ 7.67 (s, 5H), 3.56 (t, *J*= 6.4 Hz, 10H), 3.30 (t, *J*= 7.2 Hz, 10H), 2.45 (m, 10H).

^{13}C-NMR (100 MHz, $CDCl_3$): δ 139.87, 135.24, 129.86, 123.36, 34.96, 33.61, 31.67.

UV (THF) λ_{max}, nm: 261, 299.

HRMS (ESI) m/z: found 850.8714 (M + H); calc ($C_{35}H_{36}Br_5$) 850.8728.

9.3.15. *SYM*-PENTA-(1-THIOL-3-PROPYL)-CORANNULENE (**76**)

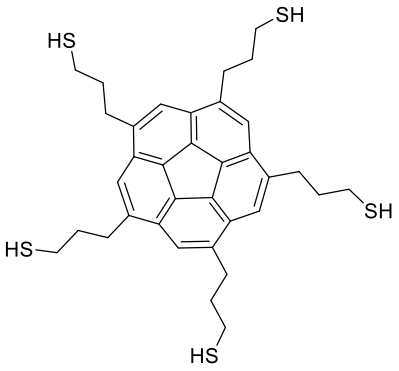

Chemical Formula: $C_{35}H_{40}S_5$
Molecular Weight: 621,01

A solution of **75** (40 mg, 46.8 μmol), thiourea (64 mg, 0.84 mmol) in ethanol (3.0 mL) and THF (1.0 mL) was heated to reflux and stirred for 2 hours. The mixture was cooled down and the solvent was evaporated. The crude was dissolved in NaOH 7.5 M (5.0 mL), heated to reflux and stirred for 2 hours. The mixture was cooled down to 0 °C and acidified to pH 1 with HCl 1 M. The solid was filtrated and washed with water and diethyl ether to yield a pale yellow solid (28 mg, 96%).

^{1}H-NMR (400 MHz, d^6-DMSO): δ 7.79 (s, 5H), 3.24 (t, *J*= 7.5 Hz, 10H), 2.66 (dt, *J*= 7.5 Hz, *J*= 7.0 Hz, 10H), 2.11 (m, 10H).

^{13}C-NMR (100 MHz, d^6-DMSO): δ 140.75, 133.96, 129.47, 122.86, 36.11, 31.20, 23.61.

UV (DMSO) λ_{max}, nm: 263, 301.

HRMS (ESI) m/z: found 621.1812 (M + H); calc ($C_{35}H_{41}S_5$) 621.1806.

9.3.16. *SYM*-PENTA-(3-(2,5-DIMETHYLPYRROLE)-1-PROPYL)-CORANNULENE (**81**)

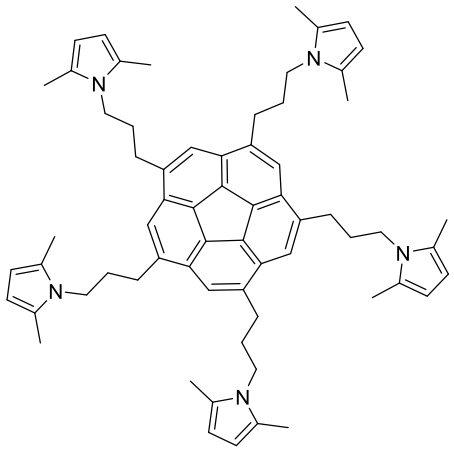

Chemical Formula: $C_{65}H_{75}N_5$
Molecular Weight: 926,35

1-(3-bromopropyl)-2,5-dimethylpyrrole (4.1 g, 19.0 mmol) was added to a suspension of Mg (557 mg, 22.3 mmol) and a crystal of iodine in THF (15 mL) at 0 °C; the mixture was stirred at room temperature for 2 hours. The Grignard solution was added to a suspension of *sym*-pentachlorocorannulene (730 mg, 1.7 mmol) and $Fe(acac)_3$ (152 mg, 0.43 mmol) in THF (15 mL) and NMP (1.5 mL) at 0 °C. The reaction was stirred at room temperature for 2.5 hours. The solution was then cooled to 0 °C and quenched by slowly addition of diethyl ether followed by a 1 M solution of HCl in water. The organic layer was separated and the aqueous phase was extracted with ethyl acetate. The collected organic phases were dried over Na_2SO_4 and evaporated to yield the crude product. The product was purified by column chromatography on silica gel eluted with a mixture hexane:ethyl acetate 8:2. The solvent was evaporated to yield a pale yellow solid (976 mg, 62%).

^{1}H-NMR (500 MHz, $CDCl_3$): δ 7.39 (s, 5H), 5.83 (s, 10H), 3.97 (t, *J*= 7.0 Hz, 10H), 3.10 (t, *J*= 7.0 Hz, 10H), 2.25 (m, 40H).

^{13}C-NMR (125 MHz, $CDCl_3$): δ 140.64, 135.35, 129.53, 127.62, 122.33, 105.59, 43.44, 33.37, 30.57, 12.87.

UV (THF) λ_{max}, nm: 262, 299.

HRMS (ESI) m/z: found 948.5905 (M + Na); calc ($C_{65}H_{75}N_5Na$) 948.5915.

9.3.17. *SYM*-PENTA-((*N*-METYL-ACETATE)3-AMINO-1-PROPYL)-CORANNULENE (**82**)

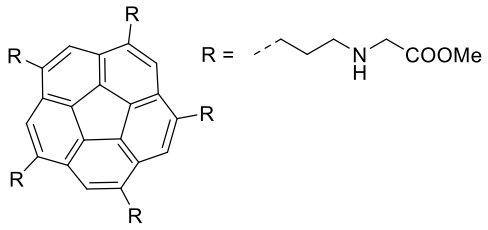

Chemical Formula: $C_{50}H_{65}N_5O_{10}$
Molecular Weight: 896,09

To solution of **70** (41 mg, 77 μmol) in methanol (2 mL) were added glycine methylester (146 mg, 1.17 mmol) and $NaBH_3CN$ (30 mg, 0.48 mmol) at 0 °C and the solution was stirred for 2 hours at room temperature. The reaction was diluted with a saturated solution of $NaHCO_3$ and extracted with AcOEt. The collected organic phases were anhydrified over Na_2SO_4 and filtrated. The solvent was evaporated to yield a yellow solid (64 mg, 93%).

^{1}H-NMR (500 MHz, $CDCl_3$): δ 7.58 (s, 5H), 3.72 (s, 15H), 3.46 (s, 10H), 3.15 (t, *J*=7.5 Hz, 10H), 2.81 (t, *J*= 6.5 Hz, 10H), 2.08 (m, 10H).

^{13}C-NMR (125 MHz, $CDCl_3$): 173.26,141.09, 135.09, 129.91, 122.78, 52.03, 51.07, 49.55, 32.79, 31.23.

UV (THF) λ_{max}, nm: 260, 300.

HRMS (ESI) m/z: found 448.7438 (M + 2H); calc ($C_{50}H_{67}N_5O_{10}$) 448.7438.

9.3.18. 5'-AZIDO-2',5'-DI-DEOXY-ADENOSINE (**85**)

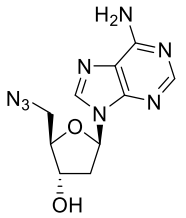

Chemical Formula: $C_{10}H_{12}N_8O_2$
Molecular Weight: 276,26

A solution of 5'-O-Toluenesulphonyl-2'-deoxy-adenosine [115] (270 mg, 6.67 mmol) in dry DMF (2.0 mL) was added dropwise to a mixture of LiN_3 (525 mg, 10.7 mmol) in dry DMF (1.0 mL). The reaction mixture was stirred at room temperature for 2 days; the solvent was evaporated and the product was purified by column chromatography on silica gel eluted with a DCM:MeOH:TEA 9:1:0.25. The solvent was evaporated to yield a colorless foam (140 mg, 76%).

^{1}H-NMR (500 MHz, *d*^{4}-MeOD): δ 8.29 (s, 1H), 8.21 (s, 1H), 6.44 (t, *J*= 7.0 Hz, 1H), 4.57 (m, 1H), 4.08 (m, 1H), 3.64 (dd, *J*= 13.5, 6.0 Hz, 1H), 3.56 (dd, *J*= 13.5, 4.0 Hz, 1H), 2.96 (m, 1H), 2.49 (m, 1H).

^{13}C-NMR (125 MHz, *d*^{4}-MeOD): δ 154.01, 141.29, 129.94, 127.12, 87.33, 85.90, 73.03, 53.46, 47.51, 40.39, 40.39.

9.3.19. *SYM*-PENTA-2-(1,2,3-TRIAZOLE-1-(5'-YL-2',5'-DI-DEOXY-ADENOSINE)-4-ETHYL)-CORANNULENE (**88**)

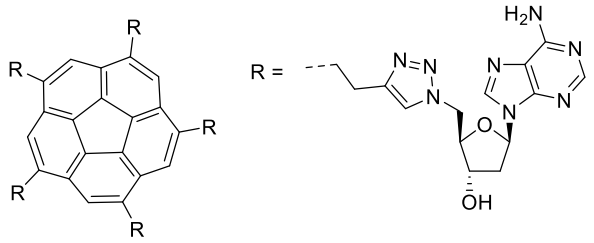

Chemical Formula: $C_{90}H_{90}N_{40}O_{10}$
Molecular Weight: 1891,98

A mixture of *sym*-penta-(1-butyn-4-yl)-corannulene **67** (10 mg, 19.6 μmol), 5'-azido-2',5'-dideoxy-adenosine **85** (65.1 mg, 0.24 mmol) and copper nanoparticles (10.1 mg, 0.16 mmol) in DMF (1.0 mL) in a microwave vessel was heated at 60 °C in a microwave reactor for 2 hours. The mixture was then filtrated over celite and the solvent was evaporated and MeOH was added to the crude. The solid was then filtrated, washed with cold MeOH and recrystallized from water to yield a reddish solid (14.5 mg, 40%).

^{1}H-NMR (500 MHz, d^6-DMSO, 373 K): δ 8.18 – 8.16 (m, 10H), 7.75 (s, 5H), 7.71 (s, 5H), 6.91 (br s, 10H), 6.35 (t, *J*= 6.5 Hz, 5H), 5.31 (d, *J*= 5.0 Hz, 5H), 4.70 (dd, *J*= 14.0, 4.5 Hz, 5H), 4.61 (dd, *J*= 14.5, 7.0 Hz, 5H), 4.53 (br s, 5H), 4.23 (br s, 5H), 3.42 (t, *J*= 7.0 Hz, 10H), 3.14 (t, *J*= 7.5 Hz, 10H), 2.80 (m, 5H), 2.36 (m, 5H).

^{13}C-NMR (125 MHz, d^6-DMSO): δ 156.09, 152.55, 149.22, 146.29, 140.41, 139.82, 133.93, 129.35, 127.97, 125.46, 122.83, 84.90, 83.58, 71.14, 66.99, 64.88, 51.36, 38.06, 32.29, 27.72, 25.10.

IR (KBr): ν cm^{-1} 3329, 3186, 2928, 1653, 1647, 1640, 1599, 1577, 1474, 1420, 1366, 1331, 1299, 1248, 1217, 1087, 1056, 939, 797, 726, 649.

UV (DMSO) λ_{max}, nm: 265, 299.

$[\alpha]_D$ = +25.6 (*c*= 0.008 in DMSO).

HRMS (ESI) m/z: found 946.3962 (M + 2H); calc ($C_{90}H_{92}N_{40}O_{10}$) 946.3955.

9.3.20. *SYM*-PENTA-2-(1,2,3-TRIAZOLE-1-(5'-YL-2'-DEOXY-RIBO-THYMIDINE)-4-ETHYL)-CORANNULENE (**89**)

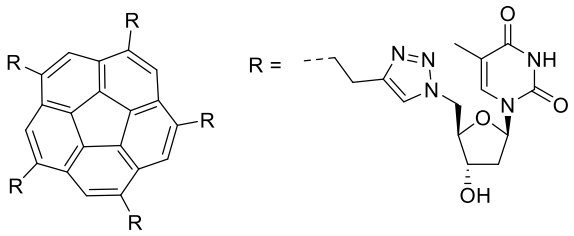

Chemical Formula: $C_{90}H_{95}N_{25}O_{20}$
Molecular Weight: 1846,91

A mixture of *sym*-penta-(1-butyn-4-yl)-corannulene **67** (9.9 mg, 19.4 μmol), 5'-azido thymidine **87** [116] (43.0 mg, 0.16 mmol) and copper nanoparticles (10.9 mg, 0.17 mmol) in DMF (1.0 mL) in a microwave vessel was heated at 60 °C in a microwave reactor for 2 hours. The mixture was then filtrated over celite and the solvent was evaporated and MeOH was added to the crude. The solid was then filtrated and washed with cold MeOH to yield a pale yellow solid (24.6 mg, 69%).

^{1}H-NMR (500 MHz, *d*^{6}-DMSO): δ 11.30 (s, 5H), 7.98 (s, 5H), 7.77 (s, 5H), 7.31 (s, 5H), 6.15 (t, *J*= 6.5 Hz, 5H), 5.49 (d, *J*= 4.5 Hz, 5H), 4.69 – 4.58 (m, 10H), 4.27 (m, 5H), 4.06 (m, 5H), 3.45 (br, 10H), 3.17 (d, *J*= 5.0 Hz, 10H), 2.15 – 2.07 (m, 10H), 1.75 (s, 15H).

^{13}C-NMR (125 MHz, *d*^{6}-DMSO): δ 163.67, 150.41, 146.35, 140.43, 136.05, 134.06, 129.41, 123.06, 109.83, 84.06, 83.96, 70.70, 51.06, 48.62, 37.93, 32.43, 27.85, 12.10.

IR (KBr): ν cm^{-1} 3421, 2926, 1688, 1472, 1438, 1273, 1221, 1135, 1084, 1056, 958, 874, 766, 558.

UV (DMSO) λ_{max}, nm: 265, 298.

$[\alpha]_D$ = +108.5 (*c*= 0.012 in DMSO).

HRMS (ESI) m/z: found 923.8662 (M + 2H); calc ($C_{90}H_{97}N_{25}O_{20}$) 923.8665.

9.3.21. *N*-(2-AZIDE-PROPIONYL)-DI-*L*-ALANINE METHYL ESTER (**92**)

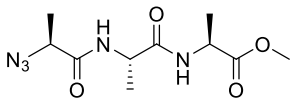

Chemical Formula: $C_{10}H_{17}N_5O_4$
Molecular Weight: 271,28

Triflic anhydride (0.65 mL, 3.88 mmol) was added to a solution of NaN_3 (1.2 g, 18.5 mmol) in DCM (3.0 mL) and water (2.0 mL) at 0 °C; the reaction was stirred at room temperature for 2 hours. The organic phase was separated and the aqueous extracted with DCM. The reunited organic phases were washed with a saturated solution of $NaHCO_3$.The organic phase was then added to a solution of H-Ala-Ala-Ala-OMe acetate salt (454 mg, 1.49 mmol), $CuSO_4*5H_2O$ (5.6 mg, 0.02 mmol) and K_2CO_3 (387 mg, 2.80 mmol) in methanol (6.6 mL) and water (3.2 mL) at room temperature; the mixture was stirred for 22 hours. The organic layer was then separated and the aqueous phase was extracted with DCM. The reunited organic phases were dried over Na_2SO_4 and evaporated to yield the crude product. The product was purified by column chromatography on silica gel eluted with a mixture DCM:MeOH 9:1. The solvent was evaporated to yield a white solid (211 mg, 52%).

^{1}H-NMR (500 MHz, $CDCl_3$): δ 6.89 (d, *J*= 6.5 Hz, 1H), 6.43 (d, *J*= 6.5 Hz, 1H), 4.56 (quint, J= 7.0 Hz, 1H), 4,42 (quint, *J*= 7.0 Hz, 1H), 4.07 (q, *J*= 7.0 Hz, 1H), 3.76 (s, 3H), 1.53 (d, *J*= 7.0 Hz, 3H), 1.42 (d, *J*= 7.0 Hz, 3H), 1.41 (d, *J*= 7.0 Hz, 3H).

^{13}C-NMR (125 MHz, $CDCl_3$): δ 173.21, 171.25, 169.83, 59.12, 52.73, 48.93, 48.37, 18.45, 18.44, 17.18.

IR (KBr): ν cm^{-1} 3312, 2972, 2116, 2078, 1740, 1641, 1546, 1450, 1376, 1344, 1325, 1218, 1162, 1106, 1073, 1063, 1008, 984, 956, 855, 663, 572.

$[\alpha]_D$ = -104.7 (*c*= 0.0040 in $CHCl_3$).

HRMS (ESI) m/z: found 294.1174 (M + Na); calc ($C_{10}H_{17}N_5NaO_4$) 294.1173.

9.3.22. *SYM*-PENTA-2-(1,2,3-TRIAZOLE-1-(*N*-(2-METHYL-ACETYL)-DI-*L*-ALANINE METHYL ESTER)-4-ETHYL)-CORANNULENE (**91**)

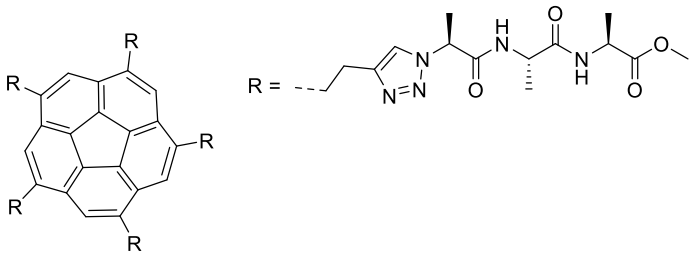

Chemical Formula: $C_{90}H_{115}N_{25}O_{20}$
Molecular Weight: 1867,07

A mixture of *sym*-penta-(1-butyn-4-yl)-corannulene **67** (9.1 mg, 18 μmol), N-(2-azide-propionyl)-di-L-alanine methyl ester **91** (50.3 mg, 0.19 mmol) and copper nanoparticles (13.4 mg, 0.21 mmol) in DMF (0.5 mL) in a microwave vessel was heated at 80 °C in a microwave reactor for 8 hours. The mixture was then filtrated over celite and the solvent was evaporated. The product was purified by column chromatography on silica gel eluted with a DCM:MeOH 9:1. The solvent was evaporated to yield a yellow solid (19 mg, 57%).

^{1}H-NMR (500 MHz, *d*^{6}-DMSO): δ 8.60 (d, *J*= 7.5 Hz, 5H), 8.39 (d, *J*= 7.0 Hz, 5H), 8.09 (s, 5H), 7.82 (s, 5H), 5.43 (q, *J*= 7.0 Hz, 5H), 4.27 (m, 10H), 3.61 (s, 15H), 3.47 (br, 10H), 3.18 (br, 10H), 1.60 (d, *J*= 7.0 Hz, 15H), 1.27 (d, *J*= 7.5 Hz, 15H), 1.21 (d, *J*= 7.0 Hz, 15H).

^{13}C-NMR (125 MHz, *d*^{6}-DMSO): δ 172.97, 171.83, 168.36, 145.99, 140.58, 134.05, 129.48, 123.05, 121.45, 57.68, 51.91, 47.95, 47.53, 32.45, 28.07, 18.15, 18.10, 16.83.

IR (KBr): ν cm^{-1} 3290, 2930, 1741, 1645, 1551, 1455, 1383, 1329, 1222, 1164, 1052, 998, 953, 684.

UV (DMSO) λ_{max}, nm: 264, 299.

$[\alpha]^{25}_{D}$ = +3.7 (*c*= 0.055 in DMSO).

HRMS (ESI) m/z: found 955.9273 (M + 2Na); calc ($C_{90}H_{115}N_{25}Na_2O_{20}$) 955.9267.

9.3.23. *SYM*-PENTA-2-(1,2,3-TRIAZOLE-1-(*N*-(2-ETHYL)OCTADEC-9-ENAMIDE)-4-ETHYL)-CORANNULENE (**84**)

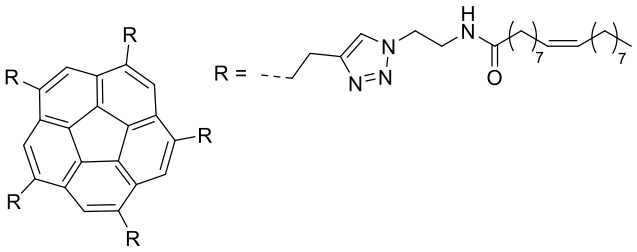

Chemical Formula: $C_{140}H_{220}N_{20}O_5$
Molecular Weight: 2263,43

A mixture of *sym*-penta-(1-butyn-4-yl)-corannulene **67** (25 mg, 49.0μmol), *N*-(2-azidoethyl)octadec-9-enamide **95** [119] (132 mg, 0.38mmol) and copper nanoparticles (25 mg, 0.39 mmol) in DMF (2.5 mL) in a microwave vessel was heated at 60 °C in a microwave reactor for 2 hours. The mixture was then filtrated over celite and the solvent was evaporated. The product was purified by column chromatography on silica gel eluted with a DCM:MeOH 93:7. The solvent was evaporated to yield a yellow wax (89 mg, 80%).

^{1}H-NMR (500 MHz, $CDCl_3$): δ 7.47 (s br, 10H), 6.87 (s, 5H), 5.28 (m, 10H), 4.44 (s, 10H), 3.69 (s br, 10H), 3.40 (s br, 10H), 3.16 (s br, 10H), 2.11 (t, J= 7.5 Hz, 10H), 1.95 (m, 20H), 1.54 (s br, 10H), 1.23 (s, 100H), 0.85 (t, J= 7.0 Hz, 15H).

^{13}C-NMR (125 MHz, $CDCl_3$): δ 174.13, 139.94, 134.67, 130.07, 129.73, 129.65, 122.82, 49.65, 31.98, 29.84, 29.81, 29.60, 29.40, 29.26, 27.30, 27.26, 25.78, 22.76, 14.20.

IR (KBr): ν cm^{-1} 3298, 2925, 2854, 1649, 1547, 1456, 1374, 1217, 1145, 1052, 874, 722.

UV ($CHCl_3$) λ_{max}, nm: 232, 264, 299.

HRMS (ESI) m/z: found 1164.3731 (M + 2Na); calc ($C_{140}H_{220}N_{20}Na_2O_5$) 1154.3696.

9.3.24. *SYM*-PENTA-(2-(1,2,3-TRIAZOLE-4-ETHYL)-ETHYL-β-D-GALACTOPYRANOSIDE)-CORANNULENE (**100**)

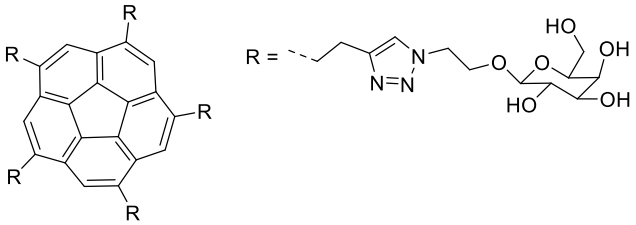

Chemical Formula: $C_{80}H_{105}N_{15}O_{30}$
Molecular Weight: 1756,79

A mixture of **96** [122,123] (42.0 mg, 0.17 mmol), *sym*-penta-(1-butyn-4-yl)-corannulene **67** (11.6 mg, 23 μmol) and copper nanoparticles (10.8 mg, 0.17 mmol) in DMF (1 mL) in a microwave vessel was heated at 60 °C in a microwave reactor for 2 hours. The mixture was then filtrated over celite, the solvent was evaporated and MeOH was added to the crude. The solid was then filtrated and washed with cold MeOH to yield a white solid (24 mg, 59%)

^{1}H-NMR (500 MHz, *d*^{6}-DMSO): δ 8.19 (s, 5H), 7.81 (s, 5H), 5.01 (d, *J*= 4.5 Hz, 5H), 4.77 (d, *J*= 5.5 Hz, 5H), 4.62-4.51 (m, 15H), 4.17 (d, *J*= 7.5 Hz, 5H), 4.08 (m, 5H), 3.86 (m, 5H), 3.62 (t, *J*= 4.0 Hz, 5H), 3.51 (m, 20H), 3.16 (t br, *J*= 7.0 Hz, 10H).

^{13}C-NMR (125 MHz, $CDCl_3$): δ 146.14, 140.6, 134.02, 129.48, 123.08, 103.45, 75.36, 73.30, 70.41, 68.16, 67.26, 60.48, 49.50, 32.43, 27.99.

UV (DMSO) λ_{max}, nm: 264, 300.

$[\alpha]_D$ = +349.3 (*c*=0.15 in H_2O).

HRMS (ESI) m/z: found 878.8647 (M + 2H); calc ($C_{80}H_{107}N_{15}O_{30}$) 878.8649.

9.3.25. *SYM*-PENTA-2-(1,2,3-TRIAZOLE-1-(2,3,5-TRI-O-ACETYL-β-RIBOFURANOSYL)-4-ETHYL)-CORANNULENE (**101**)

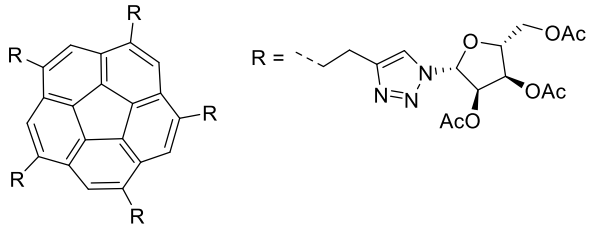

Chemical Formula: $C_{95}H_{105}N_{15}O_{35}$
Molecular Weight: 2016,95

A mixture of *sym*-penta-(1-butyn-4-yl)-corannulene **67** (10.0 mg, 20 μmol), 2,3,5-tri-*O*-acetyl-β-D-ribofuranosyl-1-azide [124] (62.0 mg, 21 mmol) and copper nanoparticles (13.2 mg, 0.21 mmol) in DMF (1.0 mL) in a microwave vessel was heated at 80 °C in a microwave reactor for 8 hours. The mixture was then filtrated over celite and the solvent was evaporated. The product was purified by column chromatography on silica gel eluted with a DCM:MeOH 96:4. The solvent was evaporated to yield a yellow solid (21.6 mg, 54%).

^{1}H-NMR (500 MHz, $CDCl_3$): δ 7.62 (s, 5H), 7.55 (s, 5H), 6.11 (d, *J*= 3.5 Hz, 5H), 5.81 (t, *J*= 4.0 Hz, 5H), 5.60 (t, *J*= 5.0 Hz, 5H), 4.42 (m, 5H), 4.32 (dd, *J*= 12.5, 3.5 Hz, 5H), 4.19 (dd, *J*= 12.5, 4.5 Hz, 5H), 3.50 (m, 10H), 3.29 (m, 10H), 2.10 (s, 15H), 2.08 (s, 15H), 1.97 (s, 15H).

^{13}C-NMR (125 MHz, $CDCl_3$): δ 170.47, 169.54, 169.35, 147.69, 140.26, 135.06, 129.74, 123.07, 120.87, 89.97, 80.88, 74.38, 71.00, 63.14, 33.09, 29.82, 28.29, 20.76, 20.61, 20.52.

IR (KBr): ν cm^{-1} 3422, 2927, 2854, 1750, 1445, 1437, 1373, 1231, 1091, 1062, 1041, 923, 900, 811, 730, 602.

UV (DMSO) λ_{max}, nm: 264, 299.

$[\alpha]_D$ = - 17.4 (*c*= 0.008 in DMSO).

HRMS (ESI) m/z: found 1030.8341 (M + 2Na); calc ($C_{95}H_{105}N_{15}Na_2O_{35}$) 1030.8341.

9.3.26. *SYM*-PENTA-2-(1,2,3-TRIAZOLE-1-(-β-RIBOFURANOSYL)-4-ETHYL)-CORANNULENE (**103**)

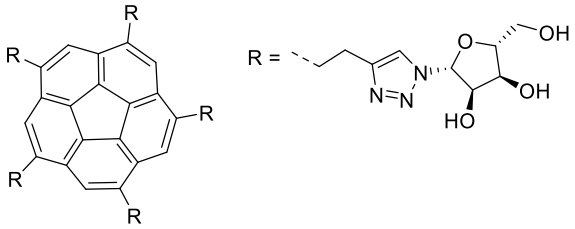

Chemical Formula: $C_{65}H_{75}N_{15}O_{20}$
Molecular Weight: 1386,40

A solution of **101** (9.2 mg, 4.6 μmol) and MeONa (16.5 mg, 0.31 mmol) in MeOH (1.5 mL) was stirred under nitrogen at room temperature for 2 days. Dowex 50 was added until pH 6 was reached. The mixture was filtrated and the solvent was evaporated. The product is a yellow solid (6.0 mg, 94%).

^{1}H-NMR (500 MHz, *d*^{6}-DMSO): δ 8.25 (s, 5H), 7.86 (s, 5H), 5.91 (d, *J*= 4.5 Hz, 5H), 5.63 (d, *J*= 5.5 Hz, 5H), 5.30 (d, *J*= 3.5 Hz, 5H), 4.99 (t, *J*= 5.0 Hz, 5H), 4.36 (d, *J*= 4.5 Hz, 5H), 4.11 (d, *J*= 3.5 Hz, 5H), 3.95 (q, *J*= 4.5 Hz, 5H), 3.61 – 3.48 (m, 20H), 3.21 (br, 10H).

^{13}C-NMR (125 MHz, *d*^{6}-DMSO): δ 146.68, 140.60, 134.12, 129.50, 123.02, 120.76, 109.54, 91.96, 85.72, 75.07, 70.42, 61.46, 32.37, 28.01.

IR (KBr): ν cm^{-1} 3359, 2924, 2853, 1595, 1454, 1383, 1331, 1228, 1101, 1047, 863, 824, 755, 102, 621.

UV (DMSO) λ_{max}, nm: 264, 300.

[α]$_{D}$ = +255.0 (*c*= 0.004 in DMSO).

HRMS (ESI) m/z: found 1408.5211 (M + Na); calc ($C_{65}H_{75}N_{15}NaO_{20}$) 1408.5205.

9.3.27. *SYM*-PENTA-2-(1,2,3-TRIAZOLE-1-(1-TRIISOPROPYL-3-(2-(2-(2-YL-1-ETHOXY)ETHOXY)ETHOXY)-PROP-1-YNE)-4-ETHYL)-CORANNULENE (**113**)

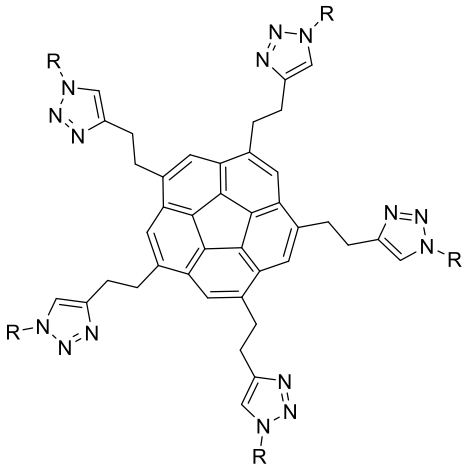

Chemical Formula: $C_{130}H_{205}N_{15}O_{15}Si_5$
Molecular Weight: 2358,59

A mixture of **67** (15.1 mg, 29 μmol), **108** (67.3 mg, 0.18 mmol) and copper nanoparticles (12.3 mg, 0.19 mmol) in DMF (1.5 mL) was loaded in a microwave vessel was heated at 60 °C in a microwave reactor for 2 h. The mixture was filtrated over celite and the solvent evaporated. The crude was purified by column chromatography on silica gel (DCM:MeOH 95:5) to yield a reddish oil (58 mg, 83%).

^{1}H-NMR (500 MHz, $CDCl_3$): δ 7.64 (s, 5H), 7.52 (s, 5H), 4.49 (t, *J*=5.5 Hz, 10H), 4.18 (s, 10H), 3.82 (t, *J*=5.5 Hz, 10H), 3.66-3.45 (m, 50H), 3.26 (t, *J*=8.0 Hz, 10H), 1.02 (s, 105H).

^{13}C-NMR (125 MHz, $CDCl_3$): δ 147.08, 140.36, 134.89, 129.71, 123.02, 122.39, 103.19, 87.73, 70.54, 70.50, 70.42, 69.68, 68.68, 59.18, 50.19, 33.39, 28.51, 18.62, 11.16.

HRMS (ESI) m/z: found 1201.2173 (M+2Na); calc ($C_{130}H_{205}N_{15}Na_2O_{15}Si_5$) 1201.2185.

9.3.28. COMPOUND (**114**)

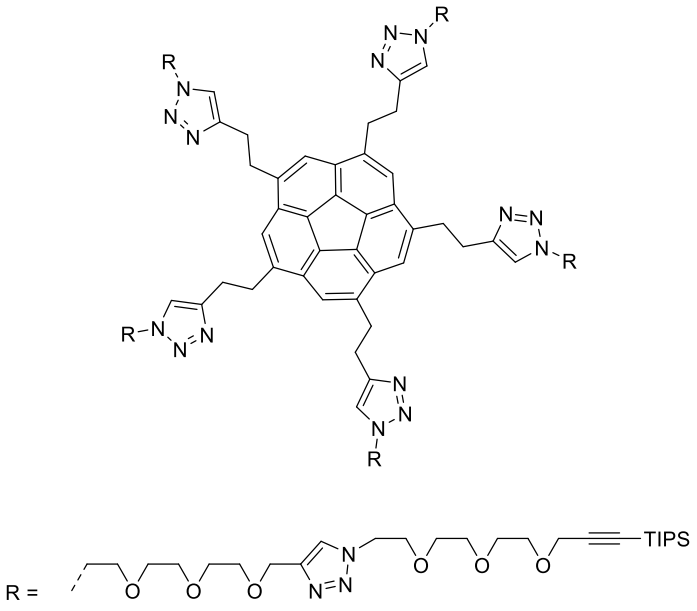

Chemical Formula: $C_{175}H_{280}N_{30}O_{30}Si_5$
Molecular Weight: 3424,77

A mixture of **67** (9.4 mg, 18 μmol), **111** (83.0 mg, 0.14 mmol) and copper nanoparticles (11.7 mg, 0.18 mmol) in DMF (1.0 mL) was loaded in a microwave vessel and was heated at 80 °C in a microwave reactor for 2 h. The reaction mixture was filtrated over celite and the solvent evaporated. The crude mixture was purified by column chromatography on silica gel (from DCM:MeOH 94:6 to DCM:MeOH 9:1) to yield a reddish oil (49 mg, 79%).

^{1}H-NMR (500 MHz, $CDCl_3$): δ 7.69 (s, 5H), 7.64 (s, 5H), 7.53 (s, 5H), 4.62 (s, 10H), 4.48 (q, *J*=5.5 Hz, 20 H), 4.21 (s, 10H), 3.82 (t, *J*=5.0 Hz, 20H), 3.69 – 3.47 (m, 90H), 3.26 (t, *J*=8.0 Hz, 10H), 1.04 (s, 105H).

^{13}C-NMR (125 MHz, $CDCl_3$): δ 147.07, 144.81, 140.42, 134.88, 129.74, 123.91, 123.06, 122.47, 103.21, 87.81, 70.55, 70.54 70.51, 70.47, 69.68, 69.64, 69.52, 68.72, 64.58, 59.28, 50.32, 50.27, 33.38, 28.49, 18.66, 11.20.

HRMS (ESI) m/z: found 1163.6590 (M+3Na); calc ($C_{175}H_{280}N_{30}Na_3O_{30}Si_5$) 1163.6609.

9.3.29. COMPOUND (**115**)

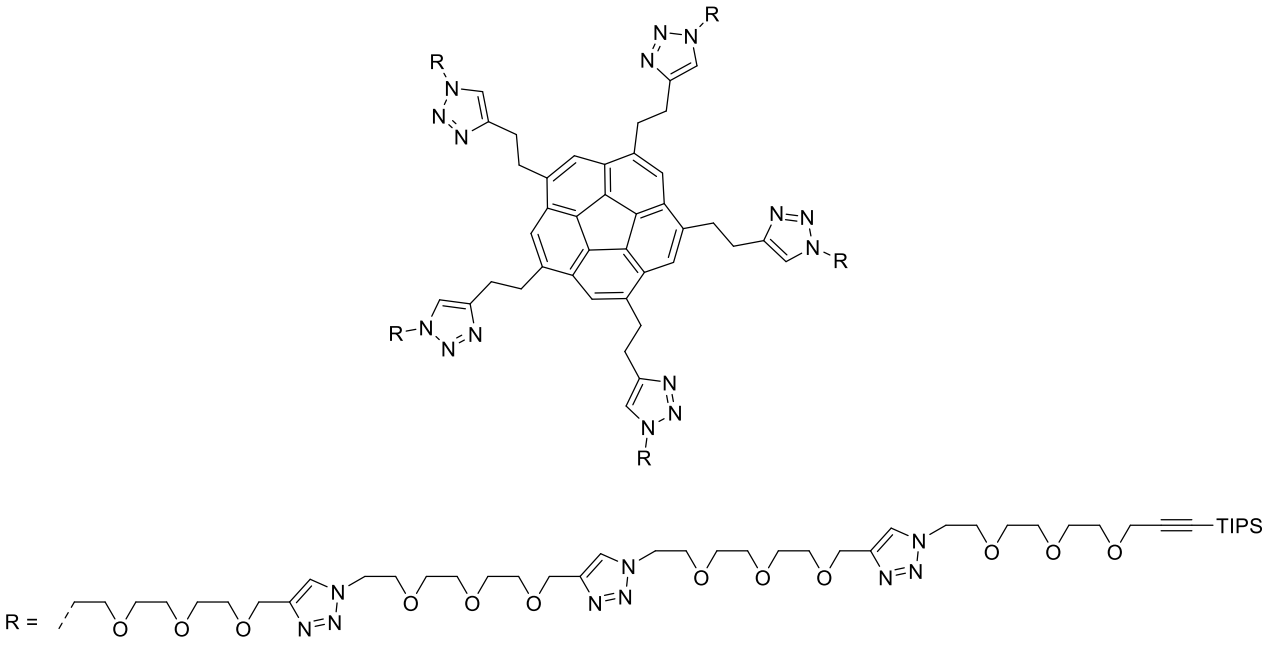

Chemical Formula: $C_{265}H_{430}N_{60}O_{60}Si_5$
Molecular Weight: 5557,14

A mixture of **67** (19.5 mg, 38 μmol), **112** (296.0 mg, 0.29 mmol) and copper nanoparticles (23.0 mg, 0.36 mmol) in DMF (2.0 mL) was loaded in a microwave vessel and was heated at 80 °C in a microwave reactor for 2 h. The reaction mixture was filtrated over celite and the solvent evaporated. The crude mixture was purified by column chromatography on silica gel (DCM:MeOH 9:1) to yield a reddish oil (147 mg, 70%).

^{1}H-NMR (500 MHz, $CDCl_3$): δ 7.66 – 7.62 (m, 15H), 7.56 (s, 5H), 7.47 (s, 5H), 4.56 – 4.52 (m, 30H), 4.43 – 4.38 (m, 40H), 4.11 (s, 10H), 3.77 – 3.73 (m, 40H), 3.61 – 3.41 (m, 165H), 3.17 (s br, 10H), 0.96 (s, 105H).

^{13}C-NMR (125 MHz, $CDCl_3$): δ 146.80, 144.51, 140.18, 134.59, 129.48, 123.73, 122.80, 122.24, 103.00, 87.53, 70.36, 70.34, 70.29, 70.24, 69.38, 69.26, 69.30, 68.53, 64.37, 64.35, 58.93, 50.02, 50.07, 50.00, 49.96, 49.91, 33.08, 28.22, 18.42, 10.93.

HRMS (ESI) m/z: found 794.3097 (M+7H); calc ($C_{265}H_{437}N_{60}O_{60}Si_5$) 794.3114.

9.3.30. SYM-PENTA-2-(1,2,3-TRIAZOLE-1-(3-(2-(2-(2-YL-1-ETHOXY)ETHOXY)ETHOXY)-PROP-1-YNE)-4-ETHYL)-CORANNULENE (**116**)

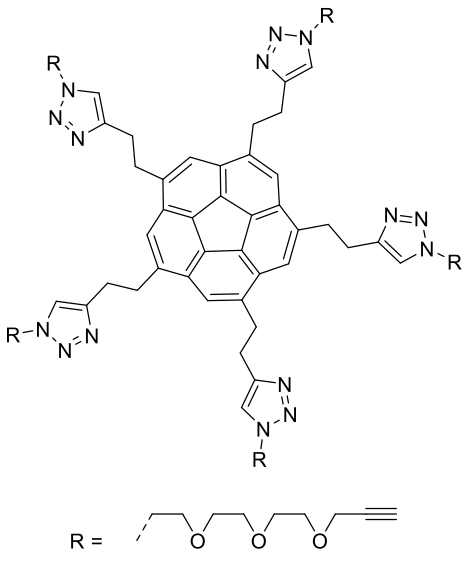

Chemical Formula: $C_{85}H_{105}N_{15}O_{15}$
Molecular Weight: 1576,86

A solution of TBAF in THF (1M, 0.77 mL, 0.77 mmol) was added to a solution of **113** (55.4 mg, 23.5 μmol) in THF (0.33 mL) and the reaction mixture was stirred at r.t. for 2 h. The solution was then diluted with a saturated aqueous solution of NH_4Cl and extracted with ethyl acetate. The combined organic phases were dried over Na_sSO_4 and evaporated to yield the crude product. The crude was then heated at 75 °C under high vacuum for 18 h. The product was then purified by column chromatography on silica gel (DCM:MeOH 95:5) to yield a reddish oil (15 mg, 40%).

^{1}H-NMR (500 MHz, $CDCl_3$): δ 7.64 (s, 5H), 7.53 (s, 5H), 4.50 (t, *J*=5.0 Hz, 10H), 4.13 (d, *J*=2.0Hz, 10H), 3.82 (t, *J*=5.0 Hz, 10H), 3.62-3.50 (m, 50H), 3.26 (t, *J*=8.0 Hz, 10H), 2.40 (t, *J*=2.0 Hz, 5H).

^{13}C-NMR (125 MHz, $CDCl_3$): δ 147.10, 140.45, 134.90, 129.77, 123.10, 122.54, 79.69, 74.82, 70.55, 70.43, 69.70, 69.13, 58.48, 50.26, 33.42, 28.53.

HRMS (ESI) m/z: found 526.2709 (M+3H); calc ($C_{85}H_{108}N_{15}O_{15}$) 526.2711.

9.3.31. COMPOUND (**117**)

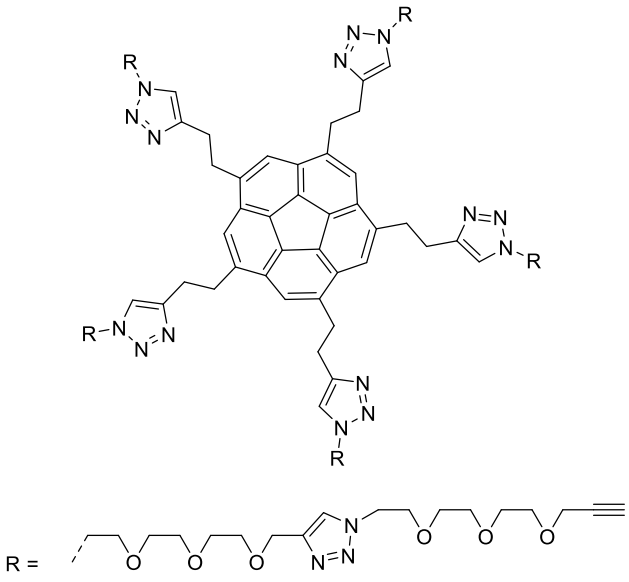

Chemical Formula: $C_{130}H_{180}N_{30}O_{30}$
Molecular Weight: 2643,05

A solution of TBAF in THF (1M, 1.0 mL, 1.0 mmol) was added to a solution of **114** (103 mg, 30.1 μmol) in THF (1.0 mL) and the reaction mixture was stirred at r.t. for 2 h. The solution was then diluted with a saturated aqueous solution of NH_4Cl and extracted with ethyl acetate. The collected organic phases were dried over Na_sSO_4 and evaporated to yield the crude product. The crude was then heated at 75 °C under high vacuum for 18 h. The product was then purified by column chromatography on silica gel (DCM:MeOH 9:1) to yield a reddish oil (24 mg, 30%).

^{1}H-NMR (500 MHz, $CDCl_3$): ^{1}H-NMR (500 MHz, $CDCl_3$): δ 7.70 (s, 5H), 7.64 (s, 5H), 7.53 (s, 5H), 4.62 (s, 10H), 4.50 – 4.46 (m, 20 H), 4.16 (d, *J*=2.5 Hz, 10H), 3.82 (t, *J*=5.0 Hz, 20H), 3.64 – 3.51 (m, 90H), 3.23 (t, *J*=8.0 Hz, 10H), 2.44 (d, *J*=2.5 Hz, 5H).

^{13}C-NMR (125 MHz, $CDCl_3$): δ 147.11, 144.83, 140.47, 134.89, 129.76, 123.97, 123.07, 122.47, 79.70, 74.86, 70.57, 70.55, 70.47, 69.65, 69.52, 69.14, 64.72, 58.48, 50.26, 50.20, 33.39, 28.52.

HRMS (ESI) m/z: found 529.2767 (M+5H); calc ($C_{130}H_{185}N_{30}O_{30}$) 529.2769.

9.3.32. COMPOUND (**118**)

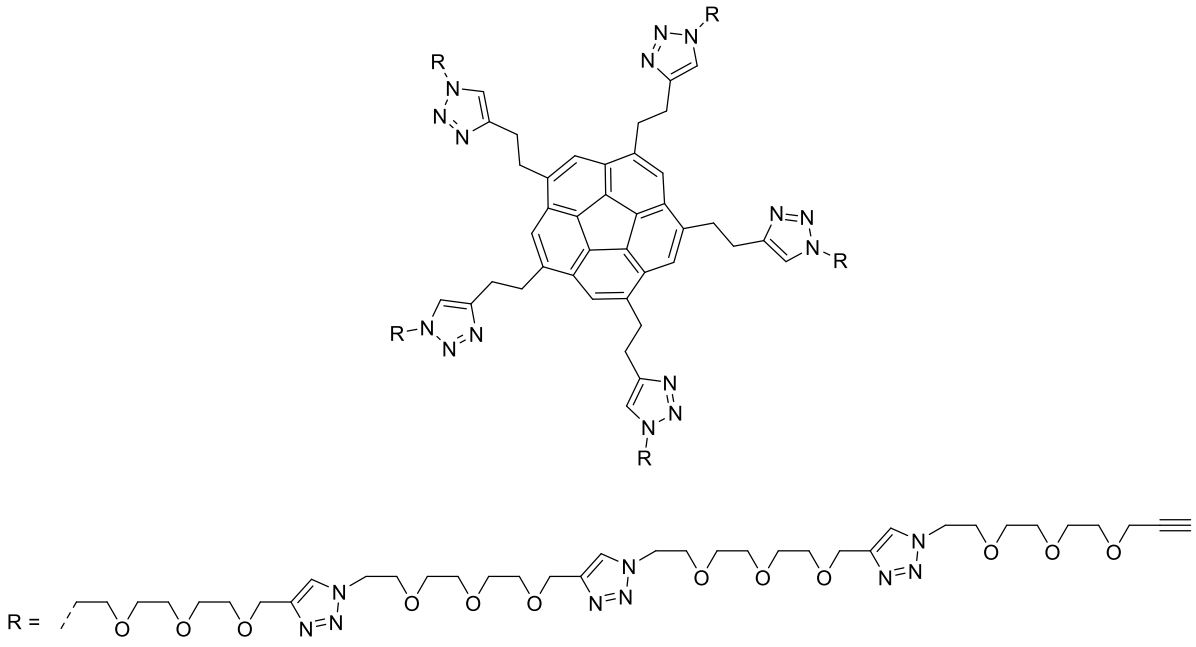

Chemical Formula: $C_{220}H_{330}N_{60}O_{60}$
Molecular Weight: 4775,42

A solution of TBAF in THF (1M, 0.9 mL, 0.9 mmol) was added to a solution of **115** (143 mg, 25.7 μmol) in THF (1.0 mL) and the reaction mixture was stirred at r.t. for 2 h. The solution was then diluted with a saturated aqueous solution of NH_4Cl and extracted with ethyl acetate. The collected organic phases were dried over Na_sSO_4 and evaporated to yield the crude product. The crude was then heated at 75 °C under high vacuum for 18 h. The product was then purified by column chromatography on silica gel (DCM:MeOH 9:1) to yield a reddish oil (81 mg, 66%).

^{1}H-NMR (500 MHz, $CDCl_3$): δ 7.69 – 7.65 (m, 15H), 7.60 (s, 5H), 7.50 (s, 5H), 4.60 – 4.56 (m, 30H), 4.48 – 4.41 (m, 40H), 4.13 (d, *J*=2.0 Hz, 10H), 3.81 – 3.80 (m, 40H), 3.62 – 3.52 (m, 165H), 3.18 (t br, *J*=7.5 Hz, 10H), 2.41 (s, 5H).

^{13}C-NMR (125 MHz, $CDCl_3$): δ 146.93, 144.71, 140.34, 134.76, 129.65, 123.80, 123.78, 122.92, 122.31, 79.62, 74.72, 70.47, 70.46, 70.44, 70.42, 70.35, 69.55, 69.41, 69.39, 69.04, 64.47, 58.35, 50.17, 50.16, 50.12, 50.07, 33.21, 28.35.

HRMS (ESI) m/z: found 1216.1057 (M+4Na); calc ($C_{220}H_{330}N_{60}Na_4O_{60}$) 1216.1052.

9.3.33. 1-AZIDO-6-(β-D-(2,3,4,6-TETRAACETATE)-GALACTOPYRANOSIDE)-1-DEOXYHEXAETHYLENEGLYCOL (**120**)

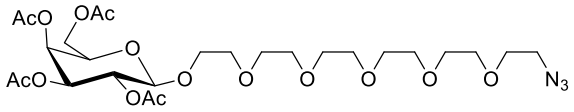

Chemical Formula: $C_{26}H_{43}N_3O_{15}$
Molecular Weight: 637,6

A mixture of 2,3,4,6-tetra-*O*-acetyl-*a*-D-galactopyranosyl bromide (**67**, 1.63 g, 4.0 mmol), 2[-2-(2-{2-[2-(2-hydroxyethoxy)-ethoxy]-ethoxy}-ethoxy)-ethoxy]- ethyl azide (**119**, 1.73 g, 5.6 mmol) and molecular sieves in dry dichloromethane (35 mL) was stirred at r.t. for 50 min; $HgBr_2$ (1.43 g, 4.0 mmol) was added to the reaction and the mixture was stirred at r. t. for 3 days. The mixture was then filtrated and the solid washed with dichloromethane, methanol and THF. The filtrate was concentrated *in vacuo*. The product was purified by column chromatography on silica gel eluted with AcOEt:Hexane 1:1. The solvent was evaporated to yield a yellow syrup (1.39 g, 55%).

^{1}H-NMR (500 MHz, $CDCl_3$): δ 5.36 (d, *J*=3.0 Hz, 1H), 5.17 (dd, *J*=10.0 Hz, *J*=8.0 Hz, 1H), 5.00 (dd, *J*=10.5 HZ, *J*=3.5 Hz, 1H), 4.55 (d, *J*=8.00 Hz, 1H), 4.16 – 4.10 (m, 2H), 3.97 – 3.89 (m, 2H) 3.76 – 3.62 (m, 23H), 3.39 (t, *J*=5.00 Hz, 2H), 2.12 (s, 3H), 2.07 (s, 3H), 2.05 (s, 3H), 1.99 (s, 3H).

^{13}C-NMR (135 MHz, $CDCl_3$): δ 170.60, 170.42, 170.33, 101.65, 71.06, 70.89, 70.80, 70.61, 70.45, 70.06, 69.31, 69.08, 67.27, 61.46, 50.85, 21.04, 20.90, 20.87, 20.79.

HRMS (ESI) m/z: found 660.2580 (M+Na); calc ($C_{26}H_{43}N_3NaO_{15}$) 660.2586.

9.3.34. 1-AZIDO-6-(β-D-GALACTOPYRANOSIDE)-1-DEOXYHEXAETHYLENEGLYCOL (**121**)

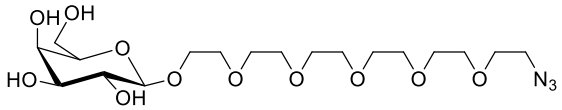

Chemical Formula: $C_{18}H_{35}N_3O_{11}$
Molecular Weight: 469,5

A solution of sodium methoxide (3 g in 10 mL of methanol) was added to a solution of **120** (1.31 g, 2.1 mmol) in methanol (10 mL.) until pH 12 was reached. The reaction mixture was stirred at r. t. for 2 days. Dowex 50 was added to the reaction until pH 6 was reached; the mixture was then filtrated and the solvent evaporated. The crude was purified by chromatography (DCM:MeOH 85:15). The product is a yellow syrup (560 mg, 58%).

^{1}H-NMR (500 MHz, D_2O): δ 4.44 (d, J=8.0 Hz, 1H), 4.12 – 4.08 (m, 1H), 3.94 (d, J=3.5, 1H), 3.88 – 3.66 (m, 25H), 3.58 – 3.52 (m, 3H).

^{13}C-NMR (125 MHz, d^4-MeOD): δ 104.26, 76.36, 74.08, 72.06, 71.01, 70.91, 70.87, 70.83, 70.54, 69.89, 69.73, 62.14, 51.39. HRMS (ESI) m/z: found 492.2159 (M+Na); calc ($C_{18}H_{35}N_3NaO_{11}$) 492.2164.

9.3.35.*SYM*-PENTA-(2-(1,2,3-TRIAZOLE-1-(1-YL-6-(β-D-GALACTOPYRANOSIDE)-1-DEOXYHEXAETHYLENEGLYCOL)-4-ETHYL)-CORANNULENE (**122**)

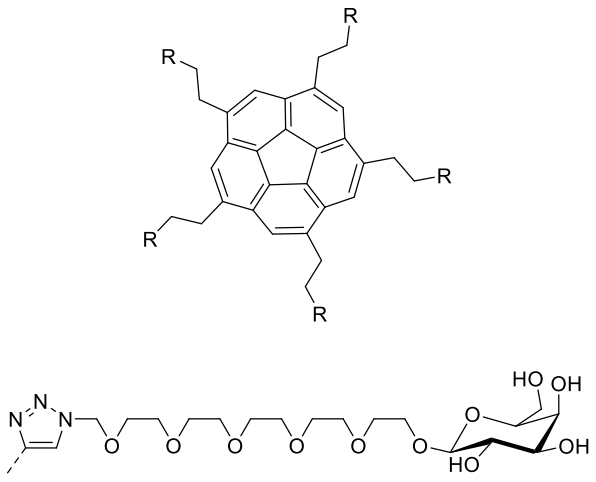

Chemical Formula: $C_{130}H_{205}N_{14}O_{55}$
Molecular Weight: 2844,11

A mixture of **67** (11.0 mg, 21.5 μmol), **121** (89.2 mg, 0.19 mmol) and copper nanoparticles (12.3 mg, 0.19 mmol) in DMF (1.0 mL) Cwas loaded in a microwave vessel was heated at 80 °C in a microwave reactor for 2 h. The mixture was filtrated over celite and the solvent evaporated. The crude was purified by size exclusion chromatography (Sephadex® G-25, water) to yield a reddish solid (147 mg, 47%).

^{1}H-NMR (600 MHz, d^4-MeOD): δ 7.83 (s, 5H), 7.71 (s, 5H), 4.54 (t br, J=5.0 Hz, 10H), 4.26 (d, J=5.0 Hz, 5H), 3.99 – 3.85 (m, 5H), 3.82 – 3.70 (m, 20H), 3.68 – 3.59 (m, 30H), 3.53 – 3.29 (m, 125H).

^{13}C-NMR (150 MHz, d^4-MeOD): δ 148.05, 141.66, 135.82, 130.90, 124.67, 124.43, 104.87, 76.70, 74.88, 72.50, 71.41, 71.31, 71.27, 71.25, 71.24, 71.22, 70.43, 70.28, 69.50, 62.52, 51.33, 34.11, 29.14.

HRMS (ESI) m/z: found 737.0824 (M+4Na); calc ($C_{130}H_{205}N_{14}Na_4O_{55}$) 737.0819.

9.3.36. COMPOUND (**123**)

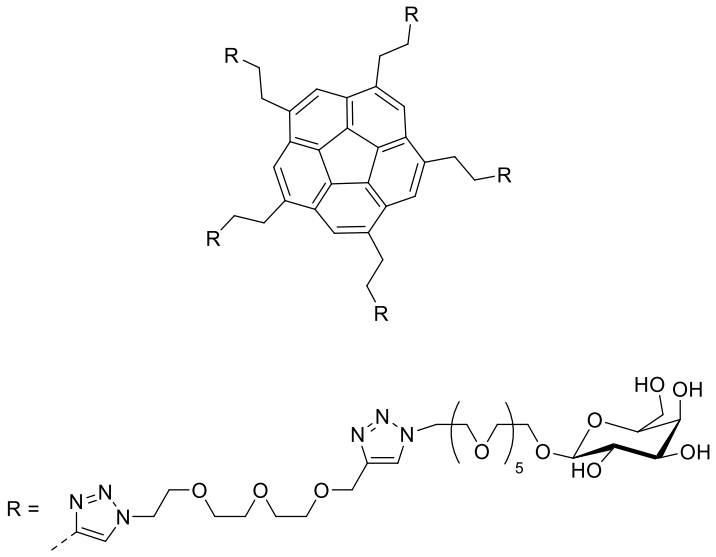

Chemical Formula: $C_{175}H_{280}N_3O_{70}$
Molecular Weight: 3546,12

A mixture of **116** (4.5 mg, 2.9 μmol), **121** (11.3 mg, 24.1 μmol) and copper nanoparticles (1.5 mg, 23.6 μmol) in DMF (300 μL) was loaded in a microwave vessel and was heated at 80 °C in a microwave reactor for 2 h. The mixture was filtrated over celite and the solid was washed with water. The crude was lyophilized and purified by size exclusion chromatography (Sephadex® G-25, water) to yield a reddish solid (5.0 mg, 44%).

^{1}H-NMR (500 MHz, D_2O/*d*^{4}-MeOD): δ 7.81 (s, 5H), 7.57 (s, 5H), 7.52 (s, 5H), 4.41 – 397 (m, 40H), 3.85 (m, 5H), 3.71 – 2.99 (m, 220H).

^{13}C-NMR (125 MHz, D_2O/*d*^{4}-MeOD): δ 144.80, 141.30, 137.38, 126.06, 124.82, 124.35, 103.84, 76.11, 73.67, 71.72, 70.67, 70.47, 70.34, 70.26, 70.22, 70.18, 69.76, 69.73, 69.59, 69.53, 66.85, 63.97, 61.92, 50.88, 50.75.

HRMS (ESI) m/z: found 807.3734 (M+5Na); calc ($C_{175}H_{280}N_{30}Na_5O_{70}$) 807.3747.

9.3.37. COMPOUND (**124**)

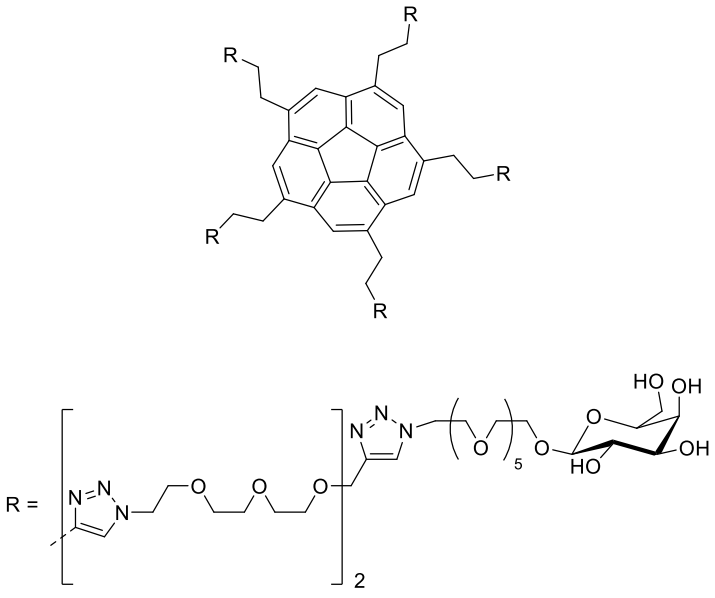

Chemical Formula: $C_{220}H_{355}N_{45}O_{85}$
Molecular Weight: 4990,49

A mixture of **117** (8.5 mg, 3.2 μmol), **121** (11.3 mg, 24.1 μmol) and copper nanoparticles (1.5 mg, 23.6 μmol) in DMF (300 μL) was loaded in a microwave vessel was heated at 80 °C in a microwave reactor for 2 h. The mixture was filtrated over celite and the solid was washed with water. The crude was lyophilized and purified by size exclusion chromatography (Sephadex® G-25, water) to yield a reddish solid (9.1 mg, 57%).

^{1}H-NMR (500 MHz, D_2O/*d*^{4}-MeOD): δ 8.01 (s, 5H), 7.88 (s, 5H), 7.68 (s, 5H), 7.60 (s, 5H), 4.58 – 4.39 (m, 50H), 4.08 – 4.06 (m, 5H), 3.98 – 3.12 (m, 255H).

^{13}C-NMR (125 MHz, D_2O/*d*^{4}-MeOD): δ 147.90, 144.84, 141.31, 134.78, 130.36, 126.25, 126.05, 124.76 124.23, 103.86, 76.12, 73.69, 71.73, 70.69, 70.57, 70.52, 70.42, 70.41, 70.35, 70.27, 70.24, 69.86, 69.79, 69.73, 69.65, 69.61, 69.54, 63.99, 61.93, 50.90, 50.77, 49.52, 33.97, 28.11.

HRMS (ESI) m/z: found 854.2378 (M+6Na); calc ($C_{220}H_{355}N_{45}Na_6O_{85}$) 854.2366.

9.3.38. COMPOUND (**125**)

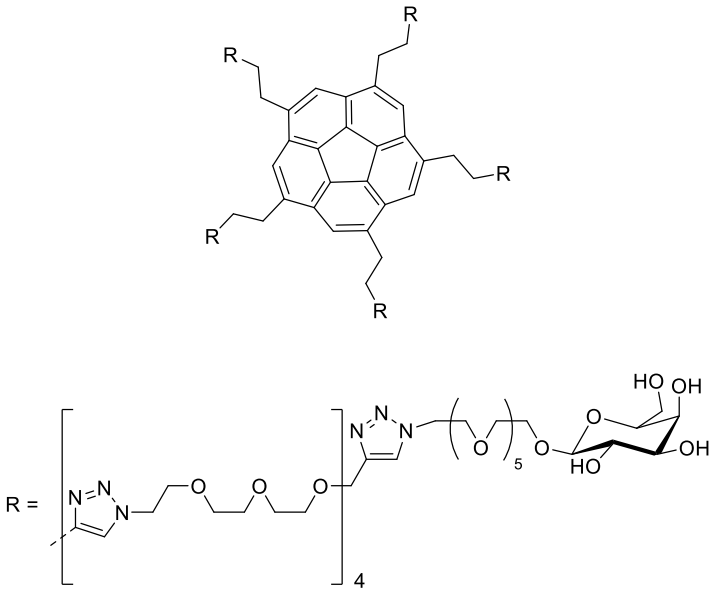

Chemical Formula: $C_{310}H_{505}N_{75}O_{115}$
Molecular Weight: 7122,86

A mixture of **118** (16.2 mg, 3.4 μmol), **121** (13.6 mg, 29.0 μmol) and copper nanoparticles (1.8 mg, 28.3 μmol) in DMF (300 μL) was loaded in a microwave vessel was heated at 80 °C in a microwave reactor for 2 h. The mixture was filtrated over celite and the solid was washed with water. The crude was lyophilized and purified by size exclusion chromatography (Sephadex® G-25, water) to yield a reddish solid (10.4 mg, 43%).

^{1}H-NMR (500 MHz, D_2O/d^4-MeOD): δ 8.07 (d, J=5.0 Hz, 5H), 8.02 (d, J=5.0 Hz, 5H), 7.98 (d, J=5.0 Hz, 5H), 7.90 (d, J=5.0 Hz, 5H), 7.89 (d, J=5.0 Hz, 5H), 7.63 (s, 5H), 4.69 – 4.39 (m, 90H), 4.08 (m, 5H), 3.96 – 3.16 (m, 345H).

^{13}C-NMR (125 MHz, D_2O/d^4-MeOD): δ 147.88, 144.97, 141.36, 134.77, 130.34, 126.15, 126.10, 126.04, 125.88, 124.59, 124.09, 103.82, 99.49, 76.02, 73.72, 71.72, 70.61, 70.58, 70.46, 70.36, 70.31, 70.26, 70.24, 69.85, 69.59, 69.57, 69.55, 69.46, 64.00, 61.87, 50.89, 50.87, 50.84, 50.74, 32.93, 28.06.

HRMS (ESI) m/z: found 912.8149 (M+8Na); calc ($C_{310}H_{505}N_{75}Na_8O_{115}$) 912.8139.

9.3.39. COMPOUND (**131**)

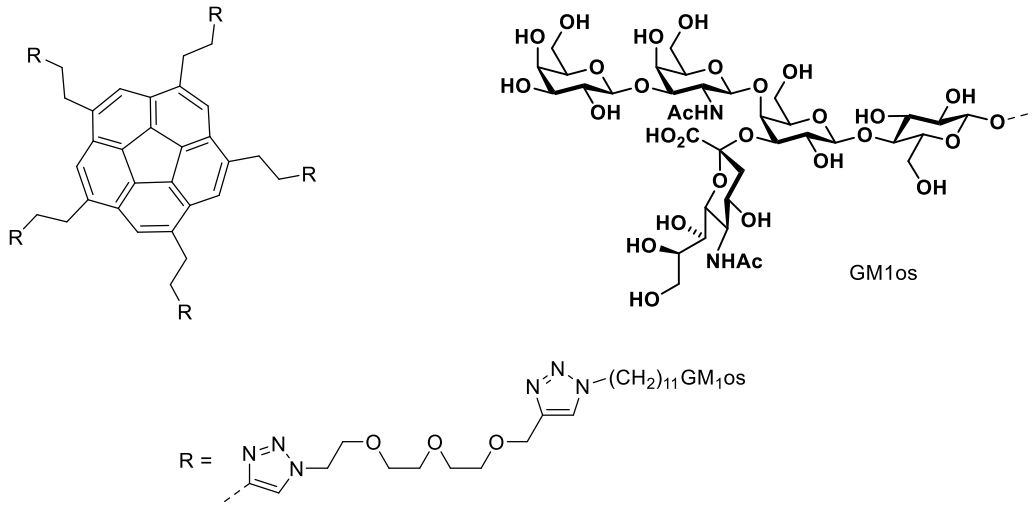

Chemical Formula: $C_{325}H_{520}N_{40}O_{160}$
Molecular Weight: 7547,85

A mixture of **116** (0.83 mg, 0.53 μmol), **130** (5.54 mg, 4.6 μmol) and copper nanoparticles (0.33 mg, 5.2 μmol) in water (150 μL) was loaded in a microwave vessel was heated at 80 °C in a microwave reactor for 2 h. The mixture was filtrated over celite and the solid was washed with water. The crude was lyophilized and purified by size exclusion chromatography (Sephadex® G-15, water) to yield a colorless solid (1.8 mg, 45%).

^{1}H-NMR (500 MHz, D_2O/*d*^{4}-MeOD): δ 7.86 – 7.70 (m, 15H), 4.55 (t, *J*=10.0 Hz, 25H), 3.81 (d, *J*=10.0 Hz, 10H), 3.76 (t, *J*=5.0 Hz, 5H), 3.85 – 3.79 (m, 15H), 3.75 3.59 (m, 40H), 3.58 – 3.52 (m, 20H), 3.47 – 3.41 (m, 20H), 3.64 – 3.33 (m, 25H), 2.69 (d, *J*=10.0 Hz, 5H), 1.98 (d, *J*=15.0 Hz, 15H), 1.93 – 1.84 (m, 5H), 1.55 – 1.54 (m br, 5H), 1.47 – 1.37 (m br, 10H), 1.26 – 1.12 (m br, 20H), 1.07 – 0.83 (m br, 30H).

^{13}C-NMR (125 MHz, D_2O/*d*^{4}-MeOD): the amount of this compound was not enough to measure a ^{13}C-NMR.

HRMS (ESI) m/z: found 1507.8678 (M–5H); calc ($C_{325}H_{515}N_{40}O_{160}$) 1507.6684.

9.3.40. COMPOUND (**132**)

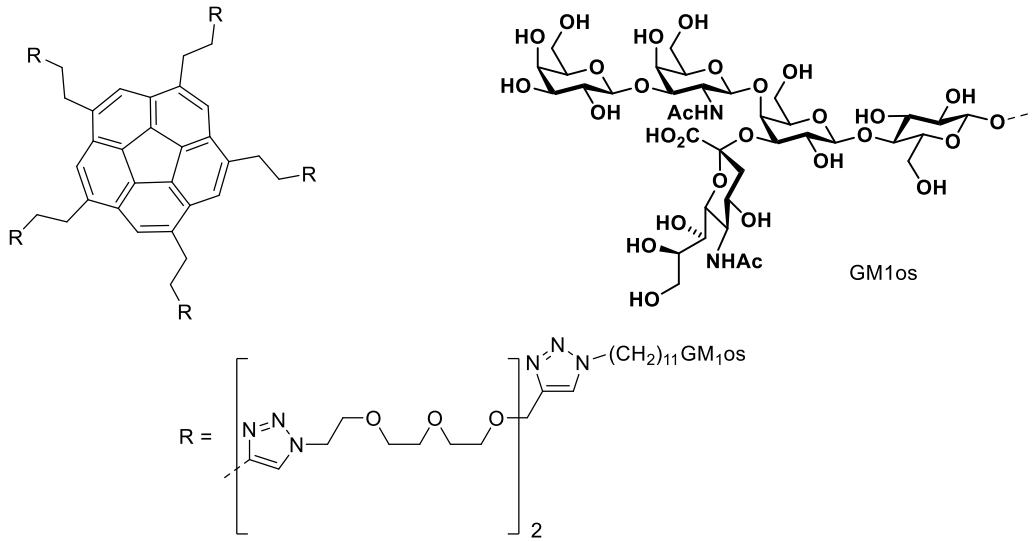

Chemical Formula: $C_{370}H_{595}N_{55}O_{175}$
Molecular Weight: 8614,04

A mixture of **117** (2.88 mg, 1.09 μmol), **130** (11.1 mg, 9.3 μmol) and copper nanoparticles (0.76 mg, 12.0 μmol) in water (300 μL) was loaded in a microwave vessel was heated at 80 °C in a microwave reactor for 2 h. The mixture was filtrated over celite and the solid was washed with water. The crude was lyophilized and purified by size exclusion chromatography (Sephadex® G-25, water) to yield a colorless solid (4.8 mg, 51%).

^{1}H-NMR (500 MHz, D_2O/*d*^{4}-MeOD): δ 7.96 – 7.75 (m, 20H), 4.57 – 4.54 (m, 70H), 4.18 – 4.05 (m, 45H), 3.94 – 3.34 (m, 286H), 2.70 (d, *J*=10.0 Hz, 5H), 2.06 (d, *J*=15.0 Hz, 35H), 1.98 – 1.94 (t, *J*=10.0 Hz, 5H), 1.62 – 1.45 (m br, 25H), 1.28 – 1.25 (m br, 20H), 1.11 – 0.90 (m br, 75H).

^{13}C-NMR (125 MHz, D_2O/*d*^{4}-MeOD): δ 175.96, 175.06, 105.70, 103.61, 103.48, 103.18, 102.70, 75.83, 75.32, 73.47, 71.66, 70.66, 70.64, 70.62, 70.52, 70.50, 70.48, 70.47, 70.45, 69.59, 69.57, 61,90, 52.61, 52.12, 51.13, 51.11, 29.73, 26.58, 26.23, 23.58, 22.99.

HRMS (ESI) m/z: found 1721.1778 (M–5H); calc ($C_{370}H_{590}N_{55}O_{175}$) 1720.7797.

9.3.41. COMPOUND (**133**)

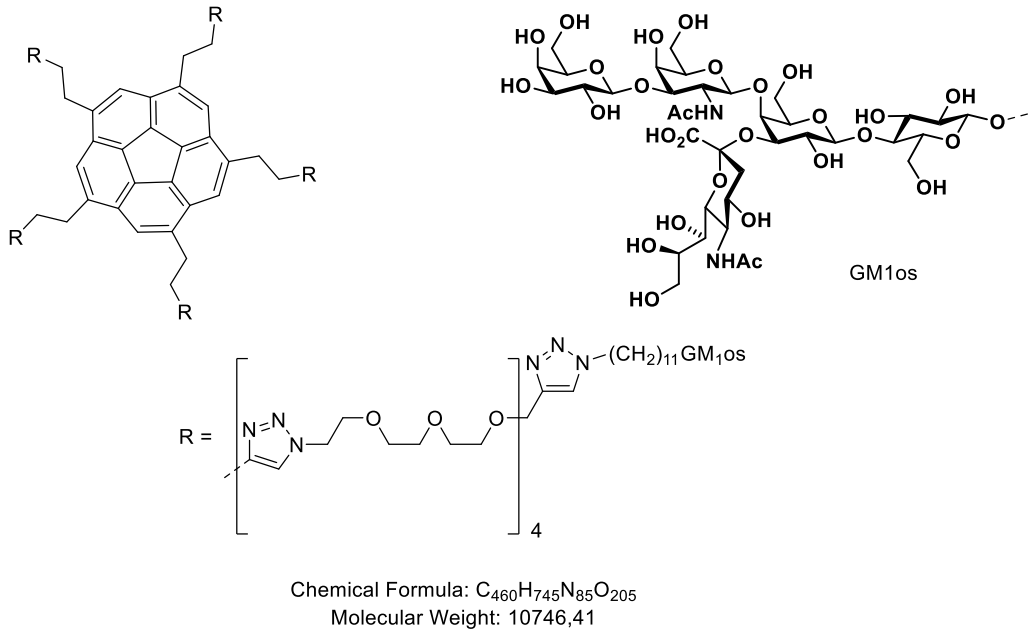

Chemical Formula: $C_{460}H_{745}N_{85}O_{205}$
Molecular Weight: 10746,41

A mixture of **118** (4.77 mg, 1.0 μmol), **130** (8.4 mg, 7.0 μmol) and copper nanoparticles (0.51 mg, 8.0 μmol) in water (300 μL) was loaded in a microwave vessel was heated at 80 °C in a microwave reactor for 2 h. The mixture was filtrated over celite and the solid was washed with water. The crude was lyophilized and purified by size exclusion chromatography (Sephadex® G-25, water) to yield a colorless solid (6.2 mg, 58%).

^{1}H-NMR (500 MHz, D_2O/*d*^{4}-MeOD): δ 7.91 – 7.67 (m, 25H), 4.47 – 4.35 (m br, 75H), 4,07 (m 20H), 3.98 (t, *J*=5.00 Hz, 10H), 3.88 – 3.15 (m, 280H), 2.60 (d, *J*=10.0 Hz, 5H), 1.95 (d, *J*=15.0 Hz, 25H), 1.85 (s, 40H), 1.55 (s br, 10H), 1.40 (s br, 10H), 1.07 – 0.91 (m br, 60H).

^{13}C-NMR (125 MHz, D_2O/*d*^{4}-MeOD): δ 175.96, 175.61, 175.05, 171.92, 144.86, 126.28, 126.25, 126.20, 126.17, 126.06, 126.05, 125.47, 105.70, 103.61, 103.47, 103.13, 102.68, 81.39, 79.72, 78.23, 75.83, 75.67, 75.50, 75.31, 75.04, 75.03, 74.07, 74.06, 73.77, 73.76, 73.74, 73.51, 73.47, 73.21, 71.66, 71.39, 70.97, 70.64, 70.62, 70.59, 70.49, 70.45, 69.91, 69.87, 69.66, 69.57, 69.00, 68.88, 64.09, 64.06, 63.80, 62.06, 61.89, 61.54, 52.60, 52.11, 51.13, 50.94, 50.83, 37.86, 30.38, 30.34, 30.33, 30.31, 29.94, 29.89, 29.86, 29.80, 29.79, 29.74, 29.72, 29.70, 29.68, 29.64, 29.62, 29.15, 26.60, 26.58, 26.18, 26.16, 24.22, 23.58, 23.00.

HRMS (ESI) m/z: found 2147.2039 (M–5H); calc ($C_{460}H_{740}N_{85}O_{205}$) 2147.0024.

9.3.42. *N*-(2-AZIDOETHYL)-HEPTANAMIDE (**142**)

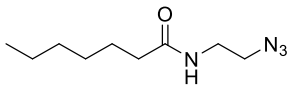

Chemical Formula: $C_9H_{18}N_4O$
Molecular Weight: 198,27

Oxalyl chloride (1.5 mL, 17.5 mmol) was added dropwise to a solution of heptanoic acid (652 mg, 5.0 mmol) in dry DCM (2 mL) and DMF (3 drops) and stirred at 0 °C under inert atmosphere. After 3.5 h, the solvent and the oxalylchoride were evaporated and the residue was dissolved in dry DCM (5 mL); this solution was then slowly added to a mixture of 2-azidoethanamine (550 mg, 6.4 mmol) in dry TEA (1.5 mL) and dry DCM (15 mL); the reaction mixture was stirred at room temperature for 24 h under inert atmosphere. The solvent was evaporated and the product was purified by column chromatography on silica gel eluted with a DCM:MeOH 97:3. The solvent was evaporated to yield a colorless solid (880 mg, 89%).

^{1}H-NMR (400 MHz, $CDCl_3$): δ 5.84 (s br, 1H), 3.42 (m, 4H), 2.18 (t, J= 7.2 Hz, 2H), 1.62 (m, 2H), 1.31 (m, 6H), 0.87 (t, J= 6.8 Hz, 3H).

^{13}C-NMR (100 MHz, $CDCl_3$): δ173.61, 51.12, 39.00, 36.80, 31.64, 29.06, 25.71, 22.61, 14.13.

HRMS (ESI) m/z: found 221.1370 (M + Na); calc ($C_9H_{18}N_4NaO$) 221.1373.

9.3.43. *N*-(2-AZIDOETHYL)-STEARAMIDE (**143**)

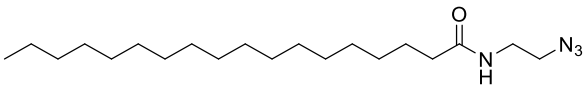

Chemical Formula: $C_{20}H_{40}N_4O$
Molecular Weight: 352,57

Oxalyl chloride (1.52 g, 12.0 mmol) was added dropwise to a solution of stearic acid (1.06 g, 3.7 mmol) in dry DCM (20 mL) and DMF (5 drops) and stirred at 0 °C under inert atmosphere. After 3.5 h, the solvent and the oxalylchoride were evaporated and the residue was dissolved in dry DCM (15 mL); this solution was then slowly added to a mixture of 2-azidoethanamine (410 mg, 4.7 mmol) in dry TEA (1.1 mL) and dry DCM (15 mL); the reaction mixture was stirred at room temperature for 18 h under inert atmosphere. The solvent was evaporated and the product was recrystallized from MeOH to yield a colorless solid (754 mg, 58%).

^{1}H-NMR (500 MHz, $CDCl_3$): δ 5.69 (s br, 1H), 3.43 (m, 4H), 2.19 (t, *J*= 7.5 Hz, 2H), 1.62 (m, 2H), 1.56 (s, 2H), 1.25 (m, 26H), 0.88 (t, *J*= 7.0 Hz, 3H).

^{13}C-NMR (125MHz, $CDCl_3$): δ 173.54, 51.21, 36.88, 32.88, 29.85, 29.83, 29.81, 29.76, 29.63, 29.51, 29.49, 29.43, 25.78, 22.85, 14.27.

HRMS (ESI) m/z: found 375.30906 (M + Na); calc ($C_{20}H_{40}N_4NaO$) 375.30943.

9.3.44. *SYM*-PENTA-2-(1,2,3-TRIAZOLE-1-(N-(2-ETHYL)HEPTANAMIDE)-4-ETHYL)-CORANNULENE (**144**)

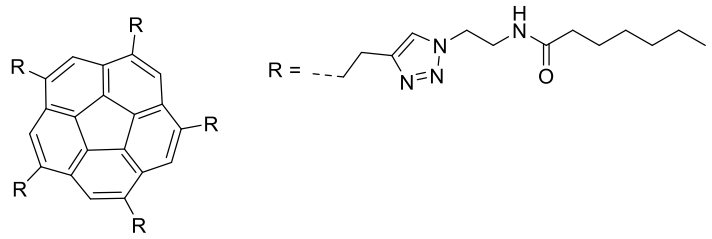

Chemical Formula: $C_{85}H_{120}N_{20}O_5$
Molecular Weight: 1502,03

A mixture of *sym*-penta-(1-butyn-4-yl)-corannulene (**67**, 10.6 mg, 20.8μmol), *N*-(2-azidoethyl)-heptanamide **142** (220 mg, 1.11mmol) and copper nanoparticles (10.1 mg, 0.16mmol) in DMF (1 mL) in a microwave vessel was heated at 60 °C in a microwave reactor for 2 hours. The mixture was then filtrated over celite and the solvent was evaporated. The product was purified by column chromatography on silica gel eluted with a DCM:MeOH 90:10. The solvent was evaporated to yield a yellow powder (19 mg, 61%).

^{1}H-NMR (500 MHz, $CDCl_3$): δ 7.48 (s, 5H), 7.43 (s, 5H), 6.71 (t br, J= 5.0 Hz, 5H), 4.43 (t br, *J*= 5.0 Hz, 10H), 3,68 (m, 10H), 3.42 (m, 10H), 3.19 (t br, *J*= 5.0 Hz, 10H), 2.08 (t, *J*= 5.0 Hz, 10H), 1.51 (t br, *J*= 5.0 Hz, 10H), 1.21 (m, 30H), 0.81 (t, *J*= 10.0 Hz, 15H).

^{13}C-NMR (125 MHz, $CDCl_3$): δ 174.19, 140.02, 134.69, 129.71, 122.95, 122.59, 49.64, 39.63, 36.56, 33.00, 31.62, 29.06, 28.02, 25.74, 22.61, 14.14.

IR (KBr): ν cm^{-1} 3294, 3072, 2927, 2856, 2102, 1657, 1548, 1455, 1368, 1217, 1143, 1052, 723.

UV ($CHCl_3$) λ_{max}, nm: 257, 264, 299.

HRMS (ESI) m/z: found 773.4762 (M + 2Na); calc ($C_{85}H_{120}N_{20}Na_2O_5$) 773..4767.

9.3.45. *SYM*-PENTA-2-(1,2,3-TRIAZOLE-1-(N-(2-ETHYL)STEARAMIDE)-4-ETHYL)-CORANNULENE (**145**)

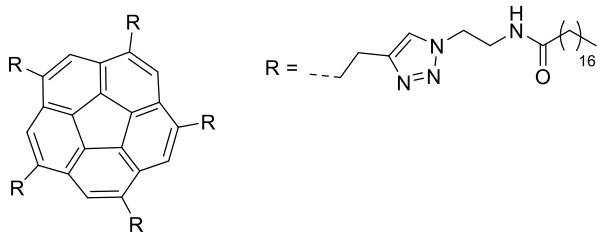

Chemical Formula: $C_{140}H_{230}N_{20}O_5$
Molecular Weight: 2273,51

A mixture of *sym*-penta-(1-butyn-4-yl)-corannulene (**67**, 29.8 mg, 58.4μmol), *N*-(2-azidoethyl)-stearamide **143** (164 mg, 0.47mmol) and copper nanoparticles (33.0 mg, 0.52mmol) in DMF (5 mL) in a microwave vessel was heated at 60 °C in a microwave reactor for 2 hours. The mixture was then filtrated over celite and the solvent was evaporated. The product was purified by column chromatography on silica gel eluted with a DCM:MeOH 93:7. The solvent was evaporated to yield a yellow powder (64 mg, 48%).

^{1}H-NMR (500 MHz, $CDCl_3$): δ 7.51 (s, 5H), 6.71 (s br, 2H), 4.47 (s br, 5H), 3.68 (s br, 10H), 3,44 (s br, 10H), 3.23 (s br, 10H), 2.10 (m, 10H), 1.53 (s br, 10H), 1.21 (m, 130H), 0.87 (t, *J*= 10.0 Hz, 15H).

^{13}C-NMR (125 MHz, $CDCl_3$): δ 174.30, 139.84, 134.75, 129.72, 123.11, 39.60, 36.63, 32.07, 29.85, 29.06, 29.80, 29.69, 29.55, 25.85, 22.83, 14.26.

IR (KBr): ν cm^{-1} 3316, 3133, 3072, 2918, 2850, 1647, 1545, 1468, 1378, 1275, 1258, 1240, 1221, 1053, 1148, 1053, 865, 720.3, 663, 585

UV ($CHCl_3$) λ_{max}, nm: 256, 263, 300.

HRMS (ESI) m/z: found 1159.4065 (M + 2Na); calc ($C_{140}H_{230}N_{20}Na_2O_5$) 1159.4086.

9.3.46. COMPOUND **147**

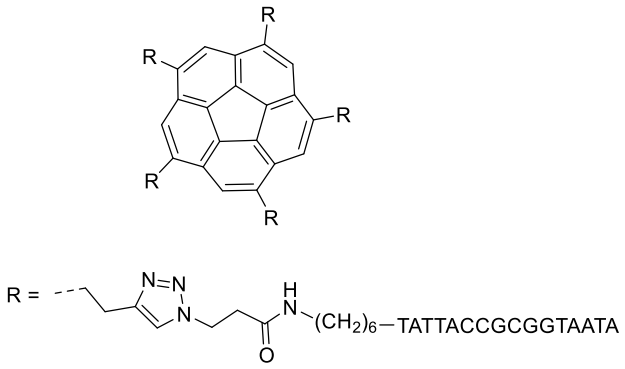

Chemical Formula: $C_{875}H_{1115}N_{315}O_{490}P_{80}$
Molecular Weight: 26363,2

10 μL of a solution of CuBr (92 μg, 0.64 μmol) and TBTA (0.546 mg, 1.0 μmol) in water:THF 1:1 (100 μl) was added to a solution of *sym*-penta-(1-butyn-4-yl)-corannulene **67** (49 μg, 96 nmol) and oligonucleotide **146** (1.1 μmol) in THF (5 μl) and water (15 μl) and heated at 60 °C for 2 days and at 80 °C for 4 days. The reaction mixture was then desalted with Sephadex G-25. The crude product was then purified by 6% D-PAGE (acrylamide:bisacrylamide 19:1, Urea 7 M) at constant power of 40 W, using TBE buffer (Tris 11 g, boric acid 5.6 g and EDTA 0.74 g in 1 L of sterile water). Following electrophoresis, the plate was wrapped in plastic and placed on a fluorescent TLC plate and illuminated with UV lamp (254 nm). The band was quickly excised, and the gel pieces were frozen with liquid nitrogen, crushed and incubated overnight in 2 volumes of NaOAc (0.5 M, pH 5.2 with HCl) at 37 °C. The samples was then centrifuges and the supernatant collected. The gel was the washed with 1/5 volume of NaOAc 0.5 M, centrifuged and the supernatant collected. The aqueous solution was then extracted with *n*-butanol to 1/3 of the original volume. 0.16 volume of a solution of LiCl 4 M and $MgCl_2$ 0.125 mM and 3 volumes of cold ethanol (100%, -80 °C) were added to the aqueous solution and stored overnight at -80 °C. The sample was then centrifuged (13200 rpm, 4 °C, 20 min) and the supernatant was removed. The precipitate was washed 3 times with cold ethanol (80 %, 0 °C), dissolved in sterile milliQ water and desalted with Float-A-Lyzer G2. The amount of **147** was quantified by UV absorption (300 nm assuming $\varepsilon=3.28\cdot10^4$) The sample was then freeze-dried yielding the desired product as a pale yellow powder (304 μg, 12%).

MALDI-TOF MS m/z found 26483.2 (M + 5Na + 18 H); calc. ($C_{875}H_{1195}N_{315}O_{490}P_{80}Na_2Li$) 26483.7241.

9.4. ELISA ASSAYS

Each well of a 96-well microtiter plate was coated with a 100 μL native GM1 solution (1.3 μM in ethanol) after which the solvent was evaporated. Unattached GM1 was removed by washing with PBS (3 × 450 μL), the remaining free binding sites were blocked by incubation with 100 μL of a 1% (w/v) BSA solution in PBS for 30 min at 37 °C. Subsequently, the wells were washed with PBS (3 × 450 μL). In separate vials, a logarithmic serial dilution, starting from 2.0 mM, of 150 μL saccharide-corannulenes in 0.1% BSA, 0.05% Tween-20 in PBS, mixed with 150 μL of a 50 ng/mL CTB-HRP solution in the same buffer were incubated. This gave an initial inhibitor concentration of 1.0 mM. In the case of potent inhibitors, based on the logarithmic experiments, a more accurate, serial dilution of a factor two was performed around the expected IC_{50} values. The inhibitor-toxin mixtures were incubated at room temperature for 2 h and then transferred to the coated wells. After 30 min of incubation at room temperature, unbound CTB-HRP-corannulene complexes were removed from the wells by washing with 0.1% BSA, 0.05% Tween-20 in PBS (3 x 500 μL). 100 μL of a freshly prepared OPD solution (25 mg OPD·2HCl, 7.5 mL 0.1M citric acid, 7.5 mL 0.1M sodium citrate and 6 μL of a 30% H_2O_2 solution, pH was adjusted to 6.0 with NaOH) was added to each well and allowed to react with HRP in absence of light, at room temperature, for 15 min. The oxidation reaction was quenched by addition of 50 μL 1M H_2SO_4. Within 5 min, the adsorbance was measured at 490 nm.

9.5. GELATION TEST

In a typical gelation experiment a weighed amount of compound and 1 mL of the solvent mixture were placed in a vial, which was sealed and then heated until the compound dissolved. The solution was allowed to cool to room temperature. Gelation was considered to have occurred when a homogeneous substance was obtained, which exhibited no gravitational flow.

9.6. ASSEMBLING STUDIES OF COMPOUND **147**

9.6.1. KINETICALLY-CONTROLLED PROCEDURE

A 2 μM solution of **22** in TE buffer (Tris 10 mM, EDTA 1 mM pH 7.5 with HCl) with NaCl 100 mM and $MgCl_2$ 5 mM was heated for 5 min at 95 °C in a heating block; the sample was then transferred in an ice-bath, kept at 0 °C for 10 min and then loaded on the gel.

9.6.2. THERMODYNAMICALLY-CONTROLLED PROCEDURE

A 1 μM solution of **22** in TE buffer (Tris 10 mM, EDTA 1 mM pH 7.5 with HCl) with $MgCl_2$ 10 mM was heated for 5 min at 95 °C in a heating block, then slowly cooled to 55 °C, kept at this temperature for 50 hours, then slowly cooled to 4 °C and loaded on the gel. *Native PAGE*: the sample from assembling studies were analyzed by 4% native-PAGE (acrylamide:bisacrylamide 19:1) at 4 °C and at constant current of 10 mA for 1.5 hours. The gels were stained with ethidium bromide.

9.7. ENZYMATIC DIGESTION

Digestion of single-stranded DNA with mung bean nuclease was performed for 3 hours at 0 °C in sodium acetate buffer (10 mM, $Zn(OAc)_2$ 0.1 mM, cysteine 1 mM, Triton X-100 0.001% and glycerol 50%) applying 10 units of mung bean nuclease per μg of **147**.

11. REFERENCES

1 R. G. Lawton and W. E. Barth, *J. Am. Chem. Soc.*, 1971, **93**, 1730–1745.

2 G. Gleicher, *Tetrahedron*, 1967, **23**, 4257–4263.

3 L. T. Scott, M. M. Hashemi, D. T. Meyer and H. B. Warren, *J. Am. Chem. Soc.*, 1991, **113**, 7082–7084.

4 S. Grabowsky, M. Weber, Y. S. Chen, D. Lentz, B. M. Schmidt, M. Hesse and P. Z. Luger, *Naturforsch.*, 2010, **65b**.

5 A. Borchardt, A. Fuchicello, K. V. Kilway, K. K. Baldridge and J. S. Siegel, *J. Am. Chem. Soc.*, 1992, **114**, 1921–1923.

6 M. Fedurco, M. M. Olmstead and W. R. Fawcett, *Inorg. Chem.*, 1995, **34**, 390–392.

7 J. C. Hanson and C. E. Nordman, *Acta Crystallogr B Struct Crystallogr Cryst Chem*, 1976, **32**, 1147–1153.

8 Y. Sevryugina, A. Y. Rogachev, E. A. Jackson, L. T. Scott and M. A. Petrukhina, *J. Org. Chem.*, 2006, **71**, 6615–6618.

9 L. T. Scott, M. M. Hashemi and M. S. Bratcher, *J. Am. Chem. Soc.*, 1992, **114**, 1920–1921.

10 T. J. Seiders, K. K. Baldridge, G. H. Grube and J. S. Siegel, *J. Am. Chem. Soc.*, 2001, **123**, 517–525.

11 W. E. Barth and R. G. Lawton, *J. Am. Chem. Soc.*, 1966, **88**, 380–381.

12 J. T. Craig and M. D. Robins, *Aust. J. Chem.*, 1968, **21**, 2237.

13 J. R. Davy, M. N. Iskander and J. A. Reiss, *Tetrahedron Letters*, 1978, **19**, 4085–4088.

14 J. R. Davy, M. N. Iskander and J. A. Reiss, *Aust. J. Chem.*, 1979, **32**, 1067.

15 H. W. Kroto, J. R. Heath, S. C. O'Brien, R. F. Curl and R. E. Smalley, *Nature*, 1985, **318**, 162–163.

16 a) R. F. Brown, F. W. Eastwood and G. P. Jackman, *Aust. J. Chem.*, 1978, **31**, 579; b) R. F. Brown, F. W. Eastwood and G. P. Jackman, *Aust. J. Chem.*, 1977, **30**, 1757; c) R. F. C. Brown, K. J. Harrington and G. L. McMullen, *J. Chem. Soc., Chem. Commun.*, 1974, 123.

17 R. F. Brown, F. W. Eastwood, K. J. Harrington and G. L. McMullen, *Aust. J. Chem.*, 1974, **27**, 2391.

18 L. T. Scott, P.-C. Cheng, M. M. Hashemi, M. S. Bratcher, D. T. Meyer and H. B. Warren, *J. Am. Chem. Soc.*, 1997, **119**, 10963–10968.

19 C. Z. Liu and P. W. Rabideau, *Tetrahedron Letters*, 1996, **37**, 3437–3440.

20 H.-J. Knölker, A. Braier, D. J. Bröcher, P. G. Jones and H. Piotrowski, *Tetrahedron Letters*, 1999, **40**, 8075–8078.

21 G. Zimmermann, U. Nuechter, S. Hagen and M. Nuechter, *Tetrahedron Letters*, 1994, **35**, 4747–4750.

22 G. Mehta and G. Panda, *Tetrahedron Letters*, 1997, **38**, 2145–2148.

23 T. J. Seiders, K. K. Baldridge and J. S. Siegel, *J. Am. Chem. Soc.*, 1996, **118**, 2754–2755.

24 T. J. Seiders, E. L. Elliott, G. H. Grube and J. S. Siegel, *J. Am. Chem. Soc.*, 1999, **121**, 7804–7813.

25 A. Sygula and P. W. Rabideau, *J. Am. Chem. Soc.*, 1999, **121**, 7800–7803.

26 A. M. Butterfield, B. Gilomen and J. S. Siegel, *Org. Process Res. Dev.*, 2012, **16**, 664–676.

27 a) G. Xu, A. Sygula, Z. Marcinow and P. W. Rabideau, *Tetrahedron Letters*, 2000, **41**, 9931–9934; b) A. Sygula and P. W. Rabideau, *J. Am. Chem. Soc.*, 2000, **122**, 6323–6324.

28 A. Sygula, G. Xu, Z. Marcinow and P. W. Rabideau, *Tetrahedron*, 2001, **57**, 3637–3644.

29 a) A. Sygula, R. Sygula and P. W. Rabideau, *Org. Lett.*, 2006, **8**, 5909–5911; b) Y.-T. Wu and J. S. Siegel, *Chem. Rev.*, 2006, **106**, 4843–4867; c) Z. Marcinow, A. Sygula, A. Ellern and P. W. Rabideau, *Org. Lett.*, 2001, **3**, 3527–3529.

30 Y.-T. Wu, T. Hayama, K. K. Baldridge, A. Linden and J. S. Siegel, *J. Am. Chem. Soc.*, 2006, **128**, 6870–6884.

31 E. A. Jackson, B. D. Steinberg, M. Bancu, A. Wakamiya and L. T. Scott, *J. Am. Chem. Soc.*, 2007, **129**, 484–485.

32 B. D. Steinberg, E. A. Jackson, A. S. Filatov, A. Wakamiya, M. A. Petrukhina and L. T. Scott, *J. Am. Chem. Soc.*, 2009, **131**, 10537–10545.

33 a) A. H. Abdourazak, A. Sygula and P. W. Rabideau, *J. Am. Chem. Soc.*, 1993, **115**, 3010–3011; b) A. Sygula and P. W. Rabideau, *J. Am. Chem. Soc.*, 1998, **120**, 12666–12667.

34 A. Sygula, S. D. Karlen, R. Sygula and P. W. Rabideau, *Org. Lett.*, 2002, **4**, 3135–3137.

35 a) A. Stanger, A. Shachter and R. Boese, *Tetrahedron*, 1998, **54**, 1207–1220; b) A. Stanger, N. Ashkenazi, A. Shachter, D. Bläser, P. Stellberg and R. Boese, *J. Org. Chem.*, 1996, **61**, 2549–2552.

36 R. M. Maag, Diploma Thesis, University of Zurich, 2006.

37 Y.-T. Wu, D. Bandera, R. Maag, A. Linden, K. K. Baldridge and J. S. Siegel, *J. Am. Chem. Soc.*, 2008, **130**, 10729–10739.

38 a) F. Alonso, I. P. Beletskaya and M. Yus, *Chem. Rev.*, 2002, **102**, 4009–4092; b) P. P. Cellier, J.-F. Spindler, M. Taillefer and H.-J. Cristau, *Tetrahedron Letters*, 2003, **44**, 7191–7195.

39 H. Miyamoto, K. Yui, Y. Aso, T. Otsubo and F. Ogura, *Tetrahedron Letters*, 1986, **27**, 2011–2014.

40 L. T. Scott, *Pure Appl. Chem.*, 1996, **68**, 291–300.

41 S. Mizyed, P. E. Georghiou, M. Bancu, B. Cuadra, A. K. Rai, P. Cheng and L. T. Scott, *J. Am. Chem. Soc.*, 2001, **123**, 12770–12774.

42 M. N. Eliseeva and L. T. Scott, *J. Am. Chem. Soc.*, 2012, **134**, 15169–15172.

43 L. T. Scott, H. E. Bronstein, D. V. Preda, R. B. M. Ansems, M. S. Bratcher and S. Hagen, *Pure Appl. Chem.*, 1999, **71**, 209–219.

44 T. J. Seiders, K. K. Baldridge, E. L. Elliott, G. H. Grube and J. S. Siegel, *J. Am. Chem. Soc.*, 1999, **121**, 7439–7440.

45 G. H. Grube, E. L. Elliott, R. J. Steffens, C. S. Jones, K. K. Baldridge and J. S. Siegel, *Org. Lett.*, 2003, **5**, 713–716.

46 T. Hayama, K. K. Baldridge, Y.-T. Wu, A. Linden and J. S. Siegel, *J. Am. Chem. Soc.*, 2008, **130**, 1583–1591.

47 T. Hayama, PhD. Thesis, University of Zurich, 2008.

48 M. R. Biscoe, B. P. Fors and S. L. Buchwald, *J. Am. Chem. Soc.*, 2008, **130**, 6686–6687.

49 L. T. Scott, E. A. Jackson, Q. Zhang, B. D. Steinberg, M. Bancu and B. Li, *J. Am. Chem. Soc.*, 2012, **134**, 107–110.

50 Adam F. Littke, Gregory C. Fu, *Angew. Chem. Int. Ed. Engl.*, 1998, **37**, 3387–3388.

51 A. F. Littke, C. Dai and G. C. Fu, *J. Am. Chem. Soc.*, 2000, **122**, 4020–4028.

52 D. Pappo, T. Mejuch, O. Reany, E. Solel, M. Gurram and E. Keinan, *Org. Lett.*, 2009, **11**, 1063–1066.

53 M. R. Eberhard, Z. Wang and C. M. Jensen, *Chem. Commun.*, 2002, 818–819.

54 P. E. Georghiou, A. H. Tran, S. Mizyed, M. Bancu and L. T. Scott, *J. Org. Chem.*, 2005, **70**, 6158–6163.
55 R. Gershoni-Poranne, D. Pappo, E. Solel and E. Keinan, *Org. Lett.*, 2009, **11**, 5146–5149.
56 M. Bancu, A. K. Rai, P. Cheng, R. D. Gilardi and L. T. Scott, *Synlett*, 2004, 173–176.
57 M. Ballester, C. Molinet and J. Castaner, *J. Am. Chem. Soc.*, 1960, **82**, 4254–4258.
58 T. Hayama, Y.-T. Wu, A. Linden, K. K. Baldridge and J. S. Siegel, *J. Am. Chem. Soc.*, 2007, **129**, 12612–12613.
59 K. K. Baldridge, K. I. Hardcastle, T. J. Seiders and J. S. Siegel, *Org. Biomol. Chem.*, 2009, **8**, 53.
60 A. Pogoreltsev, E. Solel, D. Pappo and E. Keinan, *Chem. Commun.*, 2012, **48**, 5425.
61 J. Mack, P. Vogel, D. Jones, N. Kaval and A. Sutton, *Org. Biomol. Chem.*, 2007, **5**, 2448.
62 H. Boedigheimer, G. M. Ferrence and T. D. Lash, *J. Org. Chem.*, 2010, **75**, 2518–2527.
63 I. Hargittai, *Fivefold Symmetry*, 1992.
64 a) N. S. Poonia and A. V. Bajaj, *Chem. Rev.*, 1979, **79**, 389–445; b) C. Silvestru, H. J. Breunig and H. Althaus, *Chem. Rev.*, 1999, **99**, 3277–3328; c) B. Hasenknopf, J.-M. Lehn, B. O. Kneisel, G. Baum and D. Fenske, *Angew. Chem. Int. Ed. Engl.*, 1996, **35**, 1838–1840; d) V. W. Day, T. J. Marks and W. A. Wachter, *J. Am. Chem. Soc.*, 1975, **97**, 4519–4527.
65 a) O. Pornillos, B. K. Ganser-Pornillos and M. Yeager, *Nature*, 2011, **469**, 424–427; b) G. Cardone, J. G. Purdy, N. Cheng, R. C. Craven and A. C. Steven, *Nature*, 2009, **457**, 694–698; c) D. Voet and J. G. Voet, *Biochemie*, VCH Verlagsgesellschaft, mbH, Weinheim, 1992; d) B. K. Ganser, *Science*, 1999, **283**, 80–83.
66 C. Zhang, M. Su, Y. He, X. Zhao, P.-a. Fang, A. E. Ribbe, W. Jiang and C. Mao, *Proceedings of the National Academy of Sciences*, 2008, **105**, 10665–10669.
67 Y. He, T. Ye, M. Su, C. Zhang, A. E. Ribbe, W. Jiang and C. Mao, *Nature*, 2008, **452**, 198–201.
68 P. W. K. Rothemund, *Nature*, 2006, **440**, 297–302.
69 J. M. Kim, Y.-h. Lee, C. R. Ku and E. J. Lee, *Endocrinology*, 2011, **152**, 536–544.
70 E. Fan, Z. Zhang, W. E. Minke, Z. Hou, Verlinde,Christophe L. M. J. and W. G. J. Hol, *J. Am. Chem. Soc.*, 2000, **122**, 2663–2664.
71 Z. Zhang, J. Liu, Verlinde,Christophe L. M. J., W. G. J. Hol and E. Fan, *J. Org. Chem.*, 2004, **69**, 7737–7740.
72 a) P. Dedek, V. Janout and S. L. Regen, *J. Org. Chem.*, 1993, **58**, 6553–6555; b) C. Gargiulli, G. Gattuso, C. Liotta, A. Notti, M. F. Parisi, I. Pisagatti and S. Pappalardo, *J. Org. Chem.*, 2009, **74**, 4350–4353; c) D. Mendoza-Espinosa and T. A. Hanna, *Dalton Trans.*, 2009, 5211.
73 G. Cafeo, F. H. Kohnke, M. F. Parisi, R. Pistone Nascone, G. L. La Torre and D. J. Williams, *Org. Lett.*, 2002, **4**, 2695–2697.
74 D. Bardelang, K. A. Udachin, R. Anedda, I. Moudrakovski, D. M. Leek, J. A. Ripmeester and C. I. Ratcliffe, *Chem. Commun.*, 2008, 4927.
75 T. Ogoshi, S. Kanai, S. Fujinami, T.-a. Yamagishi and Y. Nakamoto, *J. Am. Chem. Soc.*, 2008, **130**, 5022–5023.
76 a) B. Qin, W. Q. Ong, R. Ye, Z. Du, X. Chen, Y. Yan, K. Zhang, H. Su and H. Zeng, *Chem. Commun.*, 2011, **47**, 5419; b) B. Qin, X. Chen, X. Fang, Y. Shu, Y. K. Yip, Y. Yan, S. Pan, W. Q. Ong, C. Ren, H. Su and H. Zeng, *Org. Lett.*, 2008, **10**, 5127–5130.

77 M. C. Stuparu, *CHIMIA*, 2011, **65**, 799–801.

78 D. Miyajima, K. Tashiro, F. Araoka, H. Takezoe, J. Kim, K. Kato, M. Takata and T. Aida, *J. Am. Chem. Soc.*, 2009, **131**, 44–45.

79 L. Baldini, A. Casnati, F. Sansone and R. Ungaro, *Chem. Soc. Rev.*, 2007, **36**, 254.

80 a) T. Seiders, K. K. Baldridge, J. S. Siegel and R. Gleiter, *Tetrahedron Letters*, 2000, **41**, 4519–4522; b) T. Jon Seiders, K. K. Baldridge and J. S. Siegel, *Tetrahedron*, 2001, **57**, 3737–3742.

81 A. Bernardi, J. Jiménez-Barbero, A. Casnati, C. de Castro, T. Darbre, F. Fieschi, J. Finne, H. Funken, K.-E. Jaeger, M. Lahmann, T. K. Lindhorst, M. Marradi, P. Messner, A. Molinaro, P. V. Murphy, C. Nativi, S. Oscarson, S. Penadés, F. Peri, R. J. Pieters, O. Renaudet, J.-L. Reymond, B. Richichi, J. Rojo, F. Sansone, C. Schäffer, W. B. Turnbull, T. Velasco-Torrijos, S. Vidal, S. Vincent, T. Wennekes, H. Zuilhof and A. Imberty, *Chem. Soc. Rev.*, 2013, **42**, 4709.

82 Y. M. Chabre and R. Roy, *Chem. Soc. Rev.*, 2013, **42**, 4657.

83 T. R. Branson and W. B. Turnbull, *Chem. Soc. Rev.*, 2013, **42**, 4613.

84 a) J. P. Schneider and J. W. Kelly, *Chem. Rev.*, 1995, **95**, 2169–2187; b) J. W. Bryson, S. F. Betz, H. S. Lu, D. J. Suich, H. X. Zhou, K. T. O'Neil and W. F. DeGrado, *Science*, 1995, **270**, 935–941; c) M. Mutter and S. Vuilleumier, *Angew. Chem. Int. Ed. Engl.*, 1989, **28**, 535–554.

85 F. A. Aldaye, A. L. Palmer and H. F. Sleiman, *Science*, 2008, **321**, 1795–1799.

86 N. C. Seeman, *Mol Biotechnol*, 2007, **37**, 246–257.

87 a) N. Kudo, M. Perseghini and G. C. Fu, *Angew. Chem. Int. Ed.*, 2006, **45**, 1282–1284; b) Adam F. Littke, Gregory C. Fu Prof, *Angew. Chem. Int. Ed.*, 2002, **41**, 4176–4211.

88 a) S. M. Neumann and J. K. Kochi, *J. Org. Chem.*, 1975, **40**, 599–606; b) R. S. Smith and J. K. Kochi, *J. Org. Chem.*, 1976, **41**, 502–509; c) J. K. Kochi, *Acc. Chem. Res.*, 1974, **7**, 351–360; d) M. Tamura and J. K. Kochi, *J. Am. Chem. Soc.*, 1971, **93**, 1487–1489; e) M. Tamura and J. K. Kochi, *Synthesis*, 1971, **1971**, 303–305.

89 G. Cahiez and S. Marquais, *Pure Appl. Chem.*, 1996, **68**, 53–60.

90 W. Dohle, F. Kopp, G. Cahiez and P. Knochel, *Synlett*, 2001, **2001**, 1901–1904.

91 a) M. A. Fakhfakh, X. Franck, R. Hocquemiller and B. Figadère, *Journal of Organometallic Chemistry*, 2001, **624**, 131–135; b) H. M. Walborsky and R. B. Banks, *J. Org. Chem.*, 1981, **46**, 5074–5077; c) G. A. Molander, B. J. Rahn, D. C. Shubert and S. E. Bonde, *Tetrahedron Letters*, 1983, **24**, 5449–5452; d) A. Fürstner and H. Brunner, *Tetrahedron Letters*, 1996, **37**, 7009–7012.

92 E. Alvarez, T. Cuvigny, C. Du Penhoat and M. Julia, *Tetrahedron*, 1988, **44**, 119–126.

93 a) C. Cardellicchio, V. Fiandanese, G. Marchese and L. Ronzini, *Tetrahedron Letters*, 1987, **28**, 2053–2056; b) M. M. Dell'Anna, P. Mastrorilli, C. F. Nobile, G. Marchese and M. R. Taurino, *Journal of Molecular Catalysis A: Chemical*, 2000, **161**, 239–243; c) K. Ritter and M. Hanack, *Tetrahedron Letters*, 1985, **26**, 1285–1288; d) W. C. Percival, R. B. Wagner and N. C. Cook, *J. Am. Chem. Soc.*, 1953, **75**, 3731–3734; e) V. Fiandanese, G. Marchese, V. Martina and L. Ronzini, *Tetrahedron Letters*, 1984, **25**, 4805–4808; f) C. Cardellicchio, V. Fiandanese, G. Marchese and L. Ronzini, *Tetrahedron Letters*, 1985, **26**, 3595–3598.

94 a) A. Yanagisawa, N. Nomura and H. Yamamoto, *Tetrahedron*, 1994, **50**, 6017–6028; b) A. Yanagisawa, N. Nomura and H. Yamamoto, *Synlett*, 1991, **1991**, 513–514.

95 a) A. Fürstner, *Active metals. Preparation, characterization, applications*, VCH, Weinheim [Germany], New York, 1996; b) L. E. Aleandri, B. Bogdanovic, P. Bons, C. Duerr, A. Gaidies, T. Hartwig, S. C. Huckett, M. Lagarden, U. Wilczok and R. A. Brand, *Chem. Mater.*, 1995, **7**, 1153–1170.

96 B. Bogdanovic and M. Schwickardi, *Angew. Chem. Int. Ed.*, 2000, **39**, 4610–4612.

97 G. Siedlaczek, M. Schwickardi, U. Kolb, B. Bogdanovic and D. Blackmond, *Catalysis Letters*, 1998, **55**, 67–72.

98 Fürstner, A. and Leitner, A., *Angew. Chem. Int. Ed.*, 2002, **41**, 609–612.

99 A. Fürstner, A. Leitner, M. Méndez and H. Krause, *J. Am. Chem. Soc.*, 2002, **124**, 13856–13863.

100 B. D. Sherry and A. Fürstner, *Acc. Chem. Res.*, 2008, **41**, 1500–1511.

101 A. Fürstner, R. Martin, H. Krause, G. Seidel, R. Goddard and C. W. Lehmann, *J. Am. Chem. Soc.*, 2008, **130**, 8773–8787.

102 M. Mattarella and J. S. Siegel, *Org. Biomol. Chem.*, 2012, **10**, 5799.

103 Wuts, Peter G. M and T. W. Greene, *Greene's protective groups in organic synthesis*, Wiley-Interscience, Hoboken, N.J, 4th edn., 2007.

104 A. Orita, J. Yaruva, J. Otera, *Angew. Chem. Int. Ed.*, 1999, **38**, 2267–2270.

105 a) S. Winstein, E. Grunwald and H. W. Jones, *J. Am. Chem. Soc.*, 1951, **73**, 2700–2707; b) E. Grunwald and S. Winstein, *J. Am. Chem. Soc.*, 1948, **70**, 846–854.

106 J. B. Lambert, *Organic structural spectroscopy*, Prentice Hall, Boston, 2nd edn., 2010.

107 J. H. van't Hoff, *Arrangement of Atoms in Space*, Longmans, London, 2nd edn., 1898.

108 R. L. Letsinger, *J. Am. Chem. Soc.*, 1948, **70**, 406–409.

109 a) Rostovtsev, V. V., Green, L. G., Fokin, V. V. and Sharpless, K. B., *Angew. Chem. Int. Ed.*, 2002, **41**, 2596–2599; b) L. Liang and D. Astruc, *Coordination Chemistry Reviews*, 2011, **255**, 2933–2945.

110 a) J. E. Moses and A. D. Moorhouse, *Chem. Soc. Rev.*, 2007, **36**, 1249–1262; b) H. C. Kolb, M. G. Finn and K. B. Sharpless, *Angew. Chem. Int. Ed.*, 2001, **40**, 2004–2012.

111 a) R. Franke, C. Doll and J. Eichler, *Tetrahedron Letters*, 2005, **46**, 4479–4482; b) Q. Wang, T. R. Chan, R. Hilgraf, V. V. Fokin, K. B. Sharpless and M. G. Finn, *J. Am. Chem. Soc.*, 2003, **125**, 3192–3193; c) C. W. Tornøe, C. Christensen and M. Meldal, *J. Org. Chem.*, 2002, **67**, 3057–3064; d) J. Gierlich, G. A. Burley, P. M. E. Gramlich, D. M. Hammond and T. Carell, *Org. Lett.*, 2006, **8**, 3639–3642.

112 a) M. R. Whittaker, C. N. Urbani and M. J. Monteiro, *J. Am. Chem. Soc.*, 2006, **128**, 11360–11361; b) P. Wu, M. Malkoch, J. N. Hunt, R. Vestberg, E. Kaltgrad, M. G. Finn, V. V. Fokin, K. B. Sharpless and C. J. Hawker, *Chem. Commun.*, 2005, 5775; c) P. Wu, A. K. Feldman, A. K. Nugent, C. J. Hawker, A. Scheel, B. Voit, J. Pyun, J. M. J. Fréchet, K. B. Sharpless and V. V. Fokin, *Angew. Chem. Int. Ed.*, 2004, **43**, 3928–3932; d) V. Ladmiral, G. Mantovani, G. J. Clarkson, S. Cauet, J. L. Irwin and D. M. Haddleton, *J. Am. Chem. Soc.*, 2006, **128**, 4823–4830; e) B. A. Laurent and S. M. Grayson, *J. Am. Chem. Soc.*, 2006, **128**, 4238–4239; f) B. Helms, J. L. Mynar, C. J. Hawker and J. M. J. Fréchet, *J. Am. Chem. Soc.*, 2004, **126**, 15020–15021.

113 a) A. D. Moorhouse, A. M. Santos, M. Gunaratnam, M. Moore, S. Neidle and J. E. Moses, *J. Am. Chem. Soc.*, 2006, **128**, 15972–15973; b) Lewis, W. G., Green, L. G., Grynszpan, F., Radić, Z., Carlier, P. R., Taylor, P., Finn, M. G. and Sharpless, K. B., *Angew. Chem. Int. Ed.*, 2002, **41**, 1053–1057; c) H. C. Kolb

and K. Sharpless, *Drug Discovery Today*, 2003, **8**, 1128–1137; d) L. V. Lee, M. L. Mitchell, S.-J. Huang, V. V. Fokin, K. B. Sharpless and C.-H. Wong, *J. Am. Chem. Soc.*, 2003, **125**, 9588–9589.

114 F. Alonso, Y. Moglie, G. Radivoy and M. Yus, *Tetrahedron Letters*, 2009, **50**, 2358–2362.

115 T. G. Upton, B. A. Kashemirov, C. E. McKenna, M. F. Goodman, G. K. S. Prakash, R. Kultyshev, V. K. Batra, D. D. Shock, L. C. Pedersen, W. A. Beard and S. H. Wilson, *Org. Lett.*, 2009, **11**, 1883–1886.

116 I. Yamamoto, M. Sekine and T. Hata, *J. Chem. Soc., Perkin Trans. 1*, 1980, 306.

117 a) Schillinger, E.-K., Mena-Osteritz, E., Hentschel, J., Börner, H. G. and Bäuerle, P., *Adv. Mater.*, 2009, **21**, 1562–1567; b) H.-A. Klok, A. Rösler, G. Gütz, E. Mena-Osteritz and P. Bäuerle, *Org. Biomol. Chem.*, 2004, **2**, 3541.

118 Landau, E. M. and Rosenbusch, J. P., *Proceedings of the National Academy of Sciences*, 1996, **93**, 14532–14535.

119 Y. M. Osornio, P. Uebelhart, S. Bosshard, F. Konrad, J. S. Siegel and E. M. Landau, *J. Org. Chem.*, 2012, **77**, 10583–10595.

120 M. Mattarella, J. Haberl, J. Ruokolainen, E. M. Landau, R. Mezzenga and J. S. Siegel, *Chem. Commun.*, 2013, **49**, 7204–7206.

121 M. Mattarella, J. Garcia-Hartjes, T. Wennekes, H. Zuilhof and J. S. Siegel, *Org. Biomol. Chem.*, 2013, **11**, 4333.

122 M. E. Jung, E. C. Yang, B. T. Vu, M. Kiankarimi, E. Spyrou and J. Kaunitz, *J. Med. Chem.*, 1999, **42**, 3899–3909.

123 F. Fazio, M. C. Bryan, O. Blixt, J. C. Paulson and C.-H. Wong, *J. Am. Chem. Soc.*, 2002, **124**, 14397–14402.

124 S. Hou, W. Liu, D. Ji and Z. Zhao, *Bioorganic Medicinal Chemistry Letters*, 2011, **21**, 1667–1669.

125 M. Ali, A. L. Lopez, Y. Ae You, Y. Eun Kim, B. Sah, B. Maskery and J. Clemens, *Bull World Health Org*, 2012, **90**, 209–218.

126 a) E. A. Merritt and W. G. J. Hol, *Current Opinion in Structural Biology*, 1995, **5**, 165–171; b) B. D. Spangler, *Microbiol. Rev.*, 1992, **56**, 622–647.

127 E. Fan, C. J. O'Neal, D. D. Mitchell, M. A. Robien, Z. Zhang, J. C. Pickens, X. J. Tan, K. Korotkov, C. Roach, B. Krumm, C. L. M. J. Verlinde, E. A. Merritt and W. G. J. Hol, *International Journal of Medical Microbiology*, 2004, **294**, 217–223.

128 R.-G. Zhang, D. L. Scott, M. L. Westbrook, S. Nance, B. D. Spangler, G. G. Shipley and E. M. Westbrook, *Journal of Molecular Biology*, 1995, **251**, 563–573.

129 I. Lonnroth and J. Holmgren, *J. Gen. Microbiol.*, 1973.

130 a) G. Ercolani and L. Schiaffino, *Angew. Chem. Int. Ed.*, 2011, **50**, 1762–1768; b) C. A. Hunter and H. L. Anderson, *Angew. Chem. Int. Ed.*, 2009, **48**, 7488–7499.

131 D. E. Schafer and A. K. Thakur, *Cell Biophys.*, 1982, **4**, 25.

132 C. J. O'Neal, *Science*, 2005, **309**, 1093–1096.

133 Joaquín Sánchez and Jan Holmgren, *Indian J Med Res.*, 2011, **133**, 153–163.

134 E. Fan, E. A. Merritt, C. L. Verlinde and W. G. J. Hol, *Current Opinion in Structural Biology*, 2000, **10**, 680–686.

135A. Bernardi, A. Checchia, P. Brocca, S. Sonnino and F. Zuccotto, *J. Am. Chem. Soc.*, 1999, **121**, 2032–2036.

136W. E. Minke, C. Roach, W. G. J. Hol and Verlinde,Christophe L. M. J., *Biochemistry*, 1999, **38**, 5684–5692.

137J. C. Pickens, E. A. Merritt, M. Ahn, C. L. Verlinde, W. G. Hol and E. Fan, *Chemistry Biology*, 2002, **9**, 215–224.

138D. D. Mitchell, J. C. Pickens, K. Korotkov, E. Fan and W. G. Hol, *Bioorganic Medicinal Chemistry*, 2004, **12**, 907–920.

139Vrasidas, I., de Mol, Nico J., Liskamp, Rob M. J. and Pieters, Roland J., *Eur. J. Org. Chem.*, 2001, **2001**, 4685–4692.

140H. M. Branderhorst, R. M. J. Liskamp, G. M. Visser and R. J. Pieters, *Chem. Commun.*, 2007, 5043.

141D. Arosio, I. Vrasidas, P. Valentini, R. M. J. Liskamp, R. J. Pieters and A. Bernardi, *Org. Biomol. Chem.*, 2004, **2**, 2113.

142a) J. C. Pickens, D. D. Mitchell, J. Liu, X. Tan, Z. Zhang, C. L. Verlinde, W. G. Hol and E. Fan, *Chemistry Biology*, 2004, **11**, 1205–1215; b) E. A. Merritt, Z. Zhang, J. C. Pickens, M. Ahn, W. G. J. Hol and E. Fan, *J. Am. Chem. Soc.*, 2002, **124**, 8818–8824; c) Z. Zhang, E. A. Merritt, M. Ahn, C. Roach, Z. Hou, Verlinde,Christophe L. M. J., W. G. J. Hol and E. Fan, *J. Am. Chem. Soc.*, 2002, **124**, 12991–12998.

143A. V. Pukin, PhD. Thesis, Wageningen University, 2010.

144A. V. Pukin, H. M. Branderhorst, C. Sisu, Weijers,Carel A. G. M., M. Gilbert, R. M. J. Liskamp, G. M. Visser, H. Zuilhof and R. J. Pieters, *ChemBioChem*, 2007, **8**, 1500–1503.

145a) F. Sansone, L. Baldini, A. Casnati and R. Ungaro, *New J. Chem.*, 2010, **34**, 2715; b) J. Garcia-Hartjes, S. Bernardi, Weijers,Carel A. G. M., T. Wennekes, M. Gilbert, F. Sansone, A. Casnati and H. Zuilhof, *Org. Biomol. Chem.*, 2013, **11**, 4340.

146S. Binauld, C. J. Hawker, E. Fleury and E. Drockenmuller, *Angew. Chem. Int. Ed.*, 2009, **48**, 6654–6658.

147A. Bouzide and G. Sauvé, *Org. Lett.*, 2002, **4**, 2329–2332.

148M. K. Müller and L. Brunsveld, *Angewandte Chemie International Edition*, 2009, **48**, 2921–2924.

149a) A. V. Pukin, C. A. Weijers, B. van Lagen, R. Wechselberger, B. Sun, M. Gilbert, M.-F. Karwaski, D. E. Florack, B. C. Jacobs, A. P. Tio-Gillen, A. van Belkum, H. P. Endtz, G. M. Visser and H. Zuilhof, *Carbohydrate Research*, 2008, **343**, 636–650; b) S. M. Andersen, C.-C. Ling, P. Zhang, K. Townson, H. J. Willison and D. R. Bundle, *Org. Biomol. Chem.*, 2004, **2**, 1199.

150a) A.-M. Svennerholm and J. Holmgren, *Current Microbiology*, 1978, **1**, 19–23; b) R. M. Dawson, *J. Appl. Toxicol.*, 2005, **25**, 30–38.

151D. Michel, *Biophysical Chemistry*, 2007, **129**, 284–288.

152a) A. Pfeil and J.-M. Lehn, *J. Chem. Soc., Chem. Commun.*, 1992, 838; b) P. N. Taylor and H. L. Anderson, *J. Am. Chem. Soc.*, 1999, **121**, 11538–11545.

153a) G. Ercolani, C. Piguet, M. Borkovec and J. Hamacek, *J. Phys. Chem. B*, 2007, **111**, 12195–12203; b) G. Ercolani, *J. Am. Chem. Soc.*, 2003, **125**, 16097–16103.

154A. Schoen and E. Freire, *Biochemistry*, 1989, **28**, 5019–5024.

155C. Sisu, A. J. Baron, H. M. Branderhorst, S. D. Connell, Weijers,Carel A. G. M., R. de Vries, E. D. Hayes, A. V. Pukin, M. Gilbert, R. J. Pieters, H. Zuilhof, G. M. Visser and W. B. Turnbull, *ChemBioChem*, 2009, **10**, 329–337.

156R. B. Martin, *Chem. Rev.*, 1996, **96**, 3043–3064.

157a) H. Sun, K. Ye, C. Wang, H. Qi, F. Li and Y. Wang, *J. Phys. Chem. A*, 2006, **110**, 10750–10756; b) P. Taboada, D. Attwood, J. M. Ruso, M. García, F. Sarmiento and V. Mosquera, *Langmuir*, 2000, **16**, 3175–3181.

158M. Wang, G. L. Silva and B. A. Armitage, *J. Am. Chem. Soc.*, 2000, **122**, 9977–9986.

159H. Yao, K. Domoto, T. Isohashi and K. Kimura, *Langmuir*, 2005, **21**, 1067–1073.

160M. Stephen and J. Straley, *Rev. Mod. Phys.*, 1974, **46**, 617–704.

161a) B. Bahadur, *Liquid crystals. Applications and uses*, World Scientific, Singapore, River Edge, NJ, 1991; b) P. M. Chaikin and T. C. Lubensky, *Principles of condensed matter physics*, Cambridge University Press, Cambridge, New York, NY, USA, 1995; c) Gennes, Pierre Gilles de and J. Prost, *The physics of liquid crystals*, Clarendon Press; Oxford University Press, Oxford, New York, 2nd edn., 1993, vol. 83.

162F. Reinitzer, *Monatsch. Chem.*, 1888, **9**, 421.

163O. Lehmann, *Z. Physik. Chem.*, 1889, **4**, 462.

164K. K. Baldridge and J. S. Siegel, *Theoretical Chemistry Accounts: Theory, Computation, and Modeling (Theoretica Chimica Acta)*, 1997, **97**, 67–71.

165a) B. Xu and T. M. Swager, *J. Am. Chem. Soc.*, 1993, **115**, 1159–1160; b) D. Miyajima, F. Araoka, H. Takezoe, J. Kim, K. Kato, M. Takata and T. Aida, *Science*, 2012, **336**, 209–213; c) L. M. Blinov, *Liquid Crystals*, 1998, **24**, 143–152; d) J. L. Atwood, L. J. Barbour, M. J. Hardie and C. L. Raston, *Coordination Chemistry Reviews*, 2001, **222**, 3–32.

166a) I. V. Kuvychko, S. N. Spisak, Y.-S. Chen, A. A. Popov, M. A. Petrukhina, S. H. Strauss and O. V. Boltalina, *Angew. Chem. Int. Ed.*, 2012, **51**, 4939–4942; b) B. M. Schmidt, S. Seki, B. Topolinski, K. Ohkubo, S. Fukuzumi, H. Sakurai and D. Lentz, *Angew. Chem. Int. Ed.*, 2012, **51**, 11385–11388; c) A. Sygula, H. E. Folsom, R. Sygula, A. H. Abdourazak, Z. Marcinow, F. R. Fronczek and P. W. Rabideau, *J. Chem. Soc., Chem. Commun.*, 1994, 2571–2572.

167L. Leibler, *Macromolecules*, 1980, **13**, 1602–1617.

168van Esch, J. H., Schoonbeek, F., de Loos, M., Kooijman, H., Spek, A. L., Kellogg, R. M. and Feringa, *Chem. Eur. J.*, 1999, **5**, 937–950.

169a) P. Beckmann, *Aust. J. Chem.*, 1961, **14**, 229; b) E. E. JELLEY, *Nature*, 1937, **139**, 631; c) E. E. JELLEY, *Nature*, 1936, **138**, 1009–1010.

170J. Sharma, R. Chhabra, A. Cheng, J. Brownell, Y. Liu and H. Yan, *Science*, 2009, **323**, 112–116.

171H. Furukawa and O. M. Yaghi, *J. Am. Chem. Soc.*, 2009, **131**, 8875–8883.

172a) D. Vance, J. Martin, S. Patke and R. S. Kane, *Advanced Drug Delivery Reviews*, 2009, **61**, 931–939; b) D. A. Scheinberg, C. H. Villa, F. E. Escorcia and M. R. McDevitt, *Nat Rev Clin Oncol*, 2010, **7**, 266–276.

173N. Scharnagl, S. Lee, B. Hiebl, A. Sisson and A. Lendlein, *J. Mater. Chem.*, 2010, **20**, 8789.

174a) T. Murase, S. Horiuchi and M. Fujita, *J. Am. Chem. Soc.*, 2010, **132**, 2866–2867; b) C. J. Brown, R. G. Bergman and K. N. Raymond, *J. Am. Chem. Soc.*, 2009, **131**, 17530–17531; c) D. Ajami and J. Rebek, *Nature Chem*, 2009, **1**, 87–90.

175a) E. T. Pashuck, H. Cui and S. I. Stupp, *J. Am. Chem. Soc.*, 2010, **132**, 6041–6046; b) J. Schneider, H. Cui, M. J. Webber and S. I. Stupp, *Biopolymers*, 2010, **94**, 1–18; c) J. D. Hartgerink, *Proceedings of the National Academy of Sciences*, 2002, **99**, 5133–5138; d) H. Cui, T. Muraoka, A. G. Cheetham and S. I. Stupp, *Nano Lett.*, 2009, **9**, 945–951; e) J. D. Hartgerink, *Science*, 2001, **294**, 1684–1688; f) R. C. Claussen, B. M. Rabatic and S. I. Stupp, *J. Am. Chem. Soc.*, 2003, **125**, 12680–12681; g) W.-W. Tsai, L.-s. Li, H. Cui, H. Jiang and S. I. Stupp, *Tetrahedron*, 2008, **64**, 8504–8514.

176a) C. Li, J. Huang and Y. Liang, *Langmuir*, 2000, **16**, 7701–7707; b) P. Berndt, K. Kurihara and T. Kunitake, *Langmuir*, 1995, **11**, 3083–3091; c) A. Gissot, M. Camplo, M. W. Grinstaff and P. Barthélémy, *Org. Biomol. Chem.*, 2008, **6**, 1324; d) J. S. Nowick, T. Cao and G. Noronha, *J. Am. Chem. Soc.*, 1994, **116**, 3285–3289.

177a) J. S. Yang, Q. Q. Zhou and W. He, *Carbohydrate Polymers*, 2013, **92**, 223–227; b) A. G. Dal Bó, V. Soldi, F. C. Giacomelli, C. Travelet, B. Jean, I. Pignot-Paintrand, R. Borsali and S. Fort, *Langmuir*, 2012, **28**, 1418–1426; c) B.-S. Kim, D.-J. Hong, J. Bae and M. Lee, *J. Am. Chem. Soc.*, 2005, **127**, 16333–16337.

178a) J. C. MacDonald and G. M. Whitesides, *Chem. Rev.*, 1994, **94**, 2383–2420; b) G. Whitesides, J. Mathias and C. Seto, *Science*, 1991, **254**, 1312–1319; c) L. Isaacs, D. N. Chin, X. Bowden, Y. Xia and G. M. Whitesides, *Perspect. Supramol. Chem.*, 1999, **4**, 1–46; d) S. C. Zimmerman, F. Zeng, D. E. C. Reichert and S. V. Kolotuchin, *Science*, 1996, **271**, 1095–1098; e) V. Percec, C.-H. Ahn, G. Ungar, D. J. P. Yeardley, M. Möller and S. S. Sheiko, *Nature*, 1998, **391**, 161–164; f) S. D. Hudson, *Science*, 1997, **278**, 449–452; g) H. Engelkamp, *Science*, 1999, **284**, 785–788; h) M. R. Ghadiri, J. R. Granja, R. A. Milligan, D. E. McRee and N. Khazanovich, *Nature*, 1993, **366**, 324–327; i) Hartgerink, J. D., Clark, T. D. and Ghadiri, M. R., *Chem. Eur. J.*, 1998, **4**, 1367–1372; j) Clark, T. D., Kobayashi, K. and Ghadiri, M. R., *Chem. Eur. J.*, 1999, **5**, 782–792; k) E. W. Meijer, Hirschberg,J. H. K. Ky, L. Brunsveld, A. Ramzi, Vekemans,Jef A. J. M. and R. P. Sijbesma, *Nature*, 2000, **407**, 167–170; l) L. Brunsveld, B. J. B. Folmer and E. W. Meijer, *MRS Bull.*, 2000, **25**, 49–53; m) J.-M. Lehn, *Supramolecular Chemistry*, Wiley-VCH Verlag GmbH Co. KGaA, Weinheim, FRG, 1995.

179a) Y. Zhang and N. C. Seeman, *J. Am. Chem. Soc.*, 1994, **116**, 1661–1669; b) N. C. Seeman, *Angew. Chem. Int. Ed.*, 1998, **37**, 3220–3238; c) N. C. Seeman, *Journal of Theoretical Biology*, 1982, **99**, 237–247; d) J. Chen and N. C. Seeman, *Nature*, 1991, **350**, 631–633.

180a) R. M. McKinlay, S. J. Dalgarno, P. J. Nichols, S. Papadopoulos, J. L. Atwood and C. L. Raston, *Chem. Commun.*, 2007, 2393; b) Müller, A., Sarkar, S., Shah, S. Q. N., Bögge, H., Schmidtmann, M., Sarkar, S., Kögerler, P., Hauptfleisch, B., Trautwein, A. X. and Schünemann, V., *Angew. Chem. Int. Ed.*, 1999, **38**, 3238–3241; c) S. Alvarez, *Dalton Trans.*, 2005, 2209.

181A. J. Olson, Y. H. E. Hu and E. Keinan, *Proceedings of the National Academy of Sciences*, 2007, **104**, 20731–20736.

182a) H. Dietz, S. M. Douglas and W. M. Shih, *Science*, 2009, **325**, 725–730; b) S. M. Douglas, H. Dietz, T. Liedl, B. Högberg, F. Graf and W. M. Shih, *Nature*, 2009, **459**, 414–418; c) T. Liedl, B. Högberg, J. Tytell,

D. E. Ingber and W. M. Shih, *Nature Nanotech*, 2010, **5**, 520–524; d) W. M. Shih, J. D. Quispe and G. F. Joyce, *Nature*, 2004, **427**, 618–621; e) E. S. Andersen, M. Dong, M. M. Nielsen, K. Jahn, R. Subramani, W. Mamdouh, M. M. Golas, B. Sander, H. Stark, C. L. P. Oliveira, J. S. Pedersen, V. Birkedal, F. Besenbacher, K. V. Gothelf and J. Kjems, *Nature*, 2009, **459**, 73–76; f) A. Kuzuya and M. Komiyama, *Chem. Commun.*, 2009, 4182.

183 S. H. Ko, M. Su, C. Zhang, A. E. Ribbe, W. Jiang and C. Mao, *Nature Chem*, 2010, **2**, 1050–1055.

184 a) F. A. Aldaye, P. K. Lo, P. Karam, C. K. McLaughlin, G. Cosa and H. F. Sleiman, *Nature Nanotech*, 2009, **4**, 349–352; b) H. Yang, C. K. McLaughlin, F. A. Aldaye, G. D. Hamblin, A. Z. Rys, I. Rouiller and H. F. Sleiman, *Nature Chem*, 2009, **1**, 390–396; c) P. K. Lo, P. Karam, F. A. Aldaye, C. K. McLaughlin, G. D. Hamblin, G. Cosa and H. F. Sleiman, *Nature Chem*, 2010, **2**, 319–328; d) F. A. Aldaye and H. F. Sleiman, *J. Am. Chem. Soc.*, 2007, **129**, 13376–13377.

185 C. K. McLaughlin, G. D. Hamblin, F. A. Aldaye, H. Yang and H. F. Sleiman, *Chem. Commun.*, 2011, **47**, 8925.

186 Scheffler, M., Dorenbeck, A., Jordan, S., Wüstefeld, M. and von Kiedrowski, G., *Angew. Chem. Int. Ed.*, 1999, **38**, 3311–3315.

187 J. Zimmermann, M. P. J. Cebulla, S. Mönninghoff and G. von Kiedrowski, *Angew. Chem. Int. Ed.*, 2008, **47**, 3626–3630.

188 T. R. Chan, R. Hilgraf, K. B. Sharpless and V. V. Fokin, *Org. Lett.*, 2004, **6**, 2853–2855.

189 a) D. Kowalski, W. D. Kroeker and M. Laskowski, *Biochemistry*, 1976, **15**, 4457–4463; b) T. McCutchan, J. Hansen, J. Dame and J. Mullins, *Science*, 1984, **225**, 625–628.

190 M. S. Shchepinov, K. U. Mir, J. K. Elder, M. D. Frank-Kamenetskii and E. M. Southern, *Nucleic Acids Research*, 1999, **27**, 3035–3041.

191 G. B. Rocha, R. O. Freire, A. M. Simas and J. J. P. Stewart, *J. Comput. Chem.*, 2006, **27**, 1101–1111.

192 M. W. Schmidt, K. K. Baldridge, J. A. Boatz, S. T. Elbert, M. S. Gordon, J. H. Jensen, S. Koseki, N. Matsunaga, K. A. Nguyen, S. Su, T. L. Windus, M. Dupuis and J. A. Montgomery, *J. Comput. Chem.*, 1993, **14**, 1347–1363.

193 James J. P. Stewart, *MOPAC2012*, Stewart Computational Chemistry, Colorado Springs, CO, USA, 2012.

194 a) J. D. WATSON and F. H. C. CRICK, *Nature*, 1953, **171**, 737–738; b) M. Mandelkern, J. G. Elias, D. Eden and D. M. Crothers, *Journal of Molecular Biology*, 1981, **152**, 153–161.

195 Roman M. Maag, PhD Thesis, University of Zurich, 2012.

CURRICULUM VITAE

MATTARELLA Martin

Sex: Male

Date of Birth: November 30th, 1986 in Carate Brianza (MB), Italy

Nationality: Italian

Languages: Italian (mother tongue), English (fluent).

E-mail: martin.mattarella@uzh.ch

Tel: +41 44 635 39 54

Education

June 2010 – Present	**University of Zurich, Switzerland** **PhD Studies in Organic Chemistry** PhD thesis: "Five-Fold Symmetric Penta-Bioconjugated Corannulenes: Synthesis, Properties and Applications". Advisor: Prof. Dr. Jay S. Siegel
October 2008 – February 2010	**Università degli Studi di Milano, Italy** **M.S. in Organic – Inorganic Chemistry** Master thesis: "Preparation of Fluorescent Tubulin Binder". Advisor: Prof. Dr. Daniele Passarella
October 2005 – October 2008	**Università degli Studi di Milano, Italy** **B.S. in Chemical Science** Bachelor thesis: "Thermal Analysis of some Oxidizing Agent by DSC and TGA". Advisors: Prof. Dr. Lucio Forni, Dr. Paolo Cardillo

September 2000 – June 2005	**I.S.S. "A. Greppi", Italy** Diploma: Chemistry

Work Experience

	University of Zurich, Switzerland
June 2010 – Present	PhD Student in the group of Prof. Dr. Jay S. Siegel. Teaching assistant in Laboratory Courses in Organic Chemistry I and Organic Chemostry II.
	Università degli Studi di Milano, Italy
January 2009 – February 2010	Undergraduate student in the group of Prof. Dr. Daniele Passarella. Laboratory advisor for bachelor students.
	Stazione Sperimentale per i Combustibili, Italy
March 2008 – October 2008	Bachelor student in the thermoanalysis laboratory of Dr. Paolo Cardillo

Oral Presentations

June 2012	**Doktorandentag 2012**, PhD student day of the Institute of Organic Chemistry, University of Zurich

Poster Presentations

"*C*$_5$-Symmetric Penta-Bioconjugated Corannulenes: Synthesis, Properties and Applications"; *M. Mattarella*, *J. S. Siegel*; poster presented at the Rigi-Workshop 2013. Rigi Kulm, Switzerland, 2013

"*C*$_5$-Symmetric Penta-Bioconjugated Corannulenes: Synthesis, Properties and Applications"; *M. Mattarella*, *J. S. Siegel*; poster presented at the 7th Annual DCH Symposium; Zurich, Switzerland, 2012.

"Bioconjugated Corannulenes: a New Class of Penta-substituted Corannulenes"; *M. Mattarella, J. S. Siegel*; poster presented at the 5th Siegfried Symposium; Zurich, Switzerland, 2012.

"Bioconjugated Corannulenes: a New Class of Penta-substituted Corannulenes"; *M. Mattarella, J. S. Siegel*; poster presented at the Gordon Research Conference; Newport, RI, USA, 2012.

"Bioconjugated Corannulenes: a New Class of Penta-substituted Corannulenes"; *M. Mattarella, J. S. Siegel*; poster presented at the 6th Annual DCH Symposium; Zurich, Switzerland, 2011.

"Bioconjugated Corannulenes: a New Class of Penta-substituted Corannulenes"; *M. Mattarella, J. S. Siegel*; poster presented at the 17th European Symposium on Organic Chemistry; Hersonissos, Greece, 2011.

"Desymmetrization of 1,3,5,7,9-Pentachlorocorannulene via DNA-Templated Organic Synthesis"; *M. Mattarella, J. S. Siegel*; poster presented at the COST Action D34 Final Meeting; Florence, Italy, 2010.

"Desymmetrization of 1,3,5,7,9-Pentachlorocorannulene via DNA-Templated Organic Synthesis"; *M. Mattarella, J. S. Siegel*; poster presented at the 5th Annual DCH Symposium; Zurich, Switerland, 2010.

Publications

"**Nanomolar Cholera Toxin Inhibitors based on Symmetrical Pentavalent Ganglioside GM1os-*Sym*-Corannulenes**", M. Mattarella, J. Garcia-Hartjes, T. Wennekes, H. Zuilhof, J. S. Siegel, *Org. Biomol. Chem.*, **2013**, *11*, 4333-4339.

"**Five-Fold Symmetric Penta-substituted Corannulene with Gelation Properties and Liquid-Crystalline Phase**", M. Mattarella, J. M. Haberl, J. Ruokolainen, E. M. Landau, R. Mezzenga, J. S. Siegel, *Chem. Comm.*, **2013**, *49*, 7204-7206.

"**Preparation of Fluorescent Tubulin Binders**", E. Riva, M. Mattarella, S. Borrelli, M. S. Christodoulou, D. Cartelli, M. Main, S. Faulkner, D. Sykes, G. Cappelletti, J. S. Snaith, D. Passarella, *ChemPlusChem*, **2013**, *78*, 222-226.

"***Sym*-($CH_2X)_5$-corannulenes: molecular pentapods displaying functional group and bioconjugate appendages**", M. Mattarella and J. S. Siegel, *Org. Biomol. Chem.*, **2012**,*10*, 5799-5802.

"**Determinazione del potere ossidante: proposta di un metodo basato sulla calorimetria differenziale a scansione**", L. Gigante, M. Dellavedova, C. Pasturenzi, A. Lunghi, M. Mattarella, P. Cardillo, *Riv. Combustibili*, **2008**, *62*, 251.

"**Studio del meccanismo di decomposizione del carbonato di sodio peridrato mediante analisi termica**", L. Gigante, M. Dellavedova, C. Pasturenzi, A. Lunghi, M. Mattarella, P. Cardillo, *Riv. Combustibili*, **2008**, *62*, 279.